UNIVERSITY OF CALIFORNIA,
IRVINE

Retinoids Modulate *MITF*: A Novel Mechanism in the Regulation of Melanogenesis

DISSERTATION

submitted in partial satisfaction of the requirements
for the degree of

DOCTOR OF PHILOSOPHY

in Biomedical Sciences

by

Elyse Kathleen Paterson

Dissertation Committee:
Associate Professor Anand K. Ganesan, Chair
Professor Bogi Andersen
Professor Xing Dai
Associate Professor Yongsheng Shi
Professor Kyoko Yokomori

2015

DEDICATION

To my family, Doug, Julie and Marissa, for always loving me and supporting me through the good times and the bad times; to my boys, Kopitar and Quick, for being my sweet and loving guardian angels; to my family members that have passed on and whom I love and miss dearly: my grandmother Joan Mary Greenwood Paterson, my great-grandmother Annie MacKinnon Paterson, my great-grandmother Margaret "Peggy" Langlois Olauson, and my great-grandfather, Lloyd Dale Olauson; to Simon and Garfunkel, for music that is both healing and provoking; to Dr. Daniel Coleman, for at first being my friend, and for now being much, much more.

"and the sign said, 'The words of the prophets are written on the subway walls
And tenement halls
And whispered in the sound of silence.'"
Simon & Garfunkel, 'The Sound of Silence', 1966

"'Kathy, I'm lost', I said, though I knew she was sleeping
'I'm empty and aching and I don't know why'
Counting the cars on the New Jersey turnpike, they've all come to look for America"
Simon & Garfunkel, 'America', 1968

TABLE OF CONTENTS

LIST OF ABBREVIATIONS

9-*cis* RA	9-*cis* retinoic acid
all-*trans* RA	all-*trans* retinoic acid
α-MSH	alpha-melanocyte-simulating hormone
ALDH1A1	aldehyde dehydrogenase 1A1
ASIP	agouti signaling protein
BLOC	biogenesis of lysosome-related organelle complex
cAMP	cyclic adenosine monophosphate
Cya/Cy	cyanamide
CREB	cAMP-response element-binding protein
DAG	diacylglycerol
DOPA	L-3,4-dihydroxyphenylalanine
ET-1	endothelin-1
LEF-1	lymphoid enhancer-binding factor 1
LRO	lysosome-related organelle
MAPK	mitogen-activated protein kinase
MC1R	melanocortin-1 receptor
MITF-A	micropthalmia-associated transcription factor isoform A
MITF-M	micropthalmia-associated transcription factor isoform M
NCC	neural crest cell
NO	nitric oxide
PKA	protein kinase A
PMEL	premelanosome protein
POMC	pro-opiomelanocortin
qRT-PCR	quantitative real-time PCR

TYR	tyrosinase
TYRP-1	tyrosinase related-protein 1
TYRP-2	tyrosinase-related protein 2
RA	retinoic acid
RXR	retinoid X receptor
RAR	retinoic acid receptor
RNAi	RNA interference
SCF	stem cell factor
siRNA	small interfering RNA
shRNA	short hairpin RNA
SOX10	sex determining region Y-Box 10
UV-R	ultraviolet-radiation
Veh	vehicle

LIST OF FIGURES

LIST OF TABLES

ACKNOWLEDGMENTS

Here, I want to take the opportunity to thank and acknowledge the many incredible individuals who have stood by me, taught me, laughed with me, supported me, and who have been vital in forming the person and scientist that I am today. I am a constant observer of my surroundings and interactions, and this constant observation is a vital tool for me as I learn over and over how to navigate life.

Firstly, I thank **Dr. Anand Ganesan**, M.D., Ph.D., for accepting me as a graduate student into his laboratory and serving as my mentor for six years during which time he helped shape me into the scientist that I am today. From Anand, I have learned how to develop appropriate controls for every experiment, how to synthesize a clear, well thought out manuscript with an intriguing story, how to strive always for "publication quality" data, and how to have vigorous yet respectful discussions on data and what to do next.

I thank my committee members, **Dr. Bogi Andersen, Dr. Xing Dai, Dr. Yongsheng Shi** and **Dr. Kyoko Yokomori** for listening to all of my presentations over the years and giving me solid advice on how to improve my project and make it the best it could be.

I thank the **Public Library of Science (USA)** for permission to use previously published information that is open access as part of my chapter 1. I thank **John Wiley & Sons A/S** for permission to include a copyrighted manuscript as part of my dissertation, which forms all of chapter 3. Financial support was provided by a grant from the National Institute of Health (NIH) to Anand K. Ganesan (1K08AR056001) and a grant from NIAMS to Anand K. Ganesan (R01AR063116).

I thank **Dr. Amelia Soto Hopkin (Amy Hopkin)** for being a great friend, someone I can laugh with and tell anything to. Amy and I have many inside jokes and although we don't see each other everyday anymore, our friendship always picks up right where it left off. Amy is a fantastic scientist with a phenomenal capacity for teaching others what she knows. She is the bona fide ChIP expert of the second floor of Sprague Hall (if not all of Sprague Hall) and through her, I have been able to learn invaluable techniques that have advanced my project in many ways. I thank **Dr. Sohail Jahid**, the new post-doctoral scholar in the Ganesan laboratory. Sohail is genuine and compassionate and always ready to help others. She, like Amy, is a very intelligent woman who excels in science. Sohail has given me helpful ideas to improve my experiments and always seems to know a little bit about everything, highlighting her well-rounded capacity as a scientist. Both of these talented women are excellent role models for other women in the sciences, and I have learned an incredible amount from them both.

I thank **Chi-Fen Chen**, my co-worker in the Ganesan lab, for her steadfast advice and calm, quiet demeanor. I acknowledge **Marc Liggins** for his thoughtful cat-themed gifts and his listening ear. I thank **Rolando Ruiz-Vega** for being a supportive friend, reminding me of my best interests, and giving me solid advice on experiments and analysis of data. **Francisco Espitia** took over the ordering/management of the lab when he joined as lab manager, and for that I am very grateful. He has also been a steadfast friend with sound advice on fitness and life in general. I thank **Priya Vasudeva** for her honesty, her genuine friendship, and her incredible

help during my last year of graduate school. While I was away interviewing at OHSU, she took care of all of my experiments for me. She is incredibly witty, has a great sense of humor, and always listened to me when I needed her to. Priya is hugely talented in the lab and is dedicated to always performing her best and putting forth her best effort, and for that I am grateful.

I thank the individuals whom I mentored over the years, including **Jonathan Schilling**, **Sarah Carmona, Amy Sun,** and **Jessica Flesher.** They taught me valuable lessons on how to effectively mentor others. I have learned to always positively reinforce those you teach; one small word of kindness can go a long way! Thank you also for completing experiments for me, some of which are going into future publications.

I thank **Rachel Savitt,** who is one of the most genuine, caring and friendly people I have ever known. I met Rachel Savitt because she is my neighbor. Rachel is wise beyond her years, a sounding board for me, a cat lover like myself, and an incredibly independent woman who knows what she wants. She has taught so many important life lessons: always trust your gut and do what is right for you, and never settle for anything less than the absolute best for yourself.

Patty DePetris is a wonderful friend, an excellent listener and a fantastic giver-of-advice. I often stopped by Patty's office in Sprague and what was planned to be a five-minute conversation would always end up being much longer. Patty is genuine and cares for others; furthermore, she has an excellent sense of humor. She always manages to brighten my day whenever I see her, and for that I am grateful.

My boys, **Kopitar and Quick**, make my life complete- they are apart of my heart and my "guardian angels". It is hard to put into words how much I love them. They are named after Anze Kopitar and Jonathan Quick of the Los Angeles Kings (my favorite team). Kopitar is my eighteen-pound orange and white tabby cat ("Orange Tabber") that came to be mine on August 3, 2012. He was born to a "beautiful calico lady" cat named Princess in early 2012. Quick is still my kitten and came to be mine on May 25, 2014. He was found in a friend's backyard in April of 2014, along with three of his littermates. Each one of them was skin and bones and only weighed about a pound. I rescued my "Quicker" and two of his littermates (I brought them to the Irvine Animal Care Facility where they were adopted) and my friend kept the fourth kitten. I call Quicker "my survivor" because he braved incredibly hot days as a very young kitten without much food or water. I thoroughly believe in the idea that *"Until one has loved an animal, a part of one's soul remains unawakened."* (Anatole France). My boys have awakened my soul and completed me.

Thank you to the many wonderful people in the Biological Chemistry department and other departments across campus that have been amazing friends, especially the people of Sprague Hall, my second home for the last six years. This includes **Selma Alkafeef, Stacey Borrego, James Yu, Stephanie Sprowl Tanio, Dr. Haik Mkhikian, Ashley Fong, Dr. Lindsey Araujo, Rachel Herndon Klein, Dr. Briana Lee Altman, Alvaro Villarreal Ponce, Christie Mortales, Dr. Michael Salmans, Eric Cam, Dr. Hsiang Ho, Dr. Mikhail Geyfman, Dr. William Gordon, Dr. Elizabeth McReynolds Gordon, Dr. Jeniffer Hernandez, Eric Cam, Dr. Taraneh Esmailpour Angeloni, Andrew Komoto, Rubina Kapadia, and Erik Lawson.** You

brightened my days and made graduate school much more tolerable. Thank you for the advice, the support, the humor and the friendship that you have graciously given me.

My sister, **Marissa Julianne Paterson, (Belle)** has been my closest friend and confidant for my entire life. When she was born, I asked my parents if we could name her "Minnie" because I loved that Disney character and well, I loved Marissa more than anything even before she was born. Belle and I have grown together and we understand each other on a level that is unparalleled. I am incredibly thankful for her presence in my life; she balances me in a way that no one else can. I thank her for her sweetness, her sensitivity, her intelligence, her presence, her sense of humor, her kindness, and her friendship.

Andre & Kathy Beaudin, or "Mema and Gramps", my grandparents, are incredibly loving and generous people. While my grandfather, Andre, came to the US from St. Eustache, Manitoba, Canada, my grandmother, Kathy, was born here in the states. Both worked very hard their entire life to give the best life possible to their children. For years, they took care of my sister and I while after school and during summer break. We had such incredible times with them- going to museums, learning to sew and knit, cooking, going swimming, playing "office". I always enjoyed spending time with them and continue to do so. Mema and Gramps are also incredibly generous for birthdays and holidays- their kind gifts have helped me financially during difficult times. Mema and Gramps always have solid, well-thought and inspiring advice on how to be better and how to live the best life possible. I thank them for always loving me, supporting me, and being present for me.

I thank and acknowledge my parents, **Douglas "Po" & Julianne "Mo" Paterson**, for their compassion, their drive, and their incredible work ethic that allowed for my sister and I to have an amazing childhood that was filled with complete joy, play, school and constant activities. My parents always worked hard so that Marissa and I could go to private school, have a beautiful home to call our own, go on exciting, fun trips, and always have delicious food to eat. Thank you, Mo & Po, for providing for us and always being present in our lives. Po is an artist, a musician, and an athlete; not to mention, he basically built our house with his own hands. I am in awe that this man is my father; he truly is a gift that I am eternally grateful for. My mother is always a source of inspiration as well- she has always worked so hard at her job while still exceling at being a wife and a mother. My parents always reminded me of my worth and instilled in me that I could do anything I set my mind to. It is largely because of them, and how they raised me, that I am who I am today. Some of the most valuable lessons I have learned from them play in my head daily. Po once told me, "If you borrow something from someone, return it in better shape than it was when you borrowed it". Mo once said, "Always take the extra time to do things the right way the first time-it will save you time in the long run". Wiser words were never spoken.

Dr. Daniel Coleman has been a true friend and my biggest cheerleader since the day I met him at a Pigment Cell Conference in Madison, Wisconsin in September, 2013. We both had and continue to have a thing for melanocytes and RXR, so we bonded at the conference (especially on our walk to the conference gala where we got lost, which was actually the best thing ever). Dan gave an amazing talk and I was the only person in the entire audience to laugh at one of his Jersey Shore jokes. On the last day, I insisted that he Gchat me so that we could keep in touch.

The rest really is history. Dan and I understand each other in ways I never thought another person could or would understand me. We have shared the same trials and tribulations, and in these times, have emerged as better people. I am in awe of what an intelligent, caring, kind, loyal man he is, and I am so grateful for his advice, his encouragement, his understanding, and his listening ear. Dan is a brilliant scientist whom I greatly admire. I continue to learn from him and bounce ideas off of him. I am eternally grateful for his presence in my life and I am so incredibly excited to begin a new chapter of my life with him.
"He's more myself than I am. Whatever our souls are made of, his and mine are the same."
-Emily Bronte, Wuthering Heights

The **music of the 1960's** claimed my heart long ago when my father introduced me to Simon & Garfunkel and The Moody Blues as a child. I have to acknowledge the musicians of this era whose incredible song has inspired me, lead me, gave me hope, and accompanied me, every day. These artists include: Janis Joplin, The Righteous Brothers, Peter, Paul and Mary, Joan Baez, Donovan, Santana, The Animals, Neil Diamond, Grateful Dead, Jefferson Airplane, Pink Floyd, The Moody Blues, Crosby, Stills & Nash, The Velvet Underground, The Byrds, Cream, Creedence Clearwater Revival, Led Zeppelin, The Doors, Jimi Hendrix, The Rolling Stones, the Beatles, and of course, Simon & Garfunkel.

All of the aforementioned people (and animals! ☺) have affected me and shaped me into the person I am today. I am so grateful to have such incredible individuals in my life. Thank you to all of you!

"I've learned that people will forget what you said, people will forget what you did, but people will never forget how you made them feel" –Maya Angelou

Elyse Kathleen Paterson, Ph.D.

18832 Florida St, #11
Huntington Beach, CA 92648
(714) 486-8866
elyse.paterson@gmail.com
www.linkedin.com/in/elysekpaterson

University of California, Irvine
Department of Biological Chemistry
839 Health Sciences Road
Irvine, CA 92617
(949) 824-0547

EDUCATION

University of California Irvine — **Irvine, CA**
Ph.D. Candidate**,** Biological Chemistry, School of Medicine *(September 2009-August 2015)*
Advisor: Dr. Anand K. Ganesan, M.D., Ph.D.
(Ph.D. defended on August 13, 2015)

Loyola Marymount University — **Los Angeles, CA**
Bachelor of Science, Biochemistry *(August 2005-May 2009)*
Minor in biology
Magna cum laude

RESEARCH EXPERIENCE

University of California, Irvine — **Irvine, CA**
Department of Biological Chemistry *(January 2010-Present)*
Graduate Research Assistant
Advisor: Dr. Anand K. Ganesan

Loyola Marymount University — **Los Angeles, CA**
Department of Chemistry and Biochemistry *(May 2007-May 2009)*
Undergraduate Student Researcher
Advisor: Dr. Jeremy McCallum
Project: Guanine derivatives as precursors for G-Quadruplex Formation

Brandeis University — **Waltham, MA**
Department of Biochemistry *(June 2008-August 2008)*
National Science Foundation Student Researcher
Advisor: Dr. Anne Gershenson
Project: Analysis of the Unfolding and Refolding of α1-antitrypsin protein using fluorescence correlation spectroscopy

PEER-REVIEWED PUBLICATIONS & MANUSCRIPTS IN PREPARATION

Paterson, Elyse. K., Priya Vasudeva, Jessica L. Flesher, Jonathan Schilling, Amy Sun, Sohail Jahid, Jennifer Sui, Grant R. MacGregor, Jonathan Neumann and Anand K. Ganesan. "Retinoids Modulate *MITF:* A Novel Mechanism in the Regulation of Melanin Biosynthesis". Manuscript in preparation.

Paterson, Elyse K., Thomas J. Fielder, Grant R. MacGregor, Shosuke Ito, Kazumasa Wakamatsu, Victoria Eby, Raymond E. Boissy and Anand K. Ganesan. "Tyrosinase Modulates Pigmentation by Controlling the Distribution of Melanin Within the Maturing Melanosome." *In revision, PLoS One.*

Paterson, Elyse K., Hsiang Ho, Rubina Kapadia and Anand K. Ganesan. "9-*cis* Retinoic Acid is the ALDH1A1 Product That Stimulates Melanogenesis." *Experimental Dermatology* 22 (3): 202-09. 12 March 2013*.
(click to access PDF)

*This publication was commented on by the editorial board in the following publication: Kleszczynski, Konrad and Andrzej T. Slominski. "Targeting ALDH1A1 to treat pigmentary disorders." *Experimental Dermatology* 22 (5): 316-317. 25 April 2013. (click to access PDF)

ABSTRACTS

Paterson, E. K., T.J. Fielder, G. MacGregor, R.E. Boissy, and A.K. Ganesan. "An Inducible and Reversible shRNA Transgenic Mouse Model to study Melanogenesis Postnatally." *Pigment Cell and Melanoma Research* 26 (2013).

Hernandez, Jeniffer, Ryan Michalek, Brian Weist, Ryan Newton, Jose Limon, Mayra Carrillo, **Elyse Paterson**, Long Nguyen, David Fruman, Jeffrey Rathmell, and Craig Walsh. "Control of T Cell Metabolism and Regulatory T Cell Generation by a DRAK2/p70S6K1 Signaling Axis." *The Journal of Immunology* 186 (2011).

BOOK CHAPTERS

Soto Hopkin, Amelia, **Elyse K. Paterson**, Rolando Ruiz Vega, and Anand K. Ganesan. "Pigment Production Analysis in Human Melanoma Cells." *Melanoma: Methods and Protocols*. Ed. John Walker. New York: Humana, 2015. *In press.*

TECHNICAL SKILLS

Extensive experience with RNAi, pigment production assays, and gene expression analysis via western blotting and quantitative real-time PCR. Highly experienced in cell culture of many cell types and lines, cloning, lentiviral production and infection, transfection, mouse husbandry and maintenance of mouse colonies, genotyping, PCR and DNA gel electrophoresis, human three-dimensional skin equivalents, PCR primer design, chromatin immunoprecipitation, DNA/RNA isolation, DNA/RNA purification, CellTiter Glo assay, luciferase activity assay, tissue fixation, embedding, sectioning, and immunohistochemistry.

Computer skills: Microsoft Excel, Microsoft Word, Microsoft PowerPoint, UCSC Genome Browser, Image J, Adobe Illustrator, Adobe Photoshop, EndNote

PRESENTATIONS & POSTERS

Paterson, Elyse K. "An Inducible and Reversible shRNA Transgenic Mouse Model to Study Melanogenesis Postnatally". Oral presentation delivered at the Department of Biological Chemistry Seminar Series, University of California Irvine, Irvine, CA, April 15, 2014.

Paterson, Elyse K., Thomas J. Fielder, Grant R. MacGregor, Raymond E. Boissy and Anand K. Ganesan. "An Inducible and Reversible shRNA Transgenic Mouse Model to study Melanogenesis Postnatally". Poster presentation delivered at the Pan American Society for Pigment Cell Research Annual Meeting entitled "Advances in Melanocyte and Melanoma Biology", University of Wisconsin Madison, Madison, WI, September 8-11, 2013.

Paterson, Elyse K. "9-*cis* Retinoic Acid: A Novel Regulator of Melanogenesis". Oral presentation delivered at the Department of Biological Chemistry Seminar Series, University of California Irvine, Irvine, CA, May 15, 2013.

Paterson, Elyse K. "A Rapid and Scalable Transgenic shRNA System to Study Melanogenesis in the Mouse Hair Follicle". Oral presentation delivered at the University of California Irvine Chao Family Comprehensive Cancer Center Skin Cancer Retreat, Irvine, CA, January 30, 2012.

Paterson, Elyse K. "Characterizing the Role and Impact of Aldehyde Dehydrogenase as a Key Regulator of Melanogenesis in Human Skin Cells". Oral presentation delivered at the Loyola Marymount University Department of Chemistry and Biochemistry seminar series, Los Angeles, CA, September 23, 2011.

Paterson, Elyse K. "What to Expect in a Biological Sciences Graduate Program". Oral presentation delivered at the Loyola Marymount University Department of Chemistry and Biochemistry seminar series, Los Angeles, CA, September 23, 2011.

Paterson, Elyse K., and Abigail Fall. "Guanine derivatives as precursors for G-Quadruplex Formation". Poster presentation delivered at the Southern California Conference for Undergraduate Research, California Polytechnic University, Pomona, Pomona, California, November 22, 2008.

Paterson, Elyse K. "Using Fluorescence Correlation Spectroscopy to Monitor the Unfolding and Refolding of α1-antitrypsin". Oral presentation delivered at the National Sciences Foundation Research Experience for Undergraduates final seminar, Brandeis University, Waltham, MA, August 2008.

TEACHING EXPERIENCE

University of California Irvine, Department of Biological Sciences, Irvine, CA
Teaching Assistant
Courses Taught:

- Biochemistry Discussion, *January 2011-March 2011*
- Molecular Biology Laboratory, *January 2011-March 2011*
- Introductory Biology: DNA to Organisms, *September 2010-December 2010*

Loyola Marymount University, Department of Chemistry and Biochemistry, Los Angeles, CA
Teaching Assistant, Organic Chemistry Laboratory, *May 2007-May 2008*

MENTORING EXPERIENCE

University of California, Irvine (UCI), Research Mentor for Jessica Flesher, Graduate Student at UCI (*September 2014-December 2014)*
University of California, Irvine (UCI), Research Mentor for Sara Carmona, Graduate Student at UCI (*September 2013-December 2013)*
University of California, Irvine (UCI), Research Mentor for Amy Sun, Medical Student at St. Louis University (*June 2013-September 2013)*
University of California, Irvine (UCI), Research Mentor for Jonathan Schilling, undergraduate student at UCI (*March 2012-June 2013)*

AWARDS AND HONORS

School of Medicine Individual Fellowship Application Incentive, University of California Irvine *(March 2014)*

University of California Irvine School of Medicine Travel Award, University of California Irvine *(August 2013)*

John Wasmuth Graduate Student Research Seminar Award, University of California Irvine *(June 2013)*

Biochemistry Program Scholar, Loyola Marymount University *(May 2009)*

Magna cum laude, Loyola Marymount University *(May 2009)*

Dean's List, College of Science and Engineering, Loyola Marymount University *(2005-2009)*

COURSEWORK AND SPECIAL TRAINING

Excellence in Teaching *(April 2015-June 2015)*
University of California Irvine Graduate Division

Research Seminar *(September 2010-June 2015)*
Department of Biological Chemistry

Mouse Developmental Genetics *(March 2012-June 2012)*
Department of Biological Chemistry

Physiology of Ion Channels *(March 2011-June 2011)*
Department of Physiology and Biophysics

Regulation of Gene Expression *(March 2010-June 2010)*
Department of Microbiology and Molecular Genetics

Topics in Experimental Pathology *(January 2010-March 2010)*
Department of Pathology

Protein Structure and Function *(September 2009-December 2009)*
Department of Molecular Biology and Biochemistry

REFERENCES

Dr. Anand K. Ganesan, MD, Ph.D., PhD Advisor
Associate Clinical Professor
Departments of Dermatology and Biological Chemistry
School of Medicine
University of California Irvine
Phone: (949) 824-2926
email: aganesan@uci.edu
http://www.faculty.uci.edu/profile.cfm?faculty_id=5705
Relationship: PhD Advisor

Dr. Bogi Andersen, MD, PhD Committee Member
Professor
Department of Biological Chemistry
School of Medicine
University of California Irvine
Phone: (949) 824-9093
email: bogi@uci.edu
http://www.faculty.uci.edu/profile.cfm?faculty_id=4704
Relationship: PhD Committee Member

Dr. Sohail Jahid, Ph.D., Colleague
Post-Doctoral Scholar
Department of Dermatology
School of Medicine
University of California Irvine
Phone: (949) 824-0547
email: sjahid@uci.edu
Relationship: Colleague in Ganesan Lab

Dr. Amelia Hopkin, Ph.D., Colleague
Scientist, Biological Sciences-Dermatology
Allergan (Irvine, CA)
Phone: (949) 291-9146
email: hopkin_amy@allergan.com
Relationship: Former Colleague in Ganesan Lab

ABSTRACT OF THE DISSERTATION

Retinoids Modulate *MITF*: A Novel Mechanism in the Regulation of Melanogenesis

By

Elyse Kathleen Paterson

Doctor of Philosophy in Biomedical Sciences

University of California, Irvine, 2015

Associate Professor Dr. Anand Ganesan, Chair

Melanogenesis, the process by which specialized cells within the epidermis synthesize melanin, is an intricate and complicated process that requires the coordinated action of transcriptional, translational and trafficking processes. Melanin, a complex polymer derived from the amino acid tyrosine, is the primary determinant of hair, skin and eye color in humans. It plays a monumental role in the protection of the eyes and skin from solar ultraviolet-radiation through direct absorption mechanisms. Melanin is aberrantly regulated in melasma and vitiligo, two pigmentary disorders that are characterized by areas of skin that are hyper-pigmented and hypo-pigmented, respectively. Although a variety of treatment options exist for these disorders, many of the treatments are not very effective and have significant side effects. Tyrosinase inhibitors are used to treat melasma, and tyrosinase (TYR) is an enzyme that catalyzes the rate-limiting step in melanin synthesis. In this work, we investigate the role of TYR in regulating pigment production *in vivo* and examine the suitability of TYR as a therapeutic target for hyperpigmentary disorders. We demonstrate that the partial depletion of *Tyr* in the mouse was not sufficient to induce significant decreases in melanin accumulation in the mouse hair follicle,

suggesting that TYR may not be an ideal target for the treatment of hyperpigmentary disorders. To address the need for novel, effective treatments for pigmentary disorders, a genome-wide siRNA functional genomics approach was employed to identify pharmaceutically tractable, single gene loci that impact melanogenesis. The screen uncovered 92 novel regulators of melanogenesis, including Aldehyde dehydrogenase 1A1 (ALDH1A1), which was one of only three genes able to impact TYR expression in three distinct genetic backgrounds. We discovered that a potent catalytic inhibitor of ALDH1A1, cyanamide, was able to inhibit not only the accumulation of pigment, *TYR* and *MITF* mRNAs in melanoma cells, but also melanin synthesis in three-dimensional human skin equivalents, suggesting that inhibitors of this enzyme may be ideal to therapeutically treat hyperpigmentation disorders, including melasma. In this work, we have identified how ALDH1A1 regulates melanogenesis. We show that 9-*cis* retinoic acid, a molecule important in cellular differentiation and the product of ALDH1A1 catalysis in vitamin A metabolism, stimulates the accumulation of pigment, *TYR* and *MITF* mRNAs, and TYR protein in melanoma cells and primary human epidermal melanocytes. As the biological effects of 9-*cis* retinoic acid are mediated by two classes of nuclear receptors, the retinoic acid receptors (RARs) and the retinoid X receptors (RXRs), we searched for and identified a putative RAR/RXR binding site within the promoter of *MITF-A*, an isoform of MITF not known previously to play a role in melanin synthesis. While rigorous chromatin immunoprecipitation (ChIP) studies demonstrated significant enrichment of both RARα and RXRα upstream of the transcription start site of *MITF-A*, no enrichment was found in the promoter region of *MITF-M*, suggesting a novel mechanism in the regulation of melanogenesis. We then went on to show, through *luciferase*-activity assays, that retinoids can activate the full-length *MITF-A* promoter, but not a truncated *MITF-A* promoter that lacks the putative RAR/RXR heterodimer binding site.

Lastly, we demonstrate that when used in combination, RARα and RXRα agonists stimulate the accumulation of *MITF-A* and *MITF-M* transcripts. Taken together, our data outline a mechanism for how ALDH1A1 regulates melanogenesis. We provide key evidence that targeting this enzyme may be appropriate in the development of novel therapeutics for the treatment of melasma. Finally, we show that retinoids or retinoid-analogs may be ideal in targeting hypopigmentary disorders, including vitiligo.

Introduction to: Melanocytes, Melanin Biosynthesis and Regulation, Clinical Disorders of Melanogenesis and the Identification of Novel Genes that Regulate Melanogenesis

Chapter 1

Elyse K. Paterson and Anand K. Ganesan

1.1 Abstract

Melanogenesis, the process by which melanocytes in the epidermis synthesize melanin, is a complex and highly regulated process that requires the intricate interplay of many genes. Extensive research has elucidated many factors involved in melanogenesis, yet how these factors interact with each other and are regulated is still under investigation. Melasma and vitiligo are two pigmentary disorders that are characterized by areas of skin that are hyper-pigmented and hypo-pigmented, respectively. Although a variety of different treatment options exist to treat each disorder, there is no effective treatment option that ensures non-toxic, long-term normal pigmentation in areas of affected skin. In order to address this need, a genome-wide siRNA screen was performed to identify novel regulators of melanogensis that could act as pharmaceutical targets to either stimulate or inhibit pigment accumulation. The screen identified 92 novel regulators of melanogenesis, including aldehyde dehydrogenase 1A1 (ALDH1A1), an enzyme that has pleiotropic roles in detoxification. Intriguingly, experiments demonstrated that siRNA-mediated knockdown of ALDH1A1 lead to the depletion of *TYR* and *MITF* mRNA and protein levels in three pigment-producing cell types. Furthermore, a potent catalytic inhibitor of ALDH1A1, cyanamide, was able to significantly inhibit pigment accumulation in melanoma cells. Taken together, these studies suggest that ALDH1A1 may be an ideal pharmaceutical target to treat hyper-pigmentary disorders, such as melasma.

1.2 Skin Structure and Biology

As the body's physical barrier against mechanical, chemical and microbial factors, the skin plays an incredibly important role in maintaining homeostasis [1]. The skin also provides a unique defense mechanism against the harsh impact of UV radiation through the pigments made by specialized skin cells, melanocytes [1]. There are three individual layers that comprise the skin: the epidermis, the dermis and the hypodermis [1]. The epidermis is the topmost layer of the skin [1]. Comprised mainly of melanocytes and keratinocytes, it is a stratified epithelium tissue devoid of blood or nerve supplies and ~5-100 μM in thickness [1, 2]. The epidermis is arranged in four distinct layers, with keratinocytes constituting 95% of its total composition [1]. From the bottom layer to the top layer, the layers are: the stratum basale, the stratum spinosum, the stratum granulosum and the stratum corneum, respectively [3]. The bottom-most layer, the stratum basale, consists mainly of a single layer of cells that separates the epidermis from the dermis [1]. This single layer of cells attaches to a basement membrane and includes basal keratinocytes (which have stem-like properties) and neural-crest derived melanocytes [1]. The layer immediately above the straum basale is the stratum spinosum, which contains both keratinocytes and Langerhans' cells, antigen-presenting skin cells [1]. Here, keratinocytes are polyhedral in shape and have a decreased capacity for cell division [1]. As keratinocytes divide, the keratinocytes in the stratum spinosum flatten and are pushed toward the surface of the skin [1]. The next layer, the stratum granulosum, is comprised of keratinocytes that no longer divide and are flattened and polyhedral in shape [1]. In the topmost layer of the epidermis, the stratum corneum, keratinocytes are cornified and lack cytoplasmic organelles but contain large amounts of keratin [1, 4, 5]. Known as corneocytes, these cells are the physical and chemical barrier

against the outside environment that function not only to prevent infection, but also to reduce trans-epidermal water loss [1, 4, 5]. The epidermis is able to undergo continuous self-renewal as it harbors stem and transit-amplifying cells in the basal layer [6]. As the transit-amplifying cells leave the basement membrane, they undergo terminal differentiation and move upwards to the topmost layer of the epidermis [6]. This differentiation ends in the cornified layer with anucleate cells that are continuously sloughed off and replaced with cells migrating upwards from the lower layers of the epidermis [6].

The dermis is directly beneath the epidermis [1]. It is 2 to 4 mm-thick and is comprised of connective tissue and fibroblasts, which are required for the creation and degradation of the extracellular matrix [1, 3]. The dermis also contains excretory and secretory glands, including those of sebaceous, eccrine and apocrine nature [1]. Triglycerides and cholesterol-rich sebum secreted by the sebaceous glands not only lubricate the skin, but also keep it waterproof [1, 3]. Hair follicles and nails are also found in the dermis [1]. Hair follicles serve the unique function of providing a specialized, protective compartment for several stem cell populations in the skin, including keratinocyte stem cells, melanocyte stem cells, and the dermal stem cells [1]. Directly below the dermis is the hypodermis, a layer of loose connective tissue that functions to bind skin to internal organs [1, 7]. It is comprised of subcutaneous fat that provides cushioning, thermoregulation, and skin stability [1, 7].

1.3 Melanocyte Biology

1.3.1 The Epidermal Melanin Unit

Melanins are a group of pigments that are synthesized in specialized cells, melanocytes [1]. They act to photoprotect keratinocytes from UV radiation (UV-R) [1]. The anatomical relationship between keratinocytes and melanocytes is referred to as the "epidermal melanin unit" [1]. Melanin biosynthesis takes place in membrane-bound organelles known as melanosomes that mature through four unique stages [1]. The containment of melanin synthesis to the melanosome is significant because melanin intermediary species are toxic to the cell [8]. The final stage melanosome (stage IV) is transferred through melanocyte dendrites to neighboring keratinocytes [1]. Melanosome transport occurs on microtubules that are parallel to the long axis of the dendrite [9, 10]. Microtubule-associated motor proteins, including kinesins [9] and cytoplasmic dyneins, [10] control the movement of melanosomes along the microtubules. It is estimated that each melanocyte within the epidermis comes into contact with about 40 keratinocytes in the basal and supra-basal layers [11].

Melanin plays a monumental photo-protective role in human skin. In the keratinocyte, melanin accumulates above the nuclei where it absorbs and scatters damaging UV-radiation [12]. When melanin is properly distributed, dividing keratinocytes are protected in part from mutations that would otherwise be caused by UV-radiation [12]. Melanin accomplishes this task by absorbing, scattering, photo-oxidizing and scavenging free radicals that result from UV-R [13]. Moreover, melanin acts to minimize toxic repercussions of reactive oxygen species (ROS) and prevents damage to cellular DNA, proteins and cell membrane lipids [13].

1.3.2 Melanocyte Development

Melanocytes are derived from neural-crest cells (NCCs), pluripotent cells that develop from the dorsal-most point of the neural tube between the surface ectoderm and the neural plate [14, 15]. In addition to melanocytes, NCCs have the ability to differentiate to become neurons, glial cells, adrenal medulla, cardiac cells or craniofacial tissue [14]. NCCs that differentiate into melanoblasts, the precursor cells of melanocytes, immediately up-regulate the expression of key melanogenic genes, beginning with micropthalmia-associated transcription factor isoform M (*MITF-M)* [14-19]. Interestingly, the appearance and survival of melanoblasts that express *MITF-M* mRNA is independent of a functional MITF-M protein for approximately 48 hours; however, once expression is established, the continued expression of MITF-M is necessary for melanoblasts to survive [18, 20]. MITF-M deficiency leads to the complete absence of melanocytes in the epidermis, suggesting that MITF-M is absolutely necessary for either melanocyte lineage survival, for proliferation or to inhibit differentiation of NCCs to other neural-crest lineages [14]. Intriguingly, the expression of *MITF-M* needs to be driven above a threshold level in order for NCCs to commit to differentiate to melanoblasts [20]. This is accomplished by the coordinated effort of the transcription factors PAX3, CREB, SOX10 and LEF1 [20]. Each aforementioned transcription factor confers the ability of *MITF-M* expression to respond to specific environmental cues in the commitment and differentiation process [20].

Once differentiated, melanoblasts begin their migration to the skin by invading the dorsolateral pathway, between the somite and ectoderm [21, 22]. Melanoblasts populate various cutaneous structures, but the final destination differs between mice and humans. In humans, where hair follicles are relatively sparse, melanoblasts locate to the epidermis and form an

epidermal unit with neighboring keratinocyte cells [23]. Unlike humans, the majority of the mouse body is covered in hair. Thus, melanoblasts colonize the ectoderm and developing hair follicles prior to birth [15]. Any melanoblasts that are not located to the hair bulge or to the hair matrix disappear by P4 [24]. The differentiation of melanoblasts into melanocytes occurs concomitantly with the expression of *TYROSINASE (TYR)* and melanin production [25-28].

1.4 Melanogenesis

1.4.1 The Impact of UV-radiation on Pigmentation in Human Skin

Ultraviolet radiation (UV-R) lies between the visible and X-ray regions in the electromagnetic spectrum [29]. While the majority of the total radiant energy that reaches the earth's surface from the sun is divided between the visible (40%) and the infrared (50%), only 5-10% is ultraviolet [29]. UV-R is divided into three categories based on the specific wavelength of the energy: UV-A (320-400 nm), UV-B (280-320 nm), and UV-C (200-280 nm) [29]. While UV-C never reaches the earth's surface because it is absorbed by the ozone layer, UV-A and UV-B are able to penetrate [29]. However, the earth's surface receives much less UV-B than UV-A because UV-B is scattered and absorbed by oxygen, ozone and water molecules in the atmosphere [30]. In contrast to UV-B, UV-A is able to penetrate deeply into the dermis of human skin, and thus reach the depth of melanocytes [1]. While only ~9-14% of UV-B reaches melanocytes, anywhere from ~19-50% of solar UV-A reaches them; be that as it may, tans stimulated by UV-A are much more transient and less likely to protect against additional UV-induced insult than tans produced by exposure to UV-B [30]. Ultimately, it is UV-B that is

responsible for the sunburn reaction and for promoting skin cancer, especially if an individual sustains repeated and prolonged sun exposure [1]. However, UV-B does elicit the benefit of promoting vitamin D synthesis within the epidermis; this reaction only occurs with wavelengths of 290-310 nm in the UV-B range [30]. When UV-R infiltrates the skin and is absorbed by 7-dehydrocholesterol (7-DHC), the pre-vitamin D_3 is formed [30]. The vitamin D pathway is involved in many biological processes within the human body, including bone metabolism, the innate immune response, cell proliferation, and cell differentiation [31, 32].

1.4.2 Signaling Pathways and Cellular Mechanisms that Regulate Melanogenesis

While many factors influence melanocytes and pigment production, both are largely impacted by paracrine signals from neighboring keratinocytes and to a lesser degree, dermal fibroblasts [33]. However, autocrine signals from melanocytes themselves and environmental factors, mostly UV-R, also play a role [1]. Intriguingly, UV-R triggers the increased expression of keratinocyte-derived factors that are known to stimulate melanogenesis, while simultaneously suppressing factors that inhibit the pigment production process [1]. It is also known that UV-R can directly influence melanocytes by triggering the formation of additional dendritic processes as well as pigment production [34, 35]. Human skin undergoes a tanning response after exposure to UV-R, which is marked by increased pigmentation above the baseline level for each individual [36]. In addition to stimulating a tanning response, UV-R also affects both the survival and proliferation of melanocytes [1].

Cellular DNA directly absorbs UV-B radiation upon exposure, which causes the formation of DNA photoproducts, including thymine dimers and pyrimidine (6-4) pyrimidine

[36, 37]. There is a plethora of evidence that demonstrates that UV-induced DNA damage is the cause of the tanning response. First, the UV spectrum that causes tanning is the same for the formation of DNA photoproducts [37, 38]. Second, melanocytes treated with an agent that exclusively damages DNA were simultaneously stimulated to produce pigment [39]. Third, the tumor suppressor protein p53, which is activated by DNA damage, stimulates the increased expression of *TYR* mRNA and TYR protein, thus augmenting pigment production [40-43]. Studies in mouse keratinocytes demonstrated that post UV-R, p53 binds to a consensus sequence in the proopiomelanocortin (POMC) promoter, thus increasing the expression of the POMC-derived α-melanocyte stimulating hormone (α-MSH), a known key inducer of melanogenesis [44]. Moreover, the systemic administration of α-MSH, β-MSH or adrenocorticotropic hormone (ACTH), an analog of α-MSH also derived from the POMC gene, induces skin pigmentation in areas that are exposed to sun [45, 46].

The biological effects of α-MSH are mediated by the melanocortin-1 receptor (MC1R), a G-protein-coupled receptor specifically expressed in melanocytes [44, 47] with seven transmembrane domains [48, 49]. Binding of α-MSH to MC1R allows for G-protein dependent activation of adenylate cyclate, which in turn leads to increased levels of cyclic adenosine monopshophate (cAMP) [49]. cAMP-dependent protein kinase (PKA) is activated by cAMP, which phosphorylates the cAMP-responsive element binding protein (CREB) [49, 50]. Upon activation via phosphorylation, CREB binds to the *MITF-M* promoter and stimulates transcription [51], leading to increased expression of MITF-M, the master transcriptional regulator of melanogenesis [49]. With increased expression of MITF-M, key genes necessary for melanogenesis, including TYR, tyrosinase-related proteins 1 and 2 (TYRP-1 and TYRP-2) are also up regulated [52].

Despite the fact that the ubiquitous cAMP-CREB pathway regulates MITF-M, its expression is cell-type specific (only occurring in melanocytes) [1]. The reason for this is that CREB cooperatively binds to the MITF-M promoter in the presence of SOX10, the expression of which is limited to cells derived from neural-crest [53]. Interestingly, α-MSH can stimulate pigment production in melanocytes via a mechanism that is uniquely separate from MC1R [1]; it can bind to 6(R)-L-erythro-5,6,7,8-tetrahydrobiopterin (6BH4), an enzyme known to inhibit the catalytic activity of TYR [54, 55]. By binding to 6BH4, α-MSH destroys the inhibitory-properties of this molecule on TYR.

The aforementioned α-MSH mechanism promotes the synthesis of brown and black melanins, also known as eumelanins [49]. Interestingly, pheomelanin, or yellow/red melanins, can also be up regulated while simultaneously inhibiting the production of eumelanins through MC1R [56, 57]. Agouti signaling protein (ASP), a protein expressed in both mice and humans, has been shown to compete with α-MSH for binding to MC1R, thus preventing the activation of adenylate cyclase [56-58]. Through this mechanism, ASP inhibits the synthesis of eumelanins and drives the production of pheomelanins. Intriguingly, over-expression of ASP in mice leads to a yellow coat color phenotype [57]. As of yet, the role of ASP in humans is still poorly understood [1].

The POMC/MC1R/cAMP pathway is thought of as the key pathway that regulates melanogenesis, yet POMC-deficient mice ($POMC^{-/-}$) demonstrate normal black coat color [59]. Histological analyses of these mice demonstrated normal hair follicle structure with normal eumelanin pigmentation [59], suggesting either that MC1R has a baseline activity sufficient for normal pigmentation or that a different mechanism is able to induce pigment production in the mouse hair follicle of $POMC^{-/-}$ mice. It was later shown that melanocytes express both β_2 and α_1

adrenoreceptors (β_2-AR and α_1-AR, respectively) that can each stimulate melanogenesis through unique mechanisms [60, 61]. Epinephrine produced by keratinocytes can bind to β_2-AR on the melanocyte cell surface and increase intracellular levels of cAMP, leading to increased melanin production [60]. On the other hand, α_1-AR interacts with norepinephrine released by melanocytes, thus increasing the level of diacylglycerol and activating melanogenesis via the PCK- β pathway [60, 62].

Another pathway critical to melanogenesis is the stem-cell factor (SCF) and c-Kit mechanism [1]. SCF, which is secreted by keratinocytes after exposure to UV-R, binds to the c-Kit tyrosine kinase receptor on the cell surface of melanocytes [63]. Upon SCF binding, c-Kit autophosphorylates itself and activates mitogen activated protein kinase (MAPK) [63]. MAPKs then phosphorylate and activate MITF-M, which in turn up-regulates *TYR*, *TYRP-1* and *TYRP-2* transcription [63]. SCF is an important melanocyte survival factor [52] and can also act synergistically with specific interleukins and granulocyte-macrophage-colony stimulating factor to augment UV-induced pigment production [63, 64].

Another important modulator of melanogenesis is endothelin-1 (ET-1), a 21 amino acid peptide secreted by keratinocytes in response to UV-R [65-67]. ET-1 has been shown to increase the expression of MC1R as well as to strengthen the affinity of MC1R for α-MSH [68]. Furthermore, ET-1 activates TYR and increases expression of *TYRP-1* [65, 69], as well as stimulates melanocyte proliferation [65, 69] and the formation of additional dendritic processes [66].

Lastly, nitric oxide (NO) plays a role in stimulating pigment production in melanocytes. This diverse molecule has different effects depending on the cell/tissue type [70] and is produced by both melanocytes and keratinocytes in situations where inflammatory cytokines are abundant

[71-74]. Moreover, keratinocytes produce NO upon exposure to UV-R [75]. NO enacts its biological effects through specific secondary messengers, including cyclic guanine monophosphate (cGMP) and cGMP-dependent protein kinase, to boost TYR activity and pigment production in melanocytes [75].

1.4.3 Key Enzymes that Orchestrate Melanin Biosynthesis

TYR (monophenol, 3,4-β-dihydroxyphenylalanine oxygen oxidoreductase, EC 1.14.18.1) is a glycoprotein comprised of 529 amino acids found in the membrane of the melanosome [76, 77]. It has both an inner catalytic domain that locates to inside of the melanosome (90% of the protein) as well as a short transmembrane domain and cytoplasmic domain [76-78]. Within the catalytic domain, histidine residues bind copper ions that are required for its activity [76, 77]. TYR is regarded as one of the most important enzymes in the melanin biosynthesis pathway as it catalyzes the initial rate-limiting step, the hydroxylation of tyrosine to β-3,4-dihydroxyphenylalanine (DOPA) [76, 77]. It subsequently oxidizes DOPA to DOPAquninone. Numerous proteins regulate TYR, including PKC- β, tyrosine hydroxylase isoenzyme (THI), and phenylalanine hydroxylase [36, 79, 80]. UV-R, along with ligand-mediated activation of α_1-AR and ET-1, releases diacyl-glycerol (DAG) from the plasma membrane [80]. DAG activates PKC- β, allowing it to bind the receptor for activated C-Kinase-I (RACK-1; the receptor specific for activated PCK- β); subsequently, PKC- β translocates to the melanosome [80-82]. Once in the melanosome, PKC- β phosphorylates serine residues on TYR [80, 82], which allows it to complex with TYRP-1 [83], thus stabilizing and increasing the enzymatic activity of both proteins [84].

Like TYR, both of the tyrosinase-related proteins 1 and 2 (TYRP-1 and TYRP-2) span the melanosomal membrane, and are ~40% homologous in their amino acid sequence to TYR [85, 86]. It has been hypothesized that the genes encoding for TYR, TYRP-1 and TYRP-2 diverged from a single common ancestral gene [87], with the original gene encoding only TYR [88]. Then, two duplication/divergence events occurred to give rise to the separate proteins TYRP-1 and TYRP-2 [88]. Both TYRP-1 and TYRP-2 contain an NH_2-terminal signal sequence, EGF-like domains, two histidine-rich metal binding domains, and a COOH-terminal transmembrane segment with a short cytoplasmic tail [52]; the COOH terminus and the transmembrane segment are necessary for targeting both proteins to the melanosome [52].

TYRP-1 is an abundant 75 kDa glycoprotein produced only in melanocytes [85]. Sequence homology between TYRP-1 and TYR is most highly conserved in the copper-binding domain, the cysteine and tryptophan residues, the transmembrane domain, the signal sequences used for trafficking to the melanosome, and the glycosylation sites [85, 86]. In the mouse, mutations in *Tyrp-1* lead to a brown coat color phenotype [87, 89]; furthermore, *TYRP-1* is also mutated in the OCA3 subtype of human albinism, and individuals present reduced pigmentation in the hair, skin and eyes [90]. Intriguingly, while TYRP-1 acts as a DHICA oxidase that generates indole-5,6-quinone-carboxylic acid in the mouse [91, 92], evidence suggests that it does not share this function in humans, where it instead acts as a tyrosine hydroxylase [85]. TYRP-1 is important in eumelanogenesis and not needed in pheomelanogenesis, because in cells depleted of TYRP-1 or in cells that have TYRP-1 with defective activity, eumelanogenesis is down regulated and pheomelanogenesis is up regulated [93]. Additionally, TYRP-1 may function to stabilize TYR activity and maintain melanosomal structural integrity [94, 95]. The function of TYRP-2 (dopachrome tautomerase) is well characterized: it catalyzes the reaction of

dopachrome to DHICA in the eumelanin synthesis pathway [96-98]. Like TYRP-1, TYRP-2 is able to stabilize TYR activity, and it has been shown to play a role in melanocyte survival [94].

MITF-M is the master regulator of melanocyte development, function and survival [50]. A basic helix-loop-helix leucine zipper dimeric transcription factor [50], MITF-M is known to bind to the canonical E-box promoter sequence CACGTG and the non-palindromic seqeuence CACATG as a dimer [99-101]. The human *MITF-M* gene is comprised of nine unique promoter elements in which each promoter directs the transcription of a specific isoform of MITF [50, 102]. While the first exon of each MITF isoform is different, exons 2-9 are shared [102]. The promoter most proximal to the common downstream exons is the MITF-M promoter, which drives expression of the M isoform [50]. MITF-M is not only the smallest isoform, but also is exclusively expressed in melanocytes [50, 103]. Interestingly, the melanocyte-specific exon 1 of MITF-M only adds a few additional amino acids that have not been shown to alter the function of MITF dramatically [50]. The *MITF-M* promoter is regulated by multiple transcription factors, including paired box gene 3 (PAX3), cAMP-responsive element binding protein (CREB), SRY (sex-determining region Y)-box 10 (SOX10), lymphoid enhancer-binding factor 1 (LEF1, or TCF), one cut domain 2 (ONECUT-2) and MITF-M itself [50, 104-106]. In addition to extensive transcriptional regulation, MITF-M can be modified post-translationally as well. In particular, mitogen-activated protein kinase (MAPK), ribosomal S6 kinase (RSK), glycogen synthase kinase-3β (GSK3 β) and p38 are all known to phosphorylate MITF-M [107-110]. Although it is unclear exactly how each post-translational modifier is activated to phosphorylate MITF-M, it is generally hypothesized that environmental cues play a large role.

1.4.4 Types of Melanin

Melanocytes synthesize two unique forms of melanin: the black-brown eumelanins and the yellow-reddish pheomelanins [111]. While the absence of both melanins is associated with a white-hair phenotype, the prevalence of eumelanin is linked to black-brown hair and predominant pheomelanin composition is coupled to red or yellow hair [8]. Both melanins contain a prevailing arrangement of repeating units linked by carbon-carbon bonds [1, 111]. However, pheomelanins are characterized by sulfur-containing benzothiazine derivatives [112] while eumelanins consist of DHI (5,6-dihydroxyindole) and DHICA (5,6-dihydroxyindole-2-carboxylic acid) units in reduced or oxidized states [112].

1.4.5 The Melanosome Matures through Four Distinct Stages

Melanosomes are membrane-bound ellipsoidal organelles that mature through four morphological stages in the melanocyte [1]. The maturation stages are distinguished by their structure and the quantity, quality and arrangement of melanin within [1, 113-115]. Pre-melanosomes are produced near the Golgi apparatus in the perinuclear region [113]. A stage I melanosome lacks internal structural components and TYR, the key enzyme involved in melanin biosynthesis [113-115]. It is spherical in shape as opposed to the ellipsoidal fully mature stage IV melanosome [113-115]. In the transition of a stage I melanosome to a stage II melanosome, two main events occur. First, TYR protein is trafficked from the Golgi apparatus to the melanosome and melanin synthesis begins with minimal deposition of melanin [113-116]. Second, PMEL17, a protein involved in the structural organization of the melanosome, is

deposited [113, 114]. PMEL17 allows for the transformation of the stage I melanosome to the characteristically elongated, fibrillar stage II melanosome [113-116]. A stage III melanosome is characterized by increased melanin synthesis and the uniform deposition of melanin onto the PMEL17 fibrils [113-116]. When analyzed by electron microscopy (EM), a proper stage III melanosome is distinguished by long dark striations that stretch longitudinally across the melanosome [113, 114]. The final end-stage melanosome is either ellipsoidal or elliptical in shape and has minimal TYR activity with complete melanization [115, 116]. Eu-melanosomes and pheo-melanosomes are highly similar in maturational stages yet differ in shape: while the eu-melanosome is ellipsoidal in the final stage, the pheo-melanosome remains rounded throughout all stages [1, 115, 116].

As the main component of the protenacious internal fibrils of stage I and II melanosomes, PMEL is both necessary and sufficient for premelanosome fibril formation and proper melanosome shape [117]. Expression of PMEL alone in non-pigmented cell lines leads to the formation of fibrils that are morphologically similar to those seen in melanocytes [118, 119]. Furthermore, melanosomes from *silver* mutant mice, where total PMEL protein levels are depleted owing to a truncation mutation in the cytoplasmic domain, are enlarged and rounded due to the lack of fibrillar structure within [120]. PMEL is synthesized in melanocytes yet needs to be properly trafficked to premelanosomes [117]; it has been shown that some PMEL is routed through the plasma membrane [120]. A cytoplasmic di-leucine tail on PMEL facilitates PMEL accumulation in endosomes and in turn assists with efficient downstream sorting and fibril formation [117, 120]. As the *silver* mutant mice do not have the aforementioned di-leucine motif on PMEL protein, it aggregates on the cell surface and fails to traffic to the early-stage melanosome [120].

1.4.6 Mature Melanosome Formation requires Intricate Trafficking Processes within the Cell

An endosome is a membrane-bound compartment with the cell [117]. Early stage endosomes form major sorting stations within cells from which proteins are routed to many different locations, including the plasma membrane, the *trans*-Golgi network, and both limiting and intralumenal membranes of late endosomes and lysosomes [117, 121]. Due to the complexity of protein sorting events, endosomal trafficking is regulated by tightly-controlled molecular machinery [117]. In certain cell types, parts of the endosomal trafficking machinery are used to route specific proteins to specialized lysosome-related organelles (LROs) [117]. LROs are a class of tissue-specific intracellular organelles that share characteristics with lysosomes, including an acidic pH and lysosomal membrane protein and enzyme content [117]. Melanosomes were initially considered to be modified lysosomes [122], yet research has indicated that they instead coexist with separate lysosomes, a feature that they share with other LROs [117]. In order to synthesize LROs, host cells must separate and sort macromolecule components of lysosomes from LROs [117]; this was upheld by experiments that showed that melanosomal proteins congregate near late stage endosomes in non-pigmented cell types when they are expressed ectopically [118, 123, 124].

Hermansky-Pudlak syndrome (HPS) is a disease caused by malformation or malfunction of LROs, including melanosomes, platelet dense granules, lung lamellar bodies, and/or cytotoxic T-cell granules [125]. HPS affects multiple organ systems in the body and results in partial albinism, excessive bleeding, lung fibrosis, immunodeficiency, and granulomatous colitis [125]. While the 8 observed genes responsible for HPS are expressed in many cell types, they are essential only for LROs present in affected cell types [125]. Some of the mutated genes in HPS

encode for subunits of multi-subunit protein complexes, including AP-3 and biogenesis of lysosome-related organelles complex-1, 2 and 3 (BLOC-1, BLOC-2, and BLOC-3) [117].

AP-3 mutations have been characterized in individuals with HPS type 2 and *pearl* and *mocha* mutant mice [126]. It forms one part of the heterotetrameric adaptor complex that acts to link transmembrane cargo, through cytoplasmic sorting signals, to coated bud-formation on post-Golgi membranes [127]. AP-3 most likely acts in the trafficking of TYR from endosomes [117]. This is demonstrated by a three key findings. First, the di-leucine based sorting motif [128, 129] on the cytoplasmic domain of TYR binds to AP-3 *in vitro* and is necessary for sorting to lysosomes or neurosecretory granules in other cell types [130-132]. Secondly, in melanocytes from HPS-2 patients and *pearl* mice, TYR is misrouted to endosomes [128, 133]. Thirdly, AP-3 coats are found on buds on early endosomal tubules that also contain TYR [128, 134]. Intriguingly, in cells that are depleted of AP-3, the misrouted TYR builds up in early endosomes and in intralumenal vesicles of multi-vesicular bodies (MVBs) [128], providing evidence that AP-3 may specifically function to steer TYR away from the MVB pathway.

Although TYR protein is misrouted to endosomes (instead of melanosomes) and pigmentation is decreased in *pearl* mice and HPS-2 individuals, melanocytes from both contain pigmented, mature melanosomes with active TYR; interestingly, these melanosomes are indistinguishable from melanosomes observed in control, wild-type melanocytes [128, 133, 135]. Thus, a second pathway must exist that delivers TYR to the melanosome that is independent of AP-3. *In vitro* studies showed that the di-leucine motif on TYR is also able to bind to AP-1 [128], a second heterotetrameric adaptor complex. Moreover, in AP-3 deficient melanocytes, the amount of TYR protein in AP-1-coated endosomal buds increases [128]. Apart from delivering TYR to melanosomes, AP-1 has been shown to play additional roles in the melanocyte as well:

in vitro data demonstrates that TYRP1 is able to interact with AP-1 (but not AP-3) through its di-leucine sorting motif [124, 128]. Moreover, TYRP-1 co-localizes extensively with AP-1 in melanocytes [121]. Thus, data suggests that AP-1 probably interacts with both TYR and TYRP-1 and acts to deliver these melanogenic enzymes to the maturing melanosome.

Cargo that is sorted by AP-3 is meant for lysosomes and late endosomes; yet in melanocytes, TYR and TYRP-1 are destined for melanosomes, which requires additional proteins for sorting, including BLOCs [117]. BLOC-1 is 250-kDa protein complex comprised of eight subunits, 2 of which are mutated in human HPS [136]. BLOC-1 mutant melanocytes demonstrate complete mis-localization of TYRP-1, but only partial mis-localization of TYR [137]. Due to the fact that TYRP-1 sorting is affected differently in AP-3 and BLOC-1 mutants, AP-3 and BLOC-1 must participate in two distinct trafficking pathways from early endosomes [117]. Furthermore, because TYR and TYRP-1 are differentially affected by AP-3 and BLOC-1 depletion, the routing steps for each enzyme probably occur sequentially in space and time from distinct early endosomal domains [117].

1.5 Pigment Variation in Humans

1.5.1 Genes that contribute to human hair, skin and eye color

Human pigmentation in hair, skin and eyes is a polygenic trait that is determined by a quasi-Mendelian inheritance pattern; a few important genes have dramatic effects, while many modifier genes contribute to a lesser extent [138]. One of the most well-studied genes involved in pigment variation in humans is *MC1R* [138]. The importance of this gene was revealed by

numerous studies that showed that variation in *MC1R* contributes to a red-hair and fair-skin phenotype [138]. Intriguingly, two independent research studies that sequenced the *MC1R* gene in human samples from several continents found a lack of polymorphisms in sub-Saharan African as well as other dark-skinned populations, including Papuans and South-Asians [139, 140]. This lack of diversity in polymorphisms for *MC1R* in darker-skinned populations is explained by natural selection to remove *MC1R* mutations that may promote pheomelanin synthesis over eumelanin synthesis in regions of high UV-R [141]. On the other hand, populations in Europe, East Asia and Southeast Asia demonstrate high levels of polymorphisms in *MC1R* [138]; more than 30 alleles for *MC1R* have been documented in European populations, with more than 20 nonsynonymous variants [142]. Interestingly, there are at least 9 nonsynonymous variants of *MC1R* that occur at a frequency of 1% or greater in European populations [138], with 4 of these variants being strongly associated with the red-hair and fair-skin phenotype (Asp84Glu, Arg151Cys, Arg160Trp and Asp294His) and 3 only being weakly associated (Val60Leu, Val92Met, and Arg163Gln) [143]. Studies performed *in vitro* demonstrated that some of these variants have a reduced capacity to bind α-MSH (Val92Met) or to activate adenylyl cyclase (Arg151Cys, Arg160Trp and Asp294His) [144-146]. Such findings provide logical evidence as to why individuals with these variants in *MC1R* have hair and skin rich in pheomelanin. Significantly, individuals with these functional variants of *MC1R* sunburn easily and are at a greater risk for melanoma and non-melanoma skin cancers [147]; correlating with this, studies in melanocytes with the aforementioned functional variants of *MC1R* demonstrate decreased eumelanin synthesis and increased cytotoxicity in response to UV-R [148].

A second gene that has been shown to play a significant role in pigment variation in humans is agouti-signaling protein (ASIP*)*, which is an endogenous antagonist of MC1R [138]. Upon binding, ASIP promotes the synthesis of pheomelanin over eumelanin [138]. A recently identified SNP in the 3'-untranslated region of *ASIP* (8818A→G) correlates with dark hair, brown eyes and dark skin [149, 150]. Related studies demonstrated that the *ASIP* mRNA level is over twelve times less in melanocyte cell lines that contain the G allele (AG heterozygotes or GG homozygotes) when compared to melanocyte cell lines that contain the homozygous AA genotype [151]. Thus, decreased levels of ASIP equates to less antagonist binding to MC1R, and more activation of α-MSH and subsequent eumelanin synthesis [138].

The "golden gene", *SLC24A5*, is largely responsible for the evolution of light-skin European populations [138, 152]. The role of this gene in the evolution of human skin pigmentation was discovered by chance; researchers working with zebrafish identified a mutant (the "golden" mutant) that resulted in delayed and reduced pigmentation when compared to wild-type zebrafish [152]. A premature stop codon that that truncates SLC24A5 was determined to be responsible for the golden mutant phenotype [152]. Intriguingly, when human mRNA was injected into *golden* mutant zebrafish embryos, melanin pigmentation was rescued [152]. The golden gene encodes for a potassium-dependent sodium-calcium exchanger protein that is critical for melanogenesis [152]. Intriguingly, the HapMap database demonstrated several SNPs in the human *SLC24A5* gene, including a nonysynonymous polypmorphism (rs1426654) that encodes either an alanine or a threonine at position 111 of the protein [152]. HapMap data shows extreme frequency differences in this SNP between European human samples and West African human samples; the ancestral alanine allele occurs at a very high frequency of 93-100% in African and East Asian populations, while the threonine allele occurs at a fixed frequency of

98.7-100% in European populations [152]. Research also showed that rs1426654 is associated with melanin levels as measured by reflectometry in two admixed populations (African Americans and African Caribbeans): individuals with one or two threonine alleles demonstrated lighter skin than individuals homozygous for the ancestral alanine allele [152]. Strikingly, it has been estimated that the SNP in *SLC24A5* is responsible for 25-38% of the differences in skin melanin index between European and African populations [152].

1.5.2 Hypotheses on the Evolution of Skin Pigmentation in Humans

Human skin pigmentation correlates incredibly well with latitude; it tends to be darker in groups of people that populate equatorial and tropical areas of the globe (sub-Saharan Africa, South Asia, and Australia) and lighter in populations that reside farther from the equator [138]. The reason for this phenomenon is UV-R intensity, which is intense at the equator and gradually diminishes with increasing latitudes [138]. Multiple hypotheses have been developed to address the evolution of human skin pigmentation with regard to latitude [138].

One hypothesis that addresses this question theorizes that darker skinned individuals with higher melanin content were selected for at the equatorial latitudes due to their increased protection from sunburn and skin cancer [138]. Melanin is a natural sunblock that protects skin cells from the damaging effects of UV-R [147, 153]. One of the initial effects of UV-R on the skin is a sunburn, which is accompanied by pain, blistering, edema and erythema; often, severe sunburns can damage sweat glands and subsequently disturb thermoregulation processes while exposing the body to infection [138]. Severe sunburns also have the capacity to impair skin cells [147, 153]. Thus, it is hypothesized that dark skin was selected for in tropical environments

close to the equator because its higher eumelanin content is more advantageous than light skin in preventing sunburns [138]. Furthermore, dark skin is much less susceptible to skin cancers when compared to light skin [147]; hence, it has also been hypothesized that dark skin was selected for against white skin in equatorial latitudes for protection against skin cancer [138]. In support of this hypothesis, albino individuals in sub-Saharan Africa often develop pre-malignant lesions or skin cancer in early adulthood; additionally, records indicate that less than 10% of albinos in Nigeria and Tanzania survive beyond the age of thirty [8, 154].

A second important hypothesis on the evolution of human skin pigmentation centers on folate, an essential nutrient that is needed for DNA synthesis and repair [138] as well as spermatogenesis in males [155]. In pregnancy, folate deficiency can lead to neural tube defects, including spina bifida and anencephalus [156, 157]. Folate is very sensitive to UV-R [157]; studies demonstrated that folate levels dropped significantly in human plasma post UV-R exposure, and lighter-skin individuals showed lower folate levels after UV-R when compared to controls [158]. Due to the importance of folate in many biological processes and the fact that it is highly sensitive to UV-R, light-skin was naturally selected against in latitudes near the equator where UV-R levels are high [138].

One of the most highly debated hypotheses regarding the evolution of human skin color across the globe is the vitamin D hypothesis [138]. While it is well known that UV-R is very damaging to skin, it is necessary for the production of vitamin D, a molecule that is vital for bone metabolism, immunoregulation, regulation of cell proliferation and differentiation, prevention of invading pathogens, and in preventing autoimmune diseases [159-161]. The original hypothesis surmised that dark skin was favored near the equator so as to prevent potentially toxic overproduction of vitamin D while light skin was selected for at higher latitudes with lower UV-

R so as to maximize vitamin D production [162]. However, it was recently demonstrated that sun exposure is not able to induce vitamin D toxicity, disproving the original hypothesis [163]. The current theory describes the distribution of human skin pigmentation across the globe as a combination and balance of distinct factors: dark skin was selected for at equatorial latitudes so as to protect against sunburn and skin cancer and to allow for folate synthesis, while light skin was ideal at higher latitudes with lower UV-R to enhance vitamin D production [138]. This theory is supported by the fact that individuals with dark skin require at least ten times more sunlight compared to individuals with light skin in order to make the same amount of vitamin D [160]; thus, dark skin is at a large disadvantage in higher latitudes far from the equator [138].

1.6 Disorders of Pigmentation

1.6.1 Melasma: An acquired Disorder of Hyperpigmentation

Melasma, also known as chloasma or "mask of pregnancy" is a disfiguring disorder of pigmentation that primarily affects women of color during their childbearing years [1, 164, 165]. Melasma appears as a symmetrical hypermelanosis characterized by irregular coloration; the hyperpigmented area can range from light brown to gray to dark brown in color [164]. Although the exact causation of melasma is unknown, it correlates with pregnancy and the use of estrogen-containing oral contraceptives [165-167]. However, multiple other factors can contribute to its development, including UV exposure, hormone therapy, genetic influences, cosmetics, endocrine or hepatic dysfunction, and certain antiepileptic drugs [165, 168].

Intriguingly, studies have demonstrated that hyperpigmented areas characterized by melasma show increased deposition of melanin in both the dermis and the epidermis [169, 170]. However, the same studies showed that there was no increase in the actual number of melanocytes; the melanocytes were larger in size, contained more dendritic processes, and demonstrated increased melanogenesis with higher levels of eumelanin accumulation [169, 170]. Moreover, in lesional skin, there was an increase in the number of melanosomes within keratinocytes, melanocytes and dendrites [170].

The increased levels of estrogen, progesterone and MSH during pregnancy, especially the third trimester, have correlated with melasma [171]. Interestingly, sex hormones have been shown to increase the expression of key melanogenic genes, including TYRP-2 and TYR [172]. Furthermore, when cultured melanocytes are treated with β-estradiol, TYR activity increases [173]. Both these studies demonstrate that sex hormones are likely vital in producing hyperpigmented skin lesions associated with melasma on otherwise healthy skin.

Although a large range of treatments for melasma exist, they are associated with varying degrees of success and efficacy, with no single treatment standing out as preferable [174]. There are three main therapeutic therapies to treat melasma, including topical agents, chemical peels and laser light therapy [174]. To treat moderate to severe melasma, topical de-pigmenting agents are the most effective [174]. While a combination topical therapy is more effective than a monotherapy, triple combination therapy is the most effective at treating melasma (such as hydroquinone, tretinoin and fluocinolone acetonide) [174]. However, 40% of patients will experience erythema and peeling side effects when exposed to a triple combination therapy [174]. On the other hand, chemical peels and laser therapies are associated with an increased risk of skin irritation and future recurrence of hyperpigmentation, especially in individuals of

color [174]. Overall, current treatments for melasma remain unsatisfactory, with the need to identify novel regulators of melanogenesis to serve as innovative targets in decreasing pigment accumulation in hyper-pigmented skin lesion areas.

1.6.2 Vitiligo: A Hypo-melanosis of the Skin and Hair

Vitiligo is the most common pigmentary disorder, affecting between 0.1-2% of the worldwide population, irrespective of age, ethnic skin color or race [175-177]. Vitiligo, a disorder characterized by hypo-pigemented areas of skin, is caused by the loss of functional melanocytes [178, 179]. Vitiliginous skin exhibits one to several amelanotic macules that are chalk-white or milk-white in color and surrounded by either normal or a hyperpigmented border [180]; microscopically, melanocytes are completely absent [181]. While initial lesions are most frequently seen on the hands, forearms, feet and face, lesions can appear anywhere on the body [180]. Although it can develop at any age, it commonly begins manifestation in childhood or young adulthood [180]. Interestingly, its incidence decreases with increasing age [180]. Due to the lack of melanin, hypo-pigmented areas of skin in vitiligo patients are at a higher risk for sunburn and melanoma [177].

As a multi-factorial disorder, vitiligo is caused by a combination of genetic and non-genetic, environmental factors [175, 176, 180]. There is clinical evidence that localized trauma, stress and an autoimmune disposition can act in synergy to drive the loss of melanocytes in the epidermal-dermal junction [180]. In particular, autoimmune/autocytotoxic factors [182], toxic compounds [180], altered cellular environment [180], dysfunctional melanocyte migration and

proliferation [183] and viral infection [183, 184] can all contribute to the onset of vitiligo. However, the exact mechanism of initiation and maintenance of vitiligo remains unknown.

In the autocytotoxic theory, precursors of melanin synthesis that are cytotoxic accumulate in melanocytes and cause the cells to undergo apoptosis [182]. However, the autoimmune theory is regarded as the most plausible explanation, as sufferers of vitiligo very often tend to present other common autoimmune diseases, including autoimmune thyroid disease (particularly Hashimoto thyroiditis and Grave's disease), pernicious anemia, lupus, diabetes mellitus, Addison's disease, hypoparathyroidism, inflammatory bowel disease, rheumatoid arthritis, and psoriasis [180]. To further support this theory, blood analysis of vitiligo patients consistently shows serum autoantibodies and circulating auto-reactive T cells directed at melanocytes [185-187]. Analysis of vitiliginous skin often shows infiltrates of cytotoxic T cells [186, 187]. Lastly, vitiligo patients present increased serum levels of soluble IL-2 receptor, IL-6 and IL-8, advocating that T-cell activation may contribute to the pathogenesis of vitiligo [182, 188]. All of these studies point to an autoimmune mechanism as the likely cause for vitiligo, yet much remains unknown about the etiology of this disease.

Vitiligo is resistant to most current therapies, yet clinical research has reported that re-pigmentation spontaneously occurs in 1-25% of patients [177, 189]. As vitiligo is still a poorly understood disorder, the therapies are broad in nature. These include: topical corticosteroids, calcineurin inhibitors, vitamin-D derivatives, phototherapy (UV-A and narrowband UV-B wavelengths), photochemotherapy, surgical techniques, excimer laser, topical prostaglandin E and combinations of the aforementioned treatments [180]. The most common and effective treatment is the use of a combination light therapy with a photoactive pharmaceutical [179]. However, this treatment can take anywhere from 100-300 sessions to achieve complete re-

pigmentation [180], and adverse side effects including severe blistering [179], photo-allergic reactions [180], hyper-keratinosis of lesioned skin [180], and skin malignancies [190] are known to occur. Thus, treatment options that decrease the aforementioned side effects and that result in complete re-pigmentation reliably are needed to address vitiligo.

1.6.3 Albinism with an Emphasis on Oculocutaneous Albinism Type 1 (OCA1)

Albinism in humans is recognized as a hypopigmentation of the skin, hair and eyes [191]. It is characterized by a deficiency in melanin biosynthesis; however, melanocyte structure and number are normal [191]. Reduced pigment in the skin of affected individuals is linked with extreme UV-R sensitivity and predisposition to cancer [191]. In the eyes, foveal hypoplasia and mis-routing of the optic fibers from the retina to the optic cortex is known to occur [192]. Mutations in seven genes have been linked to different forms of albinism, including: *TYR* and oculocutaneous albinism type 1 (OCA1), the *P* gene and oculocutaneous albinism type 2 (OCA2), *TYRP-1* and oculocutaneous albinism type 3 (OCA3), the *HPS1* gene and Hermansky-Pudlak syndrome, the *CHS1* gene and Chediak-Higashi syndrome, and the *OA1* gene and X-linked ocular albinism [191].

OCA1 is an autosomal recessive disorder caused by mutations in the *TYR* gene; it has been estimated that it occurs in 1 in 40,000 in most populations [191]. The OCA1 phenotype is characterized by a complete lack of melanin biosynthesis in the hair, skin and eyes, with an inability to tan [191]. However, recent research has demonstrated that the level of skin pigmentation in individuals with OCA1 can vary greatly [191]. OCA1A is marked by a lifelong absence of pigmentation, while OCA1B individuals are able to tan and have near normal levels

of pigment in their hair, skin and eyes [191]. Both types of OCA1 are characterized by complete hypopigmentation at birth, yet individuals with OCA1B acquire pigment as they age [191]. The common feature between both subtypes of OCA1 is nystagmus (involuntary eye movement that may result in reduced or limited vision) and foveal hypoplasia with reduced visual acuity [191].

To date, over 90 mutations in *TYR* have been identified that lead to OCA1, which include missense, nonsense, frameshift, splice site mutations, and deletion of the entire coding sequence [193, 194]. Most missense mutations in *TYR* are found in or flanking the two copper binding domains [191]. The two copper atoms within TYR are held in place by six histidine ligands that keep the atoms 3.6 angstroms apart; any alteration in the secondary structure of TYR has the potential to affect this distance, which would prevent the two copper atoms from forming a peroxide with molecular oxygen and thus preventing function of the protein [191]. Other missense mutations in *TYR* have been shown to cause changes in protein folding and glycosylation, which results in the failure of TYR being trafficked out of the endoplasmic reticulum to the melanosome, its final destination [195, 196].

1.7 Identification of Novel Regulators of Melanogenesis via RNAi-based functional genomics

Much of the core machinery that drives melanogenesis has been identified, yet its full regulation and the genes that participate in said regulation are still poorly understood. A deeper understanding of the molecular underpinnings that regulate melanogenesis may aid in more effective and less toxic compounds that can either simulate or inhibit pigmentation in areas of skin marked by vitiligo or melasma, respectively. To address this need, a Dharmacon genome-

wide siRNA screen consisting of 84,508 siRNAs targeting each of the 21,127 unique human genes was employed to identify single-gene loci that modulate melanocyte pigmentation [197]. Four unique siRNA duplexes per gene were used in a one-gene to one-well format of a 96-well plate [197]. MNT-1 melanoma cells were utilized for the screen because they produce substantial amounts of melanin in culture and also because they possess a gene expression profile that is the most similar to normal human epidermal melanocytes [198]. Other groups have previously used MNT-1 cells to establish pigment regulatory mechanisms that modulate melanogenesis [115, 128, 137, 199]. Five days after transfection, a spectrophotometric melanin quantitation assay that measures absorbance at 405 nm (to account for both eumelanin and pheomelanin) was employed along with an ATP-dependent luminescence-based cell viability assay (CellTiter-Glo) [197]. The CellTiter-Glo assay eliminates siRNAs that impact pigment production because of cell proliferation or cell survival. Using TYR depletion as a positive control, it was determined that a 5-day post-transfection incubation period was optimal for quantitative detection of impaired melanin production in MNT-1 melanoma cells (Fig 1A) [197].

In order to permit plate-to-plate comparisons, the raw A_{405nm} values were normalized to internal reference samples on each plate [197]. Next, each sample was normalized to the experimental mean for each well position calculated from the full data set [197]. This controls for pigment variations due to plate position effects. In order to control for cell number in each well, adjusted luminescence values from the multiplexed cell viability assay (Cell-TiterGlo) were used [197]. This allowed for the calculation of the "normalized absorbance ratio" (absorbance/cell number) for each siRNA [197]. In Fig. 1B, the $\log_2$ transformation of the average normalized absorbance ratio is shown for each gene, with two standard deviations from the mean shown in red [197].

In order to determine the false-positive rate, 35 genes identified from the screen were randomly selected and re-tested using individually synthesized, pooled siRNAs in MNT-1 cells [197]. A keratin-7 siRNA pool, which does not affect pigmentation, was used as a negative control [197]. The ability of each re-tested siRNA to impact pigmentation was compared against the ability of the tyrosinase siRNA to inhibit pigmentation using a standard normalized percent inhibition calculation (Fig. 2A) [197]. From this analysis, it was determined that 4 of the 35 re-tested siRNAs were not able to impact pigment production, establishing a false-positive rate of 12.1% (Fig. 2A) [197]. A simple plate assay was used to compare the ability of each re-tested siRNA to affect pigmentation visually (Fig. 2B).

Intriguingly, the genes identified in the screen have broad roles in many different cellular mechanisms and processes [197]. In order to identify genes that may play a role in phenotypic variation in pigmentation, identified genes were knocked down via siRNA and analyzed for their impact on TYR protein accumulation in three different melanocyte cell lines with distinct genetic backgrounds (MNT-1 melanoma cells, darkly-pigmented human epidermal melanoctyes and medium-pigmented human epidermal melanocytes) (Figs. 3A-3B, 4A-4B) [197]. Aldehyde dehydrogenase 1A1 (ALDH1A1) was one of only two genes able to impact TYR protein accumulation in the three cell lines tested (Figs. 3A-3C, 4A-4B) [197]. Moreover, depletion of ALDH1A1 impacted pigment production visually in MNT-1 cells, as seen in the plate assay (Fig. 2B) [197].

ALDH1A1 is one of 19 in the ALDH superfamily of enzymes, all of which require $NAD(P)^+$ for catalytic activity and play pleiotropic roles in many cellular pathways [200]. ALDH enzymes are constitutively expressed in mammalian tissues with the highest expression occurring in the liver, kidney, uterus and brain [201]. ALDH enzymatic activity is necessary for

the synthesis of retinoic acid, an important regulator during embryogenesis and beyond, and for the metabolism of GABA, a neurotransmitter [202-208]. It is also needed in the alcohol detoxification process and in converting toxic aldehydes synthesized from lipid peroxidation reactions to non-toxic carboxylic acid forms [205]. In particular, ALDH1A1 protects the lens in the eye from reactive oxygen species generated in times of cellular stress [209, 210]; it also plays non-enzymatic maintenance roles in the lens by directly absorbing damaging UV-R and acting as a chaperone protein [211, 212].

ALDH1A1 has a high affinity for two intermediates apart of the Vitamin A pathway: all-*trans* retinal and 9-*cis* retinal [202, 209]. ALDH1A1 acts on these substrates and catalyzes the formation of all-*trans* retinoic and 9-*cis* retinoic acid, respectively [202, 209]. Both play important roles in retinoic acid-mediated signaling. As retinoic acid is crucial in embryogenesis, ALDH1A1 is expressed in specific tissues during embryo development in a spatial-temporal model [213, 214]. Hematopoietic stem cells express especially high levels of ALDH1A1, which can be used for isolation of these cells from other cell populations [215, 216].

In order to pharmacologically validate that ALDH1A1 modulates melanogenesis, two well-characterized catalytic inhibitors, cyanamide and Angeli's salt, were analyzed for their effects on key melanogenic gene expression [197]. Both compounds were able to inhibit TYR protein accumulation as well as pigment accumulation in melanoma cells (Figs. 3D-3E) [197], suggesting that ALDH1A1 may be an ideal pharmaceutical target for the treatment of melasma and other related hyper-pigmentary disorders. These critical initial studies led to the laboratory's interest in this enzyme, which is a major focus of this dissertation.

1.8 References

1. Costin GE, Hearing VJ. Human skin pigmentation: melanocytes modulate skin color in response to stress. FASEB journal : official publication of the Federation of American Societies for Experimental Biology. 2007;21(4):976-94. doi: 10.1096/fj.06-6649rev. PubMed PMID: 17242160.

2. Tobin DJ. Biochemistry of human skin--our brain on the outside. Chemical Society reviews. 2006;35(1):52-67. doi: 10.1039/b505793k. PubMed PMID: 16365642.

3. Freedberg IM, Fitzpatrick TB. Fitzpatrick's dermatology in general medicine. 5th ed. New York: McGraw-Hill, Health Professions Division; 1999.

4. Elias PM. Stratum corneum defensive functions: an integrated view. The Journal of investigative dermatology. 2005;125(2):183-200. doi: 10.1111/j.0022-202X.2005.23668.x. PubMed PMID: 16098026.

5. Elias PM, Choi EH. Interactions among stratum corneum defensive functions. Exp Dermatol. 2005;14(10):719-26. doi: 10.1111/j.1600-0625.2005.00363.x. PubMed PMID: 16176279.

6. Koria P, Andreadis ST. Epidermal morphogenesis: the transcriptional program of human keratinocytes during stratification. The Journal of investigative dermatology. 2006;126(8):1834-41. doi: 10.1038/sj.jid.5700325. PubMed PMID: 16645587.

7. Farage MA, Miller KW, Elsner P, Maibach HI. Structural characteristics of the aging skin: a review. Cutaneous and ocular toxicology. 2007;26(4):343-57. doi: 10.1080/15569520701622951. PubMed PMID: 18058308.

8. Rees JL. Genetics of hair and skin color. Annual review of genetics. 2003;37:67-90. doi: 10.1146/annurev.genet.37.110801.143233. PubMed PMID: 14616056.

9. Hara M, Yaar M, Byers HR, Goukassian D, Fine RE, Gonsalves J, et al. Kinesin participates in melanosomal movement along melanocyte dendrites. The Journal of investigative dermatology. 2000;114(3):438-43. doi: 10.1046/j.1523-1747.2000.00894.x. PubMed PMID: 10692101.

10. Byers HR, Yaar M, Eller MS, Jalbert NL, Gilchrest BA. Role of cytoplasmic dynein in melanosome transport in human melanocytes. The Journal of investigative dermatology. 2000;114(5):990-7. doi: 10.1046/j.1523-1747.2000.00957.x. PubMed PMID: 10771482.

11. Fitzpatrick TB, Breathnach AS. [the Epidermal Melanin Unit System]. Dermatologische Wochenschrift. 1963;147:481-9. PubMed PMID: 14172128.

12. Kobayashi N, Nakagawa A, Muramatsu T, Yamashina Y, Shirai T, Hashimoto MW, et al. Supranuclear melanin caps reduce ultraviolet induced DNA photoproducts in human epidermis. The Journal of investigative dermatology. 1998;110(5):806-10. doi: 10.1046/j.1523-1747.1998.00178.x. PubMed PMID: 9579550.

13. Pathak MA, Stratton K. Free radicals in human skin before and after exposure to light. Archives of biochemistry and biophysics. 1968;123(3):468-76. PubMed PMID: 4297037.

14. Lin JY, Fisher DE. Melanocyte biology and skin pigmentation. Nature. 2007;445(7130):843-50. doi: 10.1038/nature05660. PubMed PMID: 17314970.

15. Harris ML, Baxter LL, Loftus SK, Pavan WJ. Sox proteins in melanocyte development and melanoma. Pigment Cell Melanoma Res. 2010;23(4):496-513. doi: 10.1111/j.1755-148X.2010.00711.x. PubMed PMID: 20444197; PubMed Central PMCID: PMC2906668.

16. Lister JA, Robertson CP, Lepage T, Johnson SL, Raible DW. nacre encodes a zebrafish microphthalmia-related protein that regulates neural-crest-derived pigment cell fate. Development. 1999;126(17):3757-67. PubMed PMID: 10433906.

17. Nakayama A, Nguyen MT, Chen CC, Opdecamp K, Hodgkinson CA, Arnheiter H. Mutations in microphthalmia, the mouse homolog of the human deafness gene MITF, affect neuroepithelial and neural crest-derived melanocytes differently. Mechanisms of development. 1998;70(1-2):155-66. PubMed PMID: 9510032.

18. Opdecamp K, Nakayama A, Nguyen MT, Hodgkinson CA, Pavan WJ, Arnheiter H. Melanocyte development in vivo and in neural crest cell cultures: crucial dependence on the Mitf basic-helix-loop-helix-zipper transcription factor. Development. 1997;124(12):2377-86. PubMed PMID: 9199364.

19. Thomas AJ, Erickson CA. FOXD3 regulates the lineage switch between neural crest-derived glial cells and pigment cells by repressing MITF through a non-canonical mechanism. Development. 2009;136(11):1849-58. doi: 10.1242/dev.031989. PubMed PMID: 19403660; PubMed Central PMCID: PMC2680109.

20. Goding CR. Mitf from neural crest to melanoma: signal transduction and transcription in the melanocyte lineage. Genes & development. 2000;14(14):1712-28. PubMed PMID: 10898786.

21. Erickson CA, Duong TD, Tosney KW. Descriptive and experimental analysis of the dispersion of neural crest cells along the dorsolateral path and their entry into ectoderm in the chick embryo. Developmental biology. 1992;151(1):251-72. PubMed PMID: 1577191.

22. Serbedzija GN, Bronner-Fraser M, Fraser SE. A vital dye analysis of the timing and pathways of avian trunk neural crest cell migration. Development. 1989;106(4):809-16. PubMed PMID: 2562671.

23. Holbrook KA, Underwood RA, Vogel AM, Gown AM, Kimball H. The appearance, density and distribution of melanocytes in human embryonic and fetal skin revealed by the anti-melanoma monoclonal antibody, HMB-45. Anatomy and embryology. 1989;180(5):443-55. PubMed PMID: 2619087.

24. Hirobe T. Histochemical survey of the distribution of the epidermal melanoblasts and melanocytes in the mouse during fetal and postnatal periods. The Anatomical record. 1984;208(4):589-94. doi: 10.1002/ar.1092080414. PubMed PMID: 6731864.

25. Botchkareva NV, Botchkarev VA, Gilchrest BA. Fate of melanocytes during development of the hair follicle pigmentary unit. The journal of investigative dermatology Symposium proceedings / the Society for Investigative Dermatology, Inc [and] European Society for Dermatological Research. 2003;8(1):76-9. doi: 10.1046/j.1523-1747.2003.12176.x. PubMed PMID: 12894999.

26. Slominski A, Paus R, Costantino R. Differential expression and activity of melanogenesis-related proteins during induced hair growth in mice. The Journal of investigative dermatology. 1991;96(2):172-9. PubMed PMID: 1671405.

27. Slominski A, Paus R. Melanogenesis is coupled to murine anagen: toward new concepts for the role of melanocytes and the regulation of melanogenesis in hair growth. The Journal of investigative dermatology. 1993;101(1 Suppl):90S-7S. PubMed PMID: 8326158.

28. Sviderskaya EV, Wakeling WF, Bennett DC. A cloned, immortal line of murine melanoblasts inducible to differentiate to melanocytes. Development. 1995;121(5):1547-57. PubMed PMID: 7540532.

29. Wang SQ, Setlow R, Berwick M, Polsky D, Marghoob AA, Kopf AW, et al. Ultraviolet A and melanoma: a review. Journal of the American Academy of Dermatology. 2001;44(5):837-46. doi: 10.1067/mjd.2001.114594. PubMed PMID: 11312434.

30. Jablonski NG, Chaplin G. Colloquium paper: human skin pigmentation as an adaptation to UV radiation. Proceedings of the National Academy of Sciences of the United States of America. 2010;107 Suppl 2:8962-8. doi: 10.1073/pnas.0914628107. PubMed PMID: 20445093; PubMed Central PMCID: PMC3024016.

31. Kostner K, Denzer N, Muller CS, Klein R, Tilgen W, Reichrath J. The relevance of vitamin D receptor (VDR) gene polymorphisms for cancer: a review of the literature. Anticancer research. 2009;29(9):3511-36. PubMed PMID: 19667145.

32. Norman AW. From vitamin D to hormone D: fundamentals of the vitamin D endocrine system essential for good health. The American journal of clinical nutrition. 2008;88(2):491S-9S. PubMed PMID: 18689389.

33. Archambault M, Yaar M, Gilchrest BA. Keratinocytes and fibroblasts in a human skin equivalent model enhance melanocyte survival and melanin synthesis after ultraviolet irradiation. The Journal of investigative dermatology. 1995;104(5):859-67. PubMed PMID: 7738368.

34. Friedmann PS, Gilchrest BA. Ultraviolet radiation directly induces pigment production by cultured human melanocytes. Journal of cellular physiology. 1987;133(1):88-94. doi: 10.1002/jcp.1041330111. PubMed PMID: 2822734.

35. Scott G, Leopardi S, Printup S, Madden BC. Filopodia are conduits for melanosome transfer to keratinocytes. Journal of cell science. 2002;115(Pt 7):1441-51. PubMed PMID: 11896192.

36. Park HY, Kosmadaki M, Yaar M, Gilchrest BA. Cellular mechanisms regulating human melanogenesis. Cellular and molecular life sciences : CMLS. 2009;66(9):1493-506. doi: 10.1007/s00018-009-8703-8. PubMed PMID: 19153661.

37. Freeman SE, Hacham H, Gange RW, Maytum DJ, Sutherland JC, Sutherland BM. Wavelength dependence of pyrimidine dimer formation in DNA of human skin irradiated in situ with ultraviolet light. Proceedings of the National Academy of Sciences of the United States of America. 1989;86(14):5605-9. PubMed PMID: 2748607; PubMed Central PMCID: PMC297671.

38. Parrish JA, Jaenicke KF, Anderson RR. Erythema and melanogenesis action spectra of normal human skin. Photochemistry and photobiology. 1982;36(2):187-91. PubMed PMID: 7122713.

39. Eller MS, Ostrom K, Gilchrest BA. DNA damage enhances melanogenesis. Proceedings of the National Academy of Sciences of the United States of America. 1996;93(3):1087-92. PubMed PMID: 8577719; PubMed Central PMCID: PMC40035.

40. Nylander K, Bourdon JC, Bray SE, Gibbs NK, Kay R, Hart I, et al. Transcriptional activation of tyrosinase and TRP-1 by p53 links UV irradiation to the protective tanning response. The Journal of pathology. 2000;190(1):39-46. doi: 10.1002/(SICI)1096-9896(200001)190:1<39::AID-PATH492>3.0.CO;2-V. PubMed PMID: 10640990.

41. Khlgatian MK, Hadshiew IM, Asawanonda P, Yaar M, Eller MS, Fujita M, et al. Tyrosinase gene expression is regulated by p53. The Journal of investigative dermatology. 2002;118(1):126-32. doi: 10.1046/j.0022-202x.2001.01667.x. PubMed PMID: 11851885.

42. Eller MS, Gilchrest BA. Tanning as part of the eukaryotic SOS response. Pigment cell research / sponsored by the European Society for Pigment Cell Research and the International Pigment Cell Society. 2000;13 Suppl 8:94-7. PubMed PMID: 11041364.

43. Gilchrest BA, Park HY, Eller MS, Yaar M. Mechanisms of ultraviolet light-induced pigmentation. Photochemistry and photobiology. 1996;63(1):1-10. PubMed PMID: 8577860.

44. Cui R, Widlund HR, Feige E, Lin JY, Wilensky DL, Igras VE, et al. Central role of p53 in the suntan response and pathologic hyperpigmentation. Cell. 2007;128(5):853-64. doi: 10.1016/j.cell.2006.12.045. PubMed PMID: 17350573.

45. Lerner AB, McGuire JS. Effect of alpha- and betamelanocyte stimulating hormones on the skin colour of man. Nature. 1961;189:176-9. PubMed PMID: 13761067.

46. Levine N, Sheftel SN, Eytan T, Dorr RT, Hadley ME, Weinrach JC, et al. Induction of skin tanning by subcutaneous administration of a potent synthetic melanotropin. Jama. 1991;266(19):2730-6. PubMed PMID: 1658407.

47. Luger TA, Scholzen T, Grabbe S. The role of alpha-melanocyte-stimulating hormone in cutaneous biology. The journal of investigative dermatology Symposium proceedings / the Society for Investigative Dermatology, Inc [and] European Society for Dermatological Research. 1997;2(1):87-93. PubMed PMID: 9487022.

48. Mountjoy KG, Robbins LS, Mortrud MT, Cone RD. The cloning of a family of genes that encode the melanocortin receptors. Science. 1992;257(5074):1248-51. PubMed PMID: 1325670.

49. Rouzaud F, Kadekaro AL, Abdel-Malek ZA, Hearing VJ. MC1R and the response of melanocytes to ultraviolet radiation. Mutation research. 2005;571(1-2):133-52. doi: 10.1016/j.mrfmmm.2004.09.014. PubMed PMID: 15748644.

50. Levy C, Khaled M, Fisher DE. MITF: master regulator of melanocyte development and melanoma oncogene. Trends in molecular medicine. 2006;12(9):406-14. doi: 10.1016/j.molmed.2006.07.008. PubMed PMID: 16899407.

51. Price ER, Horstmann MA, Wells AG, Weilbaecher KN, Takemoto CM, Landis MW, et al. alpha-Melanocyte-stimulating hormone signaling regulates expression of microphthalmia, a gene deficient in Waardenburg syndrome. The Journal of biological chemistry. 1998;273(49):33042-7. PubMed PMID: 9830058.

52. Slominski A, Tobin DJ, Shibahara S, Wortsman J. Melanin pigmentation in mammalian skin and its hormonal regulation. Physiological reviews. 2004;84(4):1155-228. doi: 10.1152/physrev.00044.2003. PubMed PMID: 15383650.

53. Huber WE, Price ER, Widlund HR, Du J, Davis IJ, Wegner M, et al. A tissue-restricted cAMP transcriptional response: SOX10 modulates alpha-melanocyte-stimulating hormone-triggered expression of microphthalmia-associated transcription factor in melanocytes. The Journal of biological chemistry. 2003;278(46):45224-30. doi: 10.1074/jbc.M309036200. PubMed PMID: 12944398.

54. Schallreuter KU. A review of recent advances on the regulation of pigmentation in the human epidermis. Cellular and molecular biology. 1999;45(7):943-9. PubMed PMID: 10643998.

55. Schallreuter KU, Wood JM, Pittelkow MR, Gutlich M, Lemke KR, Rodl W, et al. Regulation of melanin biosynthesis in the human epidermis by tetrahydrobiopterin. Science. 1994;263(5152):1444-6. PubMed PMID: 8128228.

56. Lu D, Willard D, Patel IR, Kadwell S, Overton L, Kost T, et al. Agouti protein is an antagonist of the melanocyte-stimulating-hormone receptor. Nature. 1994;371(6500):799-802. doi: 10.1038/371799a0. PubMed PMID: 7935841.

57. Ollmann MM, Wilson BD, Yang YK, Kerns JA, Chen Y, Gantz I, et al. Antagonism of central melanocortin receptors in vitro and in vivo by agouti-related protein. Science. 1997;278(5335):135-8. PubMed PMID: 9311920.

58. Siegrist W, Drozdz R, Cotti R, Willard DH, Wilkison WO, Eberle AN. Interactions of alpha-melanotropin and agouti on B16 melanoma cells: evidence for inverse agonism of agouti. Journal of receptor and signal transduction research. 1997;17(1-3):75-98. doi: 10.3109/10799899709036595. PubMed PMID: 9029482.

59. Slominski A, Plonka PM, Pisarchik A, Smart JL, Tolle V, Wortsman J, et al. Preservation of eumelanin hair pigmentation in proopiomelanocortin-deficient mice on a nonagouti (a/a) genetic background. Endocrinology. 2005;146(3):1245-53. doi: 10.1210/en.2004-0733. PubMed PMID: 15564334; PubMed Central PMCID: PMC1201461.

60. Grando SA, Pittelkow MR, Schallreuter KU. Adrenergic and cholinergic control in the biology of epidermis: physiological and clinical significance. The Journal of investigative dermatology. 2006;126(9):1948-65. doi: 10.1038/sj.jid.5700151. PubMed PMID: 16912692.

61. Gillbro JM, Marles LK, Hibberts NA, Schallreuter KU. Autocrine catecholamine biosynthesis and the beta-adrenoceptor signal promote pigmentation in human epidermal melanocytes. The Journal of investigative dermatology. 2004;123(2):346-53. doi: 10.1111/j.0022-202X.2004.23210.x. PubMed PMID: 15245435.

62. Kauser S, Schallreuter KU, Thody AJ, Gummer C, Tobin DJ. Regulation of human epidermal melanocyte biology by beta-endorphin. The Journal of investigative dermatology. 2003;120(6):1073-80. doi: 10.1046/j.1523-1747.2003.12242.x. PubMed PMID: 12787137.

63. Hachiya A, Kobayashi A, Ohuchi A, Takema Y, Imokawa G. The paracrine role of stem cell factor/c-kit signaling in the activation of human melanocytes in ultraviolet-B-induced pigmentation. The Journal of investigative dermatology. 2001;116(4):578-86. doi: 10.1046/j.1523-1747.2001.01290.x. PubMed PMID: 11286626.

64. Imokawa G, Kobayasi T, Miyagishi M. Intracellular signaling mechanisms leading to synergistic effects of endothelin-1 and stem cell factor on proliferation of cultured human melanocytes. Cross-talk via trans-activation of the tyrosine kinase c-kit receptor. The Journal of biological chemistry. 2000;275(43):33321-8. doi: 10.1074/jbc.M004346200. PubMed PMID: 10921922.

65. Imokawa G, Yada Y, Miyagishi M. Endothelins secreted from human keratinocytes are intrinsic mitogens for human melanocytes. The Journal of biological chemistry. 1992;267(34):24675-80. PubMed PMID: 1280264.

66. Hara M, Yaar M, Gilchrest BA. Endothelin-1 of keratinocyte origin is a mediator of melanocyte dendricity. The Journal of investigative dermatology. 1995;105(6):744-8. PubMed PMID: 7490466.

67. Yohn JJ, Morelli JG, Walchak SJ, Rundell KB, Norris DA, Zamora MR. Cultured human keratinocytes synthesize and secrete endothelin-1. The Journal of investigative dermatology. 1993;100(1):23-6. PubMed PMID: 8423387.

68. Funasaka Y, Chakraborty AK, Hayashi Y, Komoto M, Ohashi A, Nagahama M, et al. Modulation of melanocyte-stimulating hormone receptor expression on normal human melanocytes: evidence for a regulatory role of ultraviolet B, interleukin-1alpha, interleukin-1beta, endothelin-1 and tumour necrosis factor-alpha. The British journal of dermatology. 1998;139(2):216-24. PubMed PMID: 9767234.

69. Yada Y, Higuchi K, Imokawa G. Effects of endothelins on signal transduction and proliferation in human melanocytes. The Journal of biological chemistry. 1991;266(27):18352-7. PubMed PMID: 1917960.

70. Moncada S, Palmer RM, Higgs EA. Nitric oxide: physiology, pathophysiology, and pharmacology. Pharmacological reviews. 1991;43(2):109-42. PubMed PMID: 1852778.

71. Joshi M, Strandhoy J, White WL. Nitric oxide synthase activity is up-regulated in melanoma cell lines: a potential mechanism for metastases formation. Melanoma research. 1996;6(2):121-6. PubMed PMID: 8791269.

72. Heck DE, Laskin DL, Gardner CR, Laskin JD. Epidermal growth factor suppresses nitric oxide and hydrogen peroxide production by keratinocytes. Potential role for nitric oxide in the regulation of wound healing. The Journal of biological chemistry. 1992;267(30):21277-80. PubMed PMID: 1383221.

73. Becherel PA, Mossalayi MD, Ouaaz F, Le Goff L, Dugas B, Paul-Eugene N, et al. Involvement of cyclic AMP and nitric oxide in immunoglobulin E-dependent activation of Fc epsilon RII/CD23+ normal human keratinocytes. The Journal of clinical investigation. 1994;93(5):2275-9. doi: 10.1172/JCI117227. PubMed PMID: 8182161; PubMed Central PMCID: PMC294386.

74. Fecker LF, Eberle J, Orfanos CE, Geilen CC. Inducible nitric oxide synthase is expressed in normal human melanocytes but not in melanoma cells in response to tumor necrosis factor-alpha, interferon-gamma, and lipopolysaccharide. The Journal of investigative dermatology. 2002;118(6):1019-25. doi: 10.1046/j.1523-1747.2002.01744.x. PubMed PMID: 12060397.

75. Romero-Graillet C, Aberdam E, Clement M, Ortonne JP, Ballotti R. Nitric oxide produced by ultraviolet-irradiated keratinocytes stimulates melanogenesis. The Journal of clinical investigation. 1997;99(4):635-42. doi: 10.1172/JCI119206. PubMed PMID: 9045865; PubMed Central PMCID: PMC507845.

76. Hearing VJ, Jimenez M. Mammalian tyrosinase--the critical regulatory control point in melanocyte pigmentation. The International journal of biochemistry. 1987;19(12):1141-7. PubMed PMID: 3125075.

77. Jimenez M, Kameyama K, Maloy WL, Tomita Y, Hearing VJ. Mammalian tyrosinase: biosynthesis, processing, and modulation by melanocyte-stimulating hormone. Proceedings of the National Academy of Sciences of the United States of America. 1988;85(11):3830-4. PubMed PMID: 3131764; PubMed Central PMCID: PMC280313.

78. Kwon BS, Haq AK, Pomerantz SH, Halaban R. Isolation and sequence of a cDNA clone for human tyrosinase that maps at the mouse c-albino locus. Proceedings of the National Academy of Sciences of the United States of America. 1987;84(21):7473-7. PubMed PMID: 2823263; PubMed Central PMCID: PMC299318.

79. Park HY, Gilchrest BA. Signaling pathways mediating melanogenesis. Cellular and molecular biology. 1999;45(7):919-30. PubMed PMID: 10643996.

80. Goldsmith LA, Fitzpatrick TB. Fitzpatrick's dermatology in general medicine. 8th ed. New York: McGraw-Hill Professional; 2012. p. p.

81. Mochly-Rosen D. Localization of protein kinases by anchoring proteins: a theme in signal transduction. Science. 1995;268(5208):247-51. PubMed PMID: 7716516.

82. Park HY, Wu H, Killoran CE, Gilchrest BA. The receptor for activated C-kinase-I (RACK-I) anchors activated PKC-beta on melanosomes. Journal of cell science. 2004;117(Pt 16):3659-68. doi: 10.1242/jcs.01219. PubMed PMID: 15252133.

83. Wu H, Park HY. Protein kinase C-beta-mediated complex formation between tyrosinase and TRP-1. Biochemical and biophysical research communications. 2003;311(4):948-53. PubMed PMID: 14623273.

84. Kobayashi T, Imokawa G, Bennett DC, Hearing VJ. Tyrosinase stabilization by Tyrp1 (the brown locus protein). The Journal of biological chemistry. 1998;273(48):31801-5. PubMed PMID: 9822646.

85. Boissy RE, Sakai C, Zhao H, Kobayashi T, Hearing VJ. Human tyrosinase related protein-1 (TRP-1) does not function as a DHICA oxidase activity in contrast to murine TRP-1. Exp Dermatol. 1998;7(4):198-204. PubMed PMID: 9758418.

86. Hearing VJ, Jimenez M. Analysis of mammalian pigmentation at the molecular level. Pigment cell research / sponsored by the European Society for Pigment Cell Research and the International Pigment Cell Society. 1989;2(2):75-85. PubMed PMID: 2497450.

87. Jackson IJ. Molecular and developmental genetics of mouse coat color. Annual review of genetics. 1994;28:189-217. doi: 10.1146/annurev.ge.28.120194.001201. PubMed PMID: 7893123.

88. Sturm RA, O'Sullivan BJ, Box NF, Smith AG, Smit SE, Puttick ER, et al. Chromosomal structure of the human TYRP1 and TYRP2 loci and comparison of the tyrosinase-related protein gene family. Genomics. 1995;29(1):24-34. doi: 10.1006/geno.1995.1211. PubMed PMID: 8530077.

89. Jackson IJ, Chambers D, Rinchik EM, Bennett DC. Characterization of TRP-1 mRNA levels in dominant and recessive mutations at the mouse brown (b) locus. Genetics. 1990;126(2):451-9. PubMed PMID: 2245917; PubMed Central PMCID: PMC1204199.

90. Manga P, Kromberg JG, Box NF, Sturm RA, Jenkins T, Ramsay M. Rufous oculocutaneous albinism in southern African Blacks is caused by mutations in the TYRP1 gene. American journal of human genetics. 1997;61(5):1095-101. doi: 10.1086/301603. PubMed PMID: 9345097; PubMed Central PMCID: PMC1716031.

91. Kobayashi T, Urabe K, Winder A, Jimenez-Cervantes C, Imokawa G, Brewington T, et al. Tyrosinase related protein 1 (TRP1) functions as a DHICA oxidase in melanin biosynthesis. The EMBO journal. 1994;13(24):5818-25. PubMed PMID: 7813420; PubMed Central PMCID: PMC395555.

92. Jackson IJ, Chambers DM, Budd PS, Johnson R. The tyrosinase-related protein-1 gene has a structure and promoter sequence very different from tyrosinase. Nucleic acids research. 1991;19(14):3799-804. PubMed PMID: 1907365; PubMed Central PMCID: PMC328466.

93. del Marmol V, Ito S, Jackson I, Vachtenheim J, Berr P, Ghanem G, et al. TRP-1 expression correlates with eumelanogenesis in human pigment cells in culture. FEBS letters. 1993;327(3):307-10. PubMed PMID: 8348959.

94. Hearing VJ. The melanosome: the perfect model for cellular responses to the environment. Pigment cell research / sponsored by the European Society for Pigment Cell Research and the International Pigment Cell Society. 2000;13 Suppl 8:23-34. PubMed PMID: 11041354.

95. Le Poole IC, Boissy RE, Sarangarajan R, Chen J, Forristal JJ, Sheth P, et al. PIG3V, an immortalized human vitiligo melanocyte cell line, expresses dilated endoplasmic reticulum. In vitro cellular & developmental biology Animal. 2000;36(5):309-19. doi: 10.1290/1071-2690(2000)036<0309:PAIHVM>2.0.CO;2. PubMed PMID: 10937834.

96. Yokoyama K, Suzuki H, Yasumoto K, Tomita Y, Shibahara S. Molecular cloning and functional analysis of a cDNA coding for human DOPAchrome tautomerase/tyrosinase-related protein-2. Biochimica et biophysica acta. 1994;1217(3):317-21. PubMed PMID: 8148378.

97. Jackson IJ, Chambers DM, Tsukamoto K, Copeland NG, Gilbert DJ, Jenkins NA, et al. A second tyrosinase-related protein, TRP-2, maps to and is mutated at the mouse slaty locus. The EMBO journal. 1992;11(2):527-35. PubMed PMID: 1537334; PubMed Central PMCID: PMC556483.

98. Tsukamoto K, Jackson IJ, Urabe K, Montague PM, Hearing VJ. A second tyrosinase-related protein, TRP-2, is a melanogenic enzyme termed DOPAchrome tautomerase. The EMBO journal. 1992;11(2):519-26. PubMed PMID: 1537333; PubMed Central PMCID: PMC556482.

99. Hemesath TJ, Steingrimsson E, McGill G, Hansen MJ, Vaught J, Hodgkinson CA, et al. microphthalmia, a critical factor in melanocyte development, defines a discrete transcription factor family. Genes & development. 1994;8(22):2770-80. PubMed PMID: 7958932.

100. Bentley NJ, Eisen T, Goding CR. Melanocyte-specific expression of the human tyrosinase promoter: activation by the microphthalmia gene product and role of the initiator. Molecular and cellular biology. 1994;14(12):7996-8006. PubMed PMID: 7969139; PubMed Central PMCID: PMC359338.

101. Yasumoto K, Yokoyama K, Shibata K, Tomita Y, Shibahara S. Microphthalmia-associated transcription factor as a regulator for melanocyte-specific transcription of the human tyrosinase gene. Molecular and cellular biology. 1994;14(12):8058-70. PubMed PMID: 7969144; PubMed Central PMCID: PMC359344.

102. Hershey CL, Fisher DE. Genomic analysis of the Microphthalmia locus and identification of the MITF-J/Mitf-J isoform. Gene. 2005;347(1):73-82. doi: 10.1016/j.gene.2004.12.002. PubMed PMID: 15715979.

103. Fuse N, Yasumoto K, Suzuki H, Takahashi K, Shibahara S. Identification of a melanocyte-type promoter of the microphthalmia-associated transcription factor gene. Biochemical and biophysical research communications. 1996;219(3):702-7. PubMed PMID: 8645245.

104. Yasumoto K, Takeda K, Saito H, Watanabe K, Takahashi K, Shibahara S. Microphthalmia-associated transcription factor interacts with LEF-1, a mediator of Wnt signaling. The EMBO journal. 2002;21(11):2703-14. doi: 10.1093/emboj/21.11.2703. PubMed PMID: 12032083; PubMed Central PMCID: PMC126018.

105. Saito H, Yasumoto K, Takeda K, Takahashi K, Fukuzaki A, Orikasa S, et al. Melanocyte-specific microphthalmia-associated transcription factor isoform activates its own gene promoter through physical interaction with lymphoid-enhancing factor 1. The Journal of biological chemistry. 2002;277(32):28787-94. doi: 10.1074/jbc.M203719200. PubMed PMID: 12048204.

106. Jacquemin P, Lannoy VJ, O'Sullivan J, Read A, Lemaigre FP, Rousseau GG. The transcription factor onecut-2 controls the microphthalmia-associated transcription factor gene. Biochemical and biophysical research communications. 2001;285(5):1200-5. doi: 10.1006/bbrc.2001.5294. PubMed PMID: 11478782.

107. Weilbaecher KN, Motyckova G, Huber WE, Takemoto CM, Hemesath TJ, Xu Y, et al. Linkage of M-CSF signaling to Mitf, TFE3, and the osteoclast defect in Mitf(mi/mi) mice. Molecular cell. 2001;8(4):749-58. PubMed PMID: 11684011.

108. Wu M, Hemesath TJ, Takemoto CM, Horstmann MA, Wells AG, Price ER, et al. c-Kit triggers dual phosphorylations, which couple activation and degradation of the essential melanocyte factor Mi. Genes & development. 2000;14(3):301-12. PubMed PMID: 10673502; PubMed Central PMCID: PMC316361.

109. Takeda K, Takemoto C, Kobayashi I, Watanabe A, Nobukuni Y, Fisher DE, et al. Ser298 of MITF, a mutation site in Waardenburg syndrome type 2, is a phosphorylation site with functional significance. Human molecular genetics. 2000;9(1):125-32. PubMed PMID: 10587587.

110. Mansky KC, Sankar U, Han J, Ostrowski MC. Microphthalmia transcription factor is a target of the p38 MAPK pathway in response to receptor activator of NF-kappa B ligand signaling. The Journal of biological chemistry. 2002;277(13):11077-83. doi: 10.1074/jbc.M111696200. PubMed PMID: 11792706.

111. Prota G. Melanins, melanogenesis and melanocytes: looking at their functional significance from the chemist's viewpoint. Pigment Cell Research. 2000;13(4):283-93.

112. Ito S, Wakamatsu K, Ozeki H. Chemical analysis of melanins and its application to the study of the regulation of melanogenesis. Pigment cell research / sponsored by the European Society for Pigment Cell Research and the International Pigment Cell Society. 2000;13 Suppl 8:103-9. PubMed PMID: 11041366.

113. Seiji M, Shimao K, Birbeck M, Fitzpatrick TB. Subcellular localization of melanin biosynthesis. Annals of the New York Academy of Sciences. 1963;100(1):497-533.

114. Seiji M, Fitzpatrick TB, Simpson RT, Birbeck MS. Chemical composition and terminology of specialized organelles (melanosomes and melanin granules) in mammalian melanocytes. Nature. 1963;197:1082-4. PubMed PMID: 13992623.

115. Kushimoto T, Basrur V, Valencia J, Matsunaga J, Vieira WD, Ferrans VJ, et al. A model for melanosome biogenesis based on the purification and analysis of early melanosomes. Proceedings of the National Academy of Sciences of the United States of America. 2001;98(19):10698-703. doi: 10.1073/pnas.191184798. PubMed PMID: 11526213; PubMed Central PMCID: PMC58529.

116. Basrur V, Yang F, Kushimoto T, Higashimoto Y, Yasumoto K, Valencia J, et al. Proteomic analysis of early melanosomes: identification of novel melanosomal proteins. Journal of proteome research. 2003;2(1):69-79. PubMed PMID: 12643545.

117. Raposo G, Marks MS. Melanosomes--dark organelles enlighten endosomal membrane transport. Nature reviews Molecular cell biology. 2007;8(10):786-97. doi: 10.1038/nrm2258. PubMed PMID: 17878918; PubMed Central PMCID: PMC2786984.

118. Berson JF, Harper DC, Tenza D, Raposo G, Marks MS. Pmel17 initiates premelanosome morphogenesis within multivesicular bodies. Molecular biology of the cell. 2001;12(11):3451-64. PubMed PMID: 11694580; PubMed Central PMCID: PMC60267.

119. Fowler DM, Koulov AV, Alory-Jost C, Marks MS, Balch WE, Kelly JW. Functional amyloid formation within mammalian tissue. PLoS biology. 2006;4(1):e6. doi: 10.1371/journal.pbio.0040006. PubMed PMID: 16300414; PubMed Central PMCID: PMC1288039.

120. Theos AC, Berson JF, Theos SC, Herman KE, Harper DC, Tenza D, et al. Dual loss of ER export and endocytic signals with altered melanosome morphology in the silver mutation of Pmel17. Molecular biology of the cell. 2006;17(8):3598-612. doi: 10.1091/mbc.E06-01-0081. PubMed PMID: 16760433; PubMed Central PMCID: PMC1525253.

121. Raposo G, Tenza D, Murphy DM, Berson JF, Marks MS. Distinct protein sorting and localization to premelanosomes, melanosomes, and lysosomes in pigmented melanocytic cells. The Journal of cell biology. 2001;152(4):809-24. PubMed PMID: 11266471; PubMed Central PMCID: PMC2195785.

122. Orlow SJ. Melanosomes are specialized members of the lysosomal lineage of organelles. The Journal of investigative dermatology. 1995;105(1):3-7. PubMed PMID: 7615972.

123. Bouchard B, Fuller BB, Vijayasaradhi S, Houghton AN. Induction of pigmentation in mouse fibroblasts by expression of human tyrosinase cDNA. The Journal of experimental medicine. 1989;169(6):2029-42. PubMed PMID: 2499655; PubMed Central PMCID: PMC2189346.

124. Vijayasaradhi S, Xu Y, Bouchard B, Houghton AN. Intracellular sorting and targeting of melanosomal membrane proteins: identification of signals for sorting of the human brown locus protein, gp75. The Journal of cell biology. 1995;130(4):807-20. PubMed PMID: 7642699; PubMed Central PMCID: PMC2199968.

125. Wei ML. Hermansky-Pudlak syndrome: a disease of protein trafficking and organelle function. Pigment cell research / sponsored by the European Society for Pigment Cell Research and the International Pigment Cell Society. 2006;19(1):19-42. doi: 10.1111/j.1600-0749.2005.00289.x. PubMed PMID: 16420244.

126. Robinson MS, Bonifacino JS. Adaptor-related proteins. Current opinion in cell biology. 2001;13(4):444-53. PubMed PMID: 11454451.

127. Bonifacino JS, Traub LM. Signals for sorting of transmembrane proteins to endosomes and lysosomes. Annual review of biochemistry. 2003;72:395-447. doi: 10.1146/annurev.biochem.72.121801.161800. PubMed PMID: 12651740.

128. Theos AC, Tenza D, Martina JA, Hurbain I, Peden AA, Sviderskaya EV, et al. Functions of adaptor protein (AP)-3 and AP-1 in tyrosinase sorting from endosomes to melanosomes. Molecular biology of the cell. 2005;16(11):5356-72. doi: 10.1091/mbc.E05-07-0626. PubMed PMID: 16162817; PubMed Central PMCID: PMC1266432.

129. Honing S, Sandoval IV, von Figura K. A di-leucine-based motif in the cytoplasmic tail of LIMP-II and tyrosinase mediates selective binding of AP-3. The EMBO journal. 1998;17(5):1304-14. doi: 10.1093/emboj/17.5.1304. PubMed PMID: 9482728; PubMed Central PMCID: PMC1170479.

130. Calvo PA, Frank DW, Bieler BM, Berson JF, Marks MS. A cytoplasmic sequence in human tyrosinase defines a second class of di-leucine-based sorting signals for late endosomal and lysosomal delivery. The Journal of biological chemistry. 1999;274(18):12780-9. PubMed PMID: 10212263.

131. Simmen T, Schmidt A, Hunziker W, Beermann F. The tyrosinase tail mediates sorting to the lysosomal compartment in MDCK cells via a di-leucine and a tyrosine-based signal. Journal of cell science. 1999;112 (Pt 1):45-53. PubMed PMID: 9841903.

132. Blagoveshchenskaya AD, Hewitt EW, Cutler DF. Di-leucine signals mediate targeting of tyrosinase and synaptotagmin to synaptic-like microvesicles within PC12 cells. Molecular biology of the cell. 1999;10(11):3979-90. PubMed PMID: 10564285; PubMed Central PMCID: PMC25693.

133. Huizing M, Sarangarajan R, Strovel E, Zhao Y, Gahl WA, Boissy RE. AP-3 mediates tyrosinase but not TRP-1 trafficking in human melanocytes. Molecular biology of the cell. 2001;12(7):2075-85. PubMed PMID: 11452004; PubMed Central PMCID: PMC55657.

134. Peden AA, Oorschot V, Hesser BA, Austin CD, Scheller RH, Klumperman J. Localization of the AP-3 adaptor complex defines a novel endosomal exit site for lysosomal membrane proteins. The Journal of cell biology. 2004;164(7):1065-76. doi: 10.1083/jcb.200311064. PubMed PMID: 15051738; PubMed Central PMCID: PMC2172074.

135. Nguyen T, Novak EK, Kermani M, Fluhr J, Peters LL, Swank RT, et al. Melanosome morphologies in murine models of hermansky-pudlak syndrome reflect blocks in organelle development. The Journal of investigative dermatology. 2002;119(5):1156-64. doi: 10.1046/j.1523-1747.2002.19535.x. PubMed PMID: 12445206.

136. Di Pietro SM, Dell'Angelica EC. The cell biology of Hermansky-Pudlak syndrome: recent advances. Traffic. 2005;6(7):525-33. doi: 10.1111/j.1600-0854.2005.00299.x. PubMed PMID: 15941404.

137. Setty SR, Tenza D, Truschel ST, Chou E, Sviderskaya EV, Theos AC, et al. BLOC-1 is required for cargo-specific sorting from vacuolar early endosomes toward lysosome-related organelles. Molecular biology of the cell. 2007;18(3):768-80. doi: 10.1091/mbc.E06-12-1066. PubMed PMID: 17182842; PubMed Central PMCID: PMC1805088.

138. Parra EJ. Human pigmentation variation: evolution, genetic basis, and implications for public health. American journal of physical anthropology. 2007;Suppl 45:85-105. doi: 10.1002/ajpa.20727. PubMed PMID: 18046745.

139. Rana BK, Hewett-Emmett D, Jin L, Chang BH, Sambuughin N, Lin M, et al. High polymorphism at the human melanocortin 1 receptor locus. Genetics. 1999;151(4):1547-57. PubMed PMID: 10101176; PubMed Central PMCID: PMC1460552.

140. Harding RM, Healy E, Ray AJ, Ellis NS, Flanagan N, Todd C, et al. Evidence for variable selective pressures at MC1R. American journal of human genetics. 2000;66(4):1351-61. doi: 10.1086/302863. PubMed PMID: 10733465; PubMed Central PMCID: PMC1288200.

141. Makova K, Norton H. Worldwide polymorphism at the MC1R locus and normal pigmentation variation in humans. Peptides. 2005;26(10):1901-8. doi: 10.1016/j.peptides.2004.12.032. PubMed PMID: 15979202.

142. Sturm RA, Teasdale RD, Box NF. Human pigmentation genes: identification, structure and consequences of polymorphic variation. Gene. 2001;277(1-2):49-62. PubMed PMID: 11602344.

143. Duffy DL, Box NF, Chen W, Palmer JS, Montgomery GW, James MR, et al. Interactive effects of MC1R and OCA2 on melanoma risk phenotypes. Human molecular genetics. 2004;13(4):447-61. doi: 10.1093/hmg/ddh043. PubMed PMID: 14709592.

144. Xu X, Thornwall M, Lundin LG, Chhajlani V. Val92Met variant of the melanocyte stimulating hormone receptor gene. Nature genetics. 1996;14(4):384. doi: 10.1038/ng1296-384. PubMed PMID: 8944016.

145. Frandberg PA, Doufexis M, Kapas S, Chhajlani V. Human pigmentation phenotype: a point mutation generates nonfunctional MSH receptor. Biochemical and biophysical research communications. 1998;245(2):490-2. doi: 10.1006/bbrc.1998.8459. PubMed PMID: 9571181.

146. Schioth HB, Phillips SR, Rudzish R, Birch-Machin MA, Wikberg JE, Rees JL. Loss of function mutations of the human melanocortin 1 receptor are common and are associated with red hair. Biochemical and biophysical research communications. 1999;260(2):488-91. doi: 10.1006/bbrc.1999.0935. PubMed PMID: 10403794.

147. Rees JL. The genetics of sun sensitivity in humans. American journal of human genetics. 2004;75(5):739-51. doi: 10.1086/425285. PubMed PMID: 15372380; PubMed Central PMCID: PMC1182105.

148. Scott MC, Wakamatsu K, Ito S, Kadekaro AL, Kobayashi N, Groden J, et al. Human melanocortin 1 receptor variants, receptor function and melanocyte response to UV radiation. Journal of cell science. 2002;115(Pt 11):2349-55. PubMed PMID: 12006619.

149. Kanetsky PA, Swoyer J, Panossian S, Holmes R, Guerry D, Rebbeck TR. A polymorphism in the agouti signaling protein gene is associated with human pigmentation. American journal of human genetics. 2002;70(3):770-5. doi: 10.1086/339076. PubMed PMID: 11833005; PubMed Central PMCID: PMC384954.

150. Bonilla C, Boxill LA, Donald SA, Williams T, Sylvester N, Parra EJ, et al. The 8818G allele of the agouti signaling protein (ASIP) gene is ancestral and is associated with darker skin color in African Americans. Human genetics. 2005;116(5):402-6. doi: 10.1007/s00439-004-1251-2. PubMed PMID: 15726415.

151. Voisey J, Gomez-Cabrera Mdel C, Smit DJ, Leonard JH, Sturm RA, van Daal A. A polymorphism in the agouti signalling protein (ASIP) is associated with decreased levels of mRNA. Pigment cell research / sponsored by the European Society for Pigment Cell Research and the International Pigment Cell Society. 2006;19(3):226-31. doi: 10.1111/j.1600-0749.2006.00301.x. PubMed PMID: 16704456.

152. Lamason RL, Mohideen MA, Mest JR, Wong AC, Norton HL, Aros MC, et al. SLC24A5, a putative cation exchanger, affects pigmentation in zebrafish and humans. Science. 2005;310(5755):1782-6. doi: 10.1126/science.1116238. PubMed PMID: 16357253.

153. Jablonski NG, Chaplin G. The evolution of human skin coloration. Journal of human evolution. 2000;39(1):57-106.

154. Yakubu A, Mabogunje OA. Skin cancer in African albinos. Acta oncologica. 1993;32(6):621-2. PubMed PMID: 8260178.

155. Mathur U, Datta SL, Mathur BB. The effect of aminopterin-induced folic acid deficiency on spermatogenesis. Fertility and sterility. 1977;28(12):1356-60. PubMed PMID: 590546.

156. Lucock M. Folic acid: nutritional biochemistry, molecular biology, and role in disease processes. Molecular genetics and metabolism. 2000;71(1-2):121-38. doi: 10.1006/mgme.2000.3027. PubMed PMID: 11001804.

157. Off MK, Steindal AE, Porojnicu AC, Juzeniene A, Vorobey A, Johnsson A, et al. Ultraviolet photodegradation of folic acid. Journal of photochemistry and photobiology B, Biology. 2005;80(1):47-55. doi: 10.1016/j.jphotobiol.2005.03.001. PubMed PMID: 15963436.

158. Branda RF, Eaton JW. Skin color and nutrient photolysis: an evolutionary hypothesis. Science. 1978;201(4356):625-6. PubMed PMID: 675247.

159. Holick MF. Evolution and function of vitamin D. Recent results in cancer research Fortschritte der Krebsforschung Progres dans les recherches sur le cancer. 2003;164:3-28. PubMed PMID: 12899511.

160. Holick MF. Vitamin D: A millenium perspective. Journal of cellular biochemistry. 2003;88(2):296-307. doi: 10.1002/jcb.10338. PubMed PMID: 12520530.

161. Holick MF. The vitamin D epidemic and its health consequences. The Journal of nutrition. 2005;135(11):2739S-48S. PubMed PMID: 16251641.

162. Loomis WF. Skin-pigment regulation of vitamin-D biosynthesis in man. Science. 1967;157(3788):501-6. PubMed PMID: 6028915.

163. Holick MF. Vitamin D deficiency. The New England journal of medicine. 2007;357(3):266-81. doi: 10.1056/NEJMra070553. PubMed PMID: 17634462.

164. Barankin B, Silver SG, Carruthers A. The skin in pregnancy. Journal of cutaneous medicine and surgery. 2002;6(3):236-40. doi: 10.1007/s10227-001-0045-6. PubMed PMID: 11951128.

165. Grimes PE. Melasma. Etiologic and therapeutic considerations. Archives of dermatology. 1995;131(12):1453-7. PubMed PMID: 7492140.

166. Resnik S. Melasma induced by oral contraceptive drugs. Jama. 1967;199(9):601-5. PubMed PMID: 6071249.

167. Resnik SS. Melasma and other skin manifestations or oral contraceptives. Transactions of the New England Obstetrical and Gynecological Society. 1967;21:101-7. PubMed PMID: 5620604.

168. Pathak MA, Riley FC, Fitzpatrick TB. Melanogenesis in human skin following exposure to long-wave ultraviolet and visible light. The Journal of investigative dermatology. 1962;39:435-43. PubMed PMID: 13941837.

169. Kang WH, Yoon KH, Lee ES, Kim J, Lee KB, Yim H, et al. Melasma: histopathological characteristics in 56 Korean patients. The British journal of dermatology. 2002;146(2):228-37. PubMed PMID: 11903232.

170. Grimes PE, Yamada N, Bhawan J. Light microscopic, immunohistochemical, and ultrastructural alterations in patients with melasma. The American Journal of dermatopathology. 2005;27(2):96-101. PubMed PMID: 15798432.

171. Smith AG, Shuster S, Thody AJ, Peberdy M. Chloasma, oral contraceptives, and plasma immunoreactive beta-melanocyte-stimulating hormone. The Journal of investigative dermatology. 1977;68(4):169-70. PubMed PMID: 845449.

172. Kippenberger S, Loitsch S, Solano F, Bernd A, Kaufmann R. Quantification of tyrosinase, TRP-1, and Trp-2 transcripts in human melanocytes by reverse transcriptase-competitive multiplex PCR--regulation by steroid hormones. The Journal of investigative dermatology. 1998;110(4):364-7. doi: 10.1038/jid.1998.1. PubMed PMID: 9540976.

173. Ranson M, Posen S, Mason RS. Human melanocytes as a target tissue for hormones: in vitro studies with 1 alpha-25, dihydroxyvitamin D3, alpha-melanocyte stimulating hormone, and beta-estradiol. The Journal of investigative dermatology. 1988;91(6):593-8. PubMed PMID: 2848074.

174. Rivas S, Pandya AG. Treatment of melasma with topical agents, peels and lasers: an evidence-based review. American journal of clinical dermatology. 2013;14(5):359-76. doi: 10.1007/s40257-013-0038-4. PubMed PMID: 23881551.

175. Daneshpazhooh M, Mostofizadeh GM, Behjati J, Akhyani M, Robati RM. Anti-thyroid peroxidase antibody and vitiligo: a controlled study. BMC dermatology. 2006;6:3. doi: 10.1186/1471-5945-6-3. PubMed PMID: 16526964; PubMed Central PMCID: PMC1431557.

176. Alkhateeb A, Fain PR, Thody A, Bennett DC, Spritz RA. Epidemiology of vitiligo and associated autoimmune diseases in Caucasian probands and their families. Pigment cell research / sponsored by the European Society for Pigment Cell Research and the International Pigment Cell Society. 2003;16(3):208-14. PubMed PMID: 12753387.

177. Lotti T, Gori A, Zanieri F, Colucci R, Moretti S. Vitiligo: new and emerging treatments. Dermatologic therapy. 2008;21(2):110-7. doi: 10.1111/j.1529-8019.2008.00178.x. PubMed PMID: 18394085.

178. Szczurko O, Boon HS. A systematic review of natural health product treatment for vitiligo. BMC dermatology. 2008;8:2. doi: 10.1186/1471-5945-8-2. PubMed PMID: 18498646; PubMed Central PMCID: PMC2432048.

179. Whitton ME, Ashcroft DM, Gonzalez U. Therapeutic interventions for vitiligo. Journal of the American Academy of Dermatology. 2008;59(4):713-7. doi: 10.1016/j.jaad.2008.06.023. PubMed PMID: 18793940.

180. Yaghoobi R, Omidian M, Bagherani N. Vitiligo: a review of the published work. The Journal of dermatology. 2011;38(5):419-31. PubMed PMID: 21667529.

181. Shameer P, Prasad PV, Kaviarasan PK. Serum zinc level in vitiligo: a case control study. Indian journal of dermatology, venereology and leprology. 2005;71(3):206-7. PubMed PMID: 16394417.

182. Namazi MR. Phenytoin as a novel anti-vitiligo weapon. Journal of autoimmune diseases. 2005;2:11. doi: 10.1186/1740-2557-2-11. PubMed PMID: 16303054; PubMed Central PMCID: PMC1308849.

183. Le Poole IC, Das PK, van den Wijngaard RM, Bos JD, Westerhof W. Review of the etiopathomechanism of vitiligo: a convergence theory. Exp Dermatol. 1993;2(4):145-53. PubMed PMID: 8162332.

184. Manolache L, Benea V. Stress in patients with alopecia areata and vitiligo. Journal of the European Academy of Dermatology and Venereology : JEADV. 2007;21(7):921-8. doi: 10.1111/j.1468-3083.2006.02106.x. PubMed PMID: 17659001.

185. Boissy RE, Spritz RA. Frontiers and controversies in the pathobiology of vitiligo: separating the wheat from the chaff. Exp Dermatol. 2009;18(7):583-5. doi: 10.1111/j.1600-0625.2008.00826.x. PubMed PMID: 19320739; PubMed Central PMCID: PMC2745236.

186. Ongenae K, Van Geel N, Naeyaert JM. Evidence for an autoimmune pathogenesis of vitiligo. Pigment cell research / sponsored by the European Society for Pigment Cell Research and the International Pigment Cell Society. 2003;16(2):90-100. PubMed PMID: 12622785.

187. Le Poole IC, Luiten RM. Autoimmune etiology of generalized vitiligo. Current directions in autoimmunity. 2008;10:227-43. doi: 10.1159/000131485. PubMed PMID: 18460889.

188. Mandelcorn-Monson RL, Shear NH, Yau E, Sambhara S, Barber BH, Spaner D, et al. Cytotoxic T lymphocyte reactivity to gp100, MelanA/MART-1, and tyrosinase, in HLA-A2-positive vitiligo patients. The Journal of investigative dermatology. 2003;121(3):550-6. doi: 10.1046/j.1523-1747.2003.12413.x. PubMed PMID: 12925214.

189. Castanet J, Ortonne JP. Pathophysiology of vitiligo. Clinics in dermatology. 1997;15(6):845-51. PubMed PMID: 9404687.

190. Huggins RH, Schwartz RA, Janniger C. Vitiligo. Acta dermatovenerologica Alpina, Pannonica, et Adriatica. 2005;14(4):137-42, 44-5. PubMed PMID: 16435042.

191. Oetting WS. The tyrosinase gene and oculocutaneous albinism type 1 (OCA1): A model for understanding the molecular biology of melanin formation. Pigment cell research / sponsored by the European Society for Pigment Cell Research and the International Pigment Cell Society. 2000;13(5):320-5. PubMed PMID: 11041207.

192. Oetting WS, Summers CG, King RA. Albinism and the associated ocular defects. Metabolic, pediatric, and systemic ophthalmology. 1994;17(1-4):5-9. PubMed PMID: 8719278.

193. Schnur RE, Sellinger BT, Holmes SA, Wick PA, Tatsumura YO, Spritz RA. Type I oculocutaneous albinism associated with a full-length deletion of the tyrosinase gene. The Journal of investigative dermatology. 1996;106(5):1137-40. PubMed PMID: 8618053.

194. Oetting WS, King RA. Molecular basis of albinism: mutations and polymorphisms of pigmentation genes associated with albinism. Human mutation. 1999;13(2):99-115. doi: 10.1002/(SICI)1098-1004(1999)13:2<99::AID-HUMU2>3.0.CO;2-C. PubMed PMID: 10094567.

195. Halaban R, Svedine S, Cheng E, Smicun Y, Aron R, Hebert DN. Endoplasmic reticulum retention is a common defect associated with tyrosinase-negative albinism. Proceedings of the National Academy of Sciences of the United States of America. 2000;97(11):5889-94. PubMed PMID: 10823941; PubMed Central PMCID: PMC18529.

196. Toyofuku K, Wada I, Spritz RA, Hearing VJ. The molecular basis of oculocutaneous albinism type 1 (OCA1): sorting failure and degradation of mutant tyrosinases results in a lack of pigmentation. The Biochemical journal. 2001;355(Pt 2):259-69. PubMed PMID: 11284711; PubMed Central PMCID: PMC1221735.

197. Ganesan AK, Ho H, Bodemann B, Petersen S, Aruri J, Koshy S, et al. Genome-wide siRNA-based functional genomics of pigmentation identifies novel genes and pathways that impact melanogenesis in human cells. PLoS genetics. 2008;4(12):e1000298. doi: 10.1371/journal.pgen.1000298. PubMed PMID: 19057677; PubMed Central PMCID: PMC2585813.

198. Hoek K, Rimm DL, Williams KR, Zhao H, Ariyan S, Lin A, et al. Expression profiling reveals novel pathways in the transformation of melanocytes to melanomas. Cancer research. 2004;64(15):5270-82. doi: 10.1158/0008-5472.CAN-04-0731. PubMed PMID: 15289333.

199. Theos AC, Truschel ST, Tenza D, Hurbain I, Harper DC, Berson JF, et al. A lumenal domain-dependent pathway for sorting to intralumenal vesicles of multivesicular endosomes involved in organelle morphogenesis. Developmental cell. 2006;10(3):343-54. doi: 10.1016/j.devcel.2006.01.012. PubMed PMID: 16516837; PubMed Central PMCID: PMC1773005.

200. Koppaka V, Thompson DC, Chen Y, Ellermann M, Nicolaou KC, Juvonen RO, et al. Aldehyde dehydrogenase inhibitors: a comprehensive review of the pharmacology, mechanism of action, substrate specificity, and clinical application. Pharmacological reviews. 2012;64(3):520-39. doi: 10.1124/pr.111.005538. PubMed PMID: 22544865; PubMed Central PMCID: PMC3400832.

201. Alnouti Y, Klaassen CD. Tissue distribution, ontogeny, and regulation of aldehyde dehydrogenase (Aldh) enzymes mRNA by prototypical microsomal enzyme inducers in mice. Toxicological sciences : an official journal of the Society of Toxicology. 2008;101(1):51-64. doi: 10.1093/toxsci/kfm280. PubMed PMID: 17998271.

202. Yoshida A, Hsu LC, Dave V. Retinal oxidation activity and biological role of human cytosolic aldehyde dehydrogenase. Enzyme. 1992;46(4-5):239-44. PubMed PMID: 1292933.

203. Sophos NA, Vasiliou V. Aldehyde dehydrogenase gene superfamily: the 2002 update. Chemico-biological interactions. 2003;143-144:5-22. PubMed PMID: 12604184.

204. Vasiliou V, Nebert DW. Analysis and update of the human aldehyde dehydrogenase (ALDH) gene family. Human genomics. 2005;2(2):138-43. PubMed PMID: 16004729; PubMed Central PMCID: PMC3525259.

205. Vasiliou V, Pappa A, Petersen DR. Role of aldehyde dehydrogenases in endogenous and xenobiotic metabolism. Chemico-biological interactions. 2000;129(1-2):1-19. PubMed PMID: 11154732.

206. Marchitti SA, Brocker C, Stagos D, Vasiliou V. Non-P450 aldehyde oxidizing enzymes: the aldehyde dehydrogenase superfamily. Expert opinion on drug metabolism & toxicology. 2008;4(6):697-720. doi: 10.1517/17425255.4.6.697. PubMed PMID: 18611112; PubMed Central PMCID: PMC2658643.

207. Niederreither K, Dolle P. Retinoic acid in development: towards an integrated view. Nature reviews Genetics. 2008;9(7):541-53. doi: 10.1038/nrg2340. PubMed PMID: 18542081.

208. Kim KJ, Pearl PL, Jensen K, Snead OC, Malaspina P, Jakobs C, et al. Succinic semialdehyde dehydrogenase: biochemical-molecular-clinical disease mechanisms, redox regulation, and functional significance. Antioxidants & redox signaling. 2011;15(3):691-718. doi: 10.1089/ars.2010.3470. PubMed PMID: 20973619; PubMed Central PMCID: PMC3125545.

209. Chen Y, Koppaka V, Thompson DC, Vasiliou V. Focus on molecules: ALDH1A1: from lens and corneal crystallin to stem cell marker. Experimental eye research. 2012;102:105-6. doi: 10.1016/j.exer.2011.04.008. PubMed PMID: 21536030; PubMed Central PMCID: PMC3423494.

210. Chen Y, Mehta G, Vasiliou V. Antioxidant defenses in the ocular surface. The ocular surface. 2009;7(4):176-85. PubMed PMID: 19948101; PubMed Central PMCID: PMC4104792.

211. Estey T, Cantore M, Weston PA, Carpenter JF, Petrash JM, Vasiliou V. Mechanisms involved in the protection of UV-induced protein inactivation by the corneal crystallin ALDH3A1. The Journal of biological chemistry. 2007;282(7):4382-92. doi: 10.1074/jbc.M607546200. PubMed PMID: 17158879.

212. Estey T, Chen Y, Carpenter JF, Vasiliou V. Structural and functional modifications of corneal crystallin ALDH3A1 by UVB light. PloS one. 2010;5(12):e15218. doi: 10.1371/journal.pone.0015218. PubMed PMID: 21203538; PubMed Central PMCID: PMC3006428.

213. Downes J, Holmes R. Development of aldehyde dehydrogenase and alcohol dehydrogenase in mouse eye: evidence for light-induced changes. Biology of the neonate. 1992;61(2):118-23. PubMed PMID: 1567930.

214. Grun F, Hirose Y, Kawauchi S, Ogura T, Umesono K. Aldehyde dehydrogenase 6, a cytosolic retinaldehyde dehydrogenase prominently expressed in sensory neuroepithelia during

development. The Journal of biological chemistry. 2000;275(52):41210-8. doi: 10.1074/jbc.M007376200. PubMed PMID: 11013254.

215. Storms RW, Green PD, Safford KM, Niedzwiecki D, Cogle CR, Colvin OM, et al. Distinct hematopoietic progenitor compartments are delineated by the expression of aldehyde dehydrogenase and CD34. Blood. 2005;106(1):95-102. doi: 10.1182/blood-2004-09-3652. PubMed PMID: 15790790; PubMed Central PMCID: PMC1895136.

216. Storms RW, Trujillo AP, Springer JB, Shah L, Colvin OM, Ludeman SM, et al. Isolation of primitive human hematopoietic progenitors on the basis of aldehyde dehydrogenase activity. Proceedings of the National Academy of Sciences of the United States of America. 1999;96(16):9118-23. PubMed PMID: 10430905; PubMed Central PMCID: PMC17742.

217. Whitehurst AW, Bodemann BO, Cardenas J, Ferguson D, Girard L, Peyton M, et al. Synthetic lethal screen identification of chemosensitizer loci in cancer cells. Nature. 2007;446(7137):815-9. doi: 10.1038/nature05697. PubMed PMID: 17429401.

Figure 1.1: Genome-wide RNAi screening for novel molecular components of melanogenesis.

A) A MNT-1 model for loss-of-function detection of pigmentation genes. MNT-1 cells were transfected with siRNAs targeting tyrosinase using a microtiter-plate based high throughput reverse transfection protocol [217]optimized for this cell line. Inhibition of pigmentation and tyrosinase expression relative to control non-targeting siRNAs is shown. B) MNT-1 pigmented melanoma cells were transfected with 84,920 siRNA duplexes targeting 21,230 genes in a one-well, one-gene reverse transfection format as we have previously described [217]. 120 hrs post transfection, Raw A_{405nm} absorbance values were collected for each well and normalized to internal reference samples on each plate, followed by normalization to the experimental mean for each well calculated from the full data set to control for variations in pigment due to plate and position effects. Similarly adjusted luminescence values from a multiplexed viability assay (CellTiter-Glo) were used to control for cell number, generating "normalized absorbance ratios" for each well (absorbance/cell number). The log2 transformation of the average normalized absorbance ratios among replicates is shown for each gene from lowest (hypopigmentation) to highest (hyperpigmentation). Values below 2 standard deviations from the mean are shown in red.

Data excerpted from:

"Genome-Wide siRNA-Based Functional Genomics of Pigmentation Identifies Novel Genes and Pathways That Impact Melanogenesis in Human Cells"

Anand K. Ganesan, Hsiang Ho, Brian Bodemann, Sean Peterson, Jayavani Aruri, Shiney Koshy, Zachary Richardson, Lu Q. Le, Tatiana Krasieva, Michael G. Roth, Pat Farmer and Michael A. White
PLoS Genetics
doi: 10.1371/journal.pgen.1000298
Published December 5, 2008
Figure doi: 10.1371/journal.pgen.1000298.s001

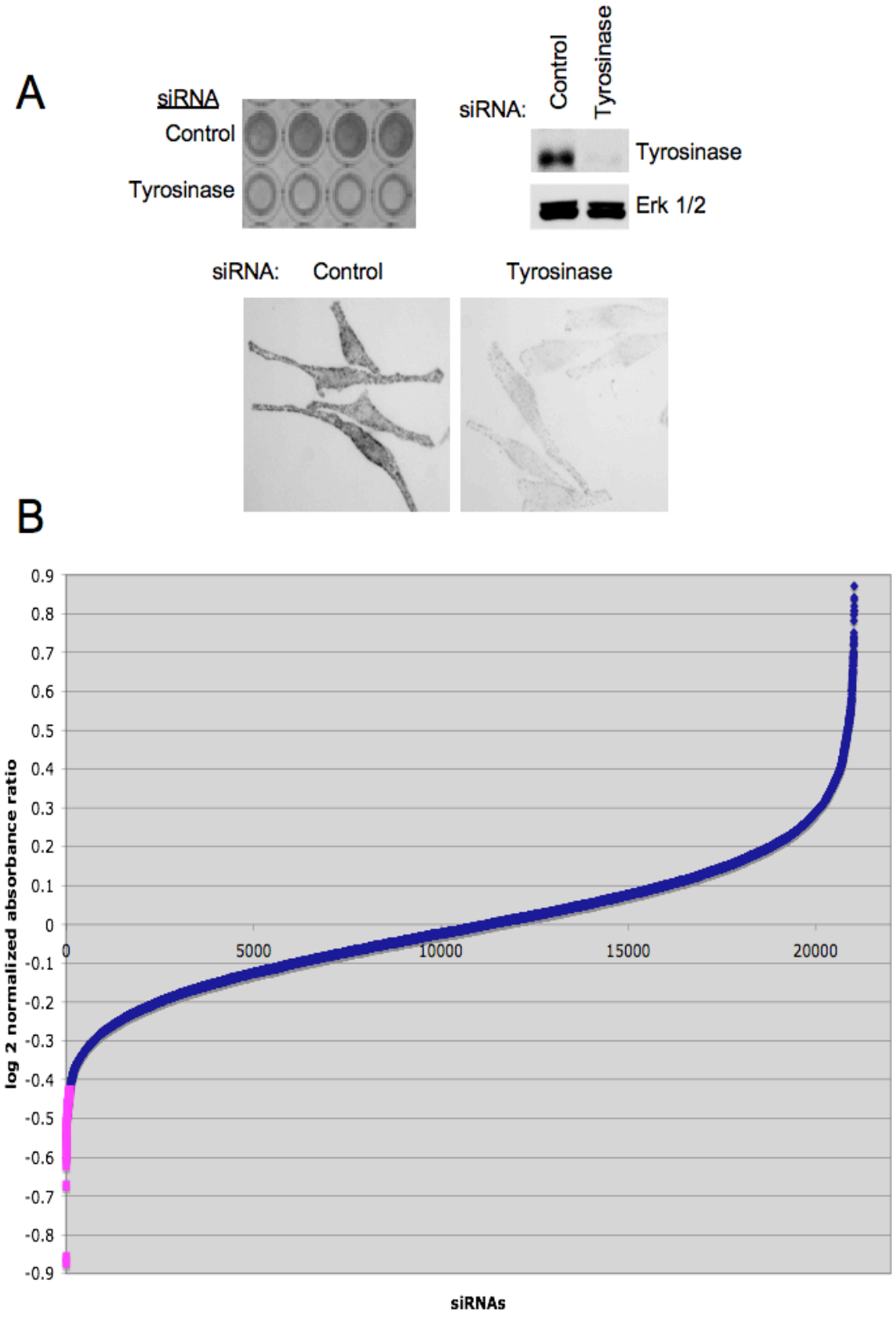
A
siRNA
Control
Tyrosinase
siRNA:
Control
Tyrosinase
Tyrosinase
Erk 1/2
siRNA:
Control
Tyrosinase
B
log 2 normalized absorbance ratio
0.9
0.8
0.7
0.6
0.5
0.4
0.3
0.2
0.1
0
-0.1
-0.2
-0.3
-0.4
-0.5
-0.6
-0.7
-0.8
-0.9
0
5000
10000
15000
20000
siRNAs

Figure 1.1

Figure 1.2: Validation of novel gene products supporting melanogenesis.

A) MNT-1 cells were transfected with the indicated siRNA pools (50 nM final concentration) targeting 35 of the 94 positive regulators of melanogenesis identified in the primary screen. siRNAs targeting Ker7, a gene that does not impact pigment production, were used as a negative control (black bar). A normalized percent inhibition calculation was employed to compare the consequences of each siRNA pool on pigmentation with that observed upon depletion of tyrosinase. Bars represent mean and s.e.m. for $n = 3$. Red bars indicate failure to significantly suppress pigmentation. The results of the analysis of these 35 genes are shown in this panel (those genes that were not putative autophagy regulators) and in Figure 3 (putative autophagy regulators). A summary of the results for all 35 genes is shown in Table S4. B) A light micrograph of a representative opaque-walled, clear-bottomed 96-well microtiter plate containing MNT-1 cell monolayers 7 days post transfection with the indicated siRNAs is shown.

Data excerpted from:

"Genome-Wide siRNA-Based Functional Genomics of Pigmentation Identifies Novel Genes and Pathways That Impact Melanogenesis in Human Cells"

Anand K. Ganesan, Hsiang Ho, Brian Bodemann, Sean Peterson, Jayavani Aruri, Shiney Koshy, Zachary Richardson, Lu Q. Le, Tatiana Krasieva, Michael G. Roth, Pat Farmer and Michael A. White
PLoS Genetics
doi: 10.1371/journal.pgen.1000298
Published December 5, 2008
Figure doi: 10.1371/journal.pgen.1000298.g001

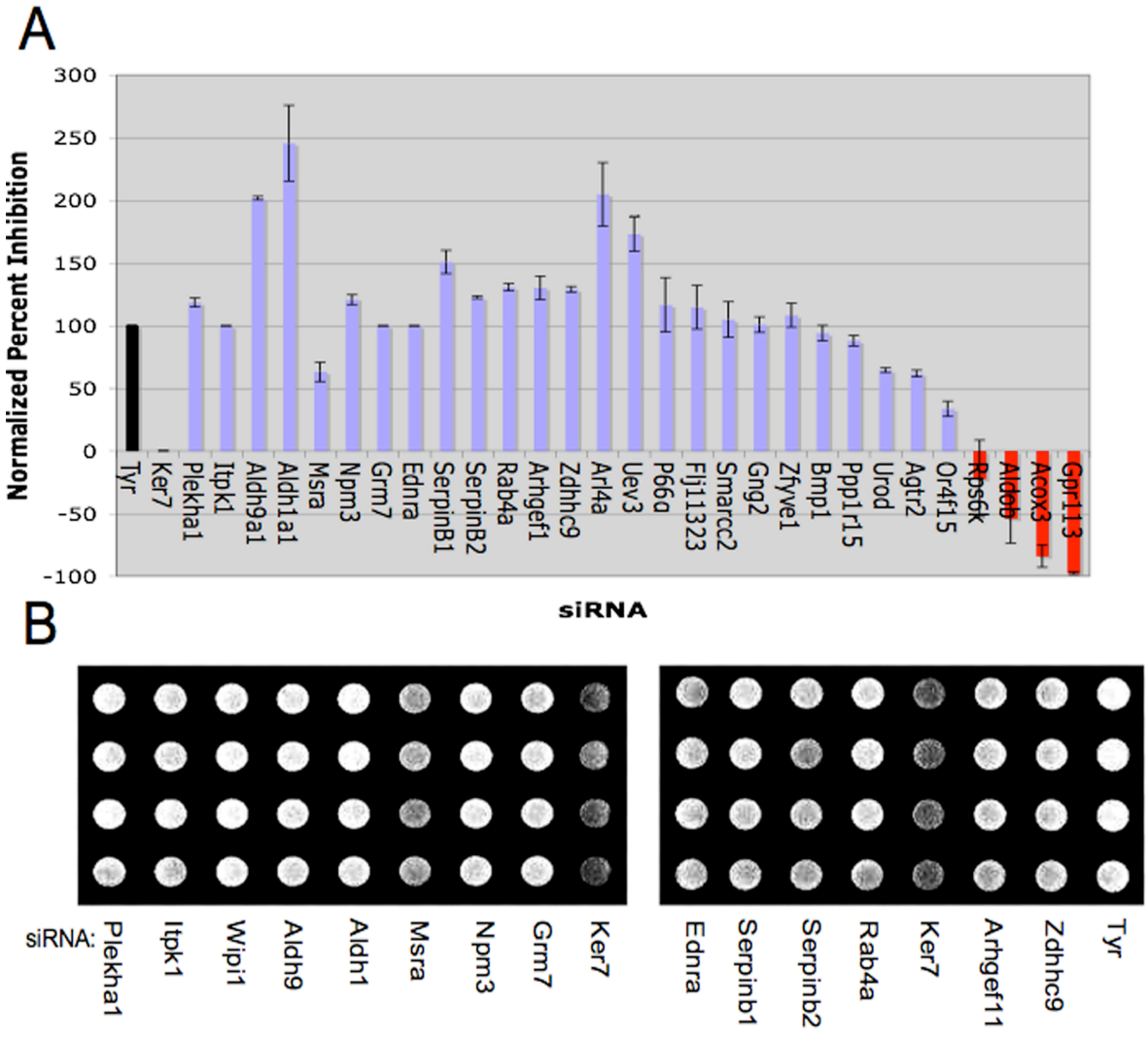
A
Normalized Percent Inhibition
300
250
200
150
100
50
0
-50
-100
Tyr
Ker7
Plekha1
Itpk1
Aldh9a1
Aldh1a1
Msra
Npm3
Grm7
Ednra
SerpinB1
SerpinB2
Rab4a
Arhgef1
Zdhhc9
Arl4a
Uev3
P66a
Fli11323
Smarcc2
Gng2
Zfyve1
Bmp1
Ppp1r15
Urod
Agtr2
Or4f15
Rps6k
Aldob
Acox3
Gpr113
siRNA
B
siRNA:
Plekha1
Itpk1
Wipi1
Aldh9
Aldh1
Msra
Npm3
Grm7
Ker7
Ednra
Serpinb1
Serpinb2
Rab4a
Ker7
Arhgef11
Zdhhc9
Tyr

Figure 1.2

Figure 1.3: Novel, pharmaceutically-tractable melanogenesis gene networks converge on tyrosinase expression.

A) 4 days post transfection with the indicated siRNAs, MNT-1 whole cell lysates were prepared and analyzed by immunoblot for the indicated proteins. A non-targeting siRNA was used as a transfection control (Control). ERK1/2 is shown as a loading control. B) Those siRNAs that inhibited tyrosinase accumulation were examined for consequences on tyrosinase and MITF gene expression by quantitative RT-PCR. 72 hours post transfection with the indicated siRNAs, equal numbers of MNT-1 cells were lysed and cDNA was prepared using a Cells to Ct kit (Ambion). Taqman qRT PCR assays (Applied Biosystems) for tyrosinase and MITF was utilized to identify siRNAs that impacted tyrosinase and MITF expression. C) The indicated siRNAs, targeting novel pigmentation genes identified in the MNT-1 screen, were tested for consequences on tyrosinase accumulation in darkly pigmented and moderately pigmented primary human melanocyte cultures 6 days post-transfection. The results presented here is a Venn diagram of the data presented in Figure S5 demonstrating that we have identified pigment regulators that differentially impact pigment production in different genetic backgrounds. D) Pharmacological inhibition of Aldh activity impacts tyrosinase protein accumulation. MNT-1 cells (left panel) and primary melanocyte cultures (right panels) were exposed to 5 mM Aldh inhibitors (cyanamide or Angeli's salt) or the tyrosinase inhibitor hydroquinone [15] for 72 hours as indicated. 24 hours post-treatment, cultures were exposed to UV-B at the doses indicated. Tyrosinase and ERK1/2 levels were assessed by immunoblot. MNT-1: Angeli's salt (5 mM), cyanamide (5 mM), or hydroquinone (5 mM); primary melanocytes: Angeli's salt (50 mM), cyanamide (100 mM), hydroquinone (1 mM). E) Aldh inhibitors impair melanogenesis in primary human melanocytes. Darkly pigmented melanocytes were cultured for seven days in the presence of the indicated dosed of cyanamide (cya), vehicle, or PTU. PTU is the most potent currently known in vitro pigment inhibitor in primary melanocytes [43]. Subsequently, cells were lysed in CellTiter-Glo and the luminescence and absorbance values were used to calculate inhibition of pigmentation as in Figure 1A.

Data excerpted from:

"Genome-Wide siRNA-Based Functional Genomics of Pigmentation Identifies Novel Genes and Pathways That Impact Melanogenesis in Human Cells"

Anand K. Ganesan, Hsiang Ho, Brian Bodemann, Sean Peterson, Jayavani Aruri, Shiney Koshy, Zachary Richardson, Lu Q. Le, Tatiana Krasieva, Michael G. Roth, Pat Farmer and Michael A. White
PLoS Genetics
doi: 10.1371/journal.pgen.1000298
Published December 5, 2008
Figure doi: 10.1371/journal.pgen.1000298.g002

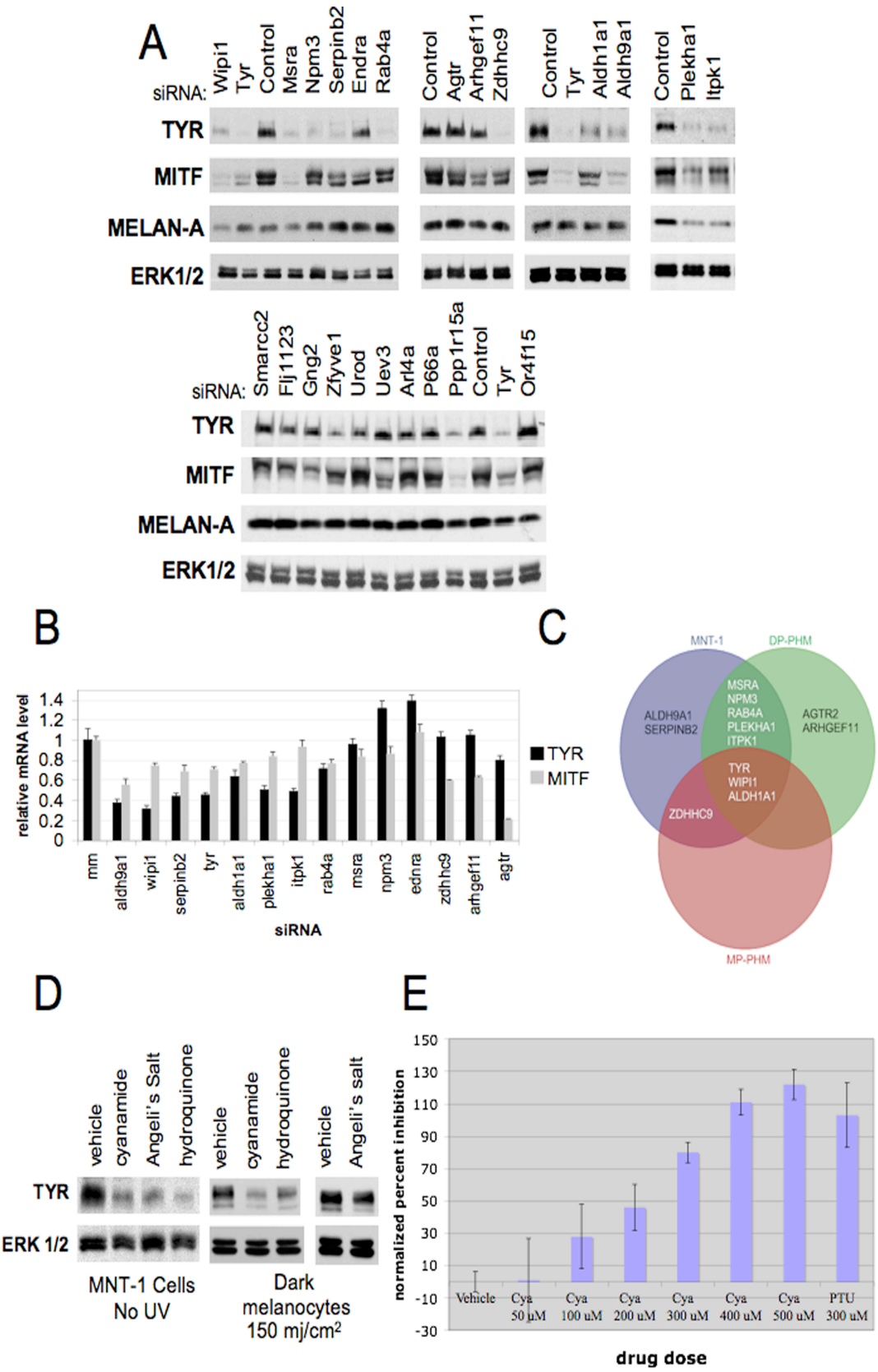
A
siRNA:
Wipi1
Tyr
Control
Msra
Npm3
Serpinb2
Endra
Rab4a
Control
Agtr
Arhgef11
Zdhhc9
Control
Tyr
Aldh1a1
Aldh9a1
Control
Plekha1
Itpk1
TYR
MITF
MELAN-A
ERK1/2
siRNA:
Smarcc2
Flj1123
Gng2
Zfyve1
Urod
Uev3
Arl4a
P66a
Ppp1r15a
Control
Tyr
Or4f15
TYR
MITF
MELAN-A
ERK1/2
B
relative mRNA level
1.4
1.2
1
0.8
0.6
0.4
0.2
0
mm
aldh9a1
wipi1
serpinb2
tyr
aldh1a1
plekha1
itpk1
rab4a
msra
npm3
ednra
zdhhc9
arhgef11
agtr
siRNA
TYR
MITF
C
MNT-1
DP-PHM
MP-PHM
ALDH9A1
SERPINB2
MSRA
NPM3
RAB4A
PLEKHA1
ITPK1
AGTR2
ARHGEF11
TYR
WIPI1
ALDH1A1
ZDHHC9
D
vehicle
cyanamide
Angeli's Salt
hydroquinone
vehicle
cyanamide
hydroquinone
vehicle
Angeli's salt
TYR
ERK 1/2
MNT-1 Cells
No UV
Dark
melanocytes
150 mj/cm2
E
normalized percent inhibition
150
130
110
90
70
50
30
10
-10
-30
Vehicle
Cya
50 uM
Cya
100 uM
Cya
200 uM
Cya
300 uM
Cya
400 uM
Cya
500 uM
PTU
300 uM
drug dose

Figure 1.3

Figure 1.4: siRNA-mediated knockdown of ALDH1A1 leads to potent decreases in TYR protein

The impact of multiple independent siRNAs, targeting the indicated genes, on tyrosinase protein accumulation was assessed by immunoblot. The impact of a given siRNA on gene expression was quantitated by densitometry (numbers below the corresponding blots). Two or more siRNAs impaired tyrosinase protein expression in all cases examined. Similarly, the impact of multiple independent siRNAs targeting tyrosinase on MITF protein accumulation was assessed by immunoblot. All three siRNAs tested had an impact on MITF expression.

Data excerpted from:

"Genome-Wide siRNA-Based Functional Genomics of Pigmentation Identifies Novel Genes and Pathways That Impact Melanogenesis in Human Cells"

Anand K. Ganesan, Hsiang Ho, Brian Bodemann, Sean Peterson, Jayavani Aruri, Shiney Koshy, Zachary Richardson, Lu Q. Le, Tatiana Krasieva, Michael G. Roth, Pat Farmer and Michael A. White
PLoS Genetics
doi: 10.1371/journal.pgen.1000298
Published December 5, 2008
Figure doi: 10.1371/journal.pgen.1000298.s003

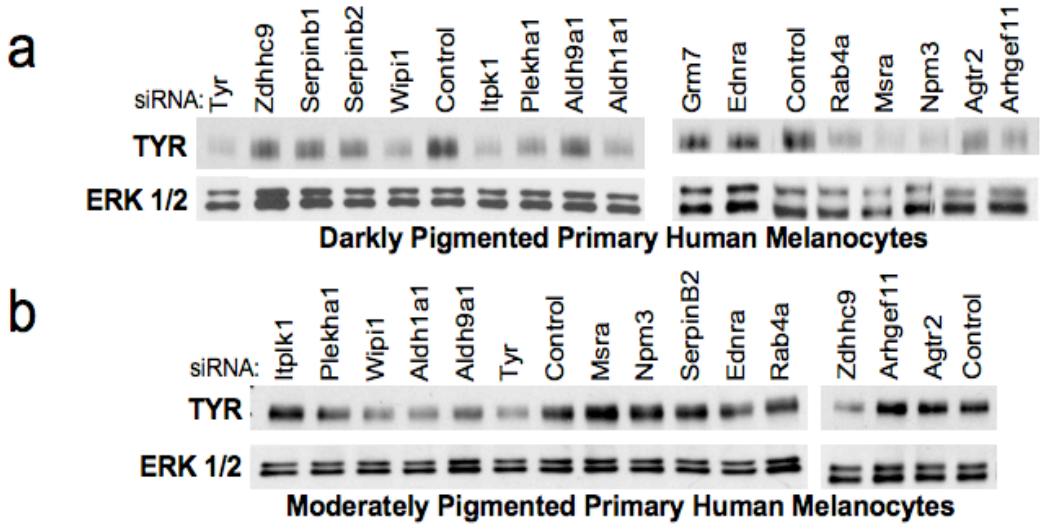
a
siRNA:
Tyr
Zdhhc9
Serpinb1
Serpinb2
Wipi1
Control
Itpk1
Plekha1
Aldh9a1
Aldh1a1
Grm7
Ednra
Control
Rab4a
Msra
Npm3
Agtr2
Arhgef11
TYR
ERK 1/2
Darkly Pigmented Primary Human Melanocytes
b
siRNA:
Itplk1
Plekha1
Wipi1
Aldh1a1
Aldh9a1
Tyr
Control
Msra
Npm3
SerpinB2
Ednra
Rab4a
Zdhhc9
Arhgef11
Agtr2
Control
TYR
ERK 1/2
Moderately Pigmented Primary Human Melanocytes

Figure 1.4

Tyrosinase Modulates Pigmentation by Controlling the Distribution of Melanin Within the Maturing Melanosome

Chapter 2

Elyse K. Paterson, Thomas J. Fielder, Grant R. MacGregor, Shosuke Ito, Kazumasa Wakamatsu, Victoria Eby, Raymond E. Boissy, Daniel Gillen and Anand K. Ganesan

Under Revision, PLoS One

Submitted June 3, 2015

2.1 Abstract

The mechanisms that lead to variation in human skin and hair color are not fully understood. To better understand the molecular control of skin and hair color variation, we modulated the expression of *Tyrosinase (Tyr),* which controls the rate-limiting step of melanogenesis, by expressing a single-copy, tetracycline-inducible shRNA against *Tyr* in mice. Moderate depletion of TYR was sufficient to alter the appearance of the mouse coat in black, agouti, and yellow coat color backgrounds, even though TYR depletion did not significantly inhibit accumulation of melanin within the mouse hair. Ultra-structural studies revealed that the reduction of *Tyr* inhibited the accumulation of terminal melanosomes, altered the pattern of melanin deposition within terminal melanosomes, and inhibited the expression of genes that regulate melanogenesis. These results indicate that color in skin and hair is determined not only by the total amount of melanin within the hair, but also by the pattern of melanin distribution within the melanosome.

2.2 Significance

Studies have identified many genes whose products regulate melanin production. However, our knowledge is incomplete about how these products interact mechanistically to control pigment variation. To phenotypically model pigment variation, we selectively depleted TYR in mice with three different coat color backgrounds. A moderate reduction of TYR was sufficient to alter the appearance of the mouse hair, although it was insufficient to significantly reduce the amount of accumulated melanin. Instead, depletion of TYR modulated maturation of the melanosome by altering expression of other genes that regulate melanogenesis. Our results indicate that TYR not only catalyzes the production of melanin but also that the level of TYR can modulate the expression of other key melanogenesis regulators. This partial loss-of-function transgenic model is a useful new experimental tool to investigate the molecular control of pigment variation *in vivo*.

2.3 Introduction

Skin color varies widely both within and between human ethnic populations, evolving over generations to be darker in indigenous equatorial populations to protect the skin from UV damage [1, 2], or to be lighter in populations at higher latitudes to facilitate Vitamin D production [3]. With human civilization, lighter skinned populations have moved to more temperate climates, resulting in the increased incidence and prevalence of UV-induced skin cancer. Indeed, one in six Americans [4] and one in two Australians will develop skin cancer during their lifetime [5]. Understanding the molecular mechanisms of skin color heterogeneity could lead to the development of new strategies to prevent skin cancer in skin types that are more susceptible to UV-induced damage. Numerous proteins have been identified that confer differences in coat color between inbred animal strains [6-8]. Despite this information, it is not yet fully understood how variation in individual pigment-related genes results in the diversity of skin color phenotypes observed in nature.

Melanin is a chemically inert yet stable pigment that gives skin and hair its color [9]. The two primary melanins found in human hair and skin are the red/yellow pheomelanins and the brown/black eumelanins [9]. Melanins are synthesized from tyrosine via an enzymatic reaction catalyzed by tyrosinase (TYR) [10, 11] with tyrosinase-related protein 1 (TYRP1) and DOPAchrome tautomerase (DCT) also being required to generate the final melanin product [10]. TYR is a membrane glycoprotein that catalyzes the conversion of tyrosine to DOPA [12] and then subsequently oxidizes DOPA to form DOPAquinone. This intermediate is further acted upon by TYRP1 and DCT to form eumelanin [9, 12]. TYRP1 and DCT are also involved in the

proper trafficking of TYR to the stage II melanosome and in detoxification processes in the melanosome, respectively [13, 14]

Melanin synthesis occurs within the melanosome, a specific lysosome-related organelle that matures through four morphologic stages (I-IV) [15-19]. Stage I melanosomes are spherical vacuoles that lack TYR activity and melanin. They contain intralumenal fibrils that are comprised mainly of luminal fragments of PMEL5/gp100, an integral membrane protein specifically expressed in pigment-producing cells [9, 16, 18, 20, 21]. In the stage II melanosome, PMEL5 is organized into sheets and thus transforms the spherical stage I melanosome to an elongated, fibrillar organelle [12, 20, 22]. TYR is transported to the stage II melanosome, initiates melanin synthesis, and deposits pigment onto internal fibrils that are characteristic of the stage III melanosome [15, 16, 18, 20]. Stage IV melanosomes are either elliptical or ellipsoidal in shape and demonstrate complete melanization with little TYR enzymatic activity [15, 18]. Stage IV melanosomes are defined by the absence of visible amyloid fibrils [23, 24]. Mature, stage IV melanosomes are transferred from melanocytes to adjacent keratinocytes where they accumulate as melanin caps above the keratinocyte nuclei and absorb disruptive UV-radiation before it can damage the DNA [25]. Correlative studies have identified biochemical and ultra-structural alterations thought to be responsible for skin and hair color variation. While light and dark skinned individuals possess similar numbers of melanocytes, melanosomes are larger (0.5-0.8 mm dia.) in highly pigmented skin compared to lightly pigmented skin (0.3-0.5 mm dia.) [26-30]. Furthermore, lightly pigmented skin contains less dense melanosomes, mostly at stage II and III, while darkly pigmented skin contains denser melanosomes mostly at stage IV [26-30]. Melanocytes from light skinned individuals also synthesize TYR protein more slowly, degrade TYR at a faster rate, and contain less TYR activity

when compared to melanocytes from dark-skinned individuals [31]. Recent RNAi-based functional genomics studies have identified a large number of novel genes that regulate melanogenesis by controlling the expression and stability of TYR [32]. Taken together, these studies suggest that subtle variations in *Tyr* expression and activity may contribute to the diversity seen in human skin color. We tested this prediction experimentally using a novel inducible and reversible partial *Tyr* loss of function mouse model. We demonstrate that partial depletion of TYR alters mouse coat color, inhibits normal melanosome maturation and inhibits expression of genes that regulate melanogenesis, while only subtly affecting eumelanin accumulation. These results support a model where TYR not only controls the synthesis of melanin, but also coordinately regulates the pattern of deposition of melanin within the melanosome, phenotypes which could have only been appreciated in a partial loss of function model.

2.4 Materials and Methods

Cell Lines and Reagents

B16F1 mouse melanoma cells (a gift from William Pavan, NHGRI obtained from ATCC) were cultured in high-glucose DMEM media supplemented with 10% FBS, 2mM glutamine, 1x NEAA, and 0.075% sodium bicarbonate at 5% CO_2 in air. The pCol-TGM plasmid was kindly provided by Scott Lowe. The pCAGGS-Flpe-puro plasmid was purchased from Addgene (Cambridge, MA). The *Tyr*-shRNAs (*Tyr*-shRNA #1 and *Tyr*-shRNA #2) were purchased from Open Biosystems/GE Dharmacon (Lafayette, CO) in the pGIPZ plasmid. The 5' to 3'mature antisense sequence for *Tyr*-shRNA #1 is: TCTTCTGAAGGCATAGCCT, while that for *Tyr*-shRNA #2 is: GATCTGCTACAAATGATCT. Antibodies used in this study are listed in Supplemental table 2. All of the primers used for genotyping the mice were taken from [33], the mouse mutant resource website, (Jackson Laboratory Bar Harbor, ME) or designed using Primer3web (http://www.primer3plus.com). Oligodeoxynucleotide primers (Eurofins Scientific, Huntsville, AL) are listed in Supplemental table 3.

Identification and characterization of a potent shRNA against *Tyr*

Short-hairpin RNAs targeting *Tyr* were analyzed using a "Sensor Rules" algorithm to identify highly potent shRNAs effective at the single copy level in the cell [34]. Two shRNAs were chosen for further analysis because they fulfilled all but one of the selected criteria of the algorithm. To generate lentiviral plasmids containing both shRNAs, TLA-HEK293T cells

(Thermo-Scientific/Open Biosystems, Grand Island, NY) were seeded at a density of 3.8 x 10^5 cells per well of a 12-well plate and transfected with 1.4 μg of pCMV packaging vector (Thermo Scientific), 0.5 μg pMP2G packaging vector (Thermo Scientific), and 2.0 μg of pGIPZ-*Tyr* or pGIPZ-*NT* (non-targeting control) (Open Biosystems/GE Dharmacon) for a total of 3.9 μg of DNA. Arrest-In was used as the transfection reagent at a 1:5 DNA:Arrest-In ratio (Thermo Scientific/Open Biosystems). Lentiviral supernatant was harvested at 48 and 72 hours post-transfection and filtered through a 0.45μm filter to remove cells. Lentivirus quantitation was carried out using a Lentivirus-Associated p24 ELISA kit (Cell Biolabs, Inc, San Diego, CA) according to the manufacturer's instructions. B16 mouse melanoma cells were infected in the presence of Polybrene (8μg/ ml) (Santa Cruz Biotechnology, Santa Cruz, CA) with lentivirus containing either pGIPZ-*Tyr* or pGIPZ-*NT* at multiplicity of infection (MOI) of 0.1. Infected B16 cells were selected for using 2 μg/mL of puromycin (Acros Organics, Pittsburgh, PA), and expanded in culture. To quantitate knockdown of Tyr mRNA and protein, infected cells were harvested for quantitative RT-PCR and western blot analysis as previously described [35].

Knock-in of a doxycycline-inducible shRNA targeting *Tyr*

KH2 cells were cultured on mitotically inactivated primary CD-1 mouse embryonic fibroblasts as described [36]. Short-hairpin RNAs were cloned into the pCol1a1 FLP-in vector [33, 37]. The shRNA was integrated immediately downstream of the *Col1a1* locus via FLPe-mediated homologous recombination (HR) via the single Frt site integrated at the mouse *Col1a1* locus [36]. Approximately 2 x 10^7 KH2 ES cells were electroporated with a mixture of 20 μg of the shRNA-containing vector and 10 μg of pCAGGS-FLPe-puro (Addgene) [38]. Selection for

HR was performed using hygromycin (150 μg/ml) beginning 48 hours post-electroporation. Correct targeting of the *Col1a1* locus in KH2 cells with the pCol-TGM vector reconstitutes the start codon for an existing hygromycin expression cassette. Sixteen independent hygromycin resistant clones were picked and expanded for Southern analysis. Targeted cells were trypsinized to single cell suspension and injected into C57BL/6NTac blastocysts and surviving embryos implanted into pseudo-pregnant ICR foster moms. Chimeric offspring were identified by agouti coat color.

Generation of *Tyr*-shRNA mutant mice on a variety of coat-color and transactivator backgrounds

All experiments involving mice conform to the Guide for the Care and Use of Laboratory Animals, 8th edition (National Academies Press, Washington, D.C.) and were approved by the Institutional Animal Care and Use Committee (IACUC) of the University of California, Irvine, approval number 2011-3020. Mice were anesthetized via injection with a sterile sodium chloride solution of 10 mg/mL ketamine and 1.25 mg/mL xylazine solution in the lower ventral area. Mice were euthanized by inhalation of carbon dioxide followed by exsanguination. Mice were housed in our approved animal facility with 12-hour light cycles. Food and water were provided ad libitum. Animals were monitored daily, and any mice exhibiting signs of distress were euthanized. The KH2 ES cell line was derived from a 129S4 x C57BL/6J F1 embryo. Four month old male ES cell chimeras, confirmed by genotyping to contain the *Tyr*-shRNA and the reverse tetracycline transactivator rtTA2, were crossed with four-month-old C57BL/6J females (stock number 000664, Jackson Laboratory, Bar Harbor, ME) to produce 129S4; C57BL/6J N2

progeny with the following genotypes: wild-type, *Tyr*-shRNA alone, rtTA2 alone, or *Tyr*-shRNA and rtTA2 together. These animals were then used to introduce the *Tyr*-shRNA/R26-rtTA2 transgenes onto three different coat color backgrounds (i.e. white-bellied agouti (A^w), yellow agouti (A^y), or non-agouti (*a/a*, black) using the following breeding strategies. Non-agouti 129S4; C57BL/6J N2 mice containing *Tyr*-shRNA and rtTA2 were bred with white-bellied agouti 129S1/SvImJ (Jackson Lab, stock number 002448) mice or yellow-agouti B6.Cg-A^y/J mice (Jackson Laboratory, stock number 000021). Agouti (A^w/+or A^y/+) progeny containing the appropriate transgenes were intercrossed for four generations to generate progeny with an agouti (A^w, or A^y) coat color and *Tyr*-shRNA and rtTA2 transgenes having the following overall strain background composition; 37.5% B6J, 12.5% 129S4, 50% 129S1 (for animals derived from crosses with 129S1/ImJ); or 87.5% B6J, 12.5% 129S4 for animals derived from crosses with B6.Cg-A^y/J mice. Transgenic mice positive for both *Tyr*-shRNA and CAG-rtTA3 were generated by crossing agouti C57BL/6J N2 progeny containing only the *Tyr*-shRNA transgene with B6N.FVB(Cg)-Tg(CAG-rtTA3)4288Slowe/J mice (Jackson Laboratory, stock number 016532). Non-agouti *Tyr*-shRNA and CAG-rtTA3 positive progeny from this mating (essentially N3 for B6) were then crossed with C57BL/6J mice, and offspring (essentially N4 for B6) containing both rTTA3 and Tyr-shRNA transgenes were intercrossed for four generations generating non-agouti mice with a composition of 93.75% C57BL/6; 6.25% 129S4. Similarly, N3 C57BL/6 non-agouti transgenic mice positive for both Tyr-shRNA and CAG-rtTA3 were crossed to yellow-agouti B6.Cg-A^y/J mice, and resulting A^y/+ progeny were intercrossed for four generations giving a final composition of 93.75% C57BL/6; 6.25% 129S4. To minimize genetic variability, all comparisons were performed using littermates. Activation of the *Tyr*-shRNA was

initiated at the time of conception for all mice, as breeding transgenic males and females were maintained on a 600 mg/kg doxycycline chow (Bio-Serv, Flemington, NJ).

Genotyping of Mutant Mice

DNA was extracted from tail biopsies taken at P21 using the Quick Genotyping^{TM} DNA Preparation Kit (Bioland Scientific, LLC, Paramount, CA) according to the manufacturer's instructions. Genomic DNA was used to genotype the mice for germline transmission of (i) the *Tyr* shRNA or the *Luc* shRNA and (ii) the specific rtTA transactivator (R26-rtTA2 or CAG-rtTA3). The mice were also genotyped at the *Col1a1* locus. A 2x Taq PCR Premix (Bioland Scientific) was used for all genotyping reactions. All PCR products were separated through a 2% (wt/vol) agarose gel. The expected sizes of the DNA products for each specific genotyping reaction are: *Tyr*-shRNA: 200 bp (with RBG-1 reverse primer); wild-type *Col1a1*: 220 bp; targeted *Col1a1*: 295 bp; ROSA26 wild-type: 500 bp; ROSA26-rtTA2: 300 bp; wild-type rtTA3: 363 bp; mutant rtTA3: 300 bp.

Quantification of Total Melanin in shaved mouse hair using Soluene-350 and Absorbance at 492 nm

Dorsal hairs of mice at P50 or P100 were shaved and 1 mg was dissolved overnight in 1 mL of hot (65°C) Soluene-350 (PerkinElmer) and 10% water. Triplicate 150 µL aliquots for each mouse hair sample were analyzed for absorbance at 492 nm as previously described to generate an average absorbance [39-42]. The values for experimental mice were normalized to

control mice, and percentage of control was calculated. This quantitation method was used only to compare littermates in order to correlate visual appearance of individual mice with melanin accumulation in the hair.

Quantification of Total Melanin, Eumelanin, and Pheomelanin in shaved mouse hair

Dorsal hairs of mice at P50 or P100 were shaved and 20 mg was homogenized with a Ten Broeck homogenizer at a concentration of 10 mg/mL. Duplicate 100 μL aliquots were solubilized in Soluene-350 (PerkinElmer, Waltham, MA) [43], and subjected to alkaline hydrogen peroxide oxidation [44], and hydroiodic acid hydrolysis [42] as previously described. Statistical inference for differences in mean outcomes between rtTA3/*Tyr*-shRNA and control were tested using a two-sample t-test with no assumption of equal variances between groups. All tests were stratified by mouse color (black vs. agouti). A Wald-based 95% confidence interval and corresponding P-value for a test of the null hypothesis of no difference in true means between the groups was computed for each outcome. To assess sensitivity of outlying observations, Wilcoxon rank sum tests were also conducted to assess any qualitative difference in findings. No differences were found. Bar plots depicting the observed mean and standard deviation of each outcome along with dot plots depicting the raw experimental data for each group were produced. All statistical analyses were carried out using the R statistical software package (Ver. 3.2.1; [45]).

RNA isolation and quantitative RT-PCR on cultured cells

RNA isolation and quantitative RT-PCR was employed as previously described [35]. Briefly, a Cells-to-Ct kit (Applied Biosystems, Grand Island, NY) was utilized to lyse the infected B16 cells after selection with puromycin. A high-capacity RNA-to-cDNA kit was then employed to generate cDNA (Applied Biosystems). Solaris qPCR gene expression assays for TYR (AX-012555-00-0200) and β-actin (AX-003451-00-0100) were obtained from Thermo Scientific/Dharmacon RNAi technologies and used with TaqMan Gene Expression Master Mix (Applied Biosystems) to complete the PCR. A 7900HT Fast Real-Time PCR system (Applied Biosystems) and SDS 2.4 (Applied Biosystems) were used to determine C_t values for each sample. Values were normalized to β-actin using the relative quantification mathematical model (Pfaffl) as previously described [32, 35]. A two-tailed Student's *t*-test was employed to determine statistical significance (**$p < 0.01$).

Tissue preparation and immunohistochemistry

Whole mouse skin was harvested from either anesthetized or euthanized mice using a 4-mm round punch biopsy (Sklar Instruments, Westchester, PA) and formalin-fixed for 24-48 hours using a 10% w/v formalin solution (Fisher Scientific, Pittsburgh, PA). Whole mouse eyes were harvested from euthanized mice and cut in half using a feather blade, followed by fixation in 10% formalin solution for 24-48 hours. Whole skin samples and eyes were then dehydrated and embedded in paraffin. Next, 7-μm thick skin and eye sections were de-waxed and rehydrated through a graded series of alcohol washes to water. After application to a microscope slide, all

samples were dried overnight at 37°C. All samples were stained with hematoxylin and eosin to view general structure. For immunohistochemistry, antigen retrieval was carried out by heating slides to 85°C for 15 minutes in 0.01 M citrate buffer (pH 6) on a hot plate. Endogenous peroxidase activity was quenched with Dual Endogenous Enzyme Block (Dako, Carpinteria, CA). Protein block was carried out using a Protein Block Solution (Dako). Skin and eye samples were then incubated with anti-GFP primary antibody overnight at 4°C at a 1:1000 dilution. Subsequently, samples were incubated with biotinylated goat anti-rabbit IgG for 2 hours at room temperature, followed by exposure to avidin-biotin enzyme complex (Vector Laboratories, Burlingame, CA). Signal was developed using diaminobenzidine (DAB) as the enzyme substrate (Dako) with a hematoxylin counterstain, followed by a final dehydration (50% ethanol for one minute, followed by two washed in 100% ethanol for one minute each) and mounting with Permount (Fisher Chemicals) at room temperature.

Immunoblotting- cultured cells

Puromycin-selected B16 mouse melanoma cells were subjected to immunoblotting as previously described [35].

Immunoblotting- whole mouse skin

Whole mouse skin samples were collected from sacrificed mice using a 4 mm punch biopsy (Sklar Instruments) and immediately flash frozen in liquid nitrogen. Skin samples were then ground using a mortar and pestle and lysed in RIPA buffer (Santa Cruz Biotechnologies)

supplemented with 1x protease and phosphatase inhibitor cocktail (Thermo Scientific). Lysates were clarified by centrifugation (18,000 x *g* for 10 min at 4°C). The relative concentration of protein in each lysate was quantified using a BCA Protein Assay Kit (Thermo Scientific). A total of 20 μg of protein per sample was separated on a 4–10% Bis-Tris gel (Life Technologies, Carlsbad, CA) under reducing conditions and transferred onto a 0.45-μm PVDF membrane (Millipore, Billerica, MA). Membranes were soaked in a blocking buffer solution composed of TBS (Fisher Scientific), 0.1% Tween-20 (Fisher Scientific) and 5% Apex (Genesee Scientific, Carlsbad, CA) non-fat milk powder. To assess immunoreactivity, either Luminata Forte chemiluminescent detection substrate (Millipore) or HyGLO Quick spray (Denville, Holliston, MA) was used. Protein levels were assessed via densitometry analysis using ImageJ (NIH) [46].

Electron Microscopy

Whole mouse skin (*n*=2 per genotype) was harvested from either anesthetized or euthanized mice using a 4-mm round punch biopsy and fixed in half-strength Karnovsky's fixative [47] for 24 hours before being transferred to sodium cacodylate buffer, 0.2M, pH 7.4 (Electron Microscopy Sciences, Hatfield, PA). Tissue was then post-fixed with 1% osmium tetroxide containing 1.5% potassium ferrocyanide. After dehydration, tissues were embedded in EPON and sections were obtained using a RMC-MT6000XL ultra-microtome and stained with uranyl acetate and lead citrate. Sections were viewed and selected images were digitally photographed using a JEOL JEM-1230 transmission electron microscope. For DOPA histochemistry and prior to post-fixation, tissues were incubated in a 0.1%solution of L-DOPA twice for 2.5 hours. The tissues were washed and processed as described above. To assess

melanosome maturation, the percentage of melanosomes in the four maturation stages was calculated visually in the electron micrographs in the knockdown and control mice using 12 melanocytes from 2 mice per group totaling ~400 melanosomes per mouse. To differentiate between Stage III and Stage IV melanosomes, stage III melanosomes were characterized as having some melanin deposition and observable melanofilaments, while stage IV melanosomes were categorized as having dark melanin and no observable melanofilaments aberrant or not in morphology.

RNA isolation on whole mouse skin and Nanostring nCounter Analysis

Whole mouse skin (*n*=3 per genotype) was harvested from either anesthetized or euthanized mice using a 4-mm round punch biopsy and immediately stabilized overnight in RNAlater RNA stabilization reagent (Life Technologies) at 4°C. Skin samples were homogenized using the Precellys24 high-throughput tissue homogenizer (Precellys, Bertin Corporation, Rockville, MD) in hard tissue homogenizing reinforced tubes that contain 2.8 mm ceramic beads (Bertin Corporation). After homogenization, RNA was extracted from each sample using the RNeasy Fibrous Tissue Mini Kit according to the manufacturer's instructions (Qiagen, Valencia, CA). The quantitative analysis of mRNA was carried out using the nCounter Nanostring Technology (NanoString Technologies, Seattle, WA). NanoString's nCounter technology is based on direct detection of target molecules using color-coded molecular barcodes, providing a digital simultaneous quantification of the number of target molecules. All data were normalized to 3 housekeeping genes quantified in the same samples. Total mRNA (100ng in 5µl) was hybridized overnight with nCounter Reporter (20µl) probes in hybridization

buffer and in excess of nCounter Capture probes (5μL) at 65°C for 16–20h. The hybridization mixture containing target/probe complexes was allowed to bind to magnetic beads containing complementary sequences on the Capture Probe. After each target found a probe pair, excess probes were washed followed by a sequential binding to sequences on the Reporter Probe. Biotinylated capture probe-bound samples were immobilized and recovered on a streptavidin-coated cartridge. The abundance of specific target molecules was then quantified using the nCounter Digital Analyzer. Individual fluorescent barcodes and target molecules present in each sample were recorded with a CCD camera by performing a high-density scan (1155 fields of view). Images were processed internally into a digital format and were normalized using the NanoString nSolver software analysis tool. Counts were normalized for all target RNAs in all samples based on the positive control RNA to account for differences in hybridization efficiency and post-hybridization processing, including purification and immobilization of complexes. The average was normalized by background counts for each sample obtained from the average of the eight negative control counts. Subsequently, a normalization of mRNA content was performed based on six internal reference housekeeping genes, including *Gapdh*, β-*Actin* and *Hprt* using nSolver Software.

2.5 Results

Modulation of *Tyr* expression alters the phenotypic appearance of the mouse hair

To develop a model to study pigment diversity *in vivo*, we generated a murine model where we could selectively modulate the expression of any gene using a tet-regulatable single-copy shRNA linked to a GFP reporter [37]. First, we utilized an algorithm [34] to identify two shRNA sequences that could effectively silence *Tyr*. Lentiviral constructs that expressed *Tyr* shRNA or *non-targeting* scrambled shRNA (negative control) were used to infect B16 mouse melanoma cells at a MOI of 0.1 to ensure that each cell was only infected with one lentivirus (single copy shRNA) [37]. Quantitative RT-PCR, western blot, and densitometry confirmed that one of the two tested shRNAs (*Tyr*-shRNA #1) efficiently suppressed *Tyr* mRNA (Fig. 1A, left panel) and protein expression (Fig. 1A, right panel). *Tyr*-shRNA #1 was cloned into the pCol-TGM targeting vector [36] (hereafter referred to as pCol-TGM-*Tyr* shRNA; Fig. 1B). To introduce the *Tyr*-shRNA into the mouse genome immediately downstream of the *Col1a1* locus, pCAGGS-Flpe and pCol-TGM-*Tyr* shRNA were co-electroporated into KH2 mouse embryonic stem cells to generate Flpe-mediated recombination between the Frt site at the *Col1a1* locus and the Frt site on the targeting vector (Fig. 1B). After recombination, the tetracycline response element (TRE), GFP, and *Tyr*-shRNA are all inserted downstream of the *Col1a1* locus in chromosome 11 in the KH2 cells (Figure 1B), a C57BL/6J x 129S4 F1 (agouti) ES cell line that is pre-engineered to express a reverse tet-trans-activator from the ROSA26 locus on chromosome 6 [36]. Southern blot analysis confirmed the correct integration of the *Tyr*-shRNA into the *Col1a1* locus in 12/12 clones tested (S1A Fig.). Modal chromosome number was verified in a

sub-set of clones that were then injected into C57BL/6NTac blastocysts, and implanted into CD-1 pseudo-pregnant female foster mice. Chimeric male agouti mice confirmed to contain both the R26-M2rtTA (hereafter referred to as rtTA2) and the *Tyr*-shRNA via genotyping were then bred to eight-week old C57BL/6J females. To verify that the *Tyr*-shRNA was expressed in the hair in a doxycycline-dependent manner, breeding pairs were placed on a 600 mg/kg doxycycline chow prior to conception of litters. Resultant pups were shaved at post-natal day (P) 50 and GFP expression within the hair was monitored by fluorescence microscopy. *Tyr*-shRNA/rtTA2 (*Tyr*-knockdown mice) mice but not *Tyr*-shRNA (control mice) mice exhibited robust expression of GFP in the hair, indicating that *Tyr*-shRNA is expressed within the hair in a tet-regulatable manner (S1B Fig., two left columns).

Having established a system to induce the expression of *Tyr*-shRNA in the hair, we next investigated whether depleting TYR in the hair and skin of *Tyr*-knockdown mice could modulate coat color similarly in mice containing different coat color compositions. To do so, we bred *Tyr*-shRNA;rtTA2 chimeric mice with mice having agouti (A^w) backgrounds and yellow agouti (A^y) as described in methods. We also bred *Tyr*-shRNA mice with mice expressing the CAG-rtTA3 (rtTA3) tet-transactivator protein, which is more effective than the rtTA2 transactivator at driving expression of tet-regulatable elements *in vivo* [48]. The rtTA3 transgene was introduced to non-agouti (black) (*a/a*) and yellow agouti (A^y/+) backgrounds as described in methods. Initial studies showed *Tyr*-shRNA/rtTA2 and *Tyr*-shRNA/rtTA3 mice to be fully viable, fertile, and without obvious developmental defects. Pregnant animals and their offspring were fed doxycycline, and progeny were photographed at P50 to make a comparison of coat color in littermates before being shaved and depilated. The shaved hair was dissolved overnight in hot Soluene-350 in 10% water as described in the methods and the absorbance of the dissolved hair

was measured at 492 nm, a wavelength at which both eumelanin and pheomelanin absorb [39-43]. These comparisons were done to correlate visual differences observed in individual mice with differences in overall melanin accumulation. We first analyzed the difference between *Tyr*-shRNA/rtTA2 mice maintained on a doxycycline (+ DOX) diet or a non-doxycycline (-DOX) regular diet. Yellow agouti *Tyr*-shRNA/rtTA2 mice on a doxycycline diet consistently demonstrated lighter coat colors compared to *Tyr*-shRNA/rtTA2 littermates fed diet without doxycycline, both visually and spectrophotometrically at P50 (Fig. 1C, compare far left mouse with far right mouse, numbers below the pictures correspond only to mice depicted). Similarly, partial depletion of *Tyr* in a white-bellied agouti coat-color background inhibited pigment accumulation in the mouse hair as two littermates with the genotype *Tyr*-shRNA/rtTA2 displayed lighter pigmentation compared to their *Tyr*-shRNA control littermate at P50 (Fig. 1D). The agouti *Tyr*-knockdown mice demonstrated 15% and 30% less absorbance at 492 nm compared to the *Tyr*-shRNA (without rtTA2) littermate control, demonstrating that partial *Tyr* depletion moderately inhibits pigment accumulation in the hair (Fig. 1D, percentage values below the images correspond only to mice depicted in the images). Non-agouti (black) *Tyr*-shRNA/rtTA3 littermates fed doxycycline also exhibited significant lightening of coat color after P50 that was dependent on genotype (Fig. 1E). Moreover, GFP was easily detected in the hair shaft of *Tyr*-shRNA/rtTA3 black mice, demonstrating the efficiency of the rtTA3 driver (S1B Fig., two right columns). Yellow agouti *Tyr*-shRNA/rtTA3 mice had more pronounced lighter coats and a 40% decrease in pigment accumulation compared with control littermates (Fig. 1F, percentages only correspond to littermates shown in the picture). Intriguingly, these mice also developed green eyes (Figure 1F, right panel). Fluorescence microscopy (S1C Fig.) and immunohistochemistry (S1D Fig.) revealed that this phenotype was related to deposition of GFP

within the mouse lens. Importantly, despite variability in the extent of coat lightening in Dox-fed *Tyr*-shRNA; rtTA (2 or 3) mice compared to their littermates, we never observed a lighter coat color in *Tyr*-shRNA single transgenic animals compared with their *Tyr*-shRNA; rtTA double transgenic littermates. Taken together, these results indicate that partial depletion of *Tyr* using inducible shRNAs can consistently modulate pigment accumulation in the hair of mice.

To investigate how the partial depletion of *Tyr* impacts melanin accumulation, we quantified melanin accumulation in hairs of mice containing primarily black coat composition and primarily agouti coat composition using established chemical methods [41, 42, 44, 49]. A comparison of five non-agouti (black) *Tyr*-shRNA/rtTA3 mice with five control mice all maintained on Dox demonstrated that partial depletion of *Tyr* leads to a 10% reduction in eumelanin content (Table 1). Dot plots of the raw experimental data revealed that this observation was not a result of outliers within the dataset (S2 Fig.). While *Tyr*-shRNA expression did inhibit eumelanin accumulation in the hair of mice with black coats, the observed differences did not reach statistical significance secondary to the intrinsic variation in eumelanin accumulation observed within experimental mice from different litters. A comparison of 13 agouti *Tyr*-shRNA/rtTA2 mice with 13 agouti control mice, however, yielded no difference in eumelanin accumulation (Table 2), and only an insignificant increase in pheomelanin accumulation (Table 2). A plot of the raw data and secondary sensitivity analyses revealed that these results were not influenced by outliers within the experimental dataset (S3 Fig.). It is conceivable that significant differences were not seen in the agouti background because the rtTA2 element is known to be less effective at inducing the expression of shRNA *in vivo* [48] suggesting that *Tyr* knockdown was not as robust as that observed in the rtTA3 mice.

Disruption of *Tyr* alters the deposition of melanin within the melanosome

To better assess how effectively our *Tyr*-shRNAs could inhibit TYR expression *in vivo*, we performed a more detailed analysis of the expression of the *Tyr*-shRNA and TYR in *Tyr*-shRNA/rtTA2 and *Tyr*-shRNA/rtTA3 knockdown mice. To do so, we performed western blot analysis on skin harvested at P50 from *Tyr*-shRNA/rtTA3 knockdown mice and *Tyr*-shRNA control mice. Western blot analysis indicated knockdown of TYR with simultaneous substantial expression of GFP, providing evidence of *Tyr* knockdown in the skin tissue (Fig. 2A). Densitometry analysis showed a 65%-73% reduction in TYR protein (Fig. 2A, numerical values under TYR protein bands). We also utilized harvested skin from mice at P50 and performed immunohistochemistry using an anti-GFP antibody. When compared to rtTA2, rtTA3, or *Tyr*-shRNA only littermate controls, *Tyr*-shRNA/rtTA2 and *Tyr*-shRNA/rtTA3 mice showed robust staining of GFP in the epidermis and the hair follicle in all coat color backgrounds, confirming co-expression of *Tyr*-shRNA when mice are fed a doxycycline diet (Fig. 2B). GFP expression co-localized with Melan-A expression, indicating that GFP is expressed in melanocytes (Fig. 2C).

Having determined how efficiently the *Tyr*-shRNA could inhibit TYR expression, we next sought to examine whether loss of endogenous *Tyr* affects the structure of the melanosome. Fresh skin harvested from *Tyr*-knockdown mice and appropriate littermate controls on both the white-bellied agouti background and the yellow agouti background were analyzed by transmission electron microscopy (TEM; Fig. 3). The respective littermate controls had normal early and late-stage melanosomes that were round with smooth, fibrillar deposits of melanin (Fig. 3A, top row, center & right). By contrast, skin from the *Tyr*-knockdown mice

demonstrated clearly irregular melanin deposition within the early-stage melanosomes unlike the even striations of melanin seen within the melanosomes of the control littermate (Fig. 3A, middle row, center and right images). Additionally, depletion of *Tyr* inhibited the maturation of the melanosome, as more stage III, but less stage IV melanosomes were present in *Tyr*-knockdown mice on both agouti coat color backgrounds (Fig. 3B, center & right graphs). The melanin in these late stage melanosomes also do not exhibit a smooth peripheral contour suggesting melanin was accumulating around intraluminal vesicles (Fig. 3A, middle row, insets of center and right images).

To determine if irregular melanin deposition occurs in black mice when *Tyr* is reduced, we harvested fresh skin from *Tyr*-shRNA/rtTA3 mice and control littermates on the black coat background. As before, the control mice displayed normal deposition of melanin within oval melanosomes (Fig. 3A, top row, left image and inset). However, the *Tyr*-knockdown mice displayed abnormal melanin deposition in late-stage melanosomes, and late stage melanosomes did not exhibit a smooth peripheral contour suggesting melanin was accumulating around intraluminal vesicles (Fig. 3A, middle row, inset of left image). As with *Tyr*- knockdown mice on the white-bellied agouti and yellow agouti background, we observed that black *Tyr*-knockdown mice possessed significantly fewer stage IV melanosomes compared to littermate controls and significantly more stage III melanosomes, suggesting that TYR is required for complete melanin deposition within the melanosome as well as maturation of the melanosome (Fig. 3B, left graph). These ultra-structural observations suggest that knockdown of endogenous *Tyr* may have a more drastic effect on the morphology of the melanosome in agouti and yellow agouti mice then in black mice (Fig. 3A, compare inset of middle image in left column to insets of middle images in center and right columns). However, upon addition of DOPA, the irregular

melanin deposition in the *Tyr*-knockdown mice in all three genotypes was not apparent. Instead, the melanosomes resembled the melanosomes of the respective control littermates (Fig. 3A, compare top row images to bottom row images). These results indicate that the block in melanosome maturation could be overcome *in vitro* by adding unlimited substrate. To verify that the differences observed were not secondary to differences in melanosome density between *Tyr*-knockdown mice and control mice, we quantified and averaged the number of melanosomes per one hundred microns^2 in fifteen melanocytes from two mice per group. We found no significant differences in the melanosome density between *Tyr*-knockdown mice and controls in all three coat colors, demonstrating that while the partial depletion of *Tyr* is sufficient to decrease total amount of stage IV melanosomes, it is not sufficient to alter the total number of melanosomes (S1 Table).

While melanosome maturation occurs predominantly in the Golgi area, mature melanosomes are localized to the dendritic processes [16, 23]. As the observed phenotype in the *Tyr*-knockdown mice was restricted to terminal melanosomes, we examined the morphology of melanosomes in the dendritic tips of melanocytes. While the melanosomes in the dendrites of the control mice displayed a normal morphology (S4A Fig., upper row), melanosomes in the dendrites of *Tyr*-knockdown mice of all three coat colors displayed the same ruffled morphology as was visualized in the Golgi area (S4A Fig., lower row).

The observed phenotypes are reversible and not a consequence of shRNA expression

To verify that the phenotypes observed in our *Tyr*-knockdown mice were not due to possible side effects caused by GFP expression, we generated mice on the black background that

expressed an shRNA directed towards *Luciferase* (*Luc*), a gene that is not expressed in the mouse. First, we examined *Luc*-knockdown mice and appropriate control mice and determined that there were no visual differences in coat color between the two groups (Fig. 4A). Next, we analyzed shaved hairs from *Luc*-knockdown mice and control mice using the previously described melanin assay and found no differences in absorbance at 492 nm, indicating that expression of GFP does not affect the production of melanin within the mouse hair follicle (Fig. 4A, percentage values below image). To determine whether the expression of a control shRNA or GFP affected the deposition of melanin within the melanosome, fresh skin harvested from *Luc* shRNA/rtTA2 mice and appropriate *Luc*-shRNA controls on the black background and was analyzed by TEM. Melanosomes from *Luc*-shRNA/rtTA2 mice demonstrated no differences in morphology when compared to melanosomes obtained from *Luc*-shRNA only mice (Fig. 4B). Both the *Luc*-shRNA and the *Luc*-shRNA/rtTA2 mice contained appropriate numbers of both early and late stage melanosomes, with stage IV melanosomes comprising the majority of the total melanosome number (Fig. 4C).

The partial depletion of *Tyr in vivo* affects the expression of key genes involved in melanogenesis

To assess whether the partial depletion of *Tyr* affected the expression of genes that play key roles in melanogenesis, we harvested fresh whole mouse skin using a 4-mm round punch biopsy and subjected the extracted RNA to Nanostring nCounter analysis. Interestingly, knockdown of *Tyr* resulted in a slight decrease in the expression levels of *Dct, Pmel5,* and *Mart1* compared to control samples (Fig. 5A). *Tyr* depletion lead to a significant decrease in the

expression levels of *Mitf-M, Sox10, Tyrp1* and, as expected, *Tyr* (Fig. 5A). These results indicate that the mechanism by which *Tyr* depletion impacts the deposition of melanin within the melanosome is secondary to an effect of TYR levels on the expression of other melanogenesis genes. Finally, depletion of *Luc* produced no significant change in expression of the same genes analyzed in *Tyr*-KD mice, demonstrating that the changes in expression resultant upon *Tyr* knockdown are specific to *Tyr* depletion (Fig. 5B).

To better understand how *Tyr* knockdown affects the expression of *Mitf-M, Sox10*, and *Tyrp1*, we compared the expression of these genes and *Tyr* between C57BL/6J wild-type mice and Tyr^{c}/Tyr^{c} mice, which express a mutant form of TYR that is trapped in the ER [50]. Interestingly, Tyr^{c}/Tyr^{c} mutant mice did not have decreased expression of *Tyr, Sox10, Mitf-M,* or *Tyrp1* (Fig. 5C), suggesting that the phenotypes observed in our *Tyr* knockdown mice were a direct consequence of reduced wild-type *Tyr* mRNA or a consequence of decreased levels of TYR in the melanosome. We had previously observed that siRNA-mediated *Tyr* knockdown also inhibited MITF expression, and validated that this phenotype could be recapitulated by three different siRNAs (S5 Fig.). Taken together, these results suggest that the effects of *Tyr* knockdown on MITF were not an off-target phenomenon *in vitro*, making it less likely that the phenotypes observed with the *Tyr*-shRNA *in vivo* were an off-target phenomenon.

Finally, to further verify that the observed phenotypes *in vivo* were reversible, we performed a longitudinal study in which we monitored coat color in three littermates during and after the administration of a doxycycline diet. At P50, the two *Tyr*-knockdown white-bellied agouti mice demonstrated less pigment in their hair both visually (Fig. 5D, left upper image) and spectrophotometrically (numerical values below image, 12.4% and 30% less absorbance at 492 nm when compared to the littermate control, respectively). The *Tyr*-knockdown mice also

exhibited visually less pigment in their tails when compared to their littermate control while on a doxycycline diet (Fig. 5D, left lower image). At P110, mice were returned to a normal diet without doxycycline. Sixty days after removing doxycycline, the coat color of the *Tyr*-knockdown mice began to return to levels comparable to the control littermate (Fig. 5D, middle upper image). At this point, we utilized shaved hair samples to establish that both *Tyr*-knockdown mice had no differences in absorbance at 492 nm when compared to the *Tyr*-shRNA alone littermate (Fig. 5D, percentage values below image). While there were no differences in hair pigmentation at P110, there was still less pigment in the tails of the *Tyr*-knockdown mice as compared to their littermate controls (Fig. 5D, lower middle image). At 90 days post doxycycline removal, neither *Tyr*-knockdown mouse showed any visible differences in coat or tail pigmentation when compared to the control littermate, demonstrating the reversibility of the tet-inducible shRNA-knockdown mouse model (Fig. 5D, upper and lower right images). Similar to our observations at 60 days post doxycycline removal, absorbance values at 492 nm for both *Tyr*-knockdown mice were at control levels at 90 days post doxycycline removal (Fig. 5D, numerical values below right image). Taken together, these studies indicate that the phenotypes observed in the *Tyr*-knockdown mice are reversible.

2.6 Discussion

This study demonstrates the utility of a conditional and reversible gene expression knockdown system to investigate the partial loss of function of gene products involved in pigmentation in an experimental system. Human skin pigmentation is a highly complex trait that relies upon the interaction of numerous gene products and environmental influences to generate the observed phenotype. Despite the complete sequencing of the human genome and recent functional genomic studies that have identified novel genes that affect pigment production *in vivo*, it is still not fully understood how pigment gene diversity leads to skin color diversity. To gain a deeper understanding of how alterations in individual genes contribute to pigment diversity, we employed a novel inducible shRNA mouse model to subtly alter TYR protein levels *in vivo*. Depletion of 65-75% of endogenous TYR (Fig. 2A) reduced the amount of eumelanin produced in the black mouse coat albeit not significantly (Table 1 and S2 Fig.). Depletion of *Tyr* in agouti mice resulted in a slight increase in pheomelanin with no observable change in eumelanin accumulation (Table 2 and S3 Fig.). Pairwise comparisons between control and *Tyr*-knockdown littermates demonstrated visual coat color differences as well as differences in absorbance at 492 nm (Figs. 1C-1F), but advanced chemical methods showed no statistically significant difference in total melanin content when all mice from a particular coat color were considered (Tables 1 and 2). The lack of statistical significance is most likely due to the variation in melanin accumulation between mouse litters and the variability of *Tyr* knockdown in the inducible shRNA mouse model. Interestingly, we found that the experimental agouti mice with *Tyr* knockdown demonstrate a slight increase in pheomelanin pigment when compared with their control counterparts. Although this observation requires more analysis, it

might implicate a role for TYR protein in regulating the eumelanin to pheomelanin switch, as has been suggested by other studies [51, 52]. Other published studies using inbred mouse strains have demonstrated a role for *Tyrp1* in specifically regulating pheomelanin production [39]. Therefore, the increased pheomelanin observed in this mouse background could be secondary to the effect of the shRNA on *Tyrp1* in this particular strain background. Future studies will be needed to confirm the relationship between *Tyr* and *Tyrp1* knockdown and the eumelanin to pheomelanin switch.

Extensive studies have characterized mutations at the *Tyr* (albino) locus in mice. Multiple mutations within the gene have demonstrated the functions and interactions of TYR with other proteins [53]. Surprisingly, none of the readily available mutations that have been characterized address how modulation of *Tyr* expression may contribute to melanin deposition within the melanosome. Some mutations within the *Tyr* gene result in an albino phenotype associated with lack of TYR activity, including the Tyr^{c}/ Tyr^{c} and $Tyr^{c\text{-}2J}$/ $Tyr^{c\text{-}2J}$ homozygous strains [50]. However, both mutations are considered null as the mutated protein is inactive *in vivo* and is retained within the endoplasmic reticulum, thus prohibiting an understanding of how changing levels of TYR may affect melanin deposition [50]. Similarly, the spontaneous *platinum* mutation in the *Tyr* locus produces mice that are very pale with pink eyes in the C57BL/6 background ($Tyr^{c\text{-}p}/Tyr^{c\text{-}p}$) [50]. Mice with this mutation possess a TYR protein that is mutated at the carboxy terminal of the protein [54, 55]. This mutation leads to the presence of a premature stop codon and lack of the essential di-leucine protein sorting motif on the cytoplasmic tail, which causes misrouting of TYR to the cell surface as opposed to the proper melanosomal location [54, 56]. Thus, although the *platinum* mutation leads to decreased melanin in the mouse coat, it does not allow for an analysis of how changing levels of TYR may affect melanin deposition. A third

spontaneous mutation in the *Tyr* locus, *Himalayan*, leads to a beige coat color phenotype in conjunction with darker pigmentation on the extremities [57]. Although an excellent model to study thermosensitive protein function, it is not helpful in understanding how TYR contributes to diversity in pigmentation. Finally, the *chinchilla* mouse mutant ($Tyr^{c\text{-}ch}/Tyr^{c\text{-}ch}$) results from a G-to-A point mutation at nucleotide +1523, which leads to the substitution of alanine for threonine at position +482 [58]. These mice are very phenotypically similar to mice that are wild-type at the *Tyr* locus, possessing black eyes and a very dark gray hair coat [50]. Interestingly, *chinchilla* mice have greatly reduced TYR activity (three-fold) [50] and it has been suggested that *chinchilla* TYR is less stable than that of the wild-type enzyme [59]. TEM studies on *chinchilla* hair bulb melanocytes showed a large number of stage II-III melanosomes without melanin deposition [60] also implicating a role for TYR in influencing melanosome maturation.

In this study we examine the consequences of partial depletion of wild-type *Tyr* mRNA and protein on melanin accumulation and melanosome maturation. Using our shRNA transgenic system, we partially deplete TYR protein at a level that is sufficient to alter coat color but not sufficient to significantly alter melanin accumulation (Figs. 1C-1F, 2A, Tables 1-2). Ultrastructural analysis revealed that the melanosomes within these mice did not have a smooth peripheral contour, suggesting that melanin is accumulating around intraluminal vesicles within melanosomes (Fig. 3A). TYR has been suggested to localize to intraluminal vesicles within melanosomes [61] and roles for intralumenal vesicles as sites of melanin deposition have been described previously [62, 63]. Taken together, these results support a model in which levels of TYR protein within the stage III melanosome can influence both the pattern and degree of melanin deposition within the fully-pigmented stage IV melanosomes *in vivo*. These observations are distinctly different from the albino mice described in the literature, which did

not exhibit a similar phenotype most likely because they had no TYR within the melanosome. Finally, our findings that the partial depletion of TYR affects the structure of the melanosome and furthermore the visual coat color in mice also correlate well with previous research showing that the modulation of the pattern of melanin deposition within the melanosome in wild turkeys and violet-backed starlings leads to a diversity in plumage color [64].

To investigate the etiology of this melanosome phenotype further, the gene expression pattern of *Tyr* shRNA transgenic mice, *Luc* shRNA transgenic mice, Tyr^c/Tyr^c mice, and C57BL/6J mice were compared. Gene expression analysis determined that *Tyr* depletion significantly modulated the expression of *Mitf-M*, *Sox10*, and *Tyrp1* (Fig. 5A) while *Luc* shRNA had no effect on the expression of *Mitf-M*, *Sox10*, and *Tyrp1* (Fig. 5B). These results indicate that the effects of the shRNA on *Mitf-M*, *Sox10*, *and Tyrp1* were not a consequence of the overexpression of shRNA or GFP in the hair of the *Tyr*-knockdown mice. To determine whether the effects of the *Tyr*-shRNA on these genes were a consequence of decreased *Tyr* expression or decreased TYR activity in the melanosome, we compared the expression of these genes between isogenic Tyr^c/Tyr^c mice and C57BL/6 mice (Fig. 5C). Interestingly, we observed that there was no change in *Mitf-M*, *Sox10*, nor *Tyrp1* between these mice. Previously published work demonstrated that *Tyr* depletion in MNT-1 cells using multiple different siRNAs (S5 Fig.) also inhibited *MITF-M* expression [32]. While it is still conceivable that the observed phenotype in our *Tyr* knockdown mice is an unpredicted *in vivo* specific off target effect, the gene expression relationship uncovered by our studies is more likely a consequence of the decreased level of tyrosinase mRNA/protein within the melanosome of these mice. Other published studies have demonstrated that overexpression of *Tyr* in fibroblasts is sufficient to induce the formation of melanin and melanosomes [65], identifying a role for *Tyr* expression in driving the expression of

other melanosome genes. Taken together, these results are consistent with a potential role for either *Tyr* mRNA levels or the level of TYR within the melanosome as modulators of the expression of other melanosome components, specifically *MITF-M,* which regulates the expression of many genes that modulate melanosome structure [66-69]. These observations are consistent with other studies that have also suggested that inhibiting melanosome maturation can feedback to regulate the expression genes involved in melanogenesis [70, 71].

The inducible and reversible shRNA mediated knockdown transgenic mouse model has several advantages over existing experimental systems. First, the model can be generated rapidly by directed recombination once a suitable shRNA sequence targeting the relevant pigment gene is identified [33]. Second, when the shRNA containing mice are crossed with mice expressing the CAG-rtTA3 driver, the double-transgenic progeny can express high levels of the shRNA (based on GFP expression) in the hair follicle and epidermis under the tight control of a doxycycline-inducible promoter (Fig. 2B). Intriguingly, the CAG-rtTA3 driver is not only efficient at driving shRNA expression within the epidermis but can also drive shRNA expression in the mouse lens (S1C-D Figs.), enabling investigators to study the function of proteins within the lens. Most importantly, this model generates partial loss-of-function phenotypes in contrast to the complete loss of function phenotypes observed in knockout mice. This unique feature allows investigators to quantify the impact of depletion of mRNA and protein on melanogenesis that normally could not be studied in null or conditional mutant null models because the knockout is lethal. On the other hand, this feature also makes these mice slightly more troublesome to characterize, as the level of shRNA expression and knockdown can vary between experimental animals. Despite these limitations, we illustrate the power of this model by using it to demonstrate that TYR controls the pattern of melanin deposition within the melanosome.

Future studies will utilize this system to better quantify the relative contributions of individual genes to pigment diversity *in vivo*.

2.7 Acknowledgements

We thank Scott W. Lowe for providing us with the reagents to generate the shRNA transgenic mice reported in this work. We thank the University of California Irvine's Transgenic Mouse Facility (TMF) for help in generating the *Tyr*-knockdown mice, the Genomics High Throughput Facility (GHTF) for help with the Nanostring experiments and the Biostatistics Shared Resource (BSR) for statistical analysis of results. The TMF, GHTF and BSR Shared Resources are funded in part by the Chao Family Comprehensive Cancer Center Support Grant (P30CA062203) from the National Cancer Institute.

2.8 References

1. Jablonski NG, Chaplin G. The evolution of human skin coloration. Journal of human evolution. 2000;39(1):57-106.

2. Jablonski NG. The evolution of human skin and skin color. Annual Review of Anthropology. 2004:585-623.

3. Loomis WF. Skin-pigment regulation of vitamin-D biosynthesis in man. Science. 1967;157(3788):501-6. PubMed PMID: 6028915.

4. Gloster HM, Jr., Brodland DG. The epidemiology of skin cancer. Dermatologic surgery : official publication for American Society for Dermatologic Surgery [et al]. 1996;22(3):217-26. PubMed PMID: 8599733.

5. Armstrong BK, Kricker A, English DR. Sun exposure and skin cancer. The Australasian journal of dermatology. 1997;38 Suppl 1:S1-6. PubMed PMID: 10994463.

6. Slominski A, Tobin DJ, Shibahara S, Wortsman J. Melanin pigmentation in mammalian skin and its hormonal regulation. Physiological reviews. 2004;84(4):1155-228. doi: 10.1152/physrev.00044.2003. PubMed PMID: 15383650.

7. Silvers WK. The Coat Colors of Mice: A Model for Mammalian Gene Action and Interaction. New York: Springer-Verlag; 1979.

8. Jackson IJ. Molecular and developmental genetics of mouse coat color. Annual review of genetics. 1994;28:189-217. doi: 10.1146/annurev.ge.28.120194.001201. PubMed PMID: 7893123.

9. Costin GE, Hearing VJ. Human skin pigmentation: melanocytes modulate skin color in response to stress. FASEB journal : official publication of the Federation of American Societies for Experimental Biology. 2007;21(4):976-94. doi: 10.1096/fj.06-6649rev. PubMed PMID: 17242160.

10. Basrur V, Yang F, Kushimoto T, Higashimoto Y, Yasumoto K, Valencia J, et al. Proteomic analysis of early melanosomes: identification of novel melanosomal proteins. Journal of proteome research. 2003;2(1):69-79. PubMed PMID: 12643545.

11. Prota G. Melanins, melanogenesis and melanocytes: looking at their functional significance from the chemist's viewpoint. Pigment Cell Research. 2000;13(4):283-93.

12. Hearing VJ, Tsukamoto K. Enzymatic control of pigmentation in mammals. FASEB journal : official publication of the Federation of American Societies for Experimental Biology. 1991;5(14):2902-9. PubMed PMID: 1752358.

13. TOYOFUKU K, WADA I, VALENCIA JC, KUSHIMOTO T, FERRANS VJ, HEARING VJ. Oculocutaneous albinism types 1 and 3 are ER retention diseases: mutation of tyrosinase or Tyrp1 can affect the processing of both mutant and wild-type proteins. The FASEB Journal. 2001;15(12):2149-61.

14. Urabe K, Aroca P, Tsukamoto K, Mascagna D, Palumbo A, Prota G, et al. The inherent cytotoxicity of melanin precursors: a revision. Biochimica et biophysica acta. 1994;1221(3):272-8. PubMed PMID: 8167148.

15. Kushimoto T, Basrur V, Valencia J, Matsunaga J, Vieira WD, Ferrans VJ, et al. A model for melanosome biogenesis based on the purification and analysis of early melanosomes. Proceedings of the National Academy of Sciences of the United States of America. 2001;98(19):10698-703. doi: 10.1073/pnas.191184798. PubMed PMID: 11526213; PubMed Central PMCID: PMC58529.

16. Marks MS, Seabra MC. The melanosome: membrane dynamics in black and white. Nature reviews Molecular cell biology. 2001;2(10):738-48. doi: 10.1038/35096009. PubMed PMID: 11584301.

17. Nordlund JJ, Boissy RE, Hearing VJ, King RA, Oetting WS, Ortonne J-P. The pigmentary system: physiology and pathophysiology: Wiley-Blackwell; 2006.

18. Seiji M, Fitzpatrick TB, Simpson RT, Birbeck MS. Chemical composition and terminology of specialized organelles (melanosomes and melanin granules) in mammalian melanocytes. Nature. 1963;197:1082-4. PubMed PMID: 13992623.

19. Seiji M, Shimao K, Birbeck M, Fitzpatrick TB. Subcellular localization of melanin biosynthesis. Annals of the New York Academy of Sciences. 1963;100(1):497-533.

20. Hearing VJ. The melanosome: the perfect model for cellular responses to the environment. Pigment cell research / sponsored by the European Society for Pigment Cell Research and the International Pigment Cell Society. 2000;13 Suppl 8:23-34. PubMed PMID: 11041354.

21. Hurbain I, Geerts WJ, Boudier T, Marco S, Verkleij AJ, Marks MS, et al. Electron tomography of early melanosomes: implications for melanogenesis and the generation of fibrillar amyloid sheets. Proceedings of the National Academy of Sciences of the United States of America. 2008;105(50):19726-31. doi: 10.1073/pnas.0803488105. PubMed PMID: 19033461; PubMed Central PMCID: PMC2604932.

22. Berson JF, Harper DC, Tenza D, Raposo G, Marks MS. Pmel17 initiates premelanosome morphogenesis within multivesicular bodies. Molecular biology of the cell. 2001;12(11):3451-64. PubMed PMID: 11694580; PubMed Central PMCID: PMC60267.

23. Raposo G, Marks MS. Melanosomes--dark organelles enlighten endosomal membrane transport. Nature reviews Molecular cell biology. 2007;8(10):786-97. doi: 10.1038/nrm2258. PubMed PMID: 17878918; PubMed Central PMCID: PMC2786984.

24. Raposo G, Tenza D, Murphy DM, Berson JF, Marks MS. Distinct protein sorting and localization to premelanosomes, melanosomes, and lysosomes in pigmented melanocytic cells. The Journal of cell biology. 2001;152(4):809-24. PubMed PMID: 11266471; PubMed Central PMCID: PMC2195785.

25. Kobayashi N, Nakagawa A, Muramatsu T, Yamashina Y, Shirai T, Hashimoto MW, et al. Supranuclear melanin caps reduce ultraviolet induced DNA photoproducts in human epidermis. The Journal of investigative dermatology. 1998;110(5):806-10. doi: 10.1046/j.1523-1747.1998.00178.x. PubMed PMID: 9579550.

26. Liu Y, Kempf VR, Nofsinger JB, Weinert EE, Rudnicki M, Wakamatsu K, et al. Comparison of the structural and physical properties of human hair eumelanin following enzymatic or acid/base extraction. Pigment cell research / sponsored by the European Society for Pigment Cell Research and the International Pigment Cell Society. 2003;16(4):355-65. PubMed PMID: 12859619.

27. Matts PJ, Dykes PJ, Marks R. The distribution of melanin in skin determined in vivo. The British journal of dermatology. 2007;156(4):620-8. doi: 10.1111/j.1365-2133.2006.07706.x. PubMed PMID: 17493065.

28. Szabó G, Gerald AB, Pathak MA, Fitzpatrick TB. Racial differences in the fate of melanosomes in human epidermis. Nature. 1969;222:1081-2.

29. Thong HY, Jee SH, Sun CC, Boissy R. The patterns of melanosome distribution in keratinocytes of human skin as one determining factor of skin colour. British Journal of Dermatology. 2003;149(3):498-505.

30. Toda K, Pathak MA, Parrish JA, Fitzpatrick TB, Quevedo WC, Jr. Alteration of racial differences in melanosome distribution in human epidermis after exposure to ultraviolet light. Nature: New biology. 1972;236(66):143-5. PubMed PMID: 4502818.

31. Halaban R, Pomerantz SH, Marshall S, Lambert DT, Lerner AB. Regulation of tyrosinase in human melanocytes grown in culture. The Journal of cell biology. 1983;97(2):480-8. PubMed PMID: 6411733; PubMed Central PMCID: PMC2112541.

32. Ganesan AK, Ho H, Bodemann B, Petersen S, Aruri J, Koshy S, et al. Genome-wide siRNA-based functional genomics of pigmentation identifies novel genes and pathways that impact melanogenesis in human cells. PLoS genetics. 2008;4(12):e1000298. doi: 10.1371/journal.pgen.1000298. PubMed PMID: 19057677; PubMed Central PMCID: PMC2585813.

33. Dow LE, Premsrirut PK, Zuber J, Fellmann C, McJunkin K, Miething C, et al. A pipeline for the generation of shRNA transgenic mice. Nature protocols. 2012;7(2):374-93. doi: 10.1038/nprot.2011.446. PubMed PMID: 22301776; PubMed Central PMCID: PMC3724521.

34. Fellmann C, Zuber J, McJunkin K, Chang K, Malone CD, Dickins RA, et al. Functional identification of optimized RNAi triggers using a massively parallel sensor assay. Molecular cell. 2011;41(6):733-46. doi: 10.1016/j.molcel.2011.02.008. PubMed PMID: 21353615; PubMed Central PMCID: PMC3130540.

35. Paterson EK, Ho H, Kapadia R, Ganesan AK. 9‐cis retinoic acid is the ALDH1A1 product that stimulates melanogenesis. Experimental dermatology. 2013;22(3):202-9.

36. Beard C, Hochedlinger K, Plath K, Wutz A, Jaenisch R. Efficient method to generate single-copy transgenic mice by site-specific integration in embryonic stem cells. Genesis. 2006;44(1):23-8. doi: 10.1002/gene.20180. PubMed PMID: 16400644.

37. Premsrirut PK, Dow LE, Kim SY, Camiolo M, Malone CD, Miething C, et al. A rapid and scalable system for studying gene function in mice using conditional RNA interference. Cell. 2011;145(1):145-58.

38. Buchholz F, Angrand PO, Stewart AF. Improved properties of FLP recombinase evolved by cycling mutagenesis. Nature biotechnology. 1998;16(7):657-62. doi: 10.1038/nbt0798-657. PubMed PMID: 9661200.

39. Lamoreux M, Wakamatsu K, Ito S. Interaction of major coat color gene functions in mice as studied by chemical analysis of eumelanin and pheomelanin. Pigment Cell Research. 2001;14(1):23-31.

40. Ozeki H, Ito S, Wakamatsu K, Hirobe T. Chemical Characterization of Hair Melanins in Various Coat—Color Mutants of Nlice. 1995.

41. Ozeki H, Ito S, Wakamatsu K, Thody AJ. Spectrophotometric characterization of eumelanin and pheomelanin in hair. Pigment cell research / sponsored by the European Society for Pigment Cell Research and the International Pigment Cell Society. 1996;9(5):265-70. PubMed PMID: 9014213.

42. Wakamatsu K, Ito S. Advanced chemical methods in melanin determination. Pigment cell research / sponsored by the European Society for Pigment Cell Research and the International Pigment Cell Society. 2002;15(3):174-83. PubMed PMID: 12028581.

43. Ozeki H, Ito S, Wakamatsu K. Chemical characterization of melanins in sheep wool and human hair. Pigment cell research / sponsored by the European Society for Pigment Cell Research and the International Pigment Cell Society. 1996;9(2):51-7. PubMed PMID: 8857665.

44. Ito S, Nakanishi Y, Valenzuela RK, Brilliant MH, Kolbe L, Wakamatsu K. Usefulness of alkaline hydrogen peroxide oxidation to analyze eumelanin and pheomelanin in various tissue

samples: application to chemical analysis of human hair melanins. Pigment cell & melanoma research. 2011;24(4):605-13.

45. Ihaka R, Gentleman, R. R: A Language for Data Analysis and Graphics. Journal of Computational and Graphical Statistics. 1995;5(3):299-314. Epub 21 Feb 2012.

46. Schneider CA, Rasband WS, Eliceiri KW. NIH Image to ImageJ: 25 years of image analysis. Nature methods. 2012;9(7):671-5. PubMed PMID: 22930834.

47. Morris JK. A formaldehyde glutaraldehyde fixative of high osmolality for use in electron microscopy. J cell Biol. 1965;27:137-9.

48. Takiguchi M, Dow LE, Prier JE, Carmichael CL, Kile BT, Turner SJ, et al. Variability of inducible expression across the hematopoietic system of tetracycline transactivator transgenic mice. PloS one. 2013;8(1):e54009. doi: 10.1371/journal.pone.0054009. PubMed PMID: 23326559; PubMed Central PMCID: PMC3543435.

49. Wakamatsu K, Ito S, Rees JL. The Usefulness of 4‐Amino‐3‐hydroxyphenylalanine as a Specific Marker of Pheomelanin. Pigment Cell Research. 2002;15(3):225-32.

50. Beermann F, Orlow SJ, Lamoreux ML. The Tyr (albino) locus of the laboratory mouse. Mammalian genome : official journal of the International Mammalian Genome Society. 2004;15(10):749-58. doi: 10.1007/s00335-004-4002-8. PubMed PMID: 15520878.

51. Ozeki H, Ito S, Wakamatsu K, Ishiguro I. Chemical characterization of pheomelanogenesis starting from dihydroxyphenylalanine or tyrosine and cysteine. Effects of tyrosinase and cysteine concentrations and reaction time. Biochimica et biophysica acta. 1997;1336(3):539-48. PubMed PMID: 9367182.

52. Burchill SA, Thody AJ, Ito S. Melanocyte-stimulating hormone, tyrosinase activity and the regulation of eumelanogenesis and phaeomelanogenesis in the hair follicular melanocytes of the mouse. The Journal of endocrinology. 1986;109(1):15-21. PubMed PMID: 3084696.

53. Kwon BS, Haq AK, Wakulchik M, Kestler D, Barton DE, Francke U, et al. Isolation, chromosomal mapping, and expression of the mouse tyrosinase gene. The Journal of investigative dermatology. 1989;93(5):589-94. PubMed PMID: 2507645.

54. Beermann F, Orlow SJ, Boissy RE, Schmidt A, Boissy YL, Lamoreux ML. Misrouting of tyrosinase with a truncated cytoplasmic tail as a result of the murine platinum (cp) mutation. Experimental eye research. 1995;61(5):599-607. PubMed PMID: 8654502.

55. Orlow SJ, Boissy RE, Moran DJ, Pifko-Hirst S. Subcellular distribution of tyrosinase and tyrosinase-related protein-1: implications for melanosomal biogenesis. The Journal of investigative dermatology. 1993;100(1):55-64. PubMed PMID: 8423398.

56. Simmen T, Schmidt A, Hunziker W, Beermann F. The tyrosinase tail mediates sorting to the lysosomal compartment in MDCK cells via a di-leucine and a tyrosine-based signal. Journal of cell science. 1999;112 (Pt 1):45-53. PubMed PMID: 9841903.

57. Green, MC. Himalayan, a new allele of albino in the mouse. Journal of Heredity. 1961;52(2):73-5.

58. Beermann F, Ruppert S, Hummler E, Bosch FX, Muller G, Ruther U, et al. Rescue of the albino phenotype by introduction of a functional tyrosinase gene into mice. The EMBO journal. 1990;9(9):2819-26. PubMed PMID: 2118105; PubMed Central PMCID: PMC551993.

59. Halaban R, Moellmann G, Tamura A, Kwon BS, Kuklinska E, Pomerantz SH, et al. Tyrosinases of murine melanocytes with mutations at the albino locus. Proceedings of the National Academy of Sciences. 1988;85(19):7241-5.

60. Imokawa G, Yada Y, Hori Y. Induction of melanization within hair bulb melanocytes in chinchilla mutant by melanogenic stimulants. Journal of investigative dermatology. 1988;91(2):106-13.

61. Theos AC, Tenza D, Martina JA, Hurbain I, Peden AA, Sviderskaya EV, et al. Functions of adaptor protein (AP)-3 and AP-1 in tyrosinase sorting from endosomes to melanosomes. Molecular biology of the cell. 2005;16(11):5356-72. doi: 10.1091/mbc.E05-07-0626. PubMed PMID: 16162817; PubMed Central PMCID: PMC1266432.

62. Turner WA, Taylor JD, Tchen TT. Melanosome formation in the goldfish: the role of multivesicular bodies. Journal of ultrastructure research. 1975;51(1):16-31. PubMed PMID: 805261.

63. Jimbow K, Oikawa O, Sugiyama S, Takeuchi T. Comparison of eumelanogenesis and pheomelanogenesis in retinal and follicular melanocytes; role of vesiculo-globular bodies in melanosome differentiation. The Journal of investigative dermatology. 1979;73(4):278-84. PubMed PMID: 479631.

64. Eliason CM, Bitton P-P, Shawkey MD. How hollow melanosomes affect iridescent colour production in birds. Proceedings of the Royal Society B: Biological Sciences. 2013;280(1767):20131505.

65. Bouchard B, Fuller BB, Vijayasaradhi S, Houghton AN. Induction of pigmentation in mouse fibroblasts by expression of human tyrosinase cDNA. The Journal of experimental medicine. 1989;169(6):2029-42. PubMed PMID: 2499655; PubMed Central PMCID: PMC2189346.

66. Chiaverini C, Beuret L, Flori E, Busca R, Abbe P, Bille K, et al. Microphthalmia-associated transcription factor regulates RAB27A gene expression and controls melanosome transport. The Journal of biological chemistry. 2008;283(18):12635-42. doi: 10.1074/jbc.M800130200. PubMed PMID: 18281284.

67. Du J, Miller AJ, Widlund HR, Horstmann MA, Ramaswamy S, Fisher DE. MLANA/MART1 and SILV/PMEL17/GP100 are transcriptionally regulated by MITF in melanocytes and melanoma. The American journal of pathology. 2003;163(1):333-43. doi: 10.1016/S0002-9440(10)63657-7. PubMed PMID: 12819038; PubMed Central PMCID: PMC1868174.

68. Levy C, Khaled M, Fisher DE. MITF: master regulator of melanocyte development and melanoma oncogene. Trends in molecular medicine. 2006;12(9):406-14. doi: 10.1016/j.molmed.2006.07.008. PubMed PMID: 16899407.

69. Vachtenheim J, Borovanský J. "Transcription physiology" of pigment formation in melanocytes: central role of MITF. Experimental dermatology. 2010;19(7):617-27.

70. Ho H, Ganesan AK. The pleiotropic roles of autophagy regulators in melanogenesis. Pigment Cell Melanoma Res. 2011;24(4):595-604. doi: 10.1111/j.1755-148X.2011.00889.x. PubMed PMID: 21777401.

71. Ho H, Kapadia R, Al-Tahan S, Ahmad S, Ganesan AK. WIPI1 coordinates melanogenic gene transcription and melanosome formation via TORC1 inhibition. The Journal of biological chemistry. 2011;286(14):12509-23. doi: 10.1074/jbc.M110.200543. PubMed PMID: 21317285; PubMed Central PMCID: PMC3069453.

Figure 2.1: *Tyr* depletion leads to coat color changes in three unique coat color backgrounds.

(A) B16 mouse melanoma cells infected with the lentiviral constructs containing individual shRNAs were harvested for quantification of *Tyr* mRNA (left panel) and protein (right panel). The values below the TYR protein bands in the western blot represent the relative intensity of the TYR band normalized to the tubulin band (loading control) for each lane divided by the relative expression of the TYR band in the mismatch-control (mm control) sample. (B) Mouse KH2 ES cells containing a FRT-hygro-pA cassette on chromosome 11 and a reverse tet-transactivator (rtTA) on chromosome 6 were co-electroporated with pCAGGS-FLPe and the targeting vector, pCol-TGM-*Tyr*. Resulting FLPe-mediated recombination between the FRT site at the *Col1a1* locus and the FRT sites present within pCol-TGM-*Tyr* results in colonies that survive hygromycin selection. (C-F) Effect of Dox-mediated Tyr shRNA on coat color was analyzed in (C,F) yellow agouti, (D) white-bellied agouti, or (E) non-agouti (black) mice by comparison of littermates. The genotype of each mouse is listed above each photo. The percentage value below each mouse corresponds to the absorbance at 492 nm for that particular mouse divided by the absorbance at 492 nm for its control littermate, which is set to 100%. (C) Yellow-agouti littermates with the rtTA2 driver; (D) agouti littermates with the rtTA2 driver; (E) black (non-agouti) littermates with the rtTA3 driver and (F) yellow agouti littermates with the rtTA3 driver were shaved on their dorsal side and then photographed. rtTA3 and *Tyr*-shRNA/rtTA3 littermates each maintained on a doxycycline diet were photographed in daylight at P100 to demonstrate the presence of GFP in the eye.

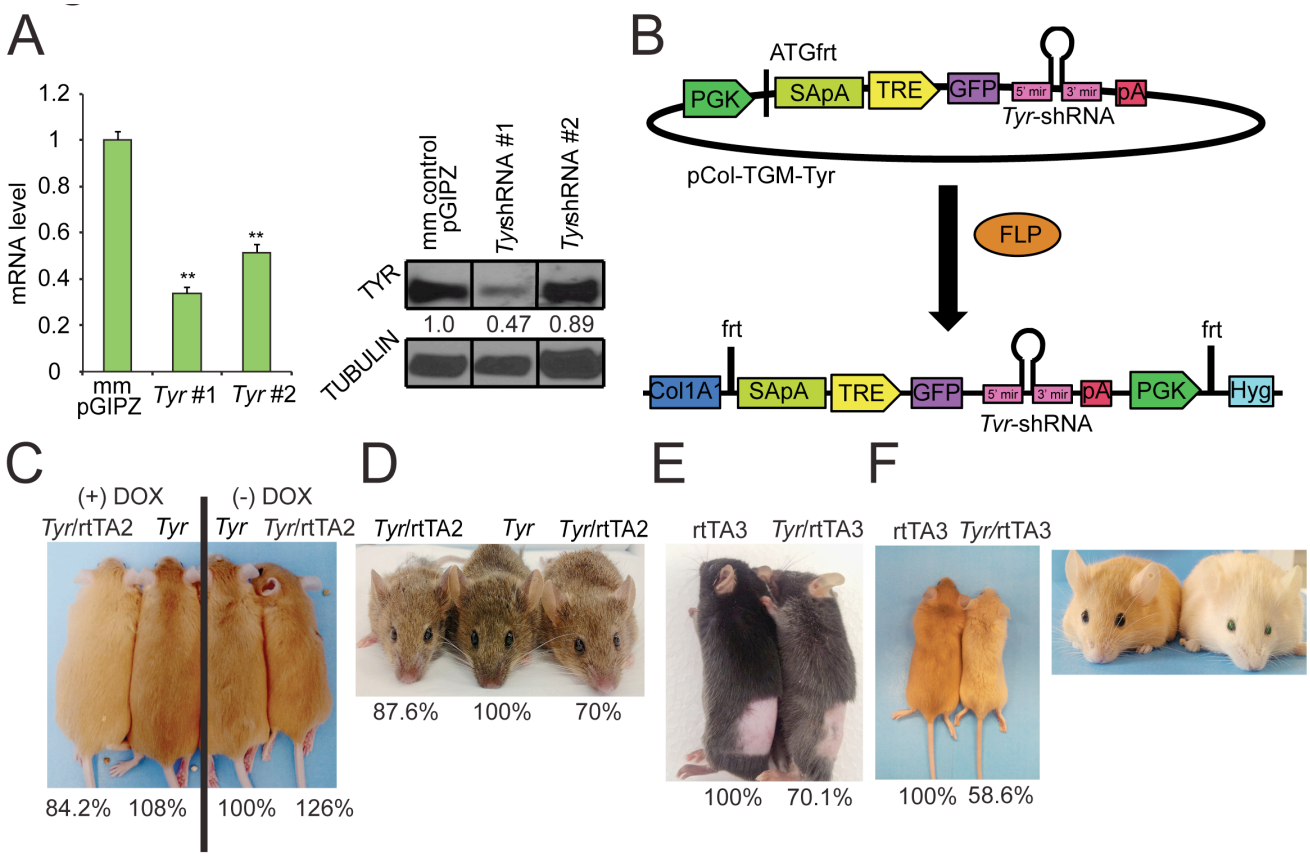
A
1.2
1
0.8
0.6
0.4
0.2
0
mRNA level
**
**
mm pGIPZ
Tyr #1
Tyr #2
mm control pGIPZ
Tyr shRNA #1
Tyr shRNA #2
TYR
TUBULIN
1.0
0.47
0.89
B
ATGfrt
PGK
SApA
TRE
GFP
5' mir
3' mir
pA
Tyr-shRNA
pCol-TGM-Tyr
FLP
frt
Col1A
SApA
TRE
GFP
5' mir
3' mir
pA
PGK
Hyg
frt
Tvr-shRNA
C
(+) DOX
(-) DOX
Tyr/rtTA2
Tyr
Tyr
Tyr/rtTA2
84.2%
108%
100%
126%
D
Tyr/rtTA2
Tyr
Tyr/rtTA2
87.6%
100%
70%
E
rtTA3
Tyr/rtTA3
100%
70.1%
F
rtTA3
Tyr/rtTA3
100%
58.6%

Figure 2.1

Figure 2.2: Depletion of TYR protein in skin in *Tyr*-shRNA; rtTA3 mice

(A) Four mm skin punch biopsies were taken at P100 from three different coat color backgrounds. Total protein was extracted and used to immunoblot for TYR and GFP. The numerical values present below the TYR protein bands in the western blot represent the relative intensity of the TYR band normalized to the beta-actin band (loading control) for each lane divided by the relative expression of the TYR band in the rtTA3 control sample. (B) Four-mm skin punch biopsies taken from the indicated mice at P100 were formalin fixed, dehydrated, and paraffin embedded. Seven-μm thick sections of the skin were cut and immunostained for GFP (brown color).

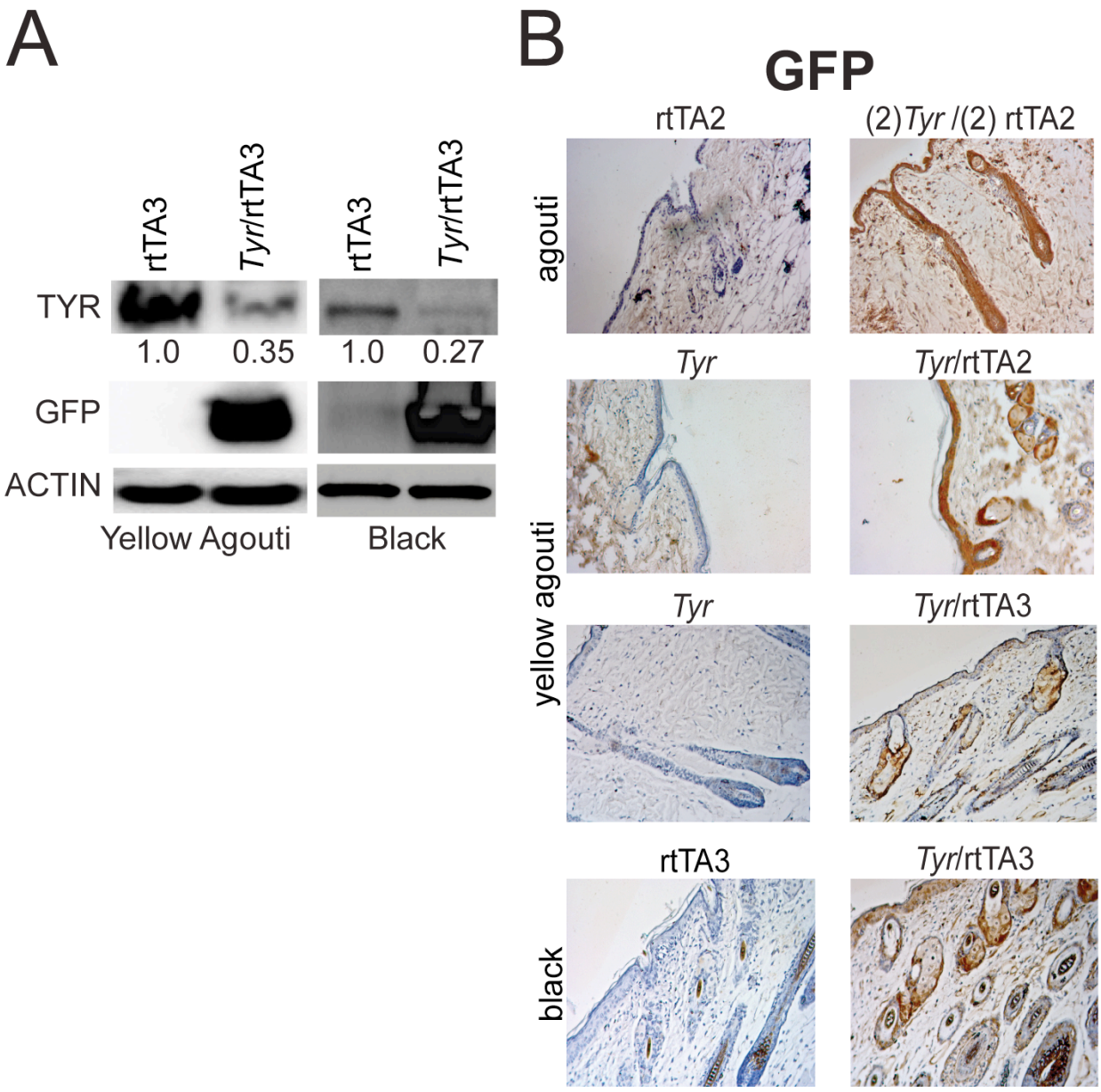
A
rtTA3
Tyr/rtTA3
rtTA3
Tyr/rtTA3
TYR
1.0
0.35
1.0
0.27
GFP
ACTIN
Yellow Agouti
Black
B
GFP
rtTA2
(2)Tyr /(2) rtTA2
agouti
Tyr
Tyr/rtTA2
yellow agouti
Tyr
Tyr/rtTA3
rtTA3
Tyr/rtTA3
black

Figure 2.2

Figure 2.3: *Tyr* depletion inhibits the normal deposition of melanin within the melanosome

(A) Fresh whole mouse skin was excised from the indicated mice using a 4-mm round punch biopsy and fixed in Karnovsky's fixative before electron microscopy analysis. Melanosomes within the Golgi area of the cell body were evaluated for maturation stage and ultra-structural morphology. DOPA histochemistry was performed to assess the relative activity of tyrosinase within the melanosome. The top row contains the relevant control images for the images listed in the middle and bottom rows, respectively. Images are representative of 15 melanocytes from 2 mice per group. (B) The relative accumulation of stage I-IV melanosomes in each coat color background was quantified as described in the methods. For black and yellow agouti coat colors, the rtTA3 driver was used. For white-bellied agouti coat color, the rtTA2 driver was used. N=nucleus; G=Golgi area. Bar=0.5 microns (Bar on inset=1.5 microns). Graph: * = $p \leq 0.05$, or ** = $p \leq 0.005$, Bars = standard deviation (n=15 melanocytes from 2 mice per group).

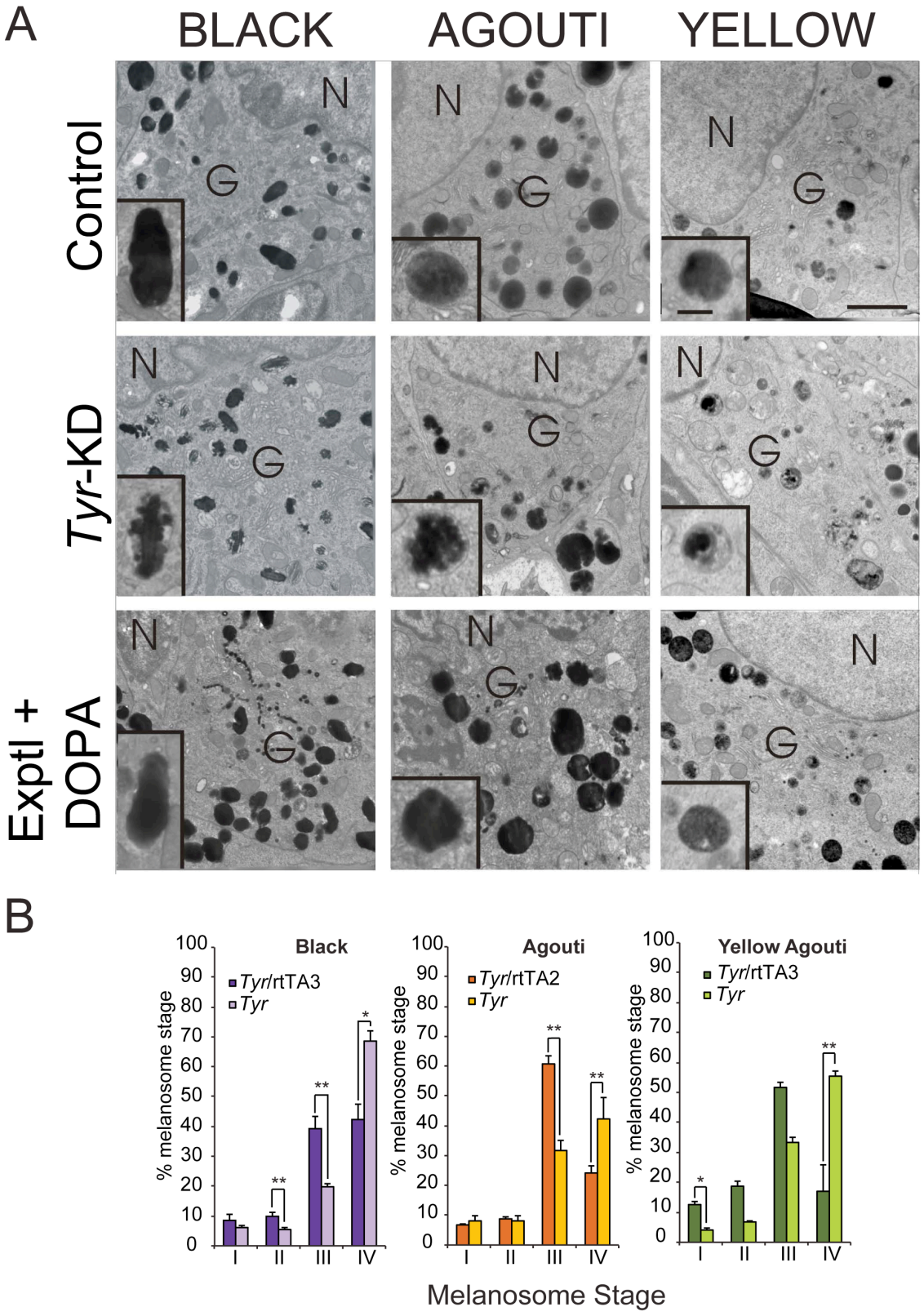
A
BLACK
AGOUTI
YELLOW
Control
Tyr-KD
Exptl + DOPA
N
G
B
Black
Agouti
Yellow Agouti
Tyr/rtTA3
Tyr
Tyr/rtTA2
% melanosome stage
Melanosome Stage
I
II
III
IV

Figure 2.3

Figure 2.4: Expression of a control shRNA does not affect pigment accumulation or melanosome maturation.

(A) Coat color in *Luc*-knockdown mice and appropriate control mice was compared both visually (genotypes of each mouse are listed above each photo) and spectrophotometrically (the percentage value below each mouse corresponds to the absorbance at 492 nm for that particular mouse divided by the absorbance at 492 nm for its control littermate, which is set to 100%). (B) Fresh whole mouse skin was excised from *Luc*-knockdown mice and corresponding control mice using a 4-mm round punch biopsy and fixed in Karnovsky's fixative before electron microscopy analysis. Melanosomes within the Golgi area of the cell body were evaluated for maturation stage and ultra-structural morphology. Images are representative of 15 melanocytes from 2 mice per group. (C) The melanosomes were also quantified as described in Figure 2D. N=nucleus; G=Golgi area. Bar=0.5 microns (Bar on inset=1.5 microns). Graph: * = $p \leq 0.05$. Bars = standard deviation (n=2 mice per group, 15 melanocytes per mouse analyzed).

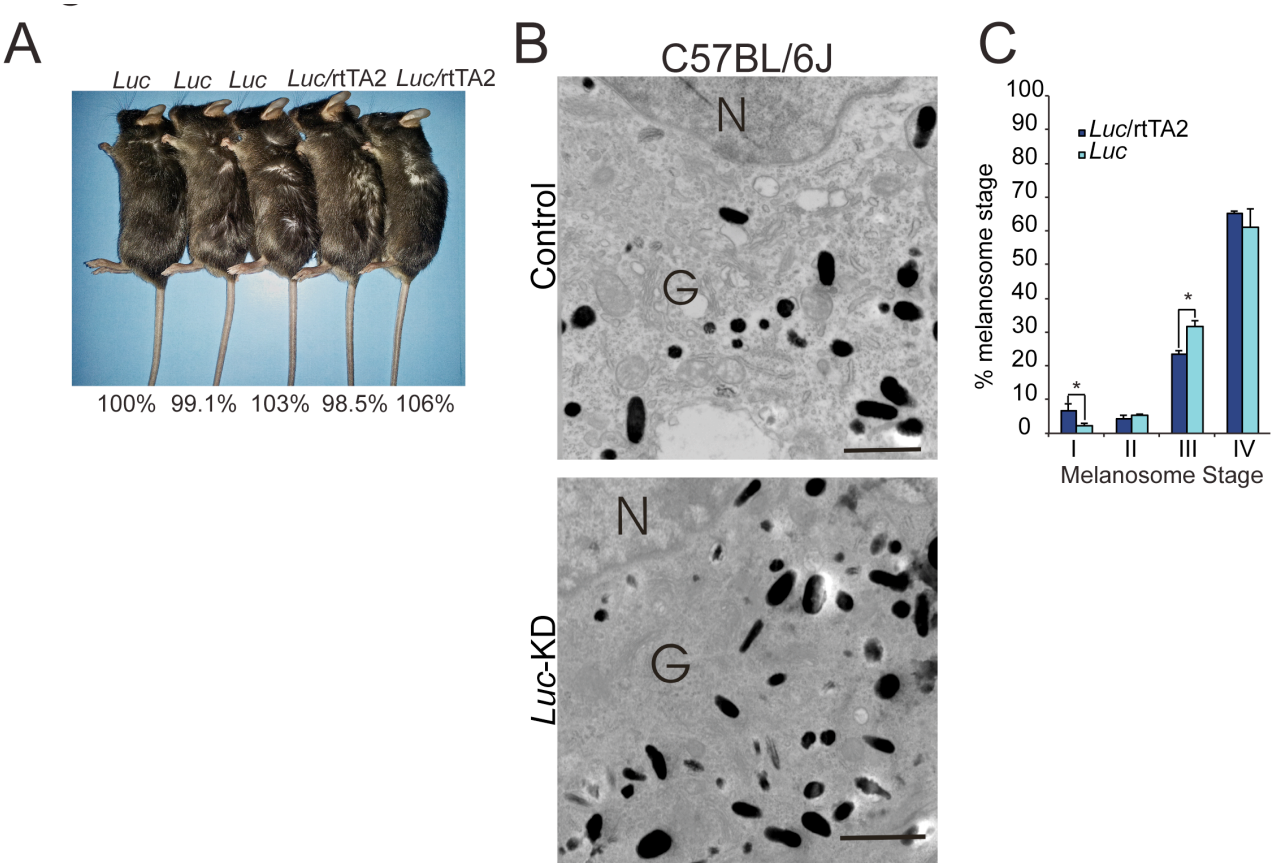
A
Luc Luc Luc Luc/rtTA2 Luc/rtTA2
100% 99.1% 103% 98.5% 106%
B
C57BL/6J
Control
N
G
Luc-KD
N
G
C
100
90
80
70
60
50
40
30
20
10
0
% melanosome stage
Luc/rtTA2
Luc
*
*
I
II
III
IV
Melanosome Stage

Figure 2.4

Figure 2.5: The partial depletion of *Tyr* impacts key genes involved in melanogenesis

4-mm skin punch biopsies were acquired from anesthetized (A) control rtTA3 mice and experimental *Tyr*-shRNA/rtTA3 mice, (B) control *Luc*-shRNA mice and experimental *Luc*-shRNA/rtTA2 mice, and (C) control C57BL/6J wild-type and Tyr^{c}/Tyr^{c} albino mice and immediately stabilized in RNAlater. Extracted RNA was subjected to Nanostring analysis on the genes listed below the bar graphs. (D) Three littermates (genotypes from left to right as shown in graphs above each figure) on continuous doxycycline were photographed at P50 (left images). After P110, doxycycline was removed from the diet for 60 days and the mice were photographed once more (middle images). Finally, the mice were fed a doxycycline-free diet for an additional 30 days and a final set of photographs were taken (right images). Pigment accumulation was measured spectrophotometrically as described in the methods. The percentage value below each mouse corresponds to the absorbance at 492 nm for that particular mouse divided by the absorbance at 492 nm for its control littermate, which is set to 100%. Data shown for all three Nanostring bar graphs (A-C) is mean normalized counts of mRNA for each gene (n = 3 mice as indicated by the error bars). * = $p \leq 0.05$ or ** = $p \leq 0.01$.

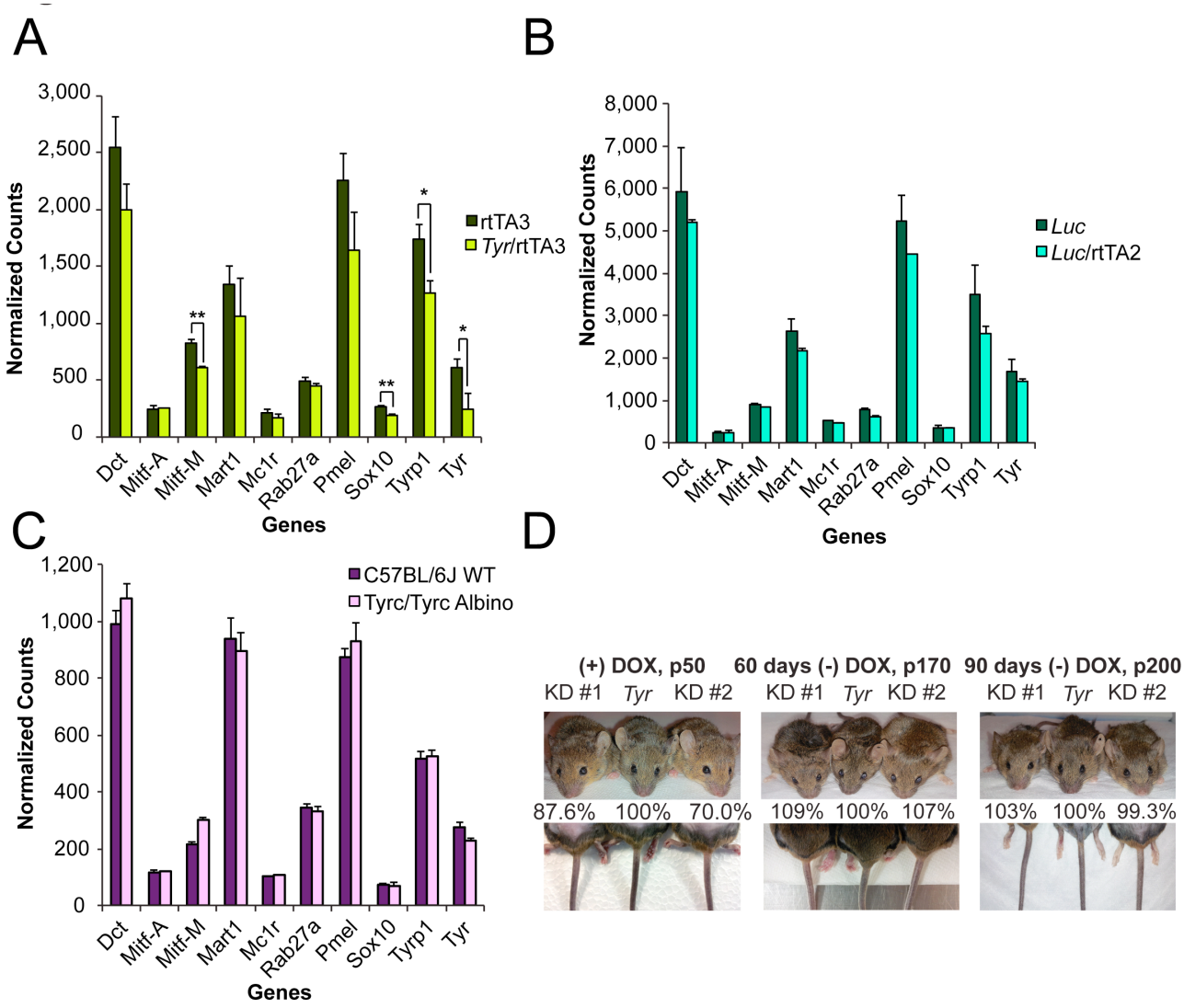
A
Normalized Counts
3,000
2,500
2,000
1,500
1,000
500
0
rtTA3
Tyr/rtTA3
**
**
*
*
Dct
Mitf-A
Mitf-M
Mart1
Mc1r
Rab27a
Pmel
Sox10
Tyrp1
Tyr
Genes
B
Normalized Counts
8,000
7,000
6,000
5,000
4,000
3,000
2,000
1,000
0
Luc
Luc/rtTA2
Dct
Mitf-A
Mitf-M
Mart1
Mc1r
Rab27a
Pmel
Sox10
Tyrp1
Tyr
Genes
C
Normalized Counts
1,200
1,000
800
600
400
200
0
C57BL/6J WT
Tyrc/Tyrc Albino
Dct
Mitf-A
Mitf-M
Mart1
Mc1r
Rab27a
Pmel
Sox10
Tyrp1
Tyr
Genes
D
(+) DOX, p50
60 days (-) DOX, p170
90 days (-) DOX, p200
KD #1
Tyr
KD #2
87.6%
100%
70.0%
109%
100%
107%
103%
100%
99.3%

Figure 2.5

Figure 2.S1: The rtTA3 transgene drives strong expression of GFP in the mouse eye lens

(A) Total genomic DNA was extracted from the parental KH2 cell line ("KH2"), or from hygromycin-resistant KH2 clones (1-12) electroporated with a shRNA targeting *Tyr*. DNA's were digested with SpeI and subjected to Southern analysis using a 0.85kb probe from the *Col1a1* locus. The sizes of the DNA fragments detected with this genomic DNA probe are wild-type allele (6.2kb); Frt-Pgk-neo allele (6.7kb); and Flp-in (*Tyr*-shRNA containing) allele (4.1kb). (B) To visualize GFP expression in the hair shaft, shaved dorsal hairs taken at P50 from an agouti *Tyr*-shRNA/rtTA2 (*Tyr/rtTA2*) and a *Tyr*-shRNA (*Tyr*) control littermate (left two columns) and a non-agouti (black) *Tyr*-shRNA/rtTA3 (*Tyr/rtTA3*) and a *Tyr*-shRNA (*Tyr*) control littermate (right two columns) were affixed to slides and subjected to both bright field microscopy and fluorescence microscopy with identical exposure times. (C) Brightfield microscopy was used to photograph the eyes of littermates to demonstrate the presence of GFP in the absence of fluorescence (left column images, middle column images). To verify that the green color in the eye was derived from GFP, eyes were also visualized using fluorescence microscopy (right column images). (D) Four-mm skin punch biopsies taken from the indicated mice at P100 were formalin fixed, dehydrated, and paraffin embedded. Seven μm thick sections of the skin were cut and stained for hematoxylin and eosin (top row), immunostained without primary GFP antibody present (second row down), or immunostained with primary GFP antibody (third row down) to demonstrate the GFP expression throughout the eye of *Tyr*-knockdown mice (right column). The fixed and dehydrated eyes were also subjected to Fontana Masson staining (F-M) to visualize melanin levels (bottom row). Ln= lens, rpe= retinal pigment epithelium.

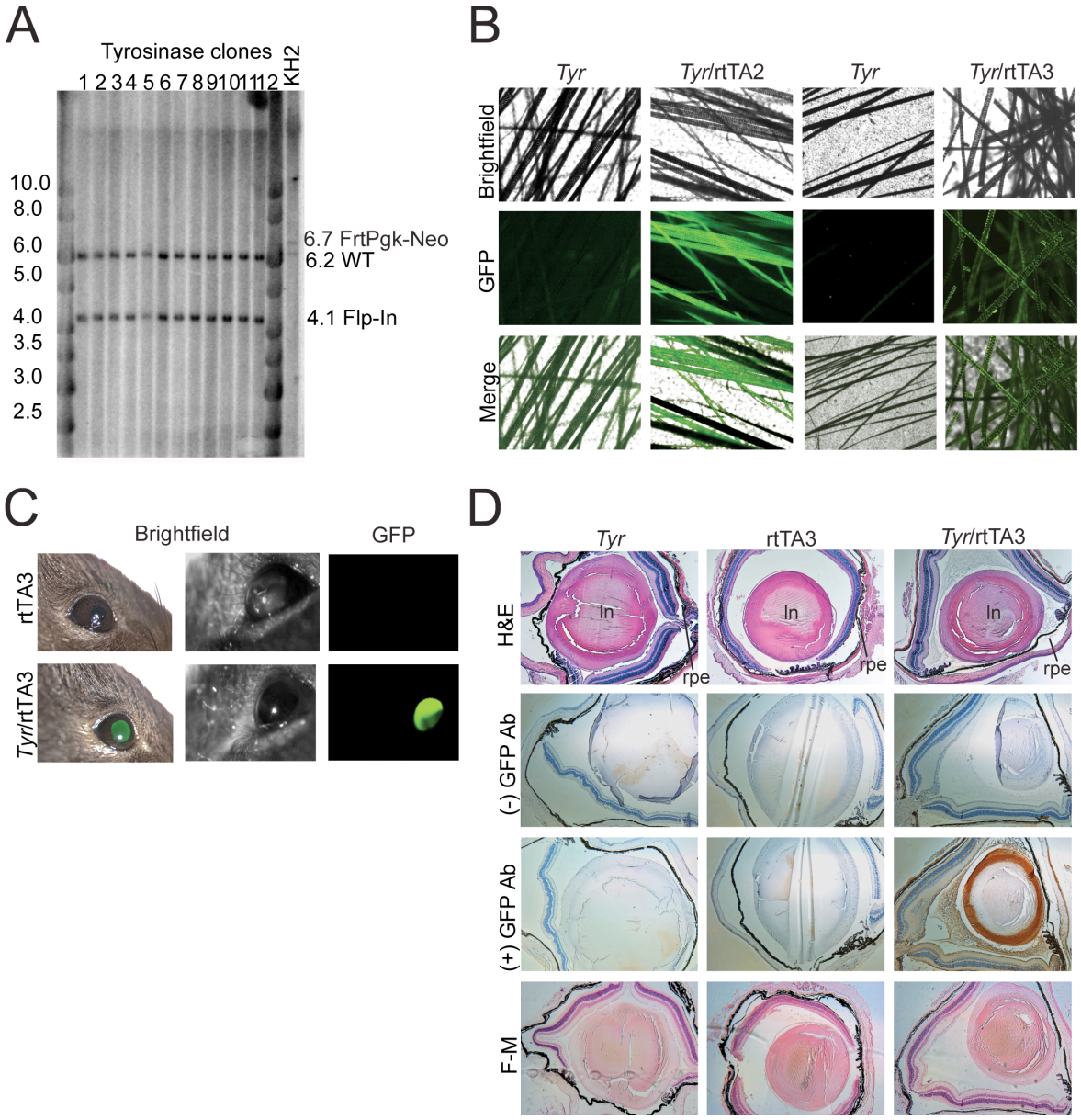
A
Tyrosinase clones
1 2 3 4 5 6 7 8 9 10 11 12 KH2
10.0
8.0
6.0
5.0
4.0
3.5
3.0
2.5
6.7 FrtPgk-Neo
6.2 WT
4.1 Flp-In
B
Tyr
Tyr/rtTA2
Tyr
Tyr/rtTA3
Brightfield
GFP
Merge
C
Brightfield
GFP
rtTA3
Tyr/rtTA3
D
Tyr
rtTA3
Tyr/rtTA3
H&E
(-) GFP Ab
(+) GFP Ab
F-M
ln
rpe

Figure 2.S1

Figure 2.S2: Bar and dot plots for black mice.

Bar plots depict the arithmetic mean and (standard deviation) for the rtTA3/*Tyr*-shRNA and control groups (actual numeric values given at the top of each subfigure). Dorsal hairs of C57BL/6J mice on continuous doxycycline treatment were shaved and processed for chemical analysis of eumelanin and of pheomelanin based upon their specific degradation products, pyrrole-2,3,5-tricarboxylic acid (PCTA) and 4-amino-3-hydroxyphenylalanine (4-AHP), respectively. Approximately 20 mg of hair was homogenized with a Tenbroeck homogenizer at a concentration of 10 mg/mL and 100 μL aliquots were subjected to Soluene-350 solubilization to quantify total melanin, alkaline hydrogen peroxide oxidation to quantify total PCTA, and hydroiodic acid hydrolysis to quantify 4-AHP in duplicate. The data corresponds to the averages of five control mice (*Tyr*-shRNA only or rtTA driver only) and five *Tyr*-knockdown mice on the C57BL/6J background, and the value is the mean of duplicate measurements. Each hair sample was derived from a single mouse. 'X' symbols on the left of each bar represent the actual data observed for each group.

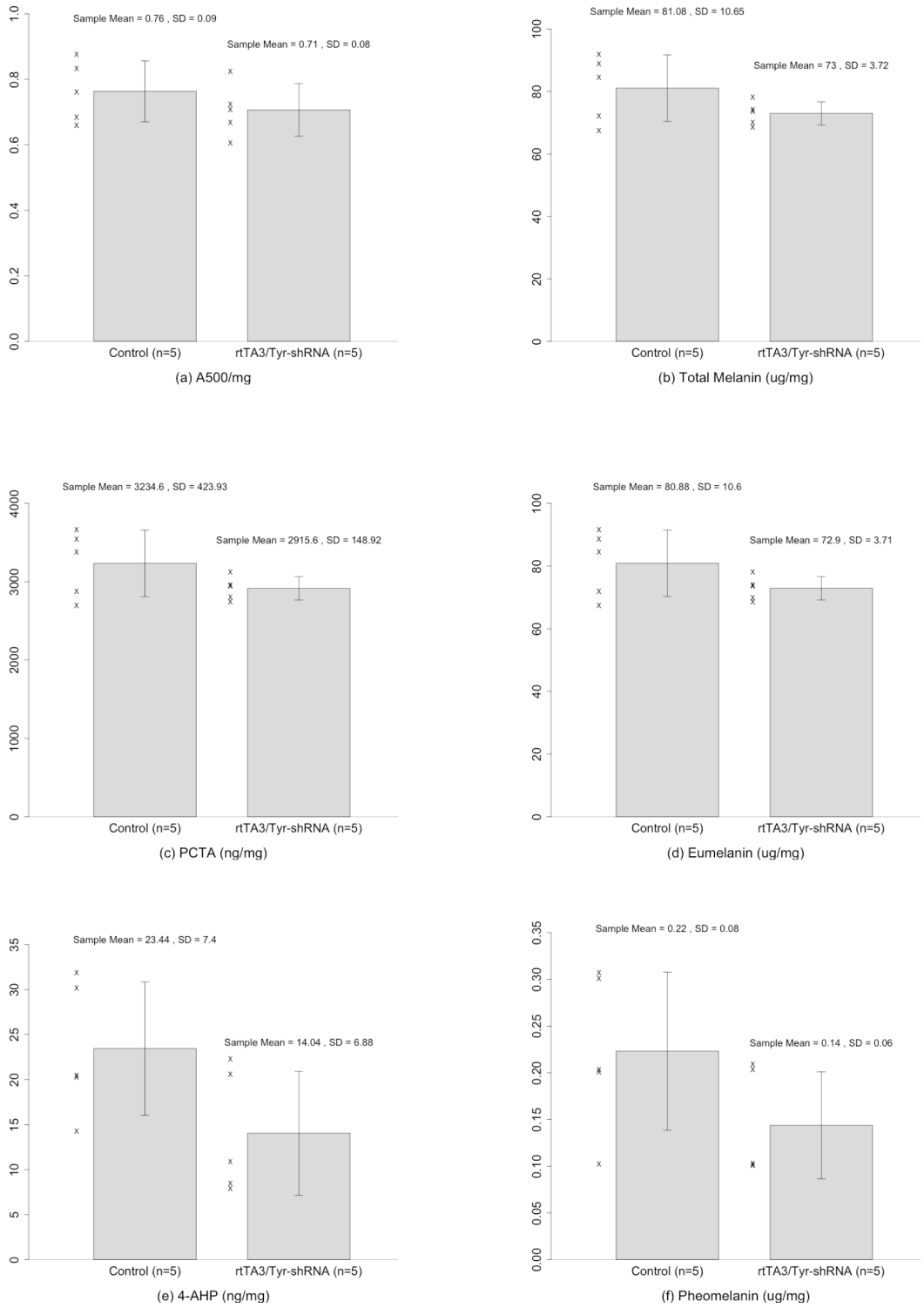
Sample Mean = 0.76 , SD = 0.09
Sample Mean = 0.71 , SD = 0.08
Control (n=5)
rtTA3/Tyr-shRNA (n=5)
(a) A500/mg
Sample Mean = 81.08 , SD = 10.65
Sample Mean = 73 , SD = 3.72
Control (n=5)
rtTA3/Tyr-shRNA (n=5)
(b) Total Melanin (ug/mg)
Sample Mean = 3234.6 , SD = 423.93
Sample Mean = 2915.6 , SD = 148.92
Control (n=5)
rtTA3/Tyr-shRNA (n=5)
(c) PCTA (ng/mg)
Sample Mean = 80.88 , SD = 10.6
Sample Mean = 72.9 , SD = 3.71
Control (n=5)
rtTA3/Tyr-shRNA (n=5)
(d) Eumelanin (ug/mg)
Sample Mean = 23.44 , SD = 7.4
Sample Mean = 14.04 , SD = 6.88
Control (n=5)
rtTA3/Tyr-shRNA (n=5)
(e) 4-AHP (ng/mg)
Sample Mean = 0.22 , SD = 0.08
Sample Mean = 0.14 , SD = 0.06
Control (n=5)
rtTA3/Tyr-shRNA (n=5)
(f) Pheomelanin (ug/mg)

Figure 2.S2

Figure 2.S3: Bar and dot plots for agouti mice.

Bar plots depict the arithmetic mean and (standard deviation) for the rtTA3/*Tyr*-shRNA and control groups (actual numeric values given at the top of each subfigure). Dorsal hairs of agouti mice on continuous doxycycline treatment were shaved and processed for chemical analysis of eumelanin and of pheomelanin based upon their specific degradation products, pyrrole-2,3,5-tricarboxylic acid (PCTA) and 4-amino-3-hydroxyphenylalanine (4-AHP), respectively as described in Table 1. 13 control (*Tyr*-shRNA only or rtTA driver only) and 13 *Tyr*-knockdown mice were analyzed. 'X' symbols on the left of each bar represent the actual data observed for each group.

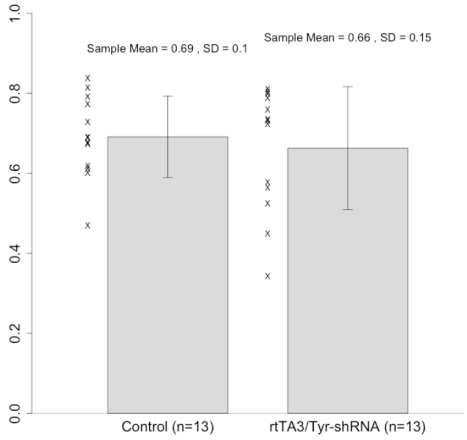

(a) A500/mg

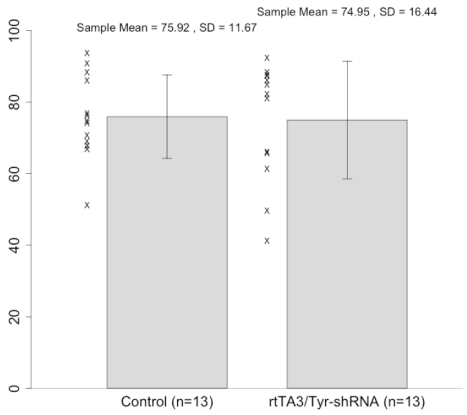

(b) Total Melanin (ug/mg)

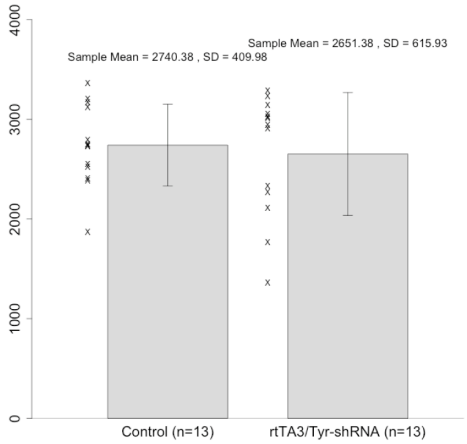

(c) PCTA (ng/mg)

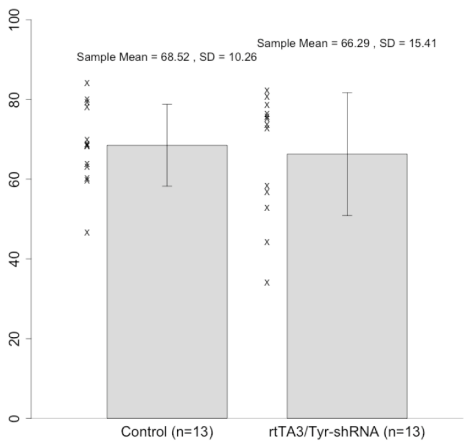

(d) Eumelanin (ug/mg)

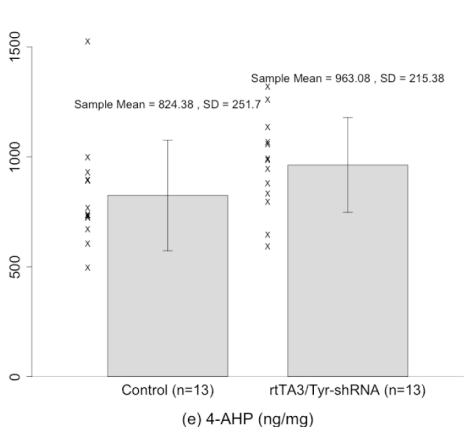

(e) 4-AHP (ng/mg)

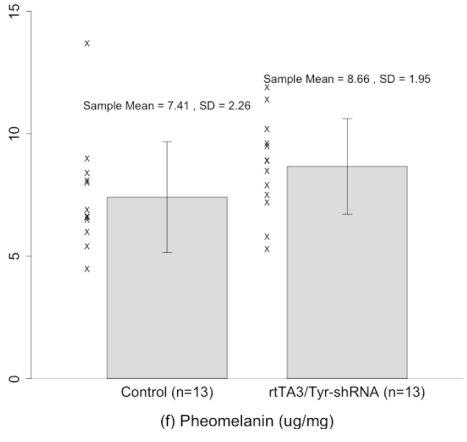

(f) Pheomelanin (ug/mg)

Figure 2.S3

Figure 2.S4: *Tyr*-knockdown mice also display aberrant melanosome structure within the melanocyte dendrites in all three mouse coat colors.

Fresh whole mouse skin was excised from *Tyr*-knockdown mice and corresponding control mice using a 4-mm round punch biopsy and fixed in Karnovsky's fixative before electron microscopy analysis. Melanosomes within the dendrites of the melanocyte were then evaluated for ultrastructural morphology. Images are representative of 15 melanocytes from 2 mice per group. Bar=2.5 microns.

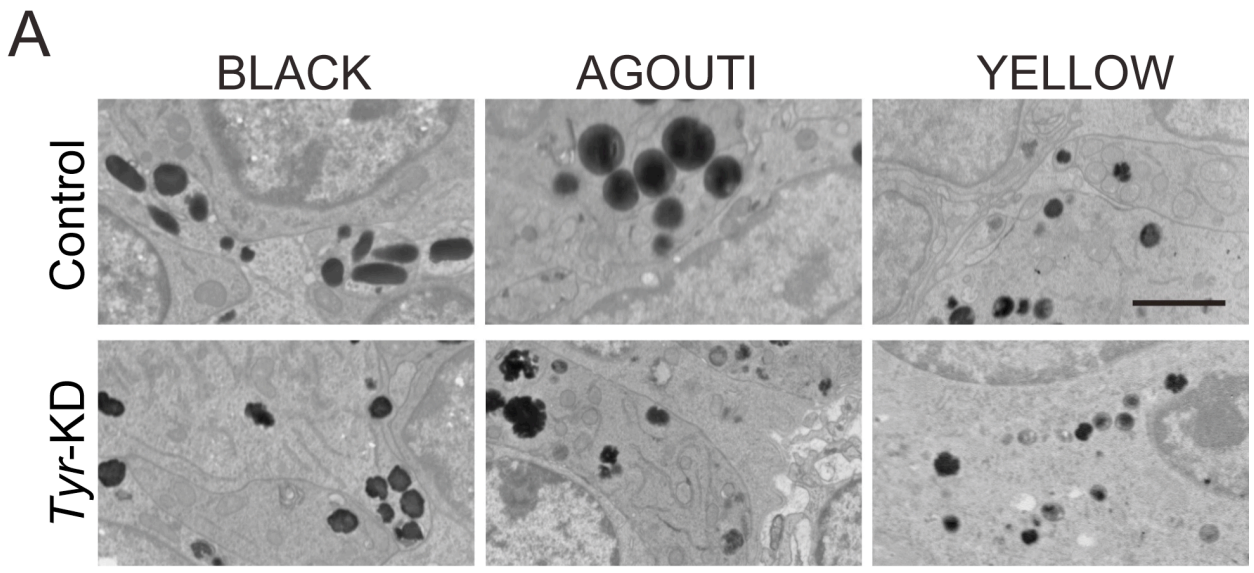

Figure 2.S4

Figure 2.S5: Multiple independent siRNAs against *TYR* impact MITF protein accumulation.

The impact of multiple independent siRNAs (1, 2, 3) targeting *TYR,* on TYR and MITF protein accumulation was assessed by immunoblot and compared to a control, mismatch siRNA (C). The impact of the given siRNAs on the protein accumulation of TYR and MITF was quantitated by densitometry (numbers below the corresponding blots).

Data excerpted from:

"Genome-Wide siRNA-Based Functional Genomics of Pigmentation Identifies Novel Genes and Pathways That Impact Melanogenesis in Human Cells"

Anand K. Ganesan, Hsiang Ho, Brian Bodemann, Sean Peterson, Jayavani Aruri, Shiney Koshy, Zachary Richardson, Lu Q. Le, Tatiana Krasieva, Michael G. Roth, Pat Farmer and Michael A. White
PLoS Genetics
doi: 10.1371/journal.pgen.1000298
Published December 5, 2008
Figure doi: 10.1371/journal.pgen.1000298.g002

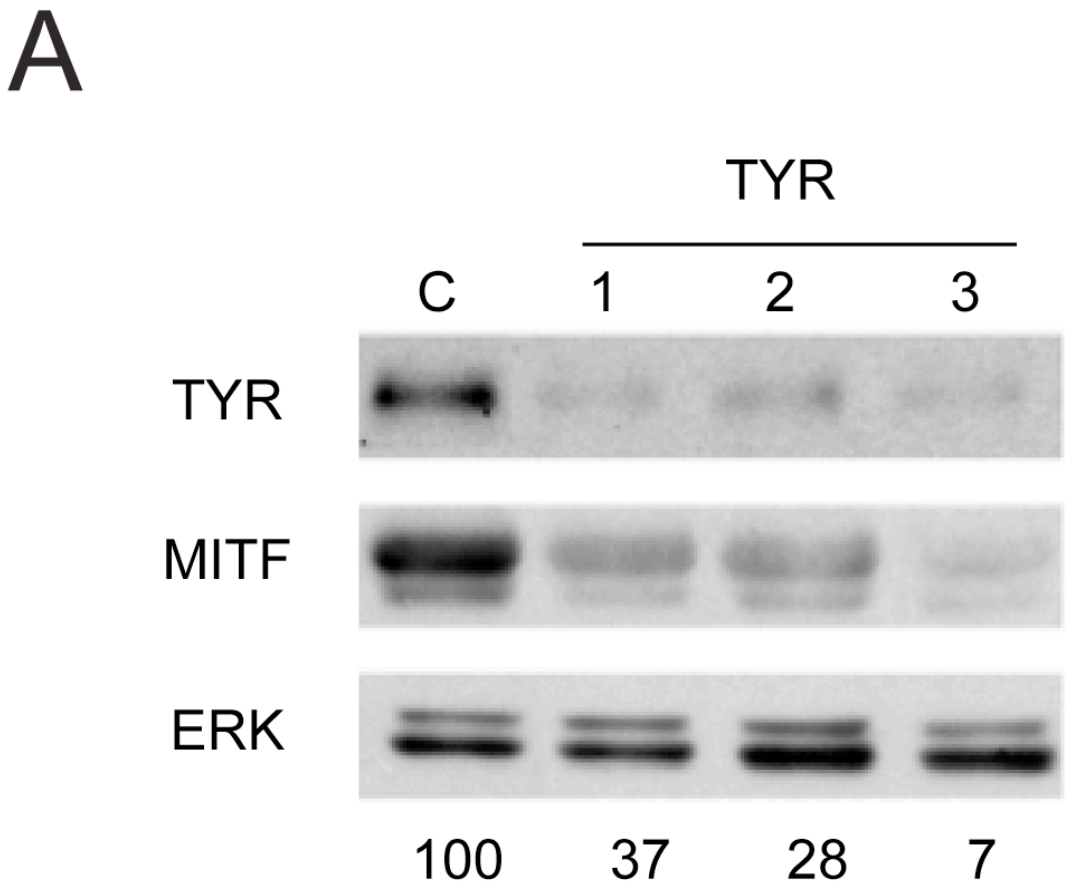

Figure 2.S5

Table 2.1: Knockdown of *Tyr in vivo* is not sufficient to induce significant melanin loss in the black mouse coat.

Outcome	Control (n=5)	rtTA3/*Tyr*-shRNA (n=5)	Difference (rtTA3/*Tyr*-shRNA – Cont)		% of Control
	Mean (SD)	Mean (SD)	Diff in Means (95% CI)	p-value	
A500/mg	0.76 (0.09)	0.71 (0.08)	-0.06 (-0.18, 0.06)	0.332	
Total melanin (μg/mg)	81.08 (10.65)	73 (3.72)	-8.08 (-19.5, 3.34)	0.148	90.1%
PCTA (ng/mg)	3234.6 (423.9)	2915.6 (148.9)	-319 (-773.6, 135.6)	0.151	
Eumelanin (μg/mg)	80.88 (10.6)	72.9 (3.71)	-7.98 (-19.34, 3.38)	0.151	90.1%
4-AHP (ng/mg)	23.44 (7.4)	14.04 (6.88)	-9.4 (-19.63, 0.83)	0.071	
Pheomelanin (μg/mg)	0.22 (0.084)	0.14 (0.055)	-0.08 (-0.18, 0.02)	0.111	63.6%
Average Phe/Eu Ratio	0.003 (0.001)	0.002 (0.001)	0.001 (-0.001, 0.001)	0.185	

Dorsal hairs of non-agouti double transgenic and control mice on continuous doxycycline treatment were shaved and processed for chemical analysis of eumelanin and of pheomelanin based upon their specific degradation products, pyrrole-2,3,5-tricarboxylic acid (PCTA) and 4-amino-3-hydroxyphenylalanine (4-AHP), respectively. Approximately 20 mg of hair was homogenized with a Ten Broeck homogenizer at a concentration of 10 mg/mL and 100 μL aliquots were subjected to Soluene-350 solubilization to quantify total melanin, alkaline hydrogen peroxide oxidation to quantify total PCTA, and hydroiodic acid hydrolysis to quantify 4-AHP in duplicate. The data corresponds to the averages of five control mice (*Tyr*-shRNA only or rtTA driver only) and five *Tyr*-knockdown mice, and the value is the mean of duplicate measurements. Each hair sample was derived from a single mouse. Within group summary statistics represent the arithmetic mean and (standard deviation). Differences in means between rtTA3/*Tyr*-shRNA and control were tested using a two-sample t-test with no assumption of equal variances between groups. P-values correspond to a test of the null hypothesis of no difference in true means between the groups. Percent of control is presented for descriptive purposes and represents the relative mean for rtTA3/*Tyr*-shRNA when compared to control. See also Supplemental Figure 2.

Table 2.2: Knockdown of *Tyr in vivo* is not sufficient to induce significant melanin loss in the agouti mouse coat.

Outcome	Control (n=13)	rtTA2/*Tyr*-shRNA (n=13)	Difference (rtTA3/*Tyr*-shRNA – Cont)		% of Control
	Mean (SD)	Mean (SD)	Diff in Means (95% CI)	p-value	
A500/mg	0.69 (0.1)	0.66 (0.15)	-0.03 (-0.14, 0.08)	0.582	
Total melanin (μg/mg)	75.92 (11.67)	74.95 (16.44)	-0.97 (-12.49, 10.55)	0.864	98.7%
PCTA (ng/mg)	2740.4 (410.0)	2651.4 (615.9)	-89 (-511.6, 333.6)	0.668	
Eumelanin (μg/mg)	68.52 (10.26)	66.29 (15.41)	-2.22 (-12.79, 8.35)	0.669	96.8%
4-AHP (ng/mg)	824.4 (251.7)	963.1 (215.4)	138.7 (-50.5, 327.9)	0.144	
Pheomelanin (μg/mg)	7.41 (2.263)	8.66 (1.95)	1.25 (-0.46, 2.96)	0.143	116.9%
Average Phe/Eu Ratio	0.108 (0.025)	0.135 (0.034)	0.027 (0.01, 0.05)	0.027	

Dorsal hairs of agouti mice on continuous doxycycline treatment were shaved and processed for chemical analysis of eumelanin and of pheomelanin based upon their specific degradation products, pyrrole-2,3,5-tricarboxylic acid (PCTA) and 4-amino-3-hydroxyphenylalanine (4-AHP), respectively as described in Table 1. 13 control (*Tyr*-shRNA only or rtTA driver only) and 13 *Tyr*-knockdown mice were analyzed. Within group summary statistics represent the arithmetic mean and (standard deviation). Differences in means between rtTA3/*Tyr*-shRNA and control were tested using a two-sample t-test with no assumption of equal variances between groups. P-values correspond to a test of the null hypothesis of no difference in true means between the groups. Percent of control is presented for descriptive purposes and represents the relative mean for rtTA3/*Tyr*-shRNA when compared to control.

Table 2.S1: The partial depletion of *Tyr in vivo* does not affect the melanosome density within the mouse melanocyte.

Mouse Coat Color and Genotype	Number of melanosomes/100 micron^2	*p*-value
Black *Tyr*-shRNA control	113.9 +15.4	0.24
Black *Tyr*-knockdown	108.9 +12.4	
Agouti *Tyr*-shRNA control	103.9 +7.5	0.29
Agouti *Tyr*-knockdown	105.9 +10.9	
Yellow agouti *Tyr*-shRNA control	105.9 +10.9	0.43
Yellow agouti *Tyr*-knockdown	94.6 +10.7	

Fresh whole mouse skin was excised from the indicated mice using a four-mm round punch biopsy and fixed in Karnovsky's fixative before electron microscopy analysis. The number of melanosomes per area for 15 melanocytes from 2 mice per mouse coat color and genotype were determined.

Table 2.S2: List of Antibodies Used in Experiments

Antibody	Host	Application	Dilution	Company	Catalog No.
polyclonal anti-GFP	Rabbit	IHC-P	1:1000	Cell Signaling	2555
anti-rabbit IgG (biotinylated)	Goat	IHC-P	1:500	Vector Labs	BA-1000
polyclonal anti-TYR	Goat	WB	1:200	Santa Cruz	sc-7834
monoclonal anti-GFP	Mouse	WB	1:1000	Cell Signaling	2955
monoclonal anti-β-actin	Rabbit	WB	1:1000	Cell Signaling	4970
anti-rabbit IgG, HRP-linked	Goat	WB	1:5000	Cell Signaling	7074
anti-mouse IgG, HRP-linked	Horse	WB	1:5000	Cell Signaling	7076
anti-goat IgG, HRP-linked	Rabbit	WB	1:1000	Santa Cruz	sc-2768

IHC-P = immunohistochemistry, paraffin-embedded tissue
WB=Western blot

Table 2.S3: List of primers used for genotyping and their sequences, 5' to 3'

Genotyping Primers	**Sequence, 5' to 3'**
Rosa26-rtTA2 common reverse	AAAGTCGCTCTGAGTTGTTAT
Rosa26-rtTA2 transgene forward	GCGAAGAGTTTGTCCTCAACC
Rosa26-rtTA2 wild-type forward	GGAGCGGGAGAAATGGATATG
CAG-rtTA3 common reverse	CGAAACTCTGGTTGACATG
CAG-rtTA3 transgene forward	CTGCTGTCCATTCCTTATTC
CAG-rtTA3 wild-type forward	TGCCTATCATGTTGTCAAA
RBG-reverse 1	GAAAGAACAATCAAGGGTCC
RGB-reverse 2	CACCCTGAAAACTTTGCCCC
Col1a1-forward	AATCATCCCAGGTGCACAGCATTGCGG
Col1a1-reverse	CTTTGAGGGCTCATGAACCTCCCAGG
SAdpA-reverse	ATCAAGGAAACCCTGGACTACTGCG
Tyr-shRNA forward 1	AAGCCACAGATGTATGATCTGCTA
Tyr-shRNA forward 2	GCCACAGATGTATGATCTGCTAC
Luc-shRNA forward	GATGTATTAATCAGAGACTTC
Luc-shRNA reverse	CACCCTGAAAACTTTGCCCC

Table 2.S4: Genotype of loci with major effect on coat color in ES cells and mice used in this study.

	Genotype at locus			
Strain	*agouti*	*Tyrp1*	*Tyr*	*Oca2*
C57BL/6J	*a/a*	+/+	+/+	+/+
B6.Cg-Ay/J	A^y/a	+/+	+/+	+/+
KH2 ES cells (129S4 x C57BL/6J F1)	A^w/a	+/+	+/+	+/+
B6N.FVB(Cg)-Tg(CAG-rtTA3)4288Slowe/J	a/a	+/+	+/+	+/+
129S1/SvImJ	A^w/A^w	+/+	+/+	+/+

A - agouti, chromosome 2.
B - tyrosinase related protein 1 (*Tyrp1*), chromosome 4.
C - Tyrosinase (*Tyr*), chromosome 7.
p - oculocutaneous albinism II (Oca2), aka pink-eyed dilution, chromosome 7.

9-*cis* Retinoic Acid is the ALDH1A1 Product that Stimulates Melanogenesis

Chapter 3

Elyse K. Paterson, Hsiang Ho, Rubina Kapadia and Anand K. Ganesan

Experimental Dermatology

Accepted for Publication January 21, 2013

First published online March 12, 2013

DOI: 10.1111/exd.12099

3.1 Abstract

Aldehyde dehydrogenase 1A1 (ALDH1A1), an enzyme that catalyzes the conversion of lipid aldehydes to lipid carboxylic acids, plays pleiotropic roles in UV-radiation resistance, melanogenesis, and stem cell maintenance. In this study, a combination of RNAi and pharmacologic approaches were used to determine which ALDH1A1 substrates and products regulate melanogenesis. Initial studies revealed that neither the UV-induced lipid aldehyde 4-hydroxy-2-nonenal nor the ALDH1A1 product all-*trans* retinoic acid appreciably induced melanogenesis. In contrast, both the ALDH1A1 substrate 9-*cis* retinal and its corresponding product 9-*cis* retinoic acid potently induced the accumulation of *MITF* mRNA, *Tyrosinase* mRNA, and melanin. ALDH1A1 depletion inhibited the ability of 9-*cis* retinal but not 9-*cis* retinoic acid to stimulate melanogenesis, indicating that ALDH1A1 regulates melanogenesis by catalyzing the conversion of 9-*cis* retinal to 9-*cis* retinoic acid. The addition of potent ALDH1A inhibitors (cyanamide or Angeli's salt) suppressed *Tyrosinase* and *MITF* mRNA accumulation *in vitro* and also melanin accumulation in skin equivalents, suggesting that 9-*cis* retinoids regulate melanogenesis in the intact epidermis. Taken together, these studies not only identify cyanamide as a potential novel treatment for hyperpigmentary disorders, but also identify 9-*cis* retinoic acid as a pigment stimulatory agent that may have clinical utility in the treatment of hypopigmentary disorders, such as vitiligo.

3.2 Introduction

Melanin, a pigment produced by the epidermal melanocyte, protects the skin from the harmful effects of UV irradiation and is aberrantly regulated in many human skin diseases including vitiligo and melasma [1, 2]. Genetic and biochemical studies have identified over 150 genes that regulate melanogenesis in mouse and human skin [3]. This knowledge has led to the identification of pigment inhibitory agents, such as hydroquinone, that can effectively inhibit melanin production *in vivo* [3]. Unfortunately, the clinical use of hydroquinone has been limited by its potential teratogenicity [4-7]. Despite the fact that many genes that regulate melanogenesis have been identified, effective pharmacologic agents that can stimulate melanogenesis in hypopigmented skin are currently unavailable [8, 9]. These observations highlight the continuing need to develop safe pigment modulatory agents for the treatment of pigmentary disorders.

Our group recently utilized a genome-wide RNAi screening approach to identify pharmaceutically tractable drug targets for the rational design of pigment modulatory agents [10]. This approach identified 92 novel regulators of melanin production in human cells, including a number of genes that control the expression of microphthalmia-associated transcription factor (MITF), the central transcriptional regulator of melanogenesis, and tyrosinase (TYR), the enzyme that catalyzes the rate-limiting step in melanogenesis [1, 10-12]. One of the novel regulators of MITF and TYR expression identified in our screen was ALDH1A1 [10], a well-characterized NAD $(P)^+$-dependent enzyme that catalyzes the irreversible oxidation of highly reactive aliphatic and aromatic aldehydes to their corresponding non-toxic carboxylic acids (EC number 1.2.1.36) [13]. The ALDH1A subfamily (ALDH1A1, ALDH1A2,

ALDH1A3) is known to catalyze, with an equal efficiency, the oxidation of all-*trans* retinal and 9-*cis* retinal to all-*trans* retinoic acid and 9-*cis* retinoic acid, respectively [14, 15]. Additionally, ALDH1A1 functions in the lens and cornea to detoxify 4-hydroxy-2-nonenal (4-HNE), a highly reactive lipid aldehyde that is generated from ultraviolet radiation induced lipid peroxidation reactions [16, 17]. Other studies have revealed that ALDH1A1 is a marker of stem cells [18]. In summary, ALDH1A1 is an enzyme that is able to regulate diverse processes ranging from stem cell maintenance [18], to UV-radiation resistance, to melanogenesis [10] by catalyzing the conversion of specific aldehydes to their corresponding carboxylic acids [1, 10, 16-20].

Previous work demonstrated that ALDH1A1 depletion in primary melanocytes and MNT-1 melanoma cells inhibited the accumulation of both *TYR* and *MITF* mRNA and protein [10]. Additionally, two potent inhibitors of the ALDH1A family (cyanamide and Angeli's salt) were shown to inhibit both TYR protein accumulation and melanin accumulation in normal human melanocytes [10]. Recent studies have suggested that human melanocytes can catalyze the light-induced isomerization of 9-*cis* retinal and revealed that the addition of 9-*cis* retinal in conjunction with UVA radiation is sufficient to induce melanin accumulation in normal human melanocytes [21]. In this study, we utilize a combination of RNAi and pharmacologic approaches to identify 9-*cis* retinal as the ALDH1A1 substrate that regulates melanogenesis.

3.3 Materials and Methods

Cell culture

Human MNT-1 melanoma cells were a gift from M. Marks (University of Pennsylvania). These cells were cultured in DMEM (CellGro) supplemented with 15% fetal bovine serum (CellGro), sodium pyruvate (Invitrogen), L-glutamine (Invitrogen), MEM vitamin solution (Invitrogen), antibiotic-antimycotic (Invitrogen), and 10% AIM-V medium (Invitrogen). For the melanin quantitation experiments, MNT-1 cells were switched to DMEM minus phenol red (CellGro) supplemented with 10% fetal bovine serum, sodium pyruvate, L-glutamine and antibiotic-antimycotic as previously described [10]. Human deeply-pigmented neonatal epidermal melanocytes (Invitrogen) were cultured in Medium 254 (Invitrogen) supplemented with phorbol 12-myristate 13-acetate-free Human Melanocyte growth supplement-2 (Invitrogen). As these melanocyte strains were purchased from commercial entities, no IRB approval was required prior to their use.

Drug Treatment

Briefly, MNT-1 cells or deeply-pigmented (DP) melanocytes were plated at a density of 1.5 x 10^4 cells per well of a 96-well microtiter plate and allowed to re-attach overnight. Subsequently, cells were incubated with varying concentrations of cyanamide (Sigma Aldrich), Angeli's salt (Sodium α-oxyhyponitrite, chemical name; disodium diazen-1-ium-1,2,2-triolate, formal name; Cayman Chemical), 4-HNE (4-hydroxy-2E-nonenal, formal name; Cayman

Chemical), 9-*cis* retinal, 9-*cis* retinoic acid, all-*trans* retinal or all-*trans* retinoic acid at the indicated concentrations (Sigma Aldrich). The cells were incubated with the retinoids for merely 30-45 minutes to avoid cellular toxicity. In the case of cyanamide, Angeli's salt and 4-HNE, cells were incubated in each drug for at least 24 hours. For the UV experiments, cells were incubated in media containing 9-*cis* retinal for 30 minutes before being irradiated with the indicated dose of UV light. Media was immediately refreshed after UV irradiation, and RNA was isolated from these cells 24 hours later. For the melanin quantitation experiments, cells were allowed to grow to confluency post 9-*cis* retinal/UVA treatment.

Real-time quantitative PCR for mRNA

A Cells-to-Ct kit was utilized to lyse the cells after the appropriate drug treatment (Applied Biosystems). A high capacity RNA-to-cDNA kit was then employed to generate cDNA (Applied Biosystems). Solaris qPCR gene expression assays for MITF (AX-008674-00-0100), TYR (AX-012555-00-0200), ALDH1A1 (AX-008722-00-0100), β-actin (AX-003451-00-0100) and GAPDH (AX-004253-00-0100) were obtained from Thermo Scientific (Dharmacon RNAi technologies) and used with TaqMan Gene Expression Master Mix (Applied Biosystems) to complete the PCR reaction. A 7900HT Fast Real-Time PCR system (Applied Biosystems) and SDS 2.4 (Applied Biosystems) were used to determine Ct values for each sample. Values were normalized to either β-actin or GAPDH using the relative quantification mathematical model (Pfaffl) as previously described [10]. A two-tailed Student's *t*-test was employed to determine statistical significance.

Western blotting

MNT-1 or DP melanocytes were plated in 96-well plates at a concentration of 2 x 10^4 cells per well, allowed to re-attach overnight, and then incubated with drug for 30 hours. After treatment, the number of cells in each well was quantified and lysates were prepared using the RIPA lysis buffer system (RIPA supplemented with protease inhibitor, PMSF and sodium orthovanadate; Santa Cruz Biotechnology). Lysates were then clarified by centrifugation (3,000 rpm for 10 minutes at 4°C). The relative concentration of protein in each lysate was quantified using both a BCA Protein Assay Kit (Thermo Scientific) and a Coomassie (Bradford) protein assay (Thermo Scientific) to eliminate the effects of interfering melanin. A total of 20 μg of protein per sample was separated on a 4-20% SDS-polyacrylamide gel (Bio-Rad) under reducing conditions and transferred onto to a 0.45-μm nitrocellulose membrane (Bio-Rad). Subsequently, membranes were blocked in a blocking buffer solution comprised of TBS (Fisher Scientific), 0.1% Tween-20 (Fisher Scientific) and 5% non-fat milk powder (Apex).

The following antibodies were used: rabbit polyclonal α/β-tubulin, #2148, Cell Signaling Technology; goat anti-rabbit IgG, HRP-linked, #7074, Cell Signaling Technology; mouse monoclonal tyrosinase, sc-20035, Santa Cruz Biotechnology; bovine anti-mouse IgG-HRP sc-2371, Santa Cruz Biotechnology. To assess immunoreactivity, either a SuperSignal West Dura Extended Duration Substrate or a SuperSignal West Pico Chemiluminescent Substrate was used according to manufacturer's directions (Pierce Protein Biology Products). Protein levels were assessed using densitometry analysis (ImageJ).

RNA interference

1.5 x 10^4 MNT-1 melanoma cells were reverse-transfected in 96-well microtiter plates with 50 nM ALDH1A1 or control siRNAs using a Dharmafect 2 transfection reagent as previously described [10]. A non-targeting control (SMARTpool; D-001810-10-20; Thermo Scientific, Dharmacon RNAi Technologies) was used as the negative control, while three different siRNA oligos purchased from Ambion (s1236, s1237, s1238) were pooled for the ALDH1A1 depletion experiments. Transfected cells were allowed to remain in the transfection media for 72 hours before drug treatment to ensure protein knockdown. Real-time quantitative RT-PCR was used to verify that ALDH1A1 siRNA effectively inhibited the expression of ALDH1A1.

Pigment Measurement

MNT-1 cells were plated at a density of 1 x 10^4 cells per well in a 96-well plate, allowed to re-attach overnight, and incubated in the indicated concentration of drug for four days. Cells were then lysed using a Cell-Titer Glo reagent (Promega), and relative melanin accumulation was quantified by measuring the absorbance of each well at 405 nm and normalizing this value to the relative cell number in each well as determined by the Cell-Titer Glo assay [10]. For the UVA experiments, cells were incubated with the indicated concentration of 9-*cis* retinal for 30 minutes, and then irradiated with the indicated dose of UVA. Media was changed immediately after UVA treatment to avoid toxicity. Cells were then lysed four days after UVA treatment according to the protocol described above. The relative pigment index (PI) was calculated by

dividing the absorbance values at 405 nm by the Cell-Titer Glo luminescence values, and then normalizing these values to the experimental control (vehicle-treated wells). To calculate the % pigment induction, the following equation was used: (PI of test – PI control (vehicle)) x 100%. A Student's two-tailed *t*-test was used to calculate the statistical significance of each value compared to the vehicle-treated control.

Maintenance and treatment of three-dimensional skin equivalents

MelanoDerm deeply-pigmented three-dimensional skin equivalents were obtained from MatTek Corporation (Ashland, MA) and maintained according to the manufacturer's instructions. The equivalents were maintained in a humidified incubator at 37°C with 5% CO_2 in EPI-100-NMM-113 media as prepared by MatTek (DMEM with 5 μg/mL gentamicin, 0.25 μg/mL amphotericin, α-MSH, β-FGF, and KGF). Both the media and the drug were refreshed every other day for three weeks before the samples were harvested for a solvable melanin assay. Cyanamide (600 μM) and kojic acid (2%) were dissolved in water before being added to the equivalents at a total volume of 20 μL. The relative melanin content of each skin equivalent after drug treatment was determined using a solvable melanin assay [22]. A Student's two-tailed *t*-test was utilized to determine whether cyanamide or kojic acid significantly inhibited the accumulation of melanin in skin equivalents.

3.4 Results

9-*cis* retinal is the ALDH1A1 substrate that stimulates melanogenesis

While published studies have defined lipid aldehydes that are detoxified by ALDH1A1 and identified ALDH1A1 substrates that promote cellular differentiation [17, 19, 23, 24], it is currently unclear which ALDH1A1 substrates regulate melanogenesis. Initial studies sought to verify that the ALDH1A family regulates melanogenesis by a catalytic mechanism. Two potent inhibitors of ALDH1A, cyanamide and Angeli's salt, inhibited the accumulation of *TYR* and *MITF* mRNA in a dose responsive manner (Figs. 1A and 1B), consistent with previous observations that ALDH1A1 depletion inhibited the accumulation of TYR and MITF protein [10].

Once we had determined that ALDH1A inhibitors could block melanogenesis, we next sought to identify putative substrates of ALDH1A that regulate melanogenesis. ALDH1A1 exhibits a high affinity for 4-HNE, one of the most abundant α, β-unsaturated aldehydes generated from UV-induced lipid peroxidation reactions [17, 19, 20]. Interestingly, 4-HNE not only inhibited the accumulation of melanin (S1A Fig.) but also the accumulation of *TYR* and *MITF* mRNA in MNT-1 cells (Fig. 1C), indicating that ALDH1A regulates melanogenesis by a mechanism that is distinct from its role in inhibiting corneal opacification [16, 17, 19].

We next sought to determine whether other known ALDH1A substrates stimulate melanogenesis. In addition to 4-HNE, ALDH1A also catalyzes the oxidation of retinal to retinoic acid [15, 25, 26]. Notably, ALDH1A can metabolize both all-*trans* retinal and 9-*cis* retinal to their corresponding carboxylic acids with equal efficiency [14]. Recently published

studies have demonstrated that 9-*cis* retinal can promote melanin accumulation in the context of UVA irradiation [14, 21]. Therefore, we sought to define specific retinaldehydes that stimulate melanogenesis. All-*trans* retinal stimulated melanogenesis at relatively high doses (S1B Fig.). These observations could be secondary to a direct stimulatory effect of all-*trans* retinal on melanogenesis, or secondary to the fact that all-*trans* retinal can be isomerized to 9-*cis* retinal, as suggested by others [21, 27]. Interestingly, 9-*cis* retinal in conjunction with UVA irradiation stimulated the accumulation of *TYR* and *MITF* mRNA in both MNT-1 melanoma cells and primary melanocytes (Figs. 1D and S1C). Similarly, the combination of 9-*cis* retinal treatment and UVA exposure induced melanin accumulation in MNT-1 cells, even though this treatment also induced cellular cytotoxicity (Figs. 1E, S2A, S2B).

The metabolic product of 9-*cis* retinal oxidation, 9-*cis* retinoic acid, acts to stimulate melanin accumulation

While *cis*-retinal isomerization to *trans*-retinal is UV dependent, the oxidation of retinal by ALDH1A is not [28]. In order to better establish whether 9-*cis* retinal or all-*trans* retinal regulates melanogenesis, we next sought to determine whether 9-*cis* retinal could stimulate melanin accumulation in the absence of UV-induced isomerization. 9-*cis* retinal induced pigment accumulation in a dose-responsive manner in the absence of UV irradiation (Fig. 2A). As 9-*cis* retinal was able to induce pigment accumulation independently of UV-irradiation, we reasoned that the addition of 9-*cis* retinoic acid, the oxidation product of 9-*cis* retinal catalyzed by ALDH1A [15, 25], should also stimulate melanin accumulation. As expected, 9-*cis* retinoic acid stimulated melanin accumulation in MNT-1 cells both visually and quantitatively (Figs. 2B

and 2C). Interestingly, 9-*cis* retinoic acid stimulated melanin accumulation more effectively than 9-*cis* retinal, providing evidence that the product of ALDH1A catalysis is the actual species that stimulates melanogenesis (Figs. 2A and 2B). In contrast, all-*trans* retinoic acid did not induce melanin accumulation (Figure 2D), providing further evidence that 9-*cis* retinoids and not all-*trans* retinoids stimulate melanogenesis.

9-*cis* retinoic acid stimulates the accumulation of TYR and MITF mRNA and TYR protein

Based on the observation that both 9-*cis* retinal and 9-*cis* retinoic acid stimulated melanin accumulation in the absence of UVA radiation, we reasoned that the 9-*cis* retinoids should also induce the accumulation of *TYR* and *MITF* mRNA. As predicted, both 9-*cis* retinal and 9-*cis* retinoic acid induced the accumulation of *TYR* (Figs 3A and 3C) and *MITF* (Figs. 3B, 3D, 3E*)* mRNAs in both primary melanocytes and MNT-1 melanoma cells, demonstrating that either species alone is sufficient to stimulate the transcription of critical regulators of melanogenesis. 9-*cis* retinal was not sufficient to induce TYR protein accumulation in either MNT-1 cells (upper panel) or primary melanocytes (lower panel) (Fig. 3F). However, 9-*cis* retinoic acid induced the accumulation of TYR protein in a dose responsive manner in both skin cell types (Fig. 3F). These observations could either be secondary to the fact that only a small fraction of 9-*cis* retinal is converted to 9-*cis* retinoic acid or due to the fact that the slow kinetics of the reaction prevented us from observing the stimulatory effect of 9-*cis* retinal on TYR protein accumulation within the experimental timeframe. Nonetheless, these results suggest that ALDH1A1 regulates melanogenesis by catalyzing the conversion of 9-*cis* retinal to 9-*cis* retinoic acid.

9-*cis* retinoic acid is able to stimulate the accumulation of *TYR* and *MITF* mRNAs in the absence of endogenous levels of ALDH1A1

To verify that ALDH1A regulates melanogenesis via the oxidation of 9-*cis* retinal, we examined whether 9-*cis* retinal could induce melanogenesis in an ALDH1A1 independent manner. Initial studies identified pooled ALDH1A1 siRNAs that effectively inhibited the expression of ALDH1A1 mRNA (S2C Fig.). As theorized, ALDH1A1 depletion inhibited the ability of 9-*cis* retinal (Fig. 3G) but not of 9-*cis* retinoic acid (Fig. 3H) to stimulate the accumulation of *TYR* and *MITF* mRNA. These results confirm that the product of ALDH1A1 oxidation, 9-*cis* retinoic acid, stimulates melanogenesis, because the addition of 9-*cis* retinal in the absence of ALDH1A1 did not induce the accumulation of *TYR* and *MITF* mRNAs.

Cyanamide is able to inhibit the production of melanin in a three-dimensional model of human skin

Once we had determined how ALDH1A regulates melanogenesis *in vitro*, we next sought to determine whether ALDH1A activity regulates melanogenesis in a more physiologic model of human skin. For these experiments, we obtained skin equivalents containing normal human epidermal keratinocytes and melanocytes from Mattek, an equivalent model that has been used by other groups to assess the efficacy of skin depigmenting agents [22]. Using doses that had been used previously to inhibit melanogenesis in primary melanocytes [10], we determined that cyanamide was able to inhibit melanin accumulation quantitatively as measured by a solvable

melanin assay (Fig. 4A), as well as both visually and histologically as measured by Fontana Masson staining (Fig. 4B).

Additionally, we sought to investigate whether 9-*cis* retinoic acid could induce melanogenesis in human skin equivalents. Preliminary studies revealed that neither forskolin (a well established pigment agonist) [29] nor 9-*cis* retinoic acid is able to quantitatively stimulate melanogenesis in lightly or darkly pigmented skin equivalents (data not shown). While an abundance of literature has documented the utility of skin equivalent models for quantifying the efficacy of melanogenesis inhibitors [22, 30-34], this system has not yet been optimized to quantify the efficacy of pigment agonists. Our preliminary results suggest that further optimization of these models is required before they can be used to quantify the efficacy of pharmacologic agents that induce melanogenesis.

3.5 Discussion

In this study, we sought to define ALDH1A substrates and products that regulate melanogenesis. Initial studies revealed that 9-*cis* retinal and 9-*cis* retinoic acid stimulated melanin accumulation, while all-*trans* retinoic acid was unable to stimulate melanin accumulation (Figs. 1E, S2A, 2A, 2B, 2D). These results identify a novel role for the 9-*cis* retinoids in regulating melanogenesis. Consistent with this observation, we observed that the addition of 9-*cis* retinoic acid potently induced the accumulation of *MITF* and *TYR* mRNA, and TYR protein in melanocytic cells (Figs. 3C-3F).

9-*cis* retinal was able to induce the accumulation of *MITF* and *TYR* mRNA at high doses, but was unable to induce the accumulation of TYR protein (Figs. 3A, 3B, 3F). It is currently unclear what percent of the added 9-*cis* retinal is converted to 9-*cis* retinoic acid in our experiments. This makes it difficult to compare the relative effects of 9-*cis* retinal and 9-*cis* retinoic acid on the accumulation of *MITF* and *TYR* mRNA. Moreover, the interpretation of the results of these experiments is further complicated by the fact that the added 9-*cis* retinoic acid could also be converted to all-*trans* retinoic acid [35], and all-*trans* retinoic acid and 9-*cis* retinoic acid can synergistically activate RXR-RAR heterodimers [35, 36].

In light of these complications, we sought to better clarify whether 9-*cis* retinoic acid independently regulates melanogenesis. Depletion of ALDH1A1 inhibited the ability of 9-*cis* retinal but not 9-*cis* retinoic acid to stimulate melanogenesis (Figs. 3G and 3H). This indicates that 9-*cis* retinoic specifically stimulates melanogenesis. Finally, ALDH1A inhibitors also inhibited the accumulation of *MITF* and *TYR* mRNAs *in vitro* and melanin accumulation in skin equivalents, further implicating a role for 9-*cis* retinoic acid in stimulating melanogenesis (Figs.

1A-1B, 4A-B). Future studies will establish better models to examine the independent effects of different retinoid isomers on melanogenesis in human skin.

A multitude of studies to date have sought to determine whether all-*trans* retinoic acid inhibits or stimulates melanogenesis. While a number of studies demonstrate that all-*trans* retinoic acid inhibits melanogenesis [37-40], an equal number of studies propose that it stimulates melanogenesis or augments UV-induced melanogenesis in a variety of mouse and human cell lines [41-44]. In this study, we approached this question by attempting to identify ALDH1A1 substrates and products that regulate melanogenesis. Our results revealed that all-*trans* retinoic acid was able to stimulate melanogenesis at high doses, while 9-*cis* retinoic acid was able to potently stimulate melanogenesis. It is particularly intriguing that 9-*cis* retinoic acid, which is not thought to have a functional role in the physiology of epidermal keratinocytes [45], appears to have a specific role in regulating the differentiation of epidermal melanocytes. Future studies will determine whether 9-*cis* retinoic acid related agents (rexinoids) are selective agents that can induce melanogenesis.

Extensive studies have sought to better define how retinoids and rexinoids regulate transcription. The biological effects of 9-*cis* retinoic acid are primarily mediated by its cognate receptor, the retinoid X receptor (RXR), of which there are three isoforms (α, β, and γ) [23, 46]. While the retinoic acid receptor (RAR) can be activated by either 9-*cis* retinoic acid or all-*trans* retinoic acid, RXRs are activated exclusively by 9-*cis* retinoic acid [46, 47]. Along with RARs, RXRs are members of the steroid hormone receptor superfamily of ligand-activated transcription factors [24, 48]. RXRs are known to dimerize with a variety of nuclear receptors, including the vitamin D receptor (VDR), the peroxisome proliferator-activated receptor (PPAR), and the thyroid hormone receptor (T3R) [49-51]. RXR homodimers act as potent inhibitors of

transcription in the absence of ligand and only activate transcription upon ligand binding [52].

In the absence of ligand, RXR interacts with co-repressor proteins including silencing mediator for retinoid and thyroid hormone receptors (SMRT) and nuclear receptor co-repressor (N-CoR) [52, 53]. These homologous proteins mediate the repressive effect of un-liganded receptors by recruiting histone deacetylase complexes to effectively silence the chromatin [52, 53]. Upon ligand binding, RXR recruits such proteins as CBP/p300, p300/CBP-associated factor and members of the SRC/p160 family (SRC-1/NCoA-1, TIF-2/GRIP-1/NCoA-2/SRC-2 and pCIP/ACTR/A1B1/TRAM1/RAC3/SRC-3), which possess intrinsic histone acetylase transferase activity and potentiate the transcriptional activity of ligand-bound receptors [52, 54, 55].

Interestingly, when we searched the MITF promoter region for putative RXR binding sites, we discovered that while this promoter did not contain RXR-VDR or RXR-T3R binding sites, it did contain a highly conserved RAR-RXR heterodimer binding site located proximal to the transcription start site [56, 57]. While only RAR agonists are required to activate transcription downstream of RAR-RXR heterodimers, it has been demonstrated that the addition of RAR and RXR agonists can synergistically stimulate transcription from these sites [58, 59]. Other studies have determined that the vitamin D receptor (VDR) binds its enhancer element as a heterodimer with RXR in the human epidermis, while the thyroid hormone receptor, another potential binding partner of RXR, is expressed in the epidermis [60-62]. Taken together, these studies indicate not only that RXR can play pleiotropic roles in regulating the differentiation of the epidermis but also that agents that can stimulate both RAR and RXR may be more effective at inducing melanogenesis as compared to RAR agonists alone.

Although there are three unique isoforms of RXR (α, β, and γ) RXRα is the most abundant isoform expressed in the epidermis [24, 50, 51]. Interestingly, RXRα mutant mice

demonstrate a premature greying phenotype, which is first visible in the snout hairs and then spreads to the truncal hair [63]. Subsequent to the hair graying, these mice develop a rapidly progressive alopecia characterized by the widespread accumulation of keratinous cysts [63]. Keratinocyte lineage-specific RXRα knockout mice develop progressive alopecia and accumulate keratinous cysts but do not exhibit premature hair graying [64, 65], suggesting that RXRα may have independent effects on melanogenesis and keratinocyte differentiation.

Vitiligo is characterized by the destruction of melanocytes [66]. New melanocytes must migrate into the de-pigmented area of skin before re-pigmentation can occur [66]. The major reservoir for melanocyte replacement is within the outer root sheath or bulge area of the hair follicle [66]. Previous studies have demonstrated that retinoic acid stimulates the differentiation of melanoblasts to melanocytes as characterized by the synthesis of pigment in the melanoblasts [67]. When coupled with our observations that RXR agonists can specifically stimulate melanogenesis in melanocytes, our studies implicate a role for RXR agonists as drugs with the potential to re-induce melanogenesis in vitiliginous skin. Future studies will optimize existing skin equivalent models to quantitatively determine whether RXR agonists can stimulate melanogenesis in skin equivalents with the goal of developing selective agents that can induce melanogenesis in vitiliginous skin.

3.6 Acknowledgements

We thank Jonathan Schilling and Priya Vasudeva for their technical assistance. This work was supported by a grant from the National Institutes of Health (1K08AR056001) to Anand K. Ganesan.

3.7 References

1. Costin GE, Hearing VJ. Human skin pigmentation: melanocytes modulate skin color in response to stress. FASEB J. 2007;21(4):976-94. doi: fj.06-6649rev [pii] 10.1096/fj.06-6649rev. PubMed PMID: 17242160.

2. Schallreuter KU, Kothari S, Chavan B, Spencer JD. Regulation of melanogenesis--controversies and new concepts. Exp Dermatol. 2008;17(5):395-404. doi: 10.1111/j.1600-0625.2007.00675.x. PubMed PMID: 18177348.

3. Bennett DC, Lamoreux ML. The color loci of mice--a genetic century. Pigment cell research / sponsored by the European Society for Pigment Cell Research and the International Pigment Cell Society. 2003;16(4):333-44. PubMed PMID: 12859616.

4. Grimes P, Nordlund JJ, Pandya AG, Taylor S, Rendon M, Ortonne JP. Increasing our understanding of pigmentary disorders. Journal of the American Academy of Dermatology. 2006;54(5 Suppl 2):S255-61. doi: 10.1016/j.jaad.2005.12.042. PubMed PMID: 16631966.

5. Brenner M, Hearing VJ. Modifying skin pigmentation - approaches through intrinsic biochemistry and exogenous agents. Drug discovery today Disease mechanisms. 2008;5(2):e189-e99. doi: 10.1016/j.ddmec.2008.02.001. PubMed PMID: 19578486; PubMed Central PMCID: PMC2678743.

6. Liang CH. Ov-16 [4-(3,4-dihydroxybenzoyloxymethyl)phenyl-O-β-D-glucopyranoside] inhibits melanin synthesis by regulating expressions of melanogenesis-regulated gene and protein. Exp Dermatol. 2011;20(9):743-8. doi: 10.1111/j.1600-0625.2011.01311.x. PubMed PMID: 21672031.

7. Ahn KS, Moon KY, Lee J, Kim YS. Downregulation of NF-kappaB activation in human keratinocytes by melanogenic inhibitors. Journal of dermatological science. 2003;31(3):193-201. PubMed PMID: 12727023.

8. Yaghoobi R, Omidian M, Bagherani N. Vitiligo: a review of the published work. The Journal of dermatology. 2011;38(5):419-31. PubMed PMID: 21667529.

9. Nicolaidou E, Antoniou C, Stratigos A, Katsambas AD. Narrowband ultraviolet B phototherapy and 308-nm excimer laser in the treatment of vitiligo: a review. Journal of the American Academy of Dermatology. 2009;60(3):470-7. doi: 10.1016/j.jaad.2008.07.053. PubMed PMID: 19157641.

10. Ganesan AK, Ho H, Bodemann B, Petersen S, Aruri J, Koshy S, et al. Genome-wide siRNA-based functional genomics of pigmentation identifies novel genes and pathways that impact melanogenesis in human cells. PLoS Genet. 2008;4(12):e1000298. doi: 10.1371/journal.pgen.1000298. PubMed PMID: 19057677; PubMed Central PMCID: PMCPMC2585813.

11. Slominski A, Zmijewski MA, Pawelek J. L-tyrosine and L-dihydroxyphenylalanine as hormone-like regulators of melanocyte functions. Pigment Cell Melanoma Res. 2012;25(1):14-27. doi: 10.1111/j.1755-148X.2011.00898.x. PubMed PMID: 21834848; PubMed Central PMCID: PMCPMC3242935.

12. Lee MS, Yoon HD, Kim JI, Choi JS, Byun DS, Kim HR. Dioxinodehydroeckol inhibits melanin synthesis through PI3K/Akt signalling pathway in α-melanocyte-stimulating hormone-treated B16F10 cells. Exp Dermatol. 2012;21(6):471-3. doi: 10.1111/j.1600-0625.2012.01508.x. PubMed PMID: 22621193.

13. Koppaka V, Thompson DC, Chen Y, Ellermann M, Nicolaou KC, Juvonen RO, et al. Aldehyde dehydrogenase inhibitors: a comprehensive review of the pharmacology, mechanism of action, substrate specificity, and clinical application. Pharmacological reviews. 2012;64(3):520-39. doi: 10.1124/pr.111.005538. PubMed PMID: 22544865; PubMed Central PMCID: PMC3400832.

14. Duester G. Families of retinoid dehydrogenases regulating vitamin A function: production of visual pigment and retinoic acid. European journal of biochemistry / FEBS. 2000;267(14):4315-24. PubMed PMID: 10880953.

15. Labrecque J, Dumas F, Lacroix A, Bhat PV. A novel isoenzyme of aldehyde dehydrogenase specifically involved in the biosynthesis of 9-cis and all-trans retinoic acid. The Biochemical journal. 1995;305 (Pt 2):681-4. PubMed PMID: 7832787; PubMed Central PMCID: PMC1136415.

16. Lassen N, Bateman JB, Estey T, Kuszak JR, Nees DW, Piatigorsky J, et al. Multiple and additive functions of ALDH3A1 and ALDH1A1: cataract phenotype and ocular oxidative damage in Aldh3a1(-/-)/Aldh1a1(-/-) knock-out mice. The Journal of biological chemistry. 2007;282(35):25668-76. doi: 10.1074/jbc.M702076200. PubMed PMID: 17567582; PubMed Central PMCID: PMC2253645.

17. Lassen N, Black WJ, Estey T, Vasiliou V. The role of corneal crystallins in the cellular defense mechanisms against oxidative stress. Seminars in cell & developmental biology. 2008;19(2):100-12. doi: 10.1016/j.semcdb.2007.10.004. PubMed PMID: 18077195.

18. Chen Y, Koppaka V, Thompson DC, Vasiliou V. Focus on molecules: ALDH1A1: from lens and corneal crystallin to stem cell marker. Experimental eye research. 2012;102:105-6. doi: 10.1016/j.exer.2011.04.008. PubMed PMID: 21536030; PubMed Central PMCID: PMC3423494.

19. Black W, Vasiliou V. Ocular Metabolism and Disposition of 4-Hydroxy-2-nonenal**.** Cutaneous and Ocular Toxicology. 2005;24(3):165-76.

20. Vasiliou V, Pappa A, Petersen DR. Role of aldehyde dehydrogenases in endogenous and xenobiotic metabolism. Chemico-biological interactions. 2000;129(1-2):1-19. PubMed PMID: 11154732.

21. Wicks NL, Chan JW, Najera JA, Ciriello JM, Oancea E. UVA phototransduction drives early melanin synthesis in human melanocytes. Current biology : CB. 2011;21(22):1906-11. doi: 10.1016/j.cub.2011.09.047. PubMed PMID: 22055294; PubMed Central PMCID: PMC3586554.

22. Ni-Komatsu L, Tong C, Chen G, Brindzei N, Orlow SJ. Identification of quinolines that inhibit melanogenesis by altering tyrosinase family trafficking. Mol Pharmacol. 2008;74(6):1576-86. doi: mol.108.050633 [pii] 10.1124/mol.108.050633. PubMed PMID: 18801917; PubMed Central PMCID: PMCPMC2747315.

23. Mangelsdorf DJ, Borgmeyer U, Heyman RA, Zhou JY, Ong ES, Oro AE, et al. Characterization of three RXR genes that mediate the action of 9-cis retinoic acid. Genes & development. 1992;6(3):329-44. PubMed PMID: 1312497.

24. Fisher GJ, Voorhees JJ. Molecular mechanisms of retinoid actions in skin. FASEB journal : official publication of the Federation of American Societies for Experimental Biology. 1996;10(9):1002-13. PubMed PMID: 8801161.

25. Molotkov A, Duester G. Genetic evidence that retinaldehyde dehydrogenase Raldh1 (Aldh1a1) functions downstream of alcohol dehydrogenase Adh1 in metabolism of retinol to retinoic acid. J Biol Chem. 2003;278(38):36085-90. doi: M303709200 [pii] 10.1074/jbc.M303709200. PubMed PMID: 12851412.

26. Fan X, Molotkov A, Manabe S, Donmoyer CM, Deltour L, Foglio MH, et al. Targeted disruption of Aldh1a1 (Raldh1) provides evidence for a complex mechanism of retinoic acid synthesis in the developing retina. Molecular and cellular biology. 2003;23(13):4637-48. PubMed PMID: 12808103; PubMed Central PMCID: PMC164835.

27. Futterman S, Rollins MH. The catalytic isomerization of all-trans-retinal to 9-cis-retinal and 13-cis-retinal. The Journal of biological chemistry. 1973;248(22):7773-9. PubMed PMID: 4750425.

28. Palczewski K. G protein-coupled receptor rhodopsin. Annual review of biochemistry. 2006;75:743-67. doi: 10.1146/annurev.biochem.75.103004.142743. PubMed PMID: 16756510; PubMed Central PMCID: PMC1560097.

29. Busca R, Ballotti R. Cyclic AMP a key messenger in the regulation of skin pigmentation. Pigment cell research / sponsored by the European Society for Pigment Cell Research and the International Pigment Cell Society. 2000;13(2):60-9. PubMed PMID: 10841026.

30. Jain P, Sonti S, Garruto J, Mehta R, Banga AK. Formulation optimization, skin irritation, and efficacy characterization of a novel skin-lightening agent. Journal of cosmetic dermatology. 2012;11(2):101-10. doi: 10.1111/j.1473-2165.2012.00610.x. PubMed PMID: 22672274.

31. Smiles KA, Dong KK, Canning MT, Grimson R, Walfield AM, Yarosh DB. A hydroquinone formulation with increased stability and decreased potential for irritation. Journal of cosmetic dermatology. 2007;6(2):83-8. doi: 10.1111/j.1473-2165.2007.00301.x. PubMed PMID: 17524123.

32. Goh MJ, Park JS, Bae JH, Kim DH, Kim HK, Na YJ. Effects of ortho-dihydroxyisoflavone derivatives from Korean fermented soybean paste on melanogenesis in B16 melanoma cells and human skin equivalents. Phytotherapy research : PTR. 2012;26(8):1107-12. doi: 10.1002/ptr.3682. PubMed PMID: 22162275.

33. Seiberg M, Paine C, Sharlow E, Andrade-Gordon P, Costanzo M, Eisinger M, et al. Inhibition of melanosome transfer results in skin lightening. The Journal of investigative dermatology. 2000;115(2):162-7. doi: 10.1046/j.1523-1747.2000.00035.x. PubMed PMID: 10951231.

34. Kondo S, Takahashi T, Yoshida K, Mizoguchi H. Inhibitory effects of autolysate of Leuconostoc mesenteroides isolated from kimoto on melanogenesis. Journal of bioscience and bioengineering. 2012;114(4):424-8. doi: 10.1016/j.jbiosc.2012.05.016. PubMed PMID: 22906413.

35. Shih TW, Lin TH, Shealy YF, Hill DL. Nonenzymatic isomerization of 9-cis-retinoic acid catalyzed by sulfhydryl compounds. Drug metabolism and disposition: the biological fate of chemicals. 1997;25(1):27-32. PubMed PMID: 9010626.

36. Minucci S, Leid M, Toyama R, Saint-Jeannet JP, Peterson VJ, Horn V, et al. Retinoid X receptor (RXR) within the RXR-retinoic acid receptor heterodimer binds its ligand and enhances retinoid-dependent gene expression. Molecular and cellular biology. 1997;17(2):644-55. PubMed PMID: 9001218; PubMed Central PMCID: PMC231790.

37. Hosoi J, Abe E, Suda T, Kuroki T. Regulation of melanin synthesis of B16 mouse melanoma cells by 1 alpha, 25-dihydroxyvitamin D3 and retinoic acid. Cancer research. 1985;45(4):1474-8. PubMed PMID: 2983883.

38. Orlow SJ, Chakraborty AK, Pawelek JM. Retinoic acid is a potent inhibitor of inducible pigmentation in murine and hamster melanoma cell lines. J Invest Dermatol. 1990;94(4):461-4. PubMed PMID: 2107263.

39. Roméro C, Aberdam E, Larnier C, Ortonne JP. Retinoic acid as modulator of UVB-induced melanocyte differentiation. Involvement of the melanogenic enzymes expression. J Cell Sci. 1994;107 (Pt 4):1095-103. PubMed PMID: 8056833.

40. Sato K, Morita M, Ichikawa C, Takahashi H, Toriyama M. Depigmenting mechanisms of all-trans retinoic acid and retinol on B16 melanoma cells. Bioscience, biotechnology, and biochemistry. 2008;72(10):2589-97. doi: 10.1271/bbb.80279. PubMed PMID: 18838813.

41. Fernandes SS, Arcuri R, Morgado-Diaz JA, Benchimol M. Increase of melanogenesis by retinoic acid: an ultrastructural and morphometric study. Tissue & cell. 2004;36(2):95-105. doi: 10.1016/j.tice.2003.10.006. PubMed PMID: 15041411.

42. Ho KK, Halliday GM, Barnetson RS. Topical retinoic acid augments ultraviolet light-induced melanogenesis. Melanoma research. 1992;2(1):41-5. PubMed PMID: 1643423.

43. Lotan R, Lotan D. Stimulation of melanogenesis in a human melanoma cell line by retinoids. Cancer research. 1980;40(9):3345-50. PubMed PMID: 6253061.

44. Welsh BM, Mason RS, Halliday GM. Topical all-trans retinoic acid augments ultraviolet radiation-induced increases in activated melanocyte numbers in mice. The Journal of investigative dermatology. 1999;112(3):271-8. doi: 10.1046/j.1523-1747.1999.00510.x. PubMed PMID: 10084301.

45. Calléja C, Messaddeq N, Chapellier B, Yang H, Krezel W, Li M, et al. Genetic and pharmacological evidence that a retinoic acid cannot be the RXR-activating ligand in mouse epidermis keratinocytes. Genes Dev. 2006;20(11):1525-38. doi: 10.1101/gad.368706. PubMed PMID: 16751185; PubMed Central PMCID: PMCPMC1475764.

46. Heyman RA, Mangelsdorf DJ, Dyck JA, Stein RB, Eichele G, Evans RM, et al. 9-cis retinoic acid is a high affinity ligand for the retinoid X receptor. Cell. 1992;68(2):397-406. doi: 0092-8674(92)90479-V [pii]. PubMed PMID: 1310260.

47. Allenby G, Bocquel MT, Saunders M, Kazmer S, Speck J, Rosenberger M, et al. Retinoic acid receptors and retinoid X receptors: interactions with endogenous retinoic acids. Proceedings of the National Academy of Sciences of the United States of America. 1993;90(1):30-4. PubMed PMID: 8380496; PubMed Central PMCID: PMC45593.

48. Tsai MJ, O'Malley BW. Molecular mechanisms of action of steroid/thyroid receptor superfamily members. Annual review of biochemistry. 1994;63:451-86. doi: 10.1146/annurev.bi.63.070194.002315. PubMed PMID: 7979245.

49. IJpenberg A, Tan NS, Gelman L, Kersten S, Seydoux J, Xu J, et al. In vivo activation of PPAR target genes by RXR homodimers. EMBO J. 2004;23(10):2083-91. doi: 7600209 [pii] 10.1038/sj.emboj.7600209. PubMed PMID: 15103326; PubMed Central PMCID: PMCPMC424365.

50. Elder JT, Astrom A, Pettersson U, Tavakkol A, Griffiths CE, Krust A, et al. Differential regulation of retinoic acid receptors and binding proteins in human skin. The Journal of investigative dermatology. 1992;98(5):673-9. PubMed PMID: 1314862.

51. Fisher GJ, Talwar HS, Xiao JH, Datta SC, Reddy AP, Gaub MP, et al. Immunological identification and functional quantitation of retinoic acid and retinoid X receptor proteins in human skin. The Journal of biological chemistry. 1994;269(32):20629-35. PubMed PMID: 8051161.

52. Nagy L, Kao HY, Love JD, Li C, Banayo E, Gooch JT, et al. Mechanism of corepressor binding and release from nuclear hormone receptors. Genes & development. 1999;13(24):3209-16. PubMed PMID: 10617570; PubMed Central PMCID: PMC317208.

53. Nagy L, Kao HY, Chakravarti D, Lin RJ, Hassig CA, Ayer DE, et al. Nuclear receptor repression mediated by a complex containing SMRT, mSin3A, and histone deacetylase. Cell. 1997;89(3):373-80. PubMed PMID: 9150137.

54. McKenna NJ, O'Malley BW. Combinatorial control of gene expression by nuclear receptors and coregulators. Cell. 2002;108(4):465-74. PubMed PMID: 11909518.

55. Vo N, Goodman RH. CREB-binding protein and p300 in transcriptional regulation. The Journal of biological chemistry. 2001;276(17):13505-8. doi: 10.1074/jbc.R000025200. PubMed PMID: 11279224.

56. Daily K, Patel VR, Rigor P, Xie X, Baldi P. MotifMap: integrative genome-wide maps of regulatory motif sites for model species. BMC bioinformatics. 2011;12:495. doi: 10.1186/1471-2105-12-495. PubMed PMID: 22208852; PubMed Central PMCID: PMC3293935.

57. Xie X, Rigor P, Baldi P. MotifMap: a human genome-wide map of candidate regulatory motif sites. Bioinformatics. 2009;25(2):167-74. doi: 10.1093/bioinformatics/btn605. PubMed PMID: 19017655; PubMed Central PMCID: PMC2732295.

58. Pogenberg V, Guichou JF, Vivat-Hannah V, Kammerer S, Pérez E, Germain P, et al. Characterization of the interaction between retinoic acid receptor/retinoid X receptor (RAR/RXR) heterodimers and transcriptional coactivators through structural and fluorescence anisotropy studies. J Biol Chem. 2005;280(2):1625-33. doi: 10.1074/jbc.M409302200. PubMed PMID: 15528208.

59. Chen JY, Clifford J, Zusi C, Starrett J, Tortolani D, Ostrowski J, et al. Two distinct actions of retinoid-receptor ligands. Nature. 1996;382(6594):819-22. doi: 10.1038/382819a0. PubMed PMID: 8752277.

60. Slominski A, Tobin DJ, Shibahara S, Wortsman J. Melanin pigmentation in mammalian skin and its hormonal regulation. Physiol Rev. 2004;84(4):1155-228. doi: 84/4/1155 [pii] 10.1152/physrev.00044.2003. PubMed PMID: 15383650.

61. Holick MF. Noncalcemic actions of 1,25-dihydroxyvitamin D3 and clinical applications. Bone. 1995;17(2 Suppl):107S-11S. PubMed PMID: 8579891.

62. Slominski A, Wortsman J. Neuroendocrinology of the skin. Endocrine reviews. 2000;21(5):457-87. doi: 10.1210/edrv.21.5.0410. PubMed PMID: 11041445.

63. Du X, Tabeta K, Mann N, Crozat K, Mudd S, Beutler B. An essential role for Rxr alpha in the development of Th2 responses. European journal of immunology. 2005;35(12):3414-23. doi: 10.1002/eji.200535366. PubMed PMID: 16259011.

64. Li M, Indra AK, Warot X, Brocard J, Messaddeq N, Kato S, et al. Skin abnormalities generated by temporally controlled RXRalpha mutations in mouse epidermis. Nature. 2000;407(6804):633-6. doi: 10.1038/35036595. PubMed PMID: 11034212.

65. Li M, Chiba H, Warot X, Messaddeq N, Gerard C, Chambon P, et al. RXR-alpha ablation in skin keratinocytes results in alopecia and epidermal alterations. Development. 2001;128(5):675-88. PubMed PMID: 11171393.

66. Boissy RE, Nordlund JJ. Vitiligo: current medical and scientific understanding. Giornale italiano di dermatologia e venereologia : organo ufficiale, Societa italiana di dermatologia e sifilografia. 2011;146(1):69-75. PubMed PMID: 21317859.

67. Dupin E, Le Douarin NM. Retinoic acid promotes the differentiation of adrenergic cells and melanocytes in quail neural crest cultures. Developmental biology. 1995;168(2):529-48. doi: 10.1006/dbio.1995.1100. PubMed PMID: 7729587.

Figure 3.1. 9-*cis* retinal is the ALDH1A1 substrate that stimulates melanogenesis.

(A) The ALDH1A inhibitor cyanamide inhibits *TYR* and *MITF* mRNA accumulation. MNT-1 melanoma cells were treated with the indicated doses of cyanamide for 24 hours and the relative expression of *TYR* and *MITF* mRNA was quantified as described in the methods. (B) The ALDH1A inhibitor Angeli's salt inhibits *TYR* and *MITF* mRNA accumulation. MNT-1 melanoma cells were treated with the indicated doses of Angeli's salt for 24 hours and the relative expression of *TYR* and *MITF* mRNA was quantified as described in the methods. (C) 4-HNE is not sufficient to induce the accumulation of either *TYR* or *MITF* mRNA. MNT-1 melanoma cells were treated with the indicated doses of 4-HNE for 24 hours, and *TYR* and *MITF* mRNA expression was quantified as described in the methods. (D) In conjunction with UVA radiation, 9-*cis* retinal induces the accumulation of both *TYR* and *MITF* mRNA. MNT-1 melanoma cells were pre-incubated with 9-*cis* retinal at the indicated concentrations for 45 minutes before being irradiated with UVA light as indicated. Relative mRNA expression was quantified as described in the methods. All data shown are mean ± S.D. (n=3 as indicated by the *error bars*). *, $p < 0.05$ or **, $p < 0.01$ using a Student's paired t-test with a two-tailed normal distribution *versus* vehicle-treated control. (E) Melanin accumulation is induced by 9-*cis* retinal in conjunction with UVA radiation. MNT-1 melanoma cells were treated with the indicated doses of 9-*cis* retinal, irradiated with UVA, and then allowed to reach confluency. Melanin accumulation was measured as described in the methods section. Data shown are mean ± S.D. (n=6 as indicated by the *error bars*). *, $p < 0.05$ or **, $p < 0.01$ using a Student's paired t-test with a two-tailed normal distribution *versus* vehicle-treated control.

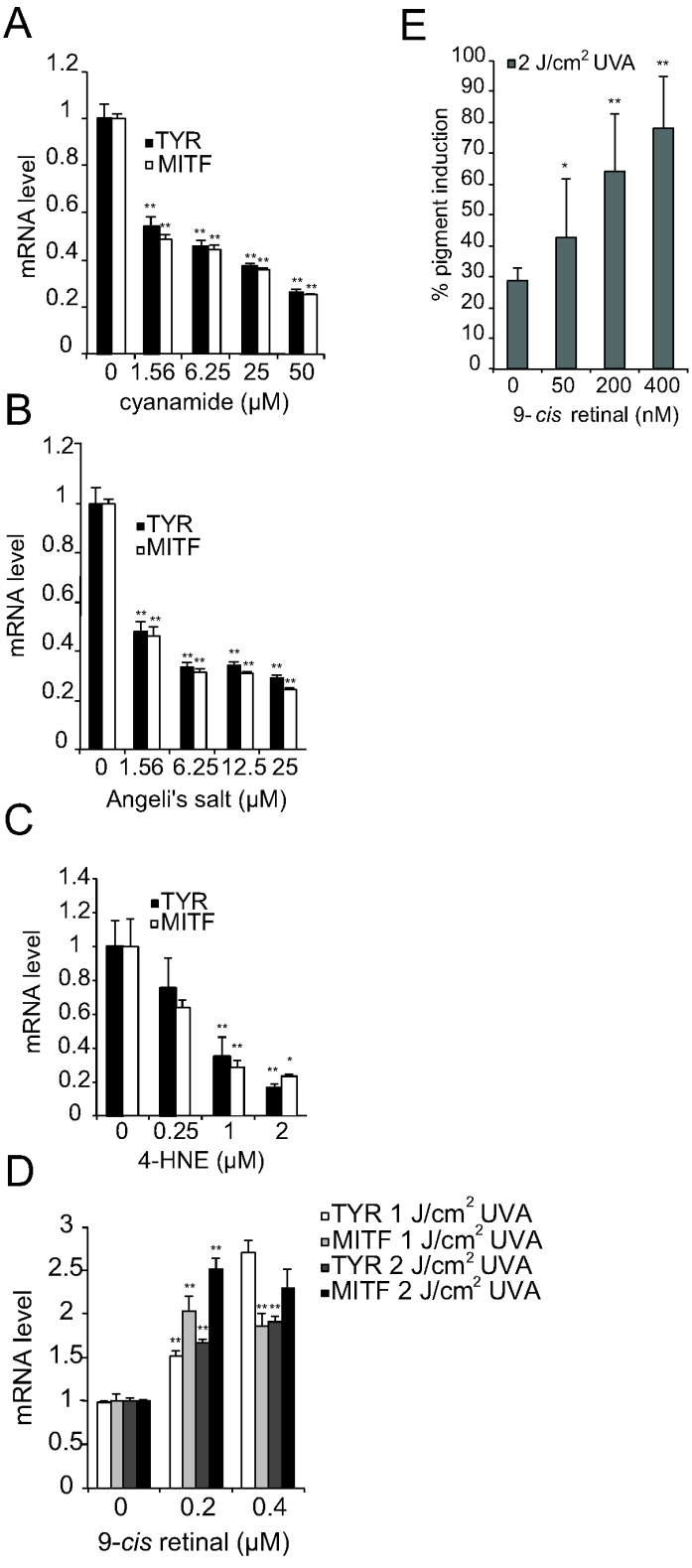
A
mRNA level
TYR
MITF
cyanamide (μM)
0 1.56 6.25 25 50
B
mRNA level
TYR
MITF
Angeli's salt (μM)
0 1.56 6.25 12.5 25
C
mRNA level
TYR
MITF
4-HNE (μM)
0 0.25 1 2
D
mRNA level
TYR 1 J/cm² UVA
MITF 1 J/cm² UVA
TYR 2 J/cm² UVA
MITF 2 J/cm² UVA
9-cis retinal (μM)
0 0.2 0.4
E
2 J/cm² UVA
% pigment induction
9-cis retinal (nM)
0 50 200 400

Figure 3.1

Figure 3.2. The metabolic product of 9-*cis* retinal oxidation, 9-*cis* retinoic acid, acts to stimulate melanin accumulation.

(A) 9-*cis* retinal alone is sufficient to induce melanin accumulation. MNT-1 melanoma cells were briefly treated with the indicated doses of 9-*cis* retinal and then allowed to reach confluency. Melanin accumulation was measured as described in the methods section. (B) 9-*cis* retinoic acid potently stimulates melanin accumulation. MNT-1 melanoma cells were briefly treated with the indicated doses of 9-*cis* retinoic acid and allowed to reach confluency. Melanin accumulation was measured as described in the methods section (C) A light micrograph of a representative opaque-walled, clear-bottomed 96-well microtiter plate containing MNT-1 cells treated with 9-*cis* retinoic acid is shown. Med, wells containing only media; Veh, cells treated with vehicle. (D) All-*trans* retinoic acid does not appreciably induce melanin accumulation. MNT-1 melanoma cells were briefly treated with the indicated doses of all-*trans* retinoic acid and allowed to reach confluency. Melanin accumulation was measured as described in the methods section. *Data* shown are mean ± S.D. (n=6 as indicated by the *error bars*). *, $p < 0.05$ or **, $p < 0.01$ using a Student's paired t-test with a two-tailed normal distribution *versus* vehicle-treated control.

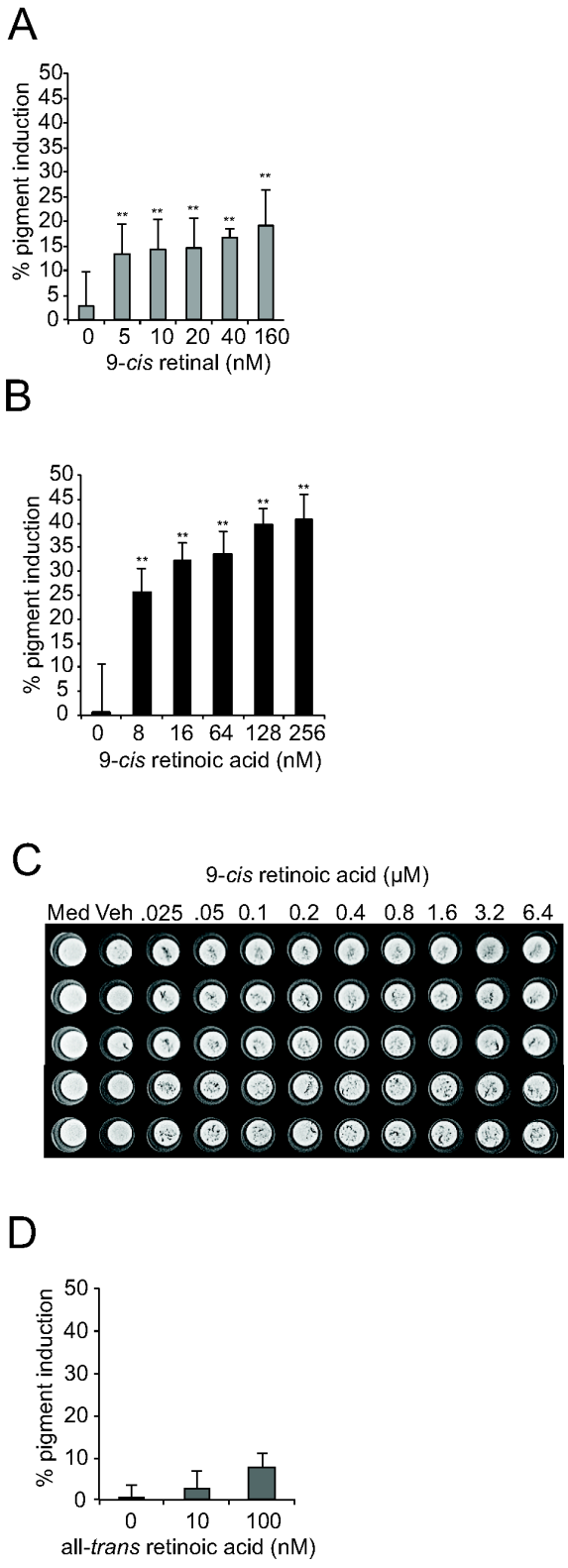
A
% pigment induction
50
45
40
35
30
25
20
15
10
5
0
0 5 10 20 40 160
9-cis retinal (nM)
B
% pigment induction
0 8 16 64 128 256
9-cis retinoic acid (nM)
C
9-cis retinoic acid (μM)
Med Veh .025 .05 0.1 0.2 0.4 0.8 1.6 3.2 6.4
D
% pigment induction
50
40
30
20
10
0
0 10 100
all-trans retinoic acid (nM)

Figure 3.2

Figure 3.3. ALDH1A Regulates Melanogenesis by Converting 9-*cis* retinal to 9-*cis* retinoic acid.

(A-B) 9-*cis* retinal induces the accumulation of *TYR* and *MITF* mRNA independently of UVA. Primary melanocytes and MNT-1 cells were pre-incubated with 9-*cis* retinal at the indicated doses for 45 minutes. Relative accumulation of *TYR* (A) and *MITF* (B) mRNA was measured as described in the methods section. (C-E) 9-*cis* retinoic acid induces the accumulation of *TYR* and *MITF* mRNA. Primary melanocytes and MNT-1 cells were pre-incubated with 9-*cis* retinoic acid at the indicated concentrations for 45 minutes. Cells were harvested 20 hours post drug treatment, and the relative accumulation of *TYR* (C) and *MITF* (D, E) mRNA was quantified as described in methods. (F) 9-*cis* retinoic acid but not 9-*cis* retinal induces the accumulation of TYR protein in both primary melanocytes and MNT-1 melanoma cells. MNT-1 melanoma cells (upper panel) and primary melanocytes (lower panel) were pre-incubated with the indicated doses of 9-*cis* retinal or 9-*cis* retinoic acid for 45 minutes. 28 hours later, the relative accumulation of TYR protein was quantified by immunoblotting. The numerical values represent the relative intensity of the TYR band normalized to the Tubulin band (loading control) for each lane divided by the relative expression of the TYR band in the vehicle control. (G-H) 9-*cis* retinal induces the accumulation of *TYR* and *MITF* mRNAs in an ALDH1A1 dependent manner. MNT-1 melanoma cells transiently transfected with either mismatch control or ALDH1A1 siRNAs for 72 hours were briefly treated with the indicated doses of 9-*cis* retinal (G) or 9-*cis* retinoic acid (H). Cells were then harvested 20 hours post drug treatment and the relative accumulation of *TYR* and *MITF* mRNA was measured. All data are mean ± S.D. (n=3 as indicated by the *error bars*). *, $p < 0.05$ or **, $p < 0.01$ using a Student's paired t-test with a two-tailed normal distribution *versus* vehicle-treated control.

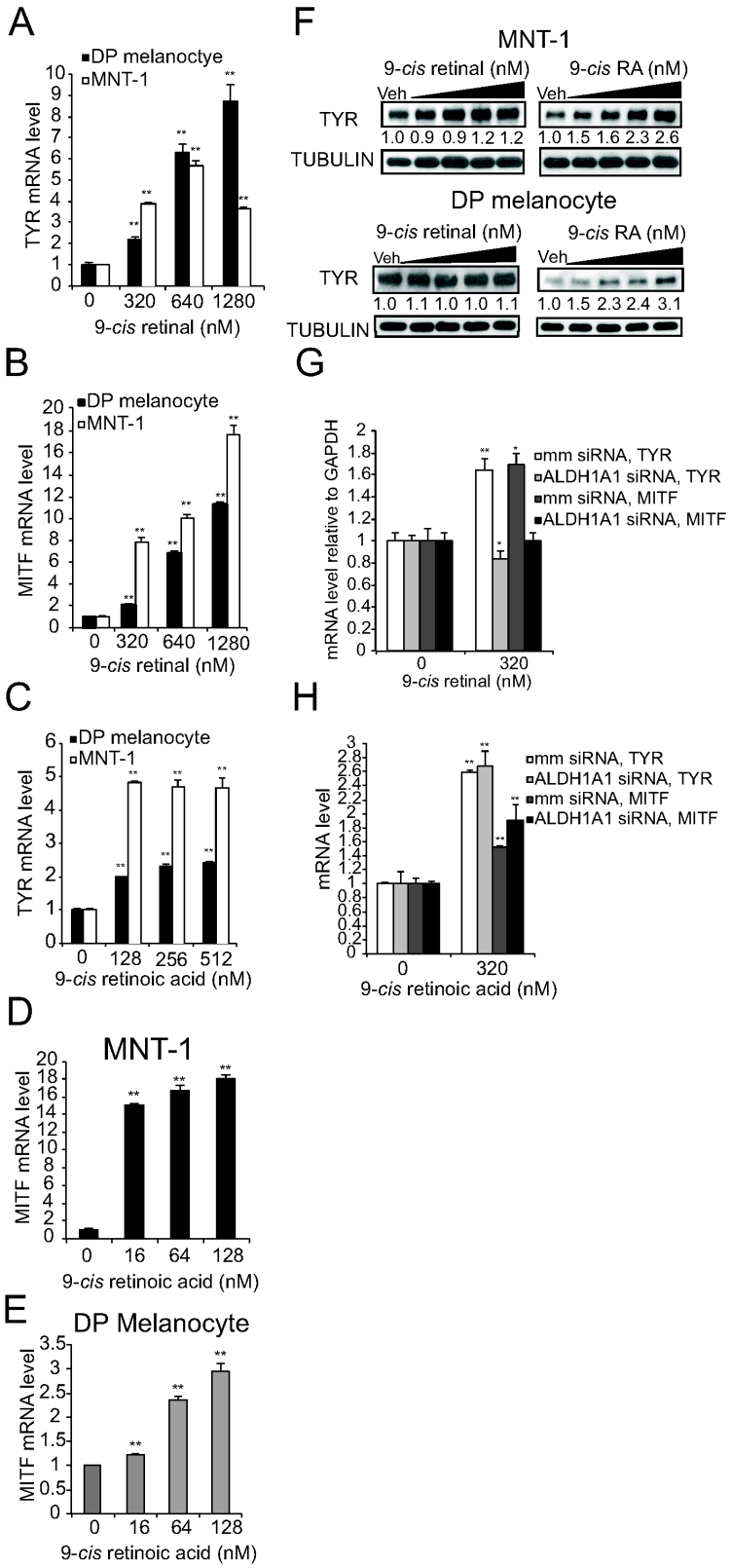
A
DP melanoctye
MNT-1
TYR mRNA level
9-cis retinal (nM)
B
DP melanocyte
MNT-1
MITF mRNA level
9-cis retinal (nM)
C
DP melanocyte
MNT-1
TYR mRNA level
9-cis retinoic acid (nM)
D
MNT-1
MITF mRNA level
9-cis retinoic acid (nM)
E
DP Melanocyte
MITF mRNA level
9-cis retinoic acid (nM)
F
MNT-1
9-cis retinal (nM)
9-cis RA (nM)
Veh
TYR
TUBULIN
1.0 0.9 0.9 1.2 1.2
1.0 1.5 1.6 2.3 2.6
DP melanocyte
1.0 1.1 1.0 1.0 1.1
1.0 1.5 2.3 2.4 3.1
G
mRNA level relative to GAPDH
mm siRNA, TYR
ALDH1A1 siRNA, TYR
mm siRNA, MITF
ALDH1A1 siRNA, MITF
9-cis retinal (nM)
H
mRNA level
9-cis retinoic acid (nM)

Figure 3.3

Figure 3.4. ALDH1A Controls Melanogenesis in Skin Equivalents.

(A) Cyanamide inhibits melanin accumulation in skin equivalents as measured by a solvable melanin assay. Mattek darkly pigmented skin equivalents were incubated with 600 μM cyanamide, 2% kojic acid or water for 21 days. Melanin accumulation was quantified using a solvable melanin assay according to the manufacturer's protocol. (B) Equivalents were photographed using a dissecting microscope and then fixed and stained with a Fontana Masson silver stain to quantify the relative accumulation of melanin.

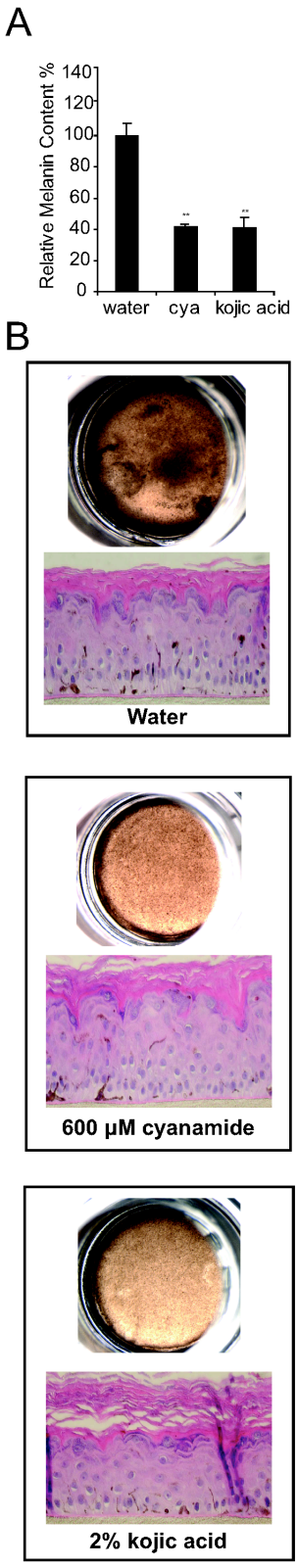
A
Relative Melanin Content %
140
120
100
80
60
40
20
0
water
cya
kojic acid
B
Water
600 µM cyanamide
2% kojic acid

Figure 3.4

Figure 3.5 ALDH1A1 Regulates Melanogenesis by Catalyzing the Production of 9-*cis* retinoic acid: a model

ALDH1A1 catalyzes the conversion of 9-*cis* retinal to 9-*cis* retinoic acid, which in turn regulates melanogenesis by stimulating the accumulation of *TYR* and *MITF* mRNA, TYR protein, and melanin production. Inhibition of ALDH1A1 catalytic activity via a potent inhibitor, such as cyanamide, prevents the catalysis of 9-*cis* retinoic acid from 9-*cis* retinal and in turn prohibits the accumulation of *TYR* and *MITF* mRNA, TYR protein, and melanin accumulation.

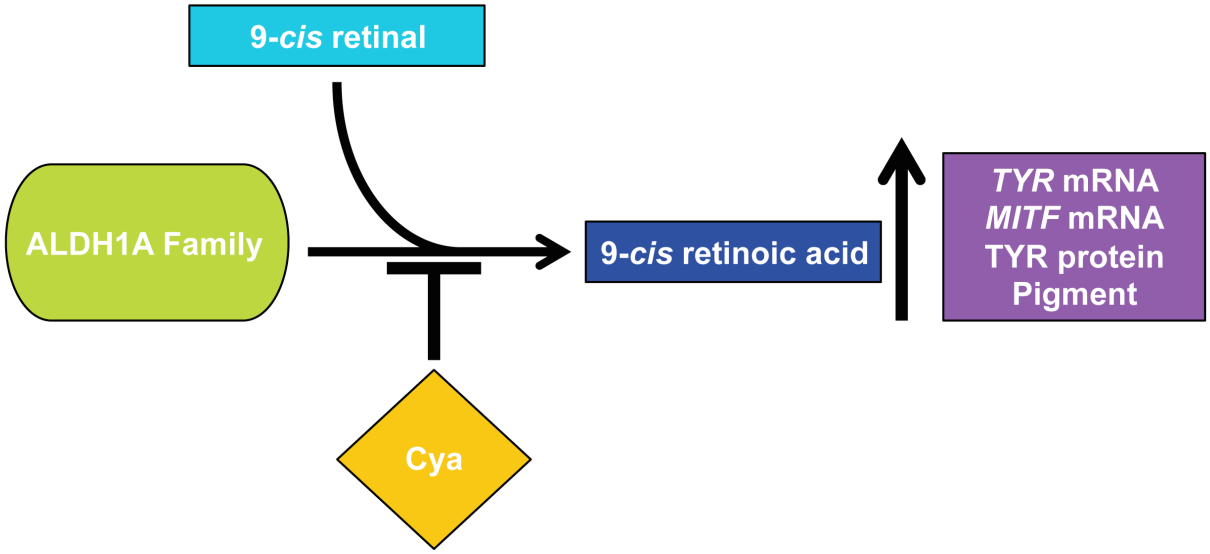
9-*cis* retinal
ALDH1A Family
9-*cis* retinoic acid
TYR mRNA
MITF mRNA
TYR protein
Pigment
Cya

Figure 3.5

Figure 3.S1

(A) UV-induced oxidation products do not stimulate melanogenesis. MNT-1 melanoma cells were treated with the indicated doses of 4-HNE and then allowed to reach confluency. Melanin accumulation was measured as described in the methods. (B) All *trans*-retinal does not induce melanogenesis. MNT-1 melanoma cells were briefly treated with the indicated doses of all-*trans* retinal and then allowed to reach confluency. Melanin accumulation was measured as described in the methods. (C) In conjunction with UVA, 9-*cis* retinal induces the accumulation of *TYR* and *MITF* mRNA in primary melanocytes. Normal human deeply-pigmented melanocytes were incubated with 9-*cis* retinal at the indicated concentrations for 45 minutes and then immediately irradiated with the indicated dose of UVA light. Cells were then harvested 24 hours post UVA treatment and the relative accumulation of *TYR* and *MITF* mRNA was quantified. Data shown in Figures S1A, and S1B are mean ± S.D. (n=6, as indicated by the *error bars*). Data shown in Figure S1C is mean ± S.D. (n=3 as indicated by the *error bars*). *, $p < 0.05$ or **, $p < 0.01$ using a Student's paired t-test with a two-tailed normal distribution *versus* vehicle-treated control.

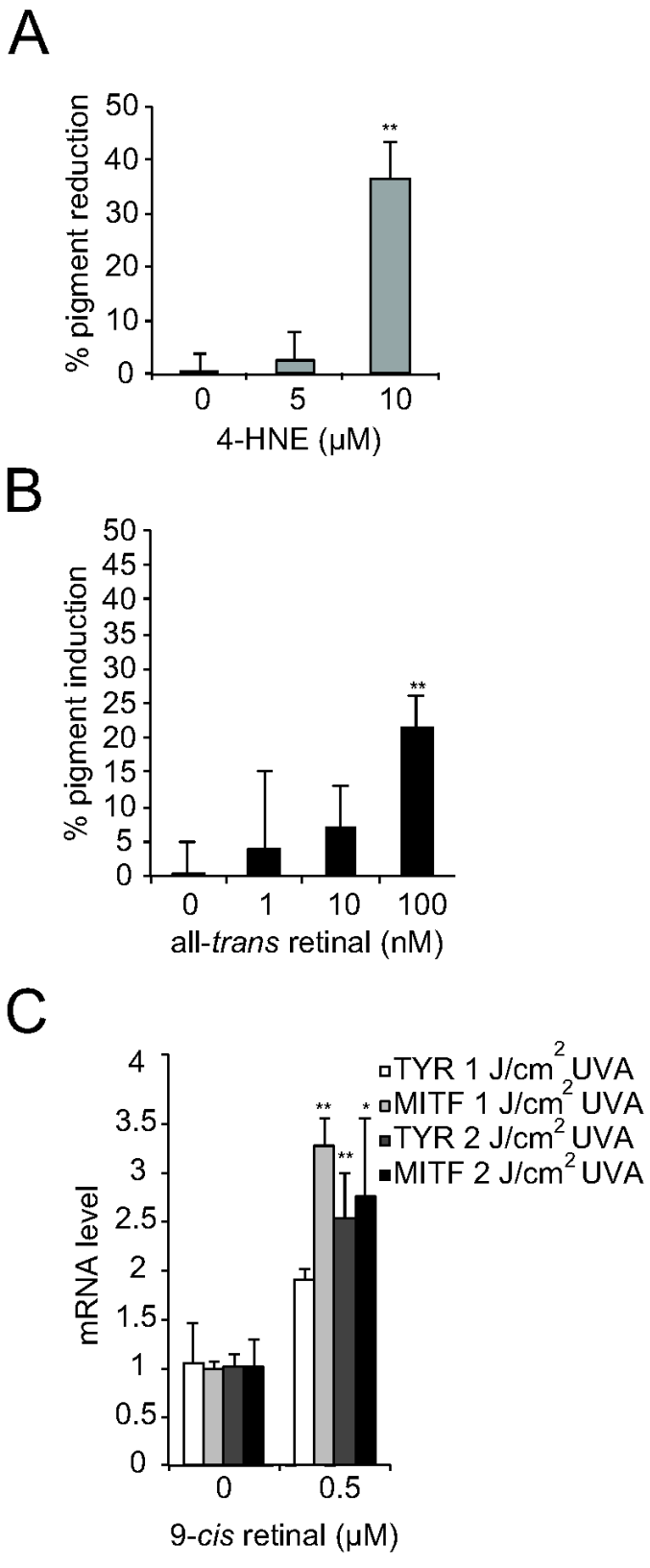
A
% pigment reduction
50
40
30
20
10
0
**
0
5
10
4-HNE (μM)
B
% pigment induction
50
45
40
35
30
25
20
15
10
5
0
**
0
1
10
100
all-trans retinal (nM)
C
mRNA level
4
3.5
3
2.5
2
1.5
1
0.5
0
**
**
*
TYR 1 J/cm2 UVA
MITF 1 J/cm2 UVA
TYR 2 J/cm2 UVA
MITF 2 J/cm2 UVA
0
0.5
9-cis retinal (μM)

Figure 3.S1

Figure 3.S2

(A) 9-*cis* retinal induces the accumulation of melanin in MNT-1 melanoma cells in conjunction with UVA radiation. MNT-1 melanoma cells were briefly treated with the indicated doses of 9-*cis* retinal and then irradiated with the indicated dose of UVA. Cells were then allowed to reach confluency. Melanin accumulation was measured as described in methods. (B) The combination of 9-*cis* retinal treatment and UVA stimulation is toxic to MNT-1 melanoma cells. MNT-1 melanoma cells were briefly treated with the indicated doses of 9-*cis* retinal and then immediately irradiated with 2 J/cm^2 of UVA light. Cells were then allowed to reach confluency and then subsequently lysed with the addition of Cell-Titer Glo reagent as previously described in the methods. The relative percentage of surviving cells was calculated by normalizing the luminescence value of drug treated cells to that of vehicle-treated control cells. (C) ALDH1A1 siRNAs inhibit *ALDH1A1* mRNA expression. MNT-1 melanoma cells were transiently transfected with either mismatch control or ALDH1A1 siRNAs. Target gene expression was measured 72 hours post transfection by RT-qPCR. Data shown in Figure S2A and S2B is mean ± S.D. (n=6). Data shown in Fig S2C is mean ± S.D. (n=3, as indicated by the *error bars*). *, $p < 0.05$ or **, $p < 0.01$ using a Student's paired t-test with a two-tailed normal distribution *versus* mismatch-transfected control.

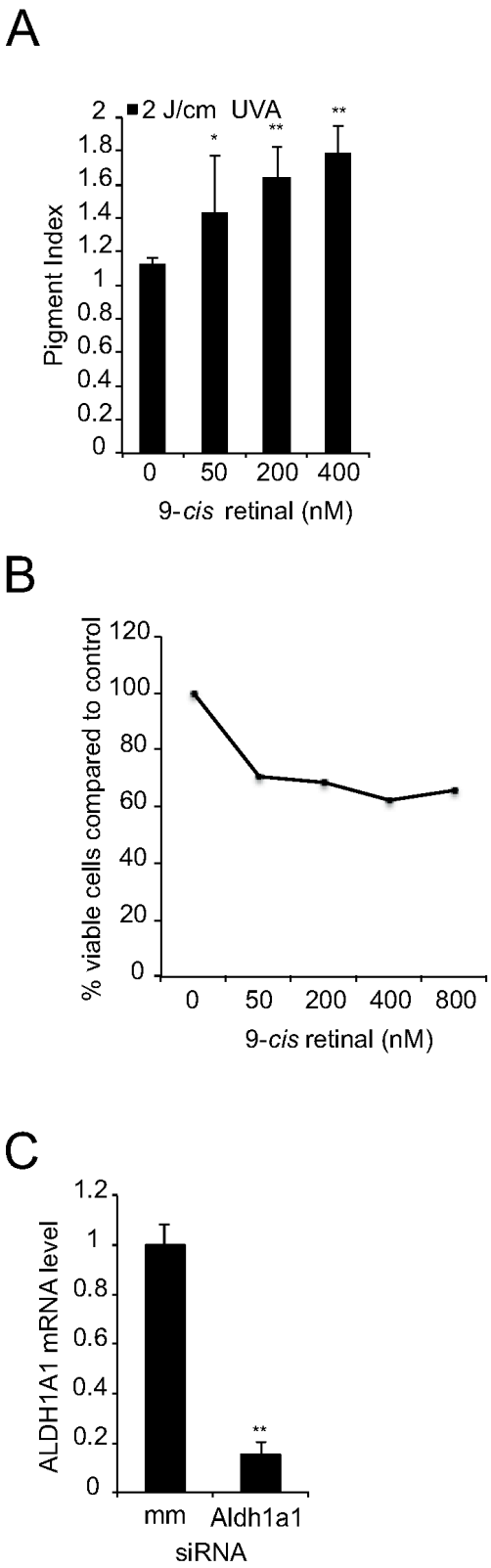
A
2 J/cm UVA
Pigment Index
9-cis retinal (nM)
B
% viable cells compared to control
9-cis retinal (nM)
C
ALDH1A1 mRNA level
mm
Aldh1a1
siRNA

Figure 3.S2

Retinoids Modulate *MITF:* A Novel Mechanism in the Regulation of Melanin Biosynthesis

Chapter 4

Elyse K. Paterson, Priya Vasudeva, Jessica L. Flesher, Jonathan Schilling, Amy Sun, Sohail Jahid, Jennifer Sui, Grant R. MacGregor, Jonathan Neumann and Anand K. Ganesan

Manuscript in Preparation

4.1 Abstract

Using a genome-wide RNAi approach, our laboratory recently identified a novel role for ALDH1A1 in regulating melanogenesis. Published work demonstrated that 9-*cis* retinoic acid, an endogenous product of ALDH1A1, stimulates *Tyrosinase* and *MITF-M* mRNA and protein accumulation as well as pigment accumulation in both primary human melanocytes and human melanoma cells. 9-*cis* retinoic acid binds to and activates both the retinoid X receptor (RXR), and the retinoic acid receptor (RAR), two nuclear receptors that regulate gene transcription. Here we show through rigorous chromatin immunoprecipitation (ChIP) studies that RXR and RAR bind in the region just upstream of the transcriptional start site of *MITF-A*, an isoform of MITF that has not been previously shown to play a role in pigment regulation. Validation studies revealed that RAR and RXR agonists induce luciferase activity in HEK293-T cells transfected with constructs containing the *MITF-A* promoter upstream of the *luciferase* gene. Taken together, our results show a specific and novel role for MITF-A in melanogenesis.

4.2 Introduction

Melanin, a light-absorbing polymer produced by the epidermal melanocyte, is widely distributed in the plant and animal kingdoms [1]. It is the primary determinant of skin, hair and eye color [1]. While its main function is to protect the skin against ultraviolet-radiation (UV-R)-induced damage through direct absorption mechanisms, melanin is also found in the stria vascularis of the inner ear, where it aids in sound conduction, and in pigment-bearing neurons of the brainstem, the substantia nigra, where it guards against toxic insult [1]. The biosynthesis of melanin requires the intricate interplay of transcriptional, translational and intracellular trafficking processes [1]. Melanin is aberrantly regulated in many skin disorders, including vitiligo and melasma, which both lack effective, non-toxic treatment plans that ensure long-term normal pigmentation [2, 3].

Previously, our group carried out a genome-wide siRNA-based pigment screen aimed at identifying pharmaceutically tractable drug targets for the rational design of pigment modulatory agents [4]. From this screen, we identified aldehyde dehydrogenase 1A1 (ALDH1A1) as a novel pigment regulator [4]. ALDH1A1, a family member of the aldehyde dehydrogenase superfamily (ALDH), plays pleiotropic roles in cellular detoxification processes [5]. It utilizes $NAD(P)^+$ to convert both endogenous and exogenous toxic lipid aldehydes to corresponding non-toxic carboxylic acids [6-10]. ALDH1A1 is also known to synthesize retinoic acid (RA) from retinal, thus establishing itself as a crucial part of the vitamin A metabolism pathway [8, 10-12]. After identifying ALDH1A1 as a novel pigment regulator [4], we then went on to show that 9-*cis* retinoic acid, one of the products of ALDH1A1 catalysis in the vitamin A pathway, was able to induce the accumulation of *TYR* and *MITF* mRNAs, TYR protein, and pigment in both MNT-1

melanoma cells and darkly-pigmented human epidermal melanocytes [13]. As the biological effects of 9-*cis* retinoic acid are mediated by nuclear receptors, namely RXRα and RARα, we sought to identify how 9-*cis* retinoic acid modulates melanogenesis.

Intriguing *in vivo* and *in vitro* studies have shown that vitamin A (retinol) and its active derivatives (retinoids) play significant roles in a number of important cellular processes, including vertebrate body shaping and organogenesis, tissue homeostasis, cell proliferation, differentiation and apoptosis [14-18]. How retinoids play such pleiotropic roles in cellular processes remained an unanswered question until the discoveries of two classes of retinoic-acid (RA)-binding receptors that were able to activate transcription of downstream genes upon binding of ligand [14, 18, 19]. The retinoic acid receptors (RARα, RARβ and RARγ) and the retinoid X receptors (RXRα, RXRβ and RXRγ) belong to the nuclear receptor (NR) superfamily [14, 18, 19]. While the RARs are activated by both all-*trans* retinoic acid and 9-*cis* retinoic acid, the RXRs are only activated by 9-*cis* retinoic acid [19]. However, data suggests that RXRs can be activated by all-*trans* retinoic acid, but only at high concentrations (1-10 μM); this may be due to an all-*trans* retinoic acid to 9-*cis* retinoic acid conversion [20, 21]. *In vitro* studies have provided strong evidence that RAR/RXR heterodimers control transcription by binding to specific DNA sequences (known as retinoic acid response elements, or RAREs) within the promoter of RA-mediated genes [18]. Due to the combination of different isoforms of RAR and RXR, a healthy reservoir of potential functional receptor dimers exists; this diversity in heterodimers allows for specific genes to be transcriptionally activated in a particular cell or tissue [22].

Unlike RARs, RXRs are promiscuous in nature; they can form a heterodimer complex with peroxisome proliferator-activated receptor (PPAR) [23, 24], stimulate the binding of thyroid

hormone receptors (TRs) to thyroid-hormone response elements (TREs) [25], and stimulate vitamin D receptors (VDRs) to bind to vitamin-D response element (VDREs) [26]. Dimerization events are achieved through the interacting surface of the ligand-binding domain (LBD) on each receptor [22]; furthermore, it is the heterodimer complex that binds a specific RARE with much higher affinity than a homodimer complex, reinforcing the idea that the functional receptor unit is a heterodimer [27-30]. Many co-regulator proteins, both co-activators and co-repressors of RAR/RXR, play important roles in the control of gene promoters regulated by RA [22]. In the absence of ligand, RAR/RXR recruits co-repressor proteins, which results in gene silencing; conversely, co-activator proteins are recruited by RAR/RXR in the presence of ligand, and transcription is initiated on what was previously a silenced gene [22].

The *microphthalmia-associated transcription factor* (*MITF)* gene, which is comprised of nine distinct promoter-exon units, codes for a basic helix-loop-helix-leucine zipper transcription factor [31, 32]. Each promoter directs the transcription of specific *MITF* isoforms that differ in their first exon but are spliced onto common downstream exons [31, 33]. The M promoter, the most proximal promoter to the downstream exons, regulates the transcription of MITF-M, the master regulator of melanocyte development, function and survival [31]. It accomplishes this regulation by mediating the downstream effects of the α-melanocyte-stimulating hormone (α-MSH) [34, 35]; in particular, MITF-M transcriptionally regulates proteins that are crucial for melanin biosynthesis in the differentiated melanocyte [31, 35, 36]. While the expression of *MITF-M* is limited to the melanocyte [37], *MITF-A* is expressed in many cell types and is the predominant isoform in retinal pigment epithelium (RPE), the pigmented cell layer that nourishes retinal visual cells [32]. In the RPE, *MITF-A* was shown to regulate the transcription of both *tyrosinase* (*TYR*) and *tyrosinase-related protein 1* (*TYRP-1*), suggesting that it plays a

significant role in melanogenesis in the eye [38]. While the functions of both MITF-A and MITF-M are known, the regulation of both isoforms is still poorly understood [31].

In the present study, we utilize rigorous chromatin immunoprecipitation studies to establish that a novel RAR/RXR heterodimer is bound directly upstream of the *MITF-A* transcription start site. Furthermore, through *luciferase*-reporter assays, we demonstrate that both retinoids (the endogenous ligands for RAR/RXR) and RAR/RXR agonists activate the full-length *MITF-A* promoter, but not a truncated *MITF-A* promoter lacking the putative RAR/RXR binding site. Through these experiments, we establish a novel mechanism in the regulation of melanin biosynthesis: after conversion from 9-*cis* retinal catalyzed by ALDH1A1, 9-*cis* retinoic acid binds to and activates a RAR/RXR heterodimer complex enriched upstream of the *MITF-A* transcription start site.

4.3 Materials and Methods

Cell Lines and Cell Culture

Human MNT-1 melanoma cells were a gift from M. Marks (University of Pennsylvania). These cells were cultured in high-glucose DMEM (containing sodium pyruvate and L-glutamine) (Caisson) supplemented with 15% fetal bovine serum (CellGro), MEM vitamin solution (Invitrogen), antibiotic-antimycotic (Invitrogen), and 10% AIM-V medium (Invitrogen). Human deeply-pigmented neonatal epidermal melanocytes (Invitrogen) were cultured in Medium 254 (Invitrogen) supplemented with phorbol 12-myristate 13-acetate-free Human Melanocyte growth supplement-2 (Invitrogen). As these melanocyte strains were purchased from commercial entities, no IRB approval was required prior to their use. B16 mouse melanoma cells (obtained from William Pavan, NHGRI) were cultured in high-glucose DMEM (containing sodium pyruvate and L-glutamine) (Caisson) media supplemented with 10% FBS (CellGro), 1x NEAA, and 0.075% sodium bicarbonate (Sigma-Aldrich) at 5% CO_2. C8161 melanoma cells were obtained from Frank Meyskens (University of California, Irvine) and cultured in DMEM (containing sodium pyruvate and L-glutamine) (Caisson) supplemented with 10% fetal bovine serum (CellGro) and antibiotic-antimycotic (Invitrogen). SK-Mel-28 melanoma cells were obtained from the ATCC. SK-Mel-28 were cultured in RPMI (containing L-glutamine) (Corning) medium with 10% fetal bovine serum and antibiotic-antimycotic (Invitrogen). HEK293T cells were purchased from the ATCC and were cultured in DMEM (containing sodium pyruvate and L-glutamine) (Caisson) supplemented with 10% fetal bovine serum (CellGro) and antibiotic-antimycotic (Invitrogen).

Real-time quantitative PCR (RT-qPCR)

Cells were harvested using Tri Reagent solution (Ambion) according to the manufacturer's protocol. RNA was extracted from the cell lysates using a Direct-zol RNA miniprep kit (Zymo Research) according to the manufacturer's guidelines. RNA concentration was measured using the Implen Nanophotometer. cDNA was then synthesized from the RNA using a high-capacity RNA to cDNA kit (Life Technologies). Primers were designed to target desired genes using Primer3. Primers targeting *MITF-A* and *MITF-M* were designed to target the first exon of each, which is different for each MITF isoform. For ChIP, primers were designed to target separate 500 base-pair tiles of the *MITF-A* and the *MITF-M* promoter. A melting curve was performed for each primer set to eradicate primers that may form primer-dimers. Power SYBR Green PCR master mix (Life Technologies) was used in the final reaction, along with pure cDNA and forward and reverse primers. All reactions were completed in biological triplicate (n=3). A 7900HT Fast Real-Time PCR system (Applied Biosystems) and SDS 2.4 (Applied Biosystems) were used to determine Ct values for each sample. Values were normalized to either β-actin or GAPDH using the relative quantification mathematical model (Pfaffl) as previously described. A two-tailed Student's t-test was employed to determine statistical significance.

RNA isolation on whole mouse skin and Nanostring nCounter Analysis

Whole mouse skin (n=3 for control mice, n=3 for experimental mice) was harvested from either anesthetized or euthanized mice using a 4-mm round punch biopsy and immediately

stabilized overnight in RNAlater RNA stabilization reagent (Life Technologies) at 4°C. Skin samples were homogenized using the Precellys24 high-throughput tissue homogenizer (Precellys) in hard tissue homogenizing reinforced tubes that contain 2.8 mm ceramic beads (Bertin Corporation). After homogenization, RNA was extracted from each sample using the RNeasy Fibrous Tissue Mini Kit according to the manufacturer's instructions (Qiagen). RNA was normalized to a concentration of 20 ng/μL and 5 μL of normalized sample was then added to a 20 μL aliquot of reporter codeset master mix (130 μL reporter codeset + 130 μL hybridization buffer). The samples were then hybridized at 65°C for 16-18 hours, and then transferred to the prep station. The prep station was run on the high sensitivity setting. Upon the completion of the prep station step, the cartridge was loaded onto the nCounter and scanned using the "max" setting which attempts to capture 1155 fields of view (FOV). Resultant data was analyzed using the nSolver analysis software (Nanostring Technologies).

Chromatin Immunoprecipitation (ChIP)

Putative RXR/RAR binding sites in the promoters of genes involved in melanogenesis were idenfitied using MotifMap [39, 40]. A total of 2 kB upstream of the transcription start site for each gene was designated as the "promoter region". The promoter region was tiled using four 500 base pair "tiles" (See Fig. 1C). Primers for quantitative real-time PCR were targeted to each of these four tiled regions in the promoter. Primers were designed using Primer3 [41, 42] and checked by melting curve analysis to eradicate any pairs that formed primer-dimers. MNT-1 and darkly-pigmented melanocytes were plated in 100-mm dishes at a density of 2.2×10^6 cells per dish. All ChIP reactions were completed in biological triplicate. For one biological

replicate, 3 100-mm dishes were pooled together per antibody. Cells were grown to 80% confluency (~8.8 x 10^6 cells per dish) and were harvested 48 hours later for ChIP using the ChIP-It Express Kit (Active Motif) according to the manufacturer's instructions without any modifications. Cultured melanoma cells were cross-linked with formaldehyde. Chromatin was sheared For each ChIP reaction, 25 μg of chromatin and 2 μg of antibody were used. Before quantitative real-time PCR analysis, eluted DNA was cleaned up using the QIAquick PCR Purification Kit (Qiagen). All RT-qPCR reactions were performed as described above. Quantitative real-time PCR analysis was completed on a 7900HT Fast Real-Time PCR system (Applied Biosystems) and SDS 2.4 (Applied Biosystems) was used to calculate the Ct values. Average Ct values were used for calculating percent input. The percent input of targeted antibody compared to its control IgG (mouse or rabbit) was used to perform a two-tailed Student's *t*-test to determine statistical significance. The following antibodies were used in the ChIP reactions: mouse monoclonal to retinoic acid receptor alpha (RARα) (ChIP-grade), ab41934, Abcam; mouse monoclonal to retinoid X receptor alpha (RXRα), c-46659, Santa Cruz Biotechnology; mouse monoclonal IgG1 isotype control, 5415S, Cell Signaling Technology; rabbit monoclonal IgG1 isotype control, 3900S, Cell Signaling Technology.

Western blotting

A375 cells, HEK293T cells, MNT-1 cells, and SKM-28 cells were plated at a density of 2.2 x 10^6 cells in 100 mm dishes and then harvested 48 hours later using 1x RIPA lysis buffer (Santa Cruz Biotechnology) supplemented with a 1x protease inhibitor cocktail (Thermo Scientific) according to the manufacturer's protocol. Lysates were then clarified by

centrifugation (14,000x*g* for 15 minutes at 4°C). The relative concentration of protein in each lysate was quantified using a BCA Protein Assay Kit (Thermo Scientific) according to the manufacturer's protocol. A total of 20 μg of protein per sample was separated on a 4-12% Bis-Tris (Life Technologies) polyacrylamide protein gel under denaturing conditions and transferred onto a 0.45-μm PVDF membrane (Millipore). Subsequently, membranes were blocked in a blocking buffer solution comprised of TBS (Fisher Scientific), 0.1% Tween-20 (Fisher Scientific) and 5% non-fat milk powder (Apex).

The following antibodies were used: mouse monoclonal to retinoic acid receptor alpha (RARα) (ChIP-grade), ab41934, Abcam; rabbit monoclonal to retinoid X receptor alpha (RXRα), 3085S, Cell Signaling Technology; rabbit monoclonal to GAPDH, 5174S, Cell Signaling Technology; anti-mouse IgG, HRP-linked, 7076S, Cell Signaling Technology; anti-rabbit IgG, HRP-linked, 7074S, Cell Signaling Technology. For detecting both RARα and RXRα, the primary antibody was diluted 1:1000 in 5% milk, and the secondary antibody was diluted 1:1000 in 5% milk. To detect GAPDH, the primary antibody was diluted 1:10,000 in 5% milk and the secondary antibody was diluted 1:5000 in 5% milk. To assess immunoreactivity, Luminata Forte Western HRP substrate was used according to manufacturer's directions (Millipore). Protein levels were assessed using densitometry analysis (ImageJ).

Drug Treatment of Cells

For real-time quantitative PCR experiments and dual-luciferase reporter assay experiments, cells were seeded at a density of 4 x 10^4 cells per well of a 24-well plate and allowed to re-attach overnight. Each treatment was completed in biological triplicate.

Subsequently, cells were incubated with increasing concentrations of either: 9-*cis* retinoic acid (Sigma Aldrich), BMS753 (Tocris Bioscience), CD3254 (Tocris Bioscience), HX531 (Tocris Bioscience), LG100268 (Sigma Aldrich), or combinations of the aforementioned drugs for 24 hours. All vehicle treatments correspond to DMSO only. All compounds were dissolved in DMSO to a stock concentration of 10 mM before being diluted to concentrations appropriate for drug treatment. Cells were treated with drug for twenty-four hours unless stated otherwise.

Transient Transfection and Dual-Luciferase Reporter Assay

HEK293T cells were transfected with 1 μg of a firefly luciferase reporter driven by MITF-A full-length promoter (MITF-A EcoRI) or 1 μg of a firefly luciferase reporter driven by a truncated MITF-A promoter (MITF-A SmaI) (both plasmids were a kind gift of Dr. Shigeki Shibahara) [43]. Both plasmids were previously described [38] and made by inserting the 5'-flanking region of the *MITF-A* isoform's first exon and the subsequent 5'-untranslated region of the gene immediately upstream of a *luciferase* gene in the pGL3 basic plasmid (Promega). The HEK293T cells were also co-transfected with 0.02 μg a Renilla luciferase reporter driven by an SV40 promoter as an internal control. All transfections were carried out using Lipofectamine 3000 transfection reagent according to the manufacturer's instructions (Life Technologies). 24 hours post-transfection, cells were treated with drug as described above. After 24 hours of drug treatment, cells were then lysed and assayed using a Dual-Glo luciferase assay system (Promega) according to the manufacturer's protocol. Measurements were recorded on a Sirius Berthold Detection System. Firefly luminescence values were normalized to Renilla luminescence. All

transfection/drug treatments were completed in biological replicate (n=3). A two-tailed Student's t-test was employed to determine statistical significance.

4.4 Results

MITF-A is expressed in pigment-producing cells and mouse skin

Previously, we demonstrated that 9-*cis* retinoic acid, a product of ALDH1A1 catalysis, is able to stimulate *TYR* and *MITF-M* mRNA, TYR protein and pigment accumulation in MNT-1 melanoma cells [13]. The intracellular actions of 9-*cis* retinoic acid are mediated by two nuclear receptors, RAR and RXR [20, 44]. Therefore, we hypothesized that RXR/RAR may be bound to the promoter-region of a gene or genes involved in melanogenesis. We utilized MotifMap [39, 40] to search for putative RXR/RAR binding sites in the promoter regions of key genes involved in melanogenesis, genes, including *MITF-A* and *MITF-M*. We determined that while no putative binding site was present in the promoter region of *MITF-M* (Table 4.1), a putative RXR:RAR binding site existed 700 base pairs upstream of the *MITF-A* transcription start site (Table 4.2), prompting us to investigate whether *MITF-A*, which has been widely studied in ocular tissues (specifically retinal pigment epithelium) [38], is expressed in melanocytes. MNT-1 melanoma cells, darkly-pigmented human epidermal melanocytes (DP Mel), and B16 mouse melanoma cells all demonstrated expression of *MITF-A* mRNA, albeit at levels significantly lower than *MITF-M* mRNA (Fig. 1A). In order to determine whether *MITF-A* is expressed in mouse skin, we utilized freshly harvested mouse skin from an unrelated study and subjected it to Nanostring nCounter analysis. Again, *MITF-A* was expressed, but at 4-fold lower levels than *MITF-M* (Fig. 1B).

RXRα and RARα are bound to the *MITF-A* promoter, but not the *MITF-M* promoter

As the MotifMap analysis did not signify which isoform of RXR/RAR is putatively bound in the *MITF-A* promoter, we first ascertained from previously published studies that RXRα is the major form expressed in the epidermis [45-50]. Furthermore, gene knockout studies in the mouse showed that RXRα is the most critical of the RXRs, with RXRβ and RXRγ being dispensable [22, 51]. Lastly, mice homozygous for a hypomorphic mutant allele (I273N) for *Rxrα* (which alters the ligand binding domain and the heterodimerization domain, leading to a 90% decline in ligand-inducible transactivation) demonstrate premature greying and progressive alopecia, suggesting a putative role for RXRα in melanogenesis in the mouse hair follicle [52]. Thus, we focused our studies on this specific isoform. First, we performed western blot analysis on MNT-1 melanoma cell lysate and darkly-pigmented human melanocyte cell lysate to ensure expression of RXRα in both cell lines (Fig. 2B). Next, in order to determine whether RXRα binds upstream of the *MITF-A* or the *MITF-M* transcription start site, we performed chromatin immunoprecipitation (ChIP) analysis using ChIP-grade antibodies against RXRα in the two aforementioned melanocyte cell lines. We used primers designed to target distinct 500 base pair tiles that together, cover the entire 2 kB promoter region for each gene (Fig. 1C). Using a host-specific isotype IgG as a control mock ChIP, we demonstrate that RXRα is significantly enriched in regions 3 and 4 upstream of the *MITF-A* transcription start site when compared to the IgG control in both MNT-1 melanoma cells and darkly-pigmented primary human melanocytes (Fig. 1D, left two graphs). Regions 3 and 4 of the *MITF-A* promoter constitute the two tiles closest to the transcription start site of the gene (Fig. 1C). Intriguingly, neither cell line showed significant

RXRα enrichment in any area of the *MITF-M* gene promoter when compared to the IgG isotype control (Fig. 1D, left two graphs).

The biological effects of 9-*cis* retinoic acid are mediated not only by RXR, but also by RAR, which can also be activated by all-*trans* retinoic acid [18, 22, 53-55]. Furthermore, while RXR can homodimerize with itself, it also commonly heterodimerizes with RAR; in fact, the RAR/RXR heterodimer is considered to be the physiologically functional unit [18, 22, 56-60]. In light of this, and also because we observed pigment accumulation in MNT-1 cells treated with all-*trans* retinal and all-*trans* retinoic acid (albeit at significantly lower levels than induced by 9-*cis* retinal and 9-*cis* retinoic acid) [13], we also performed ChIP in both MNT-1 melanoma cells and darkly-pigmented primary human melanocytes as before using an antibody against RARα. Intriguingly, we discovered that in both pigmented cell lines, RARα was significantly enriched when compared to mock IgG control in the same two regions upstream of the *MITF-A* start site as RXRα (Fig. 1D, two right graphs). As with RXRα, RARα was not enriched in the promoter of *MITF-M* relative to control IgG (Fig. 1D, two right graphs). These results demonstrate that RARα and RXRα are bound upstream of the *MITF-A* transcription start site, most likely as a heterodimer; however it is possible that they are in a complex with a different nuclear receptor.

Retinoids and retinoid-analogs are able to activate the *MITF-A* promoter

After establishing that both RARα and RXRα are enriched upstream of the *MITF-A* transcription start site, we next investigated whether retinoids and other well-established agonists of RARα and RXRα are able to activate the *MITF-A* promoter. First, we examined the expression levels of RARα and RXRα in four readily available cell lines to determine which

expresses both proteins at the highest level. We established that human epidermal kidney cells, (HEK293T) were ideal for promoter-activity experiments not only because they expressed the highest levels of RXRα protein, (Fig. 2A) but also because they are more successful than the other cell lines in transfection experiments (data not shown). Furthermore, HEK293T cells had similar levels of RARα protein when compared to the other cell lines (Fig. 2A).

Next, we transfected HEK293T cells with a previously described firefly luciferase reporter driven by the *MITF-A* full-length promoter (*MITF-A* EcoRI) or a previously described firefly luciferase reporter driven by a truncated *MITF-A* promoter that lacks our putative RAR/RXR binding site (*MITF-A* SmaI) [43] (Fig. 2B). These cells were also co-transfected with a Renilla luciferase reporter driven by an SV40 promoter as an internal control. One day after transfection, the cells were treated with either 9-*cis* retinoic acid (Fig. 2C), the endogenous ligand for RXRα, LG100268 (Fig. 2D), an agonist for RXR, BMS753 (Fig. 2E), an agonist specific for RARα, or HX531 (Fig. 2F), an antagonist for RXRα, for twenty-four hours and then harvested for a dual-luciferase activity assay. As expected, 9-*cis* retinoic acid treatment resulted in a significant, three-fold increase in luciferase activity in cells transfected with the full-length *MITF-A* promoter, but not in the cells transfected with the truncated *MITF-A* promoter (Fig. 2C). Next, we used a potent and selective rexinoid and RXR agonist, LG100268, which can bind to and activate all three isoforms of RXR [61]. It displays no activity at RAR receptors [61]. As with 9-*cis* retinoic acid treatment, we observed a significant three-fold increase in luciferase activity when HEK293T cells transfected with full-length *MITF-A* promoter were treated with LG100268 (Fig. 2D). Combined, our data suggests that both endogenous retinoids and selective, potent RXRα agonists activate the *MITF-A* promoter, providing further evidence that RXRα is enriched in the *MITF-A* promoter.

As our ChIP data suggests that RARα is also enriched upstream of the *MITF-A* transcription start site, we next investigated whether a potent RARα agonist, BMS753, could also stimulate luciferase activity. Intriguingly, as with both *9-cis* retinoic acid and LG100268 treatment, we observed a highly significant three-fold induction of luciferase activity in cells treated with RARα agonist and transfected with the full-length *MITF-A* promoter when compared to vehicle-treated control cells transfected with the same full-length promoter construct (Fig. 2E). Lastly, we treated transfected HEK293T cells with HX531, a potent RXR antagonist. In cells transfected with the full-length *MITF-A* promoter, we observed no significant increases in luciferase activity between vehicle-treated control cells and cells treated with HX531 (Fig. 2F). This demonstrates that antagonist-mediated blocking of RXRα is sufficient to inhibit increases in luciferase activity above baseline levels (vehicle-treated control), providing further evidence that RXRα is likely bound to the *MITF-A* promoter.

RXRα and RARα-specific agonists up regulate the expression of *MITF-A* and *MITF-M* in combination with each other, but not alone

Once we had established that retinoids and RXRα and RARα-specific agonists were able to regulate the activity of the full length *MITF-A* promoter, we next sought to investigate whether these compounds could induce the accumulation of *MITF-A* and *MITF-M* transcripts. We treated MNT-1 melanoma cells with an increasing dose of BMS753 (RARα-specific agonist), CD3254 (RXRα-specific agonist), or a combination of both agonists at once and then analyzed the mRNA levels of *MITF-A* and *MITF-M* using RT-qPCR with primers designed to target the specific exon 1 of both. When MNT-1 cells were treated with each agonist alone (either BMS753 or CD3254

alone), there were no significant increases in either transcript (Fig. 2G). However, when used together, the agonists were able to stimulate the accumulation of both *MITF-A* and *MITF-M* mRNAs (Fig. 2G), suggesting that both RXRα and RARα need to be activated in order to achieve stimulation of transcription. This correlates well with our previously published data that showed that 9-*cis* retinoic acid was able to induce the accumulation of *TYR* and *MITF* mRNAs [13]; unlike BMS753 and CD3254, which only activate either RXRα or RARα, 9-*cis* retinoic acid is able to activate both [18].

4.5 Discussion

We previously identified that 9-*cis* retinoic acid is the oxidative product of ALDH1A1 that stimulates melanogenesis *in vitro* [13]. However, it was unknown how 9-*cis* retinoic acid functions to modulate pigment production. Now, we demonstrate that 9-*cis* retinoic acid regulates melanogenesis through a novel RAR/RXR heterodimer enriched upstream of the *MITF-A* transcription start site (Fig. 3). Our data suggests that there are two possible ways in which the RXR/RAR heterodimer may modulate melanogenesis: either by stimulating the accumulation of *MITF-A* mRNA (which may then act in its own mechanism to modulate melanogenesis) (Fig. 3) or by acting as an enhancer to regulate expression of *MITF-M* due to chromatin looping mechanisms. In both potential mechanisms, ALDH1A1 converts 9-*cis*/all-*trans* retinal to 9-*cis*/all-*trans* retinoic acid (RA) as a part of the metabolism in the vitamin A pathway (Fig. 3). After RA is synthesized by ALDH1A1, it binds to and activates the RAR/RXR heterodimer complex that is bound upstream of the *MITF-A* transcription start site (Fig. 3). We still have not completely elucidated whether or not RAR/RXR is complexed as a heterodimer upstream of the *MITF-A* transcription start site. Our ChIP experiments demonstrate binding of both receptors in the same genomic regions; however, from this data, we cannot ascertain for sure if it is indeed a heterodimer complex of RAR/RXR. Other lines of evidence suggest that the RAR/RXR activates this upstream enhancer for two main reasons. Firstly, 9-*cis* retinoic acid, which we have shown is able to stimulate pigmentation [13], the accumulation of *TYR* and *MITF* mRNAs [13], TYR protein [13], and the full-length *MITF-A* promoter (Fig. 2C), is a specific ligand for RAR and RXR and not other well-described nuclear receptors [18]. Secondly, a combination of RAR and RXR agonists, but not the agonists individually, was able to stimulate

the accumulation of both *MITF-A* and *MITF-M* mRNAs (Fig. 2G), indicating that the activation of both receptors is necessary for transcriptional regulation. A sequential ChIP (also known as a ChIP-re-ChIP) experiment is needed to fully verify that it is a RAR/RXR heterodimer complex that we are observing. However, for ease of discussion, we will refer to the enrichment of RAR and RXR identified by our ChIP analysis as a RAR/RXR heterodimer.

A key piece of our data upholds the hypothesis that the RAR/RXR heterodimer, which is enriched directly upstream of the *MITF-A* transcription start site, stimulates the transcription of the *MITF-A* promoter and subsequently, *MITF-A* mRNA upon activation by ligand. We show that in combination, RAR and RXR agonists induce the accumulation of both *MITF-A* and *MITF-M* mRNAs in melanoma cells (Fig. 2G). Furthermore, we demonstrate that both RAR and RXR agonists stimulate the *MITF-A* promoter in *luciferase*-assay experiments (Fig. 2C-2F); however, this assay does not address the structure of chromatin in the nucleus, thus prohibiting a true understanding of whether or not retinoids can actually stimulate the *MITF-A* promoter *in vivo*. However, from the aforementioned data, we can speculate that MITF-A expression may be up regulated after activation of the RAR/RXR heterodimer. In turn, MITF-A may bind to and regulate the promoter of MITF-M, thus stimulating its increased expression and melanogenesis; this could explain why we observe the accumulation of both *MITF-M* and *MITF-A* mRNAs after treatment with both RAR and RXR agonists (Fig. 2G). It has been previously reported that MITF-M is able to bind to and regulate its own promoter [62], so it is highly possible that MITF-A may function in a similar fashion. In self-activating its own promoter, MITF-M interacts with lymphoid enhancer-binding factor 1 (LEF-1) [62], a component of the Wnt signaling pathway. Intriguingly, the recruitment of MITF-M to the *M* promoter depends on the binding of LEF-1 to three adjacent binding sites [62]; this is most likely a preventative mechanism to preclude MITF-

M from serving as a co-activator on many gene promoters containing single LEF-1 binding sites. Furthermore, the Wnt/β-catenin signaling plays a significant role in in the development of the retinal pigment epithelium (RPE), where MITF-A is highly expressed [63]. Elegant ChIP and reporter gene assays have demonstrated that Tcf/Lef (components of the Wnt/β-catenin pathway) bind to and regulate the promoters of both *Mitf-D* and *Mitf-H* [63], two isoforms of Mitf that are expressed in the RPE and important for its development [64, 65]. Combined, this data advocates that Wnt signaling plays an important part in the regulation of many isoforms of MITF; it will be interesting to determine whether, in addition to MITF-M, MITF-A is able to physically interact with LEF-1 (or other transcription factors) on the *M* promoter to stimulate its increased expression. On the other hand, two studies strongly suggest a second potential mechanism for how MITF-A may regulate melanogenesis that is separate from it possibly regulating the *MITF-M* promoter. First, in transient transfection assays, MITF-A was able to transactivate both the *TYR* and the *TYRP-1* gene promoters in HeLa human cervical cancer cells [66] and human melanoma cells [38]. Therefore, it is plausible that MITF-A may regulate the promoters of *TYR* and *TYRP-1* in pigment producing cells as well, in addition to or exclusive of regulating the *MITF-M* promoter.

Genomic DNA is defined by its linear sequence, yet the three-dimensional organization of the genome inside the nucleus forms an important role in gene expression regulation [67]. The control of gene expression often involves regulatory elements that are very far in genomic distance from the genes they control [67]. Such regulation is achieved through chromatin looping, wherein stretches of genomic sequence that lie on the same chromosome are actually in closer proximity to each other than linear sequences that separate them [67, 68]. Intriguingly, RXRα has been shown to form a heterodimeric complex with peroxisome proliferator-activated

receptor (PPAR) on a RARE within the hepatitis B virus enhancer-1; once activated, the complex transactivates the enhancer [69]. This data suggests that RXRα may have the ability to activate enhancers and thus to regulate genes that are sequentially far away upstream or downstream but close when chromatin is properly folded in the nucleus. Therefore, it is a possibility that the RAR/RXR heterodimer enriched upstream of the *MITF-A* transcription start site is also within an enhancer that may act to regulate genes that are not close in sequence of DNA. We observed that in combination, RAR/RXR agonists were able to stimulate the expression of both *MITF-M* and *MITF-A* in melanoma cells (Fig. 2G). Thus, it may be that due to specific chromatin looping, the RAR/RXR heterodimer sequentially upstream of the *MITF-A* transcription start site is, in three-dimension, close to and able to regulate the *MITF-M* promoter. It is also possible that the RAR/RXR heterodimer acts in tandem to stimulate both *MITF-A* and *MITF-M*; the heterodimer could stimulate transcription of the proximal *MITF-A* as well as stimulate transcription of the distal *MITF-M* through chromatin looping.

Vitiligo is one of the most common de-pigmenting skin disorders [2]. It occurs worldwide, with an incidence of 0.1%-2% of the total population being affected [2]. It is characterized by the acquired and progressive hypomelanosis of the hair and skin, with melanocytes completely absent in affected lesions [2]. Although the exact mechanisms of causation of vitiligo are still poorly understood, it typically co-exists with other autoimmune disorders; it is theorized that a combination of genetics, environmental stress, immunological and neurological factors synergize to destroy melanocytes, thus resulting in hypomelanosis [2]. Vitiligo leaves patients with severe physical disfigurement, which often causes serious emotional distress and prevents an individual from living a full, rewarding life. As the pathogenesis for vitiligo is still not well understood, the treatment options are broad in nature and usually not fully

effective [2]. Retinoids, especially RA, are possibly attractive candidates for the topical treatment of vitiligo for two key reasons. Firstly, multiple independent studies have shown that retinoids induce melanogenesis [13, 70-72]. We demonstrated that RA is able to induce the accumulation of pigment, *TYR* and *MITF* mRNAs, and TYR protein *in vitro* [13]. Another study, which demonstrated that RA is able to stimulate melanogenesis in B16F10 mouse melanoma cells, utilized electron microscopy analysis to show an accumulation of more late-stage melanosomes in RA-treated cells than in vehicle-treated control cells [70]. Melanosomes also showed a larger total volume across all stages when cells were treated with RA [70]. A similar study found that Hs939 human melanoma cells exposed to 1 μM of RA for longer than four days exhibited an increase in melanogenesis marked by a more than three-fold increase in melanin content and tyrosinase activity over control cells [71]. In a third study, topically applied 0.05% or 0.00375% RA augmented increases in melanocyte number after UV-B irradiation in two unrelated mouse strains, C57BL/6 and HRA:Skh-2 (lightly-pigmented, hairless mice) [72]. After two weeks of treatment, a 2-fold increase in the number of DOPA-positive melanocytes was observed concomitant with a 4-fold increase in melanogenesis [72]. In fact, RA was even able to stimulate significant increases in melanogenesis and DOPA-positive melanocytes on its own, although the effect was much more potent in conjunction with UV-B radiation [72]. A second reason why RA is possibly an attractive therapeutic candidate for the treatment of vitiligo is that all-*trans* retinoic acid has been previously shown to be a potent inducer of cellular differentiation [73]. In one convincing study, all-*trans* retinoic acid was shown to not only induce the differentiation of early-migrating trunk neural crest cells to melanocytes and adrenergic cells, but it was also able stimulate the production of pigment by melanoblasts [73]. As vitiliginous skin is marked by an absence of functional melanocytes, RA may be useful in

stimulating the differentiation of melanoblasts to pigment-producing melanocytes in lesioned areas, followed by continued stimulation of melanogenesis.

Future studies will focus on the mechanism of how RAR/RXR modulates melanogenesis, and whether or not it regulates *MITF-A*, *MITF-M* or both. We are also investigating whether retinoids and RAR/RXR agonists are able to modulate pigmentation in three-dimensional human skin equivalents, the mouse-tail and or the mouse hair. This investigation will allow us to better analyze the potential for retinoids to act as inducers of melanogenesis in a possibly therapeutic manner. To that end, we are also pursing an *in vivo* strategy to determine the importance of MITF-A to melanogenesis in the mouse hair follicle. Utilizing the novel Cas9/CRISPR gene targeting platform, we have selectively deleted regions within the first exons of *MITF-A* and *MITF-M*. This is the first time, to our knowledge, that the MITF-A isoform is being analyzed for its role in melanogenesis in the mouse hair follicle and the RPE in an *in vivo* model.

4.6 Acknowledgments

We thank Dr. Shigeki Shibahara for his kind gift of the *MITF-A*-luciferase plasmid constructs. We thank the UCI Genomics High Throughput Facility with their help on the Nanostring nCounter expression analysis.

4.7 References

1. Slominski A, Tobin DJ, Shibahara S, Wortsman J. Melanin pigmentation in mammalian skin and its hormonal regulation. Physiological reviews. 2004;84(4):1155-228. doi: 10.1152/physrev.00044.2003. PubMed PMID: 15383650.

2. Yaghoobi R, Omidian M, Bagherani N. Vitiligo: a review of the published work. The Journal of dermatology. 2011;38(5):419-31. PubMed PMID: 21667529.

3. Rivas S, Pandya AG. Treatment of melasma with topical agents, peels and lasers: an evidence-based review. American journal of clinical dermatology. 2013;14(5):359-76. doi: 10.1007/s40257-013-0038-4. PubMed PMID: 23881551.

4. Ganesan AK, Ho H, Bodemann B, Petersen S, Aruri J, Koshy S, et al. Genome-wide siRNA-based functional genomics of pigmentation identifies novel genes and pathways that impact melanogenesis in human cells. PLoS genetics. 2008;4(12):e1000298. doi: 10.1371/journal.pgen.1000298. PubMed PMID: 19057677; PubMed Central PMCID: PMC2585813.

5. Ma I, Allan AL. The role of human aldehyde dehydrogenase in normal and cancer stem cells. Stem cell reviews. 2011;7(2):292-306. doi: 10.1007/s12015-010-9208-4. PubMed PMID: 21103958.

6. Marchitti SA, Brocker C, Stagos D, Vasiliou V. Non-P450 aldehyde oxidizing enzymes: the aldehyde dehydrogenase superfamily. Expert opinion on drug metabolism & toxicology. 2008;4(6):697-720. doi: 10.1517/17425255.4.6.697. PubMed PMID: 18611112; PubMed Central PMCID: PMC2658643.

7. Black WJ, Stagos D, Marchitti SA, Nebert DW, Tipton KF, Bairoch A, et al. Human aldehyde dehydrogenase genes: alternatively spliced transcriptional variants and their suggested nomenclature. Pharmacogenetics and genomics. 2009;19(11):893-902. doi: 10.1097/FPC.0b013e3283329023. PubMed PMID: 19823103; PubMed Central PMCID: PMC3356695.

8. Vasiliou V, Nebert DW. Analysis and update of the human aldehyde dehydrogenase (ALDH) gene family. Human genomics. 2005;2(2):138-43. PubMed PMID: 16004729; PubMed Central PMCID: PMC3525259.

9. Vasiliou V, Pappa A. Polymorphisms of human aldehyde dehydrogenases. Consequences for drug metabolism and disease. Pharmacology. 2000;61(3):192-8. doi: 28400. PubMed PMID: 10971205.

10. Vasiliou V, Pappa A, Petersen DR. Role of aldehyde dehydrogenases in endogenous and xenobiotic metabolism. Chemico-biological interactions. 2000;129(1-2):1-19. PubMed PMID: 11154732.

11. Yoshida A, Hsu LC, Dave V. Retinal oxidation activity and biological role of human cytosolic aldehyde dehydrogenase. Enzyme. 1992;46(4-5):239-44. PubMed PMID: 1292933.

12. Chen Y, Koppaka V, Thompson DC, Vasiliou V. Focus on molecules: ALDH1A1: from lens and corneal crystallin to stem cell marker. Experimental eye research. 2012;102:105-6. doi: 10.1016/j.exer.2011.04.008. PubMed PMID: 21536030; PubMed Central PMCID: PMC3423494.

13. Paterson EK, Ho H, Kapadia R, Ganesan AK. 9-cis retinoic acid is the ALDH1A1 product that stimulates melanogenesis. Experimental dermatology. 2013;22(3):202-9.

14. Mark M, Ghyselinck NB, Chambon P. Function of retinoid nuclear receptors: lessons from genetic and pharmacological dissections of the retinoic acid signaling pathway during mouse embryogenesis. Annual review of pharmacology and toxicology. 2006;46:451-80. doi: 10.1146/annurev.pharmtox.46.120604.141156. PubMed PMID: 16402912.

15. Blomhoff R. Transport and metabolism of vitamin A. Nutrition reviews. 1994;52(2 Pt 2):S13-23. PubMed PMID: 8202278.

16. Kastner P, Mark M, Chambon P. Nonsteroid nuclear receptors: what are genetic studies telling us about their role in real life? Cell. 1995;83(6):859-69. PubMed PMID: 8521510.

17. Morriss-Kay GM, Ward SJ. Retinoids and mammalian development. International review of cytology. 1999;188:73-131. PubMed PMID: 10208011.

18. Chambon P. A decade of molecular biology of retinoic acid receptors. FASEB journal : official publication of the Federation of American Societies for Experimental Biology. 1996;10(9):940-54. PubMed PMID: 8801176.

19. Leid M, Kastner P, Chambon P. Multiplicity generates diversity in the retinoic acid signalling pathways. Trends in biochemical sciences. 1992;17(10):427-33. PubMed PMID: 1333659.

20. Heyman RA, Mangelsdorf DJ, Dyck JA, Stein RB, Eichele G, Evans RM, et al. 9-cis retinoic acid is a high affinity ligand for the retinoid X receptor. Cell. 1992;68(2):397-406. PubMed PMID: 1310260.

21. Levin AA, Sturzenbecker LJ, Kazmer S, Bosakowski T, Huselton C, Allenby G, et al. 9-cis retinoic acid stereoisomer binds and activates the nuclear receptor RXR alpha. Nature. 1992;355(6358):359-61. doi: 10.1038/355359a0. PubMed PMID: 1309942.

22. Wei LN. Retinoid receptors and their coregulators. Annual review of pharmacology and toxicology. 2003;43:47-72. doi: 10.1146/annurev.pharmtox.43.100901.140301. PubMed PMID: 12142470.

23. Bardot O, Aldridge TC, Latruffe N, Green S. PPAR-RXR heterodimer activates a peroxisome proliferator response element upstream of the bifunctional enzyme gene. Biochemical and biophysical research communications. 1993;192(1):37-45. doi: 10.1006/bbrc.1993.1378. PubMed PMID: 8386511.

24. Kliewer SA, Umesono K, Noonan DJ, Heyman RA, Evans RM. Convergence of 9-cis retinoic acid and peroxisome proliferator signalling pathways through heterodimer formation of their receptors. Nature. 1992;358(6389):771-4. doi: 10.1038/358771a0. PubMed PMID: 1324435.

25. Leid M, Kastner P, Lyons R, Nakshatri H, Saunders M, Zacharewski T, et al. Purification, cloning, and RXR identity of the HeLa cell factor with which RAR or TR heterodimerizes to bind target sequences efficiently. Cell. 1992;68(2):377-95. PubMed PMID: 1310259.

26. Yu VC, Delsert C, Andersen B, Holloway JM, Devary OV, Naar AM, et al. RXR beta: a coregulator that enhances binding of retinoic acid, thyroid hormone, and vitamin D receptors to their cognate response elements. Cell. 1991;67(6):1251-66. PubMed PMID: 1662118.

27. Egea PF, Rochel N, Birck C, Vachette P, Timmins PA, Moras D. Effects of ligand binding on the association properties and conformation in solution of retinoic acid receptors RXR and RAR. Journal of molecular biology. 2001;307(2):557-76. doi: 10.1006/jmbi.2000.4409. PubMed PMID: 11254382.

28. Dong D, Noy N. Heterodimer formation by retinoid X receptor: regulation by ligands and by the receptor's self-association properties. Biochemistry. 1998;37(30):10691-700. doi: 10.1021/bi980561r. PubMed PMID: 9692959.

29. Kersten S, Gronemeyer H, Noy N. The DNA binding pattern of the retinoid X receptor is regulated by ligand-dependent modulation of its oligomeric state. The Journal of biological chemistry. 1997;272(19):12771-7. PubMed PMID: 9139736.

30. Lin BC, Wong CW, Chen HW, Privalsky ML. Plasticity of tetramer formation by retinoid X receptors. An alternative paradigm for DNA recognition. The Journal of biological chemistry. 1997;272(15):9860-7. PubMed PMID: 9092522.

31. Levy C, Khaled M, Fisher DE. MITF: master regulator of melanocyte development and melanoma oncogene. Trends in molecular medicine. 2006;12(9):406-14. doi: 10.1016/j.molmed.2006.07.008. PubMed PMID: 16899407.

32. Shibahara S, Takeda K, Yasumoto K, Udono T, Watanabe K, Saito H, et al. Microphthalmia-associated transcription factor (MITF): multiplicity in structure, function, and regulation. The journal of investigative dermatology Symposium proceedings / the Society for Investigative Dermatology, Inc [and] European Society for Dermatological Research. 2001;6(1):99-104. doi: 10.1046/j.0022-202x.2001.00010.x. PubMed PMID: 11764295.

33. Hershey CL, Fisher DE. Genomic analysis of the Microphthalmia locus and identification of the MITF-J/Mitf-J isoform. Gene. 2005;347(1):73-82. doi: 10.1016/j.gene.2004.12.002. PubMed PMID: 15715979.

34. Bertolotto C, Abbe P, Hemesath TJ, Bille K, Fisher DE, Ortonne JP, et al. Microphthalmia gene product as a signal transducer in cAMP-induced differentiation of

melanocytes. The Journal of cell biology. 1998;142(3):827-35. PubMed PMID: 9700169; PubMed Central PMCID: PMC2148160.

35. Price ER, Horstmann MA, Wells AG, Weilbaecher KN, Takemoto CM, Landis MW, et al. alpha-Melanocyte-stimulating hormone signaling regulates expression of microphthalmia, a gene deficient in Waardenburg syndrome. The Journal of biological chemistry. 1998;273(49):33042-7. PubMed PMID: 9830058.

36. Goding CR. Mitf from neural crest to melanoma: signal transduction and transcription in the melanocyte lineage. Genes & development. 2000;14(14):1712-28. PubMed PMID: 10898786.

37. Fuse N, Yasumoto K, Suzuki H, Takahashi K, Shibahara S. Identification of a melanocyte-type promoter of the microphthalmia-associated transcription factor gene. Biochemical and biophysical research communications. 1996;219(3):702-7. PubMed PMID: 8645245.

38. Amae S, Fuse N, Yasumoto K, Sato S, Yajima I, Yamamoto H, et al. Identification of a novel isoform of microphthalmia-associated transcription factor that is enriched in retinal pigment epithelium. Biochemical and biophysical research communications. 1998;247(3):710-5. PubMed PMID: 9647758.

39. Daily K, Patel VR, Rigor P, Xie X, Baldi P. MotifMap: integrative genome-wide maps of regulatory motif sites for model species. BMC bioinformatics. 2011;12:495. doi: 10.1186/1471-2105-12-495. PubMed PMID: 22208852; PubMed Central PMCID: PMC3293935.

40. Xie X, Rigor P, Baldi P. MotifMap: a human genome-wide map of candidate regulatory motif sites. Bioinformatics. 2009;25(2):167-74. doi: 10.1093/bioinformatics/btn605. PubMed PMID: 19017655; PubMed Central PMCID: PMC2732295.

41. Untergasser A, Cutcutache I, Koressaar T, Ye J, Faircloth BC, Remm M, et al. Primer3--new capabilities and interfaces. Nucleic acids research. 2012;40(15):e115. doi: 10.1093/nar/gks596. PubMed PMID: 22730293; PubMed Central PMCID: PMC3424584.

42. Koressaar T, Remm M. Enhancements and modifications of primer design program Primer3. Bioinformatics. 2007;23(10):1289-91. doi: 10.1093/bioinformatics/btm091. PubMed PMID: 17379693.

43. Udono T, Yasumoto K, Takeda K, Amae S, Watanabe K, Saito H, et al. Structural organization of the human microphthalmia-associated transcription factor gene containing four alternative promoters. Biochimica et biophysica acta. 2000;1491(1-3):205-19. PubMed PMID: 10760582.

44. Mangelsdorf DJ, Borgmeyer U, Heyman RA, Zhou JY, Ong ES, Oro AE, et al. Characterization of three RXR genes that mediate the action of 9-cis retinoic acid. Genes & development. 1992;6(3):329-44. PubMed PMID: 1312497.

45. Li M, Chiba H, Warot X, Messaddeq N, Gerard C, Chambon P, et al. RXR-alpha ablation in skin keratinocytes results in alopecia and epidermal alterations. Development. 2001;128(5):675-88. PubMed PMID: 11171393.

46. Li M, Indra AK, Warot X, Brocard J, Messaddeq N, Kato S, et al. Skin abnormalities generated by temporally controlled RXRalpha mutations in mouse epidermis. Nature. 2000;407(6804):633-6. doi: 10.1038/35036595. PubMed PMID: 11034212.

47. Elder JT, Astrom A, Pettersson U, Tavakkol A, Griffiths CE, Krust A, et al. Differential regulation of retinoic acid receptors and binding proteins in human skin. The Journal of investigative dermatology. 1992;98(5):673-9. PubMed PMID: 1314862.

48. Fisher GJ, Talwar HS, Xiao JH, Datta SC, Reddy AP, Gaub MP, et al. Immunological identification and functional quantitation of retinoic acid and retinoid X receptor proteins in human skin. The Journal of biological chemistry. 1994;269(32):20629-35. PubMed PMID: 8051161.

49. Fisher GJ, Voorhees JJ. Molecular mechanisms of retinoid actions in skin. FASEB journal : official publication of the Federation of American Societies for Experimental Biology. 1996;10(9):1002-13. PubMed PMID: 8801161.

50. Reichrath J, Munssinger T, Kerber A, Rochette-Egly C, Chambon P, Bahmer FA, et al. In situ detection of retinoid-X receptor expression in normal and psoriatic human skin. The British journal of dermatology. 1995;133(2):168-75. PubMed PMID: 7547381.

51. Mark M, Ghyselinck NB, Wendling O, Dupe V, Mascrez B, Kastner P, et al. A genetic dissection of the retinoid signalling pathway in the mouse. The Proceedings of the Nutrition Society. 1999;58(3):609-13. PubMed PMID: 10604193.

52. Du X, Tabeta K, Mann N, Crozat K, Mudd S, Beutler B. An essential role for Rxr alpha in the development of Th2 responses. European journal of immunology. 2005;35(12):3414-23. doi: 10.1002/eji.200535366. PubMed PMID: 16259011.

53. Glass CK. Some new twists in the regulation of gene expression by thyroid hormone and retinoic acid receptors. The Journal of endocrinology. 1996;150(3):349-57. PubMed PMID: 8882153.

54. Mangelsdorf DJ, Kliewer SA, Kakizuka A, Umesono K, Evans RM. Retinoid receptors. Recent progress in hormone research. 1993;48:99-121. PubMed PMID: 8382832.

55. Mangelsdorf DJ, Thummel C, Beato M, Herrlich P, Schutz G, Umesono K, et al. The nuclear receptor superfamily: the second decade. Cell. 1995;83(6):835-9. PubMed PMID: 8521507.

56. Kurokawa R, Soderstrom M, Horlein A, Halachmi S, Brown M, Rosenfeld MG, et al. Polarity-specific activities of retinoic acid receptors determined by a co-repressor. Nature. 1995;377(6548):451-4. doi: 10.1038/377451a0. PubMed PMID: 7566126.

57. Dilworth FJ, Fromental-Ramain C, Remboutsika E, Benecke A, Chambon P. Ligand-dependent activation of transcription in vitro by retinoic acid receptor alpha/retinoid X receptor alpha heterodimers that mimics transactivation by retinoids in vivo. Proceedings of the National Academy of Sciences of the United States of America. 1999;96(5):1995-2000. PubMed PMID: 10051583; PubMed Central PMCID: PMC26725.

58. Dilworth FJ, Fromental-Ramain C, Yamamoto K, Chambon P. ATP-driven chromatin remodeling activity and histone acetyltransferases act sequentially during transactivation by RAR/RXR In vitro. Molecular cell. 2000;6(5):1049-58. PubMed PMID: 11106744.

59. Steinmetz AC, Renaud JP, Moras D. Binding of ligands and activation of transcription by nuclear receptors. Annual review of biophysics and biomolecular structure. 2001;30:329-59. doi: 10.1146/annurev.biophys.30.1.329. PubMed PMID: 11340063.

60. Egea PF, Klaholz BP, Moras D. Ligand-protein interactions in nuclear receptors of hormones. FEBS letters. 2000;476(1-2):62-7. PubMed PMID: 10878252.

61. Perez E, Bourguet W, Gronemeyer H, de Lera AR. Modulation of RXR function through ligand design. Biochimica et biophysica acta. 2012;1821(1):57-69. doi: 10.1016/j.bbalip.2011.04.003. PubMed PMID: 21515403.

62. Saito H, Yasumoto K, Takeda K, Takahashi K, Fukuzaki A, Orikasa S, et al. Melanocyte-specific microphthalmia-associated transcription factor isoform activates its own gene promoter through physical interaction with lymphoid-enhancing factor 1. The Journal of biological chemistry. 2002;277(32):28787-94. doi: 10.1074/jbc.M203719200. PubMed PMID: 12048204.

63. Fujimura N, Taketo MM, Mori M, Korinek V, Kozmik Z. Spatial and temporal regulation of Wnt/beta-catenin signaling is essential for development of the retinal pigment epithelium. Developmental biology. 2009;334(1):31-45. doi: 10.1016/j.ydbio.2009.07.002. PubMed PMID: 19596317.

64. Bharti K, Liu W, Csermely T, Bertuzzi S, Arnheiter H. Alternative promoter use in eye development: the complex role and regulation of the transcription factor MITF. Development. 2008;135(6):1169-78. doi: 10.1242/dev.014142. PubMed PMID: 18272592; PubMed Central PMCID: PMC2276638.

65. Bharti K, Nguyen MT, Skuntz S, Bertuzzi S, Arnheiter H. The other pigment cell: specification and development of the pigmented epithelium of the vertebrate eye. Pigment cell research / sponsored by the European Society for Pigment Cell Research and the International Pigment Cell Society. 2006;19(5):380-94. doi: 10.1111/j.1600-0749.2006.00318.x. PubMed PMID: 16965267; PubMed Central PMCID: PMC1564434.

66. Shibahara S, Yasumoto K, Amae S, Udono T, Watanabe K, Saito H, et al. Regulation of pigment cell-specific gene expression by MITF. Pigment cell research / sponsored by the European Society for Pigment Cell Research and the International Pigment Cell Society. 2000;13 Suppl 8:98-102. PubMed PMID: 11041365.

67. Kadauke S, Blobel GA. Chromatin loops in gene regulation. Biochimica et biophysica acta. 2009;1789(1):17-25. doi: 10.1016/j.bbagrm.2008.07.002. PubMed PMID: 18675948; PubMed Central PMCID: PMC2638769.

68. Cavalli G, Misteli T. Functional implications of genome topology. Nature structural & molecular biology. 2013;20(3):290-9. doi: 10.1038/nsmb.2474. PubMed PMID: 23463314.

69. Huan B, Kosovsky MJ, Siddiqui A. Retinoid X receptor alpha transactivates the hepatitis B virus enhancer 1 element by forming a heterodimeric complex with the peroxisome proliferator-activated receptor. Journal of virology. 1995;69(1):547-51. PubMed PMID: 7983754; PubMed Central PMCID: PMC188608.

70. Fernandes SS, Arcuri R, Morgado-Diaz JA, Benchimol M. Increase of melanogenesis by retinoic acid: an ultrastructural and morphometric study. Tissue & cell. 2004;36(2):95-105. doi: 10.1016/j.tice.2003.10.006. PubMed PMID: 15041411.

71. Lotan R, Lotan D. Stimulation of melanogenesis in a human melanoma cell line by retinoids. Cancer research. 1980;40(9):3345-50. PubMed PMID: 6253061.

72. Welsh BM, Mason RS, Halliday GM. Topical all-trans retinoic acid augments ultraviolet radiation-induced increases in activated melanocyte numbers in mice. The Journal of investigative dermatology. 1999;112(3):271-8. doi: 10.1046/j.1523-1747.1999.00510.x. PubMed PMID: 10084301.

73. Dupin E, Le Douarin NM. Retinoic acid promotes the differentiation of adrenergic cells and melanocytes in quail neural crest cultures. Developmental biology. 1995;168(2):529-48. doi: 10.1006/dbio.1995.1100. PubMed PMID: 7729587.

Figure 4.1: RXRα and RARα are enriched upstream of the *MITF-A* transcription start site

(A) MNT-1 melanoma cells (MNT-1), darkly-pigmented human epidermal melanocytes (DP-Mel), and B16 mouse melanoma cells (B16) were harvested for RNA extraction and subsequently checked for expression levels of *MITF-A* and *MITF-M* based on primers designed to target exon 1 of each aforementioned isoform. Data shown is relative mean mRNA level for three biological replicates of each cell line, as indicated by the error bars (n=3). (B) 4-mm skin punch biopsies were acquired from anesthetized control *Luc*-shRNA mice and experimental *Luc*-shRNA/rtTA2 and immediately stabilized in RNAlater. Extracted RNA was subjected to Nanostring analysis on *MITF*-A and *MITF-M* isoforms based on the expression levels of exon 1 for each. Data shown is mean normalized counts of mRNA for each gene (n = 3 mice as indicated by the error bars). (C) Primers used in ChIP analysis were designed to target the 2 kB region upstream of the transcription start site for both *MITF-A* and *MITF-M* isoforms (designated the "promoter region"). Four primers were made to target distinct 500-bp tiles within the entire 2 kB promoter region, designated 1-4 for each isoform (*MITF-M1, MITF-A1,* ect). (D) Enrichment of both RXRα and RARα in the promoter regions of both *MITF-A* and *MITF-M* was investigated using ChIP RT-qPCR analysis in both MNT-1 melanoma and darkly-pigmented human epidermal melanocyte cell lines. A mock ChIP using a control IgG antibody was also performed. Percent input corresponds to the mean of three ChIP biological replicates (n=3), as indicated by the *error bars*. A two-tailed student's t-test was used to determine statistical significance in enrichment between RXRα and RARα and the mock IgG control. *, $p \leq 0.05$ or **, $p \leq 0.01$

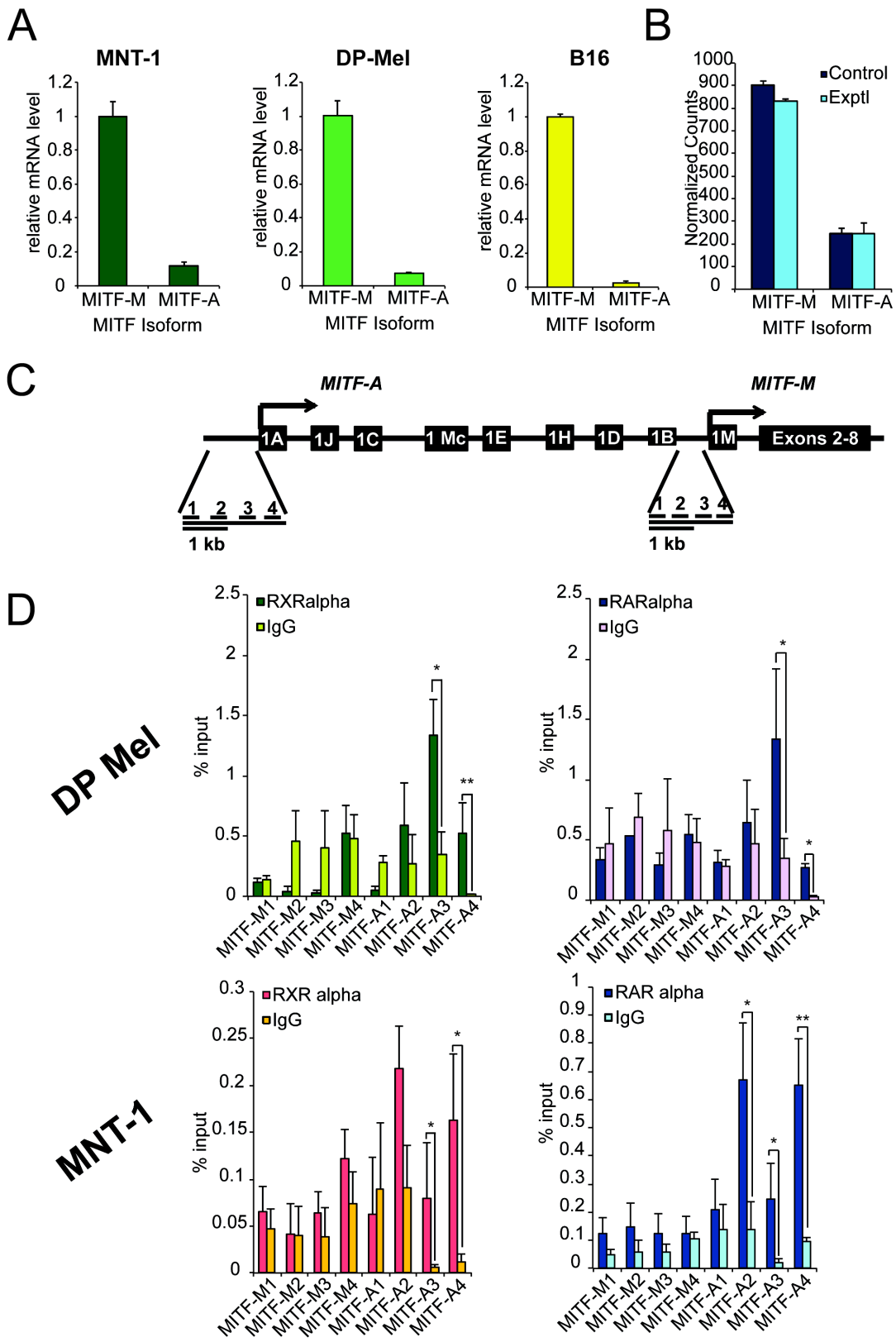
A
MNT-1
DP-Mel
B16
relative mRNA level
MITF-M
MITF-A
MITF Isoform
B
Control
Exptl
Normalized Counts
C
MITF-A
MITF-M
1A
1J
1C
1 Mc
1E
1H
1D
1B
1M
Exons 2-8
1 2 3 4
1 kb
D
DP Mel
MNT-1
RXRalpha
IgG
RARalpha
RXR alpha
RAR alpha
% input
MITF-M1
MITF-M2
MITF-M3
MITF-M4
MITF-A1
MITF-A2
MITF-A3
MITF-A4

Figure 4.1

Figure 4.2: Retinoids stimulate the *MITF-A* promoter and the expression of both *MITF-A* and *MITF-M*

(A) A375 human melanoma cells (A375), human embryonic kidney 293T cells (HEK293T), MNT-1 human melanoma cells (MNT-1), and SK-Mel-28 human melanoma cells (SKM28) were harvested and subjected to immunoblotting to quantify the amount of RXRα and RARα proteins in each. GAPDH was used as a loading control. (B) Schematic showing the size of the *MITF-A* promoter upstream of the *luciferase* gene in the pGL3-*luciferase* plasmid constructs. The full-length *MITF-A* promoter contains the full 2-kB promoter region upstream of *luciferase*, while the truncated *MITF-A* promoter only contains 60 base pairs of the *MITF-A* promoter upstream of *luciferase*. (C-F) HEK293T cells were transfected with either a firefly luciferase reporter driven by the *MITF-A* full-length promoter (MITF-A EcoRI) or a firefly luciferase reporter driven by a truncated *MITF-A* promoter (MITF-A SmaI) and co-transfected with a Renilla luciferase reporter driven by an SV40 promoter as an internal control. The cells were then treated with the indicated dose of 9-*cis* retinoic acid (endogeneous RXRα ligand) (C), LG100268 (RXR agonist) (D), BMS753 (RARα-specific agonist) (E) or HX531 (RXR antagonist) (F) for twenty four hours before being harvested and subjected to a dual-luciferase assay. Relative luciferase units (RLUs) corresponds to the mean of three biological replicates for each treatment (n=3), as indicated by the *error bars*. A two-tailed student's *t*-test was used to determine statistical significance in RLUs between drug-treated cell lysate and vehicle-control cell lysate. *, $p \leq 0.05$, **, $p \leq 0.01$, ***, $p \leq 0.001$. (G) MNT-1 melanoma cells were treated with an increasing dose (125 nM, 250 nM, 500 nM, 1000 nM) of BMS753 (RARα-specific agonist) or CD3254 (RXRα-specific agonist) or a combination of both BMS753 and CD3254 for twenty-four hours before being harvested for RNA and subsequent RT-qPCR. The expression levels of both *MITF-A* exon 1 and *MITF-M* exon 1 were analyzed and their expression was normalized to the internal housekeeping gene, β-actin. Relative mRNA level corresponds to the mean of three biological replicates for each treatment (n=3), as indicated by the *error bars*. A two-tailed student's *t*-test was employed to determine the statistical significance in mean mRNA level between drug-treated cells and vehicle-control cells. *, $p \leq 0.05$, **, $p \leq 0.01$.

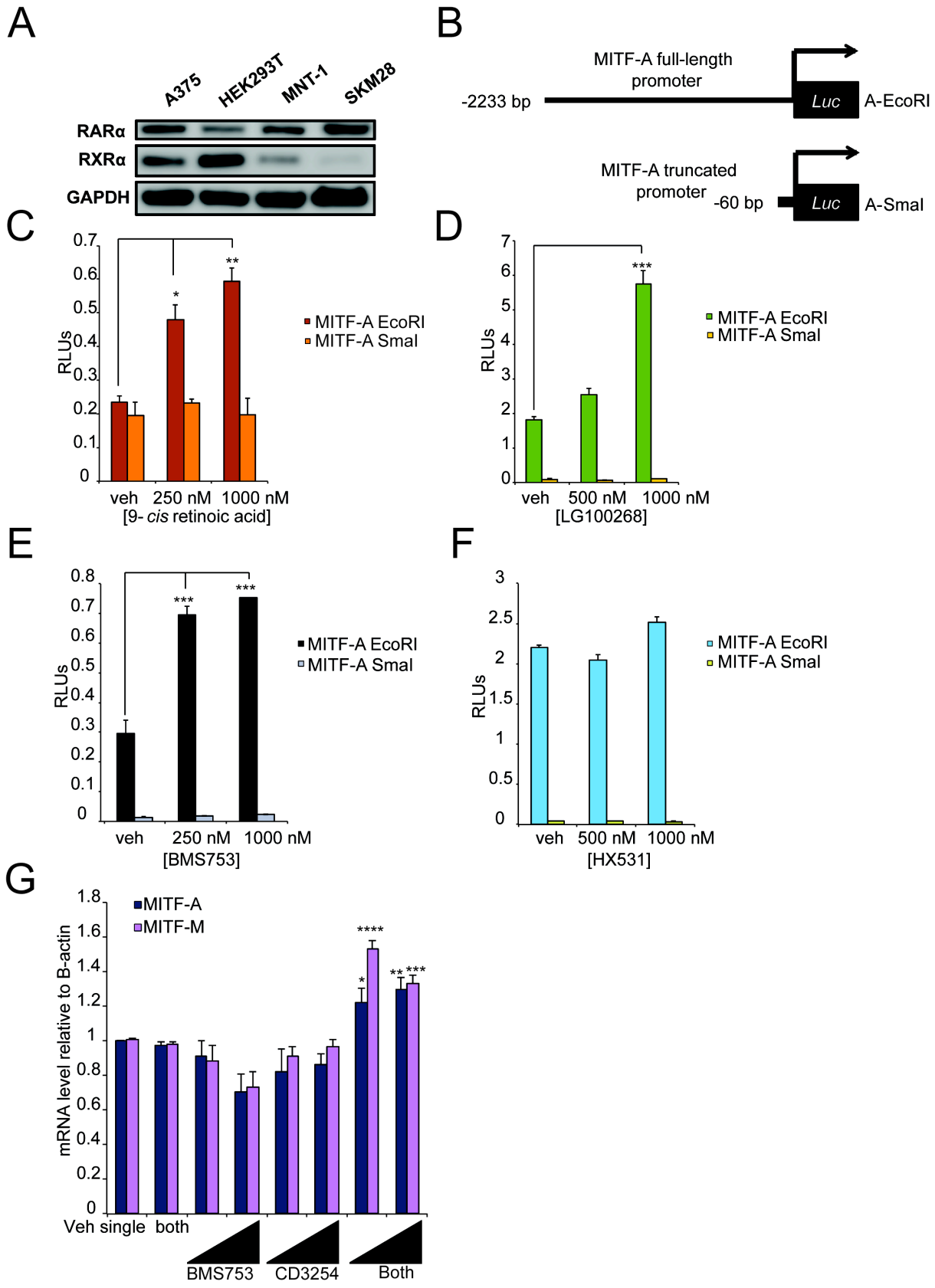
A
A375
HEK293T
MNT-1
SKM28
RARα
RXRα
GAPDH
B
MITF-A full-length promoter
-2233 bp
Luc
A-EcoRI
MITF-A truncated promoter
-60 bp
Luc
A-SmaI
C
RLUs
MITF-A EcoRI
MITF-A SmaI
veh
250 nM
1000 nM
[9- cis retinoic acid]
D
RLUs
MITF-A EcoRI
MITF-A SmaI
veh
500 nM
1000 nM
[LG100268]
E
RLUs
MITF-A EcoRI
MITF-A SmaI
veh
250 nM
1000 nM
[BMS753]
F
RLUs
MITF-A EcoRI
MITF-A SmaI
veh
500 nM
1000 nM
[HX531]
G
MITF-A
MITF-M
mRNA level relative to B-actin
Veh
single
both
BMS753
CD3254
Both

Figure 4.2

Figure 4.3: A model of how retinoids may modulate melanogenesis: stimulation of the *MITF-A* promoter through the RAR/RXR heterodimer complex

Illustration representing the regulation of the *MITF-A* promoter by retinoids. In the vitamin A pathway, ALDH1A1 catalyzes the formation of retinoic acid (both all-*trans* and 9-*cis*) from retinal. Cyanamide (Cya) prevents this reaction from occurring by inhibiting the catalytic activity of ALDH1A1. In the absence of ligand, RAR/RXR is bound to the promoter of *MITF-A*, upstream of the transcription start site. Co-repressor proteins, including histone deacetylases (HDACs), PRC2 (polycomb repressive complex 2) and silencing mediator for retinoid or thyroid-hormone receptors (SMRT) interact with the RAR/RXR heterodimer and keep the chromatin in a condensed state that is not favorable for transcription to occur. However, when retinoic acid binds to RAR/RXR, the heterodimer undergoes a conformational change and recruits co-activator proteins, including histone acetyltransferases (HATs), SWItch/Sucrose non-fermentable (SWI/SNF), TRITHORAX, and nuclear co-activator receptor proteins (NcoAs) and releases co-repressor proteins. This then allows for the chromatin to be de-compacted and more open for RNA polymerase II (Pol II) to bind and begin transcription.

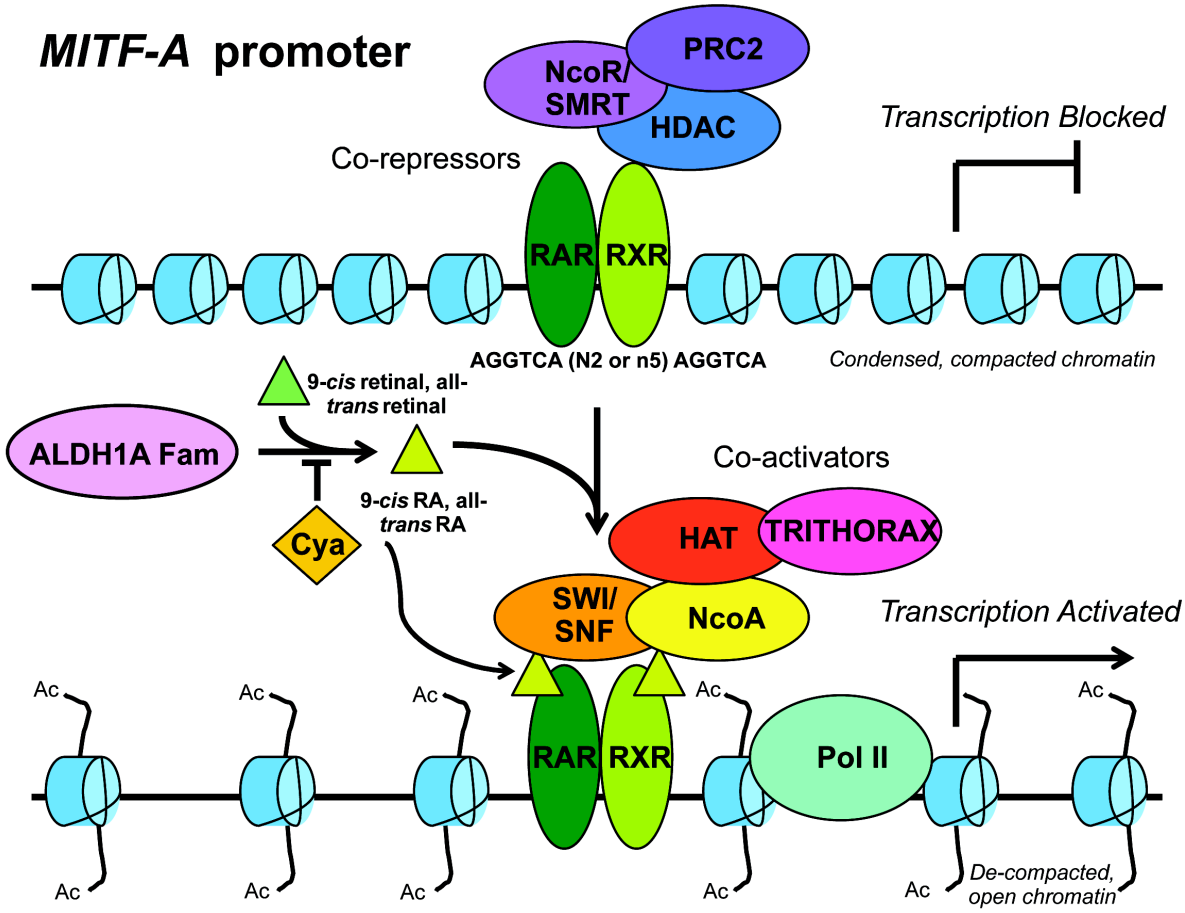
MITF-A promoter
PRC2
NcoR/
SMRT
HDAC
Co-repressors
Transcription Blocked
RAR
RXR
AGGTCA (N2 or n5) AGGTCA
Condensed, compacted chromatin
9-cis retinal, all-
trans retinal
ALDH1A Fam
9-cis RA, all-
trans RA
Cya
Co-activators
HAT
TRITHORAX
SWI/
SNF
NcoA
Transcription Activated
Ac
RAR
RXR
Pol II
De-compacted,
open chromatin

Figure 4.3

Figure 4.4: A model of how retinoids may modulate melanogenesis: the RAR/RXR heterodimer acts as an enhancer to regulate *MITF-M* through chromatin looping mechanisms

Illustration representing the regulation of the *MITF-M* promoter by retinoids. Although the putative RAR/RXR is bound almost 200 kB upstream of the *MITF-M* promoter, chromatin looping may bring the two in close physical proximity of each other. Thus, RAR/RXR may directly regulate the *MITF-M* promoter. In the presence of retinoic acid, the RAR/RXR heterodimer undergoes a conformational change and recruits co-activator proteins, including histone acetyltransferases (HATs), SWItch/Sucrose non-fermentable (SWI/SNF), TRITHORAX, and nuclear co-activator receptor proteins (NcoAs) and releases co-repressor proteins. This then allows for the chromatin to be de-compacted and more open for RNA polymerase II (Pol II) to bind and begin transcription.

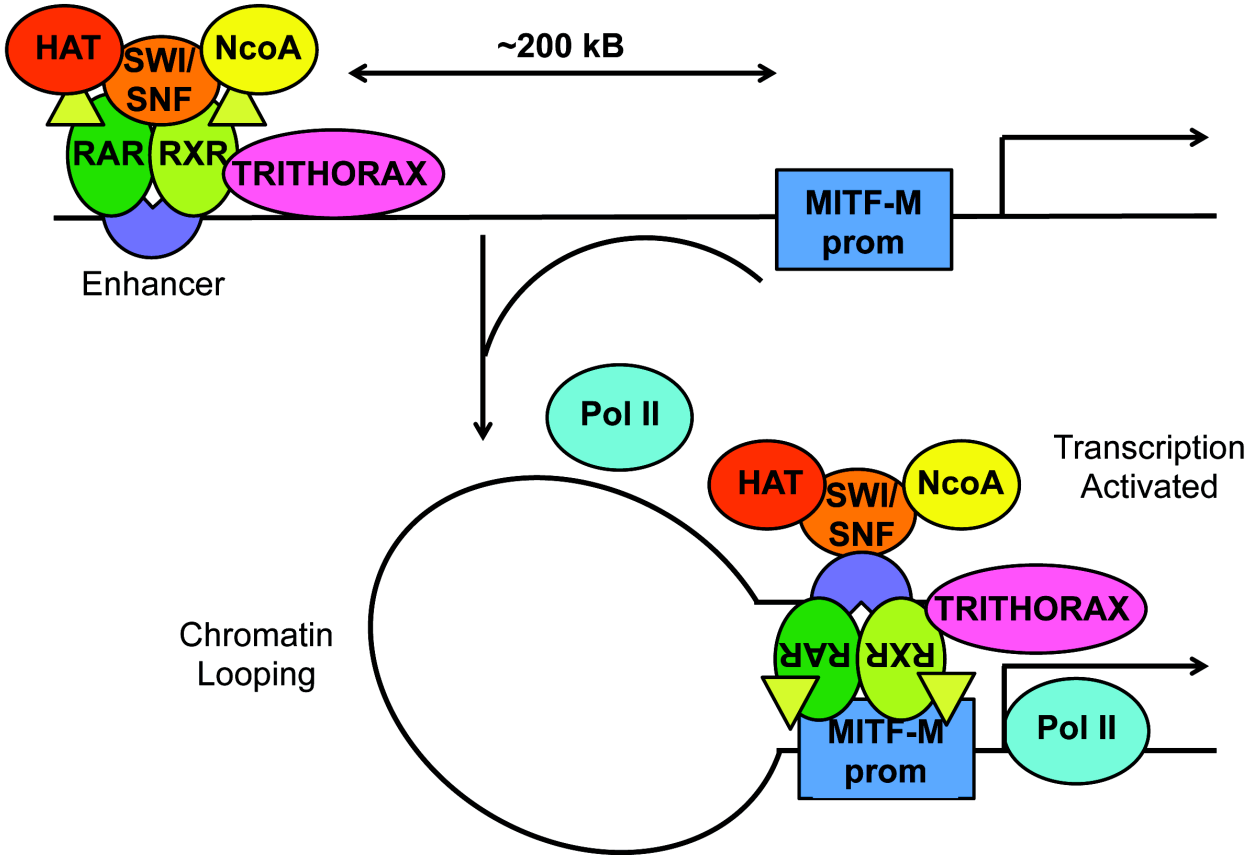
HAT
SWI/
SNF
NcoA
~200 kB
RAR
RXR
TRITHORAX
MITF-M
prom
Enhancer
Pol II
HAT
SWI/
SNF
NcoA
Transcription
Activated
TRITHORAX
RAR
RXR
Chromatin
Looping
MITF-M
prom
Pol II

Figure 4.4

Table 4.1: List of putative transcription factor binding sites in the promoter of *MITF-M*, as identified by MotifMap.

Location	BBLS	BLS	NLOD	Z-Score	FDR	TF Name	Distance (bp)	Region
chr3:70068379..70068396	1.738	2.312	0.954	5.255	0	Lhx4	-44	Upstream
chr3:70068380..70068397	1.729	2.312	0.894	4.689	0	Lhx4	-60	Upstream
chr3:70068202..70068211	2.029	2.705	0.977	4.459	0.012	SF1	-238	Upstream
chr3:70068280..70068288	2.515	2.515	1	4.856	0.013	ATF2:c-Jun	-160	Upstream
chr3:70068280..70068288	2.515	2.515	1	4.856	0.013	ATF2:c-Jun	-152	Upstream
chr3:70068279..70068288	2.139	2.737	0.968	4.596	0.014	CREB, ATF	-161	Upstream
chr3:70068280..70068289	2.135	2.737	0.927	4.296	0.019	CREB, ATF	-151	Upstream
chr3:70068202..70068210	1.938	2.607	0.973	4.362	0.022	SF1	-238	Upstream
chr3:70068277..70068288	1.573	2.515	0.919	4.403	0.028	CREB	-163	Upstream
chr3:70067895..70067902	1.931	2.612	1	3.81	0.035	ETS2	-545	Upstream
chr3:70068280..70068288	2.515	2.515	1	4.782	0.035	CREB	-152	Upstream
chr3:70068280..70068288	2.515	2.515	1	4.782	0.035	CREB	-160	Upstream
chr3:70067506..70067512	1.41	2.089	1	3.817	0.055	MAFB	-928	Upstream
chr3:70068379..70068396	1.214	2.312	0.852	4.309	0.068	K-2b	-44	Upstream
chr3:70067507..70067514	1.684	2.089	1	4.054	0.074	MAFA	-933	Upstream
chr3:70068384..70068394	0.835	2.312	0.965	4.437	0.082	ipf1	-46	Upstream
chr3:70068382..70068396	1.735	2.737	0.908	4.759	0.083	CHX10	-58	Upstream
chr3:70068380..70068397	1.316	2.312	0.934	4.73	0.084	ALX-3	-60	Upstream
chr3:70068379..70068396	1.318	2.312	0.941	4.79	0.094	ALX-3	-44	Upstream
chr3:70068380..70068397	1.233	2.312	0.918	4.936	0.1	K-2b	-60	Upstream
chr3:70069427..70069441	1.147	2.098	0.851	4.27	0.103	CHX10	1001	Downstream
chr3:70068379..70068396	0.767	2.312	0.889	4.657	0.107	Gbx2	-44	Upstream
chr3:70068426..70068435	1.504	2.376	0.929	4.531	0.113	ELK4	-5	Upstream
chr3:70068379..70068395	0.526	2.312	0.842	4.447	0.12	HOXA1	-61	Upstream
chr3:70068381..70068397	0.536	2.312	0.857	4.596	0.131	HOXA1	-43	Upstream
chr3:70069427..70069444	0.133	1.399	0.883	4.303	0.14	Shox2	987	Downstream
chr3:70069429..70069443	1.155	2.098	0.89	4.604	0.142	CHX10	989	Downstream
chr3:70068379..70068396	0.284	2.312	0.893	4.395	0.148	Shox2	-44	Upstream
chr3:70069427..70069444	0.271	1.071	0.869	4.428	0.157	Pax-4	987	Downstream
chr3:70068047..70068055	1.143	1.467	1	4.192	0.163	STAT1	-385	Upstream
chr3:70068381..70068397	0.35	2.312	0.902	4.284	0.165	Barx-2	-59	Upstream
chr3:70069427..70069444	0.222	1.796	0.872	4.408	0.165	POU6F1	987	Downstream
chr3:70068379..70068396	0.043	2.312	0.857	4.314	0.166	Pax-4	-44	Upstream
chr3:70068380..70068397	0.043	2.312	0.857	4.319	0.17	Pax-4	-60	Upstream
chr3:70068380..70068397	1.145	2.312	0.9	4.447	0.171	LH-2	-60	Upstream
chr3:70069426..70069442	0.309	1.621	0.893	4.404	0.172	PMX2A	986	Downstream
chr3:70068380..70068397	0.559	2.312	0.881	4.42	0.173	Evx-1	-60	Upstream
chr3:70068383..70068397	0.162	2.312	0.91	4.337	0.178	HOXA3	-43	Upstream
chr3:70068379..70068395	0.368	2.312	0.915	4.394	0.183	Barx-2	-45	Upstream

chr3:70068383..70068397	0.024	2.312	0.898	4.293	0.191	Dlx-1	-43	Upstream
chr3:70068379..70068396	0.568	2.312	0.892	4.523	0.194	Evx-1	-44	Upstream
chr3:70068379..70068396	0.925	2.312	0.908	4.662	0.195	Octamer	-61	Upstream
chr3:70067982..70068000	0.192	1.031	0.823	4.686	0.201	GCNF	-440	Upstream
chr3:70068381..70068397	0.002	2.312	0.882	4.278	0.202	ipf1	-59	Upstream
chr3:70068379..70068396	1.158	2.312	0.932	4.736	0.207	LH-2	-44	Upstream
chr3:70069426..70069443	0.129	1.137	0.871	4.43	0.221	PMX2B	986	Downstream
chr3:70069426..70069443	0.122	1.39	0.858	4.343	0.229	Alx-4	1003	Downstream
chr3:70068379..70068396	0.364	2.312	0.874	4.47	0.23	EMX2	-44	Upstream
chr3:70068379..70068395	0.338	2.312	0.877	4.444	0.233	HOXA5	-45	Upstream
chr3:70068379..70068396	0.211	2.312	0.849	4.422	0.236	lhx6.1	-44	Upstream
chr3:70068380..70068397	0.111	2.312	0.881	4.34	0.247	Esx1	-43	Upstream
chr3:70068177..70068188	1.355	2.376	0.916	4.485	0.288	Pax	-263	Upstream
chr3:70068379..70068395	0.077	2.312	0.851	4.343	0.29	HoxA2	-45	Upstream
chr3:70068379..70068395	0.002	2.312	0.858	4.279	0.296	Barhl-1	-61	Upstream
chr3:70069426..70069443	0.121	1.251	0.869	4.502	0.396	HOXC4	1003	Downstream
chr3:70069426..70069443	0.107	1.031	0.883	4.453	0.48	HOXC5	1003	Downstream
chr3:70068202..70068209	2.677	2.737	1	3.933	0.488	NURR1	-238	Upstream
chr3:70069036..70069046	0.464	1.935	0.982	4.519	0.49	Nkx2-2	606	Downstream
chr3:70069118..70069135	0.077	1.184	0.859	4.417	0.491	Otx2	695	Downstream

Table 4.2: List of putative transcription factor binding sites in the promoter of *MITF-A*, as identified by MotifMap.

Location	BBLS	BLS	NLOD	Z-Score	FDR	TF Name	Distance (bp)	Region
chr3:69871150..69871172	2.34	2.794	0.952	6.758	0	LM4_M2	-125	Upstream
chr3:69871219..69871241	1.417	2.794	0.843	5.562	0	LM4_M2	-34	Upstream
chr3:69871553..69871559	2.612	2.695	1	3.989	0.007	Neuro D	278	Downstream
chr3:69871553..69871559	2.612	2.695	1	3.989	0.007	Neuro D	284	Downstream
chr3:69871813..69871823	1.128	2.106	0.989	4.563	0.009	TAL1	538	Downstream
chr3:69871815..69871821	1.912	2.103	1	3.989	0.013	Neuro D	540	Downstream
chr3:69871815..69871821	1.912	2.103	1	3.989	0.013	Neuro D	546	Downstream
chr3:69871813..69871822	1.335	1.485	1	4.335	0.014	AP-4	538	Downstream
chr3:69871813..69871821	1.455	1.688	1	4.607	0.016	HEB	538	Downstream
chr3:69871080..69871086	2.591	2.591	1	3.817	0.026	MAFB	-195	Upstream
chr3:69871144..69871165	0.601	2.154	0.89	4.818	0.038	Staf	-110	Upstream
chr3:69871200..69871210	0.555	1.028	0.936	4.412	0.052	NF-kappaB	-65	Upstream
chr3:69871200..69871210	0.759	1.296	0.975	4.72	0.052	REL	-65	Upstream
chr3:69871078..69871085	2.516	2.591	1	4.054	0.058	MAFA	-190	Upstream
chr3:69871199..69871209	0.551	1.028	0.924	4.319	0.059	NF-kappaB	-76	Upstream
chr3:69871641..69871661	0.869	2.486	0.792	4.39	0.064	ESR1	386	Downstream
chr3:69871668..69871686	1.026	2.337	0.842	4.439	0.067	ESR2	411	Downstream
chr3:69871818..69871825	1.771	2.103	1	4.054	0.07	MAFA	550	Downstream
chr3:69871640..69871658	1.024	2.337	0.836	4.387	0.071	ESR2	383	Downstream
chr3:69871199..69871209	0.45	1.159	0.897	4.416	0.074	NF-kappaB (p50)	-66	Upstream
chr3:69872140..69872149	1.524	1.844	1	4.003	0.074	PUR1	865	Downstream
chr3:69871547..69871558	1.716	2.391	0.957	4.454	0.08	TGIF	283	Downstream
chr3:69871127..69871138	1.241	2.794	0.878	4.39	0.116	MYC::MAX	-137	Upstream
chr3:69871546..69871562	0.054	2.019	0.871	4.321	0.161	PKNOX2	287	Downstream
chr3:69871198..69871214	0.362	1.028	0.884	4.454	0.165	NF-kappaB	-61	Upstream
chr3:69870544..69870561	0.242	1.57	0.857	4.316	0.193	RXR::RAR_DR5	-714	Upstream
chr3:69871199..69871210	0.477	1.159	0.896	4.37	0.216	NFKB1	-76	Upstream
chr3:69871199..69871210	0.477	1.159	0.888	4.303	0.23	NFKB1	-65	Upstream
chr3:69871546..69871562	0.439	2.182	0.84	4.405	0.257	TGIF2	287	Downstream
chr3:69870735..69870762	0.554	1.898	0.817	4.578	0.276	GR	-513	Upstream
chr3:69871200..69871210	0.763	1.296	0.975	4.714	0.338	c-Rel	-65	Upstream
chr3:69871184..69871191	1.986	2.794	1	4.241	0.358	MZF1	-84	Upstream
chr3:69871055..69871062	1.868	2.591	1	4.241	0.365	MZF1	-220	Upstream
chr3:69870735..69870762	0.341	1.665	0.793	4.538	0.404	PR	-513	Upstream
chr3:69870946..69870955	1.117	1.805	0.949	4.353	0.41	AhR, Arnt, HIF-1	-329	Upstream
chr3:69871839..69871846	1.509	1.632	1	4.241	0.423	MZF1	564	Downstream
chr3:69871646..69871664	0.341	1.456	0.818	4.353	0.434	MIF-1	389	Downstream
chr3:69870944..69870955	1.024	1.805	0.935	4.552	0.474	AhR	-331	Upstream
chr3:69871149..69871156	2.459	2.794	1	3.933	0.484	NURR1	-126	Upstream

Conclusions and Future Directions

Chapter 5

Elyse K. Paterson and Anand K. Ganesan

Tyrosinase Modulates Pigmentation by Controlling the Distribution of Melanin Within the Maturing Melanosome

Melasma, an acquired disorder of pigmentation associated with symmetrical hypermelanosis, typically occurs in sun-exposed areas of skin [1, 2]. Melasma usually occurs in women of color and is difficult to treat. [1, 2]. While there is no increase in the number of melanocytes in skin marked by melasma, the melanocytes are larger and contain more dendritic processes [3, 4]. Moreover, there is more eumelanin accumulation in the epidermis and dermis [3, 4]. Multiple etiological factors contribute to its onset, including a combination of genetic influences, UV-R exposure, hormonal therapies (such as very commonly used hormonal birth-control pills), cosmetics, phototoxic drugs, and antiepileptic medications [1, 2]. Kojic acid and hydroquinone (HQ) are the most frequently used therapies for melasma [2, 5]. Both work by inhibiting the activity of tyrosinase, arguably the most important enzyme needed for melanin synthesis to occur [5]. However, both of these compounds are associated with risks and uncomfortable side effects; more importantly, they are not fully efficacious in providing continuous de-pigmentation of melasma skin lesions [5]. A once-daily triple combination formulation therapy consisting of 4.0% HQ, 0.05% tretinoin, and 0.01% fluocinolone acetonide (corticosteroid) has been shown to be one of the most efficacious treatments for melasma [6]; however, HQ was recently shown to be possibly carcinogenic at low doses, which makes its use in the treatment of melasma controversial [7]. To this effect, the FDA has recently prohibited all over-the-counter formulations of HQ until more research can be done to assess its potential carcinogenity. Furthermore, the conversion products of HQ have been shown to cause de-pigmentation side effects, which may also be possibly toxic to melanocytes [7]. Lastly, the

prolonged use of HQ has been shown to cause ochronosis, or pigmentation characterized by a blue-black color in treated areas, which is another highly undesirable side effect [7]. Taken together, it is clear that more effective, less toxic and more potent therapeutics are needed to inhibit melanogenesis in areas of skin marked by melasma.

To that end, we set out to determine whether or not whether tyrosinase is the ideal enzyme to target in the treatment of melasma. Multiple studies have demonstrated that tyrosinase inhibitors are clinically ineffective [7], meriting an analysis of the impact of what the partial loss of TYR does in the melanocyte. To address this need, we utilized a novel, partial loss of function mouse model [8, 9] to selectively deplete *Tyr* in the mouse hair follicle (Fig. 2.1). Intriguingly, while we did observe visual differences between *Tyr* knockdown mice and control mice (Fig 2.1, Fig. 2.4), we demonstrate that the partial depletion of *Tyr* (~70% knockdown) is not sufficient to induce significant decreases in the melanin accumulation in the mouse hair follicle in two distinct coat colors (Tables 2.1 and 2.2); this suggests that TYR activity is dispensable for melanogenesis to occur and that it may not be an ideal target for the treatment of melasma. We did show, however, that the partial depletion of *Tyr* is sufficient to alter the deposition of melanin within the terminal melanosome (Fig. 2.2) and to inhibit the expression of other important genes required for melanogenesis, including *Mitf-M, Sox10* and *Tyrp-1* (Fig. 2.2C). This data suggests that TYR plays a significant role in the pigment diversity seen in humans and animals, especially in subtle pigment differences. Future studies will utilize this partial loss of function mouse model to analyze the individual contributions of pigment-related genes to melanogenesis.

9-*cis* retinoic acid is the ALDH1A1 product that stimulates melanogenesis

Melanin is aberrantly regulated in vitiligo and melasma, two skin disorders characterized by hypomelanosis and hypermelanosis, respectively [1, 10]. Both diseases are not well understood and lack effective treatment options that ensure long-term, normal pigmentation in skin lesions [2, 4, 10-13]. Thus, pharmacologic agonists and antagonists are needed that either stimulate pigmentation in hypopigmented skin, or inhibit pigmentation in hyperpigmented skin. In an effort to better understand the molecular network that governs pigment production and to identify novel, single gene loci that support melanogenesis, MNT-1 melanoma cells were used to screen a genome-wide synthetic siRNA library [14]. ALDH1A1, a well-characterized enzyme involved in detoxification processes and in vitamin A metabolism [15], was one of 92 novel regulators of melanogenesis identified in the screen [14]. Intriguingly, ADLH1A1 was one of only three genes identified to impact TYR protein accumulation in three cell lines with distinct genetic backgrounds, further indicating that it regulates melanogenesis [14]. In this study, we identified at least one mechanism of how ALDH1A1 regulates pigment production. We demonstrate that 9-*cis* retinoic acid acts as a potent inducer of melanogenesis in MNT-1 melanoma cells and darkly-pigmented primary human epidermal melanocytes (Figs. 3.2-3.3). We observed dose-response increases in *TYR* and *MITF* mRNA transcript, and TYR protein when cells were exposed to 9-*cis* retinoic acid (Figs. 3.3A-3.3F). Furthermore, the depletion of ALDH1A1 by siRNA prevented the accumulation of *TYR* and *MITF* transcripts in the presence of 9-*cis* retinal (the substrate of ALDH1A1), but not in the presence of 9-*cis* retinoic acid (Figs. 3.3G-3.3H). This data provides key evidence that it is the product of ALDH1A1 catalysis that modulates melanogenesis. We utilized three-dimensional human skin equivalents to assess if

cyanamide, a potent catalytic inhibitor of ALDH1A1, would be able to impact pigment production. After three weeks of daily treatment, skin equivalents exposed to cyanamide demonstrated significantly less melanin as assessed by a melanin assay when compared to water-treated control equivalents (Fig. 3.4), suggesting that cyanamide may be an ideal pharmaceutical agent in the treatment of melasma. Currently, we are working on experiments in which a pre-formulated topical cream with cyanamide is applied to the tails of C3HeB/FeJ littermates, along with vehicle cream control. We hypothesize that due to the potent effect of cyanamide on the skin equivalents, treatment on the mouse-tails will result in visible and quantitative melanin loss. C3HeB/FeJ mice are ideal for this use because unlike other commonly used mouse strains (such as C57BL/6J), their tails are uniform in pigment.

Retinoids Modulate *MITF:* A Novel Mechanism in the Regulation of Melanin Biosynthesis

We previously identified ALDH1A1 as a novel regulator of melanogenesis [14]. However, because ALDH1A1 is a catalytic enzyme involved in multiple detoxification processes and in vitamin A metabolism [15], we hypothesized that one of its substrates or products would somehow impact pigment production. To that end, we then went on to show that its oxidation product in vitamin A metabolism, 9-*cis* retinoic acid, is the product of ALDH1A1 that stimulates melanogenesis [16]. However, the mechanism of how 9-*cis* retinoic acid achieves such modulation remained unanswered. Two classes of nuclear receptors, RARs and RXRs, exert the biological activity of 9-*cis* retinoic acid [17]. While RARs are activated by both all-*trans* retinoic acid (which we also showed stimulated the accumulation of pigment in melanoma cells, albeit not as potently as 9-*cis* retinoic acid) and 9-*cis* retinoic acid, RXRs are only activated by 9-*cis* retinoic acid [17]. Therefore, we hypothesized that a RAR/RXR heterodimer, activated by 9-*cis* retinoic acid, may be enriched in the promoter region of a key gene involved in melanogenesis. We utilized MotifMap [18, 19] to identify a putative RAR/RXR heterodimer upstream of the *MITF-A* transcription start site, an isoform of MITF not well-characterized nor previously known to play a role in pigment production in the melanocyte. We then performed ChIP RT-qPCR experiments that demonstrated the enrichment of both RARα and RXRα upstream of the *MITF-A* transcription start site (Figs. 4.1C, 4.1D); intriguingly, we identified no enrichment of RARα or RXRα anywhere upstream of the *MITF-M* transcription start site (Fig. 4.1D). We then went on to show, through *luciferase*-activity assays, that retinoids are able to activate the full-length *MITF-A* promoter, but not a truncated *MITF-A* promoter that lacks the binding site for the RAR/RXR heterodimer we identified through ChIP RT-qPCR (Figs. 4.2C-

4.2F). Finally, while RARα and RXRα agonists alone do not stimulate the accumulation of *MITF-A* or *MITF-M* transcripts, a combination of the agonists are able to do so (Fig 4.2G).

Much work needs to be completed to finish this project and to establish a full mechanism of how retinoids modulate *MITF* and melanogenesis overall. Firstly, we are in the process of performing ChIP-seq in order to fully confirm the binding of both RARα and RXRα in the promoter region of *MITF-A*. Secondly, we are planning to perform additional *luciferase*-activity assays and transfect cells with a full-length *MITF-M* promoter, as well as a truncated *MITF-M* promoter. After transfection and treatment with different retinoids, the relative luciferase activity measurements will provide us with information on whether or not retinoids are able to activate the *MITF-M* promoter in addition to activating the *MITF-A* promoter. Although ChIP RT-qPCR has shown no RAR/RXR heterodimer upstream of the *MITF-M* transcription start site, it is still as possibility that it is bound to an enhancer, and due to chromatin looping, able to regulate the transcription of *MITF-M*. The *luciferase*-activity experiments using *MITF-M* promoter constructs will provide us with information on whether the identified RAR/RXR heterodimer is able to regulate the *MITF-M* promoter directly through chromatin looping, or only able to activate the *MITF-A* promoter. To that end, we are also interested in determining if, upon activation and increased expression by RAR/RXR, MITF-A is regulating the transcription of *MITF-M*. Studies have shown that MITF-M can regulate its own promoter through an interaction with LEF-1 [20], so it is a possibility that MITF-A may function in a similar manner. The analysis of this may prove to be difficult, however, if no antibodies exist that specifically target MITF-A. To our knowledge, commercially available antibodies for MITF are pan-MITF antibodies, in that they target an exon common to all isoforms. However, if possible ChIP RT-qPCR could be used to assess whether MITF-A is able to regulate the transcription of *MITF-M*.

It would also be interesting to see whether MITF-A regulates the transcription of *TYR* and *TYRP-1*, as it has been previously shown to activate the promoters of both genes in HeLa cells and human melanoma cells [21, 22].

We are also interested in how the chromatin landscape changes in the promoters of both *MITF-M* and *MITF-A* after treatment with retinoids. If RAR/RXR is in fact enriched in the *MITF-A* promoter, activation by ligand should result in enrichment of active chromatin marks, coupled with the loss of repressive chromatin marks. We have previously observed that when treated with 9-*cis* retinoic acid, both H3K4Me3 and H3K9ac marks, which are associated with an active promoter [23], are significantly enriched in the *MITF-A* promoter regions previously identified to harbor RAR/RXR. Similarly, we observed significant decreases in enrichment for H3K9me3, a chromatin mark associated with repressed, inactive regions of chromatin [23], in the same aforementioned promoter regions of *MITF-A* when cells were treated with 9-*cis* retinoic acid. We are in the process of repeating this experiment to confirm these results, but they will provide us with a clearer picture of how the chromatin landscape changes in the presence of retinoids. It will also be interesting to analyze whether siRNA-mediated knockdown of RAR/RXR prevents changes in chromatin marks when cells are exposed to retinoids. In order to further verify that RAR and RXR are dimerized in our mechanism, ChIP re ChIP can be used [24]. In ChIP re ChIP, it is possible to identify multiple proteins that bind to the same DNA sequence, because two subsequent immunoprecipitation are carried out [24]. Thus, we plan to perform ChIP re ChIP coupled to RT-qPCR with both RARα and RXRα ChIP-grade antibodies in order to fully verify that RAR and RXR form a heterodimer complex as hinted at in our previous ChIP experiments. Lastly, we are investigating whether retinoids are able to induce the accumulation of pigment in the mouse-tail and in the previously used three-dimensional human

skin equivalents. Another *in vivo* approach that we are employing is isoform-specific knockouts of *MITF-A* and *MITF-M* utilizing the novel Cas9/CRISPR system. This is the first time that the role of MITF-A is being investigated in an *in vivo* approach. If MITF-A does contribute significantly to melanogenesis, we hope to see lightening of the coat of MITF-A knockout mice. Furthermore, we can utilize skin from MITF-A knockout mice for a variety of approaches to investigate its function in pigment synthesis in the mouse hair follicle. Currently, we are breeding the offspring of chimera *MITF-A* and *MITF-M* knockouts and using novel sequencing approaches to identify what mice have the ideal knockout for both isoforms; from there, we can establish mouse lines with appropriate backcrossing for future experiments.

Overall, this thesis work establishes a novel mechanism in the regulation of melanogenesis, which may aid in the development of therapeutics in the treatment of two of the most common and difficult to treat pigmentary disorders, melasma and vitiligo. We show a novel role for 9-*cis* retinoic acid in the stimulation of pigmentation. We also demonstrate that ALDH1A1, which is responsible for the synthesis of 9-*cis* retinoic acid, may be an ideal target for inhibiting pigment synthesis in areas of hyperpigmented skin. Lastly, we provide data to suggest that 9-*cis* retinoic acid is able to bind to and activate a RAR/RXR heterodimer upstream of the *MITF-A* transcription start site. However, we can only theorize as to what may be occurring from here: either MITF-A is a novel regulator of melanogenesis, or the RAR/RXR heterodimer may act as an enhancer and regulate the expression of *MITF-M*. Nonetheless, this work has established exciting new leads for the pigment biology field and provides new avenues to investigate in the search for better treatment options for common pigmentary disorders.

5.2 References

1. Victor FC, Gelber J, Rao B. Melasma: a review. Journal of cutaneous medicine and surgery. 2004;8(2):97-102. doi: 10.1007/s10227-004-0158-9. PubMed PMID: 15685388.

2. Gupta AK, Gover MD, Nouri K, Taylor S. The treatment of melasma: a review of clinical trials. Journal of the American Academy of Dermatology. 2006;55(6):1048-65. doi: 10.1016/j.jaad.2006.02.009. PubMed PMID: 17097400.

3. Kang WH, Yoon KH, Lee ES, Kim J, Lee KB, Yim H, et al. Melasma: histopathological characteristics in 56 Korean patients. The British journal of dermatology. 2002;146(2):228-37. PubMed PMID: 11903232.

4. Grimes PE, Yamada N, Bhawan J. Light microscopic, immunohistochemical, and ultrastructural alterations in patients with melasma. The American Journal of dermatopathology. 2005;27(2):96-101. PubMed PMID: 15798432.

5. Chang TS. An updated review of tyrosinase inhibitors. International journal of molecular sciences. 2009;10(6):2440-75. doi: 10.3390/ijms10062440. PubMed PMID: 19582213; PubMed Central PMCID: PMC2705500.

6. Torok HM. A comprehensive review of the long-term and short-term treatment of melasma with a triple combination cream. American journal of clinical dermatology. 2006;7(4):223-30. PubMed PMID: 16901182.

7. Levitt J. The safety of hydroquinone: a dermatologist's response to the 2006 Federal Register. Journal of the American Academy of Dermatology. 2007;57(5):854-72. doi: 10.1016/j.jaad.2007.02.020. PubMed PMID: 17467115.

8. Dow LE, Premsrirut PK, Zuber J, Fellmann C, McJunkin K, Miething C, et al. A pipeline for the generation of shRNA transgenic mice. Nature protocols. 2012;7(2):374-93. doi: 10.1038/nprot.2011.446. PubMed PMID: 22301776; PubMed Central PMCID: PMC3724521.

9. Premsrirut PK, Dow LE, Kim SY, Camiolo M, Malone CD, Miething C, et al. A rapid and scalable system for studying gene function in mice using conditional RNA interference. Cell. 2011;145(1):145-58.

10. Yaghoobi R, Omidian M, Bagherani N. Vitiligo: a review of the published work. The Journal of dermatology. 2011;38(5):419-31. PubMed PMID: 21667529.

11. Grimes PE. Melasma. Etiologic and therapeutic considerations. Archives of dermatology. 1995;131(12):1453-7. PubMed PMID: 7492140.

12. Boissy RE, Nordlund JJ. Vitiligo: current medical and scientific understanding. Giornale italiano di dermatologia e venereologia : organo ufficiale, Societa italiana di dermatologia e sifilografia. 2011;146(1):69-75. PubMed PMID: 21317859.

13. Whitton ME, Ashcroft DM, Gonzalez U. Therapeutic interventions for vitiligo. Journal of the American Academy of Dermatology. 2008;59(4):713-7. doi: 10.1016/j.jaad.2008.06.023. PubMed PMID: 18793940.

14. Ganesan AK, Ho H, Bodemann B, Petersen S, Aruri J, Koshy S, et al. Genome-wide siRNA-based functional genomics of pigmentation identifies novel genes and pathways that impact melanogenesis in human cells. PLoS genetics. 2008;4(12):e1000298. doi: 10.1371/journal.pgen.1000298. PubMed PMID: 19057677; PubMed Central PMCID: PMC2585813.

15. Vasiliou V, Nebert DW. Analysis and update of the human aldehyde dehydrogenase (ALDH) gene family. Human genomics. 2005;2(2):138-43. PubMed PMID: 16004729; PubMed Central PMCID: PMC3525259.

16. Paterson EK, Ho H, Kapadia R, Ganesan AK. 9-cis retinoic acid is the ALDH1A1 product that stimulates melanogenesis. Experimental dermatology. 2013;22(3):202-9.

17. Chambon P. A decade of molecular biology of retinoic acid receptors. FASEB journal : official publication of the Federation of American Societies for Experimental Biology. 1996;10(9):940-54. PubMed PMID: 8801176.

18. Daily K, Patel VR, Rigor P, Xie X, Baldi P. MotifMap: integrative genome-wide maps of regulatory motif sites for model species. BMC bioinformatics. 2011;12:495. doi: 10.1186/1471-2105-12-495. PubMed PMID: 22208852; PubMed Central PMCID: PMC3293935.

19. Xie X, Rigor P, Baldi P. MotifMap: a human genome-wide map of candidate regulatory motif sites. Bioinformatics. 2009;25(2):167-74. doi: 10.1093/bioinformatics/btn605. PubMed PMID: 19017655; PubMed Central PMCID: PMC2732295.

20. Saito H, Yasumoto K, Takeda K, Takahashi K, Fukuzaki A, Orikasa S, et al. Melanocyte-specific microphthalmia-associated transcription factor isoform activates its own gene promoter through physical interaction with lymphoid-enhancing factor 1. The Journal of biological chemistry. 2002;277(32):28787-94. doi: 10.1074/jbc.M203719200. PubMed PMID: 12048204.

21. Amae S, Fuse N, Yasumoto K, Sato S, Yajima I, Yamamoto H, et al. Identification of a novel isoform of microphthalmia-associated transcription factor that is enriched in retinal pigment epithelium. Biochemical and biophysical research communications. 1998;247(3):710-5. PubMed PMID: 9647758.

22. Shibahara S, Yasumoto K, Amae S, Udono T, Watanabe K, Saito H, et al. Regulation of pigment cell-specific gene expression by MITF. Pigment cell research / sponsored by the European Society for Pigment Cell Research and the International Pigment Cell Society. 2000;13 Suppl 8:98-102. PubMed PMID: 11041365.

23. Wang Z, Zang C, Rosenfeld JA, Schones DE, Barski A, Cuddapah S, et al. Combinatorial patterns of histone acetylations and methylations in the human genome. Nature genetics. 2008;40(7):897-903. doi: 10.1038/ng.154. PubMed PMID: 18552846; PubMed Central PMCID: PMC2769248.

24. Truax AD, Greer SF. ChIP and Re-ChIP assays: investigating interactions between regulatory proteins, histone modifications, and the DNA sequences to which they bind. Methods in molecular biology. 2012;809:175-88. doi: 10.1007/978-1-61779-376-9_12. PubMed PMID: 22113276.

Bibliography

AHN, K. S., MOON, K. Y., LEE, J. & KIM, Y. S. 2003. Downregulation of NF-kappaB activation in human keratinocytes by melanogenic inhibitors. *J Dermatol Sci,* 31**,** 193-201.

ALKHATEEB, A., FAIN, P. R., THODY, A., BENNETT, D. C. & SPRITZ, R. A. 2003. Epidemiology of vitiligo and associated autoimmune diseases in Caucasian probands and their families. *Pigment Cell Res,* 16**,** 208-14.

ALLENBY, G., BOCQUEL, M. T., SAUNDERS, M., KAZMER, S., SPECK, J., ROSENBERGER, M., LOVEY, A., KASTNER, P., GRIPPO, J. F., CHAMBON, P. & ET AL. 1993. Retinoic acid receptors and retinoid X receptors: interactions with endogenous retinoic acids. *Proc Natl Acad Sci U S A,* 90**,** 30-4.

ALNOUTI, Y. & KLAASSEN, C. D. 2008. Tissue distribution, ontogeny, and regulation of aldehyde dehydrogenase (Aldh) enzymes mRNA by prototypical microsomal enzyme inducers in mice. *Toxicol Sci,* 101**,** 51-64.

AMAE, S., FUSE, N., YASUMOTO, K., SATO, S., YAJIMA, I., YAMAMOTO, H., UDONO, T., DURLU, Y. K., TAMAI, M., TAKAHASHI, K. & SHIBAHARA, S. 1998. Identification of a novel isoform of microphthalmia-associated transcription factor that is enriched in retinal pigment epithelium. *Biochem Biophys Res Commun,* 247**,** 710-5.

ARCHAMBAULT, M., YAAR, M. & GILCHREST, B. A. 1995. Keratinocytes and fibroblasts in a human skin equivalent model enhance melanocyte survival and melanin synthesis after ultraviolet irradiation. *J Invest Dermatol,* 104**,** 859-67.

ARMSTRONG, B. K., KRICKER, A. & ENGLISH, D. R. 1997. Sun exposure and skin cancer. *Australas J Dermatol,* 38 Suppl 1**,** S1-6.

BARANKIN, B., SILVER, S. G. & CARRUTHERS, A. 2002. The skin in pregnancy. *J Cutan Med Surg,* 6**,** 236-40.

BARDOT, O., ALDRIDGE, T. C., LATRUFFE, N. & GREEN, S. 1993. PPAR-RXR heterodimer activates a peroxisome proliferator response element upstream of the bifunctional enzyme gene. *Biochem Biophys Res Commun,* 192**,** 37-45.

BASRUR, V., YANG, F., KUSHIMOTO, T., HIGASHIMOTO, Y., YASUMOTO, K., VALENCIA, J., MULLER, J., VIEIRA, W. D., WATABE, H., SHABANOWITZ, J., HEARING, V. J., HUNT, D. F. & APPELLA, E. 2003. Proteomic analysis of early melanosomes: identification of novel melanosomal proteins. *J Proteome Res,* 2**,** 69-79.

BEARD, C., HOCHEDLINGER, K., PLATH, K., WUTZ, A. & JAENISCH, R. 2006. Efficient method to generate single-copy transgenic mice by site-specific integration in embryonic stem cells. *Genesis,* 44**,** 23-8.

BECHEREL, P. A., MOSSALAYI, M. D., OUAAZ, F., LE GOFF, L., DUGAS, B., PAUL-EUGENE, N., FRANCES, C., CHOSIDOW, O., KILCHHERR, E., GUILLOSSON, J. J. & ET AL. 1994. Involvement of cyclic AMP and nitric oxide in immunoglobulin E-dependent activation of Fc epsilon RII/CD23+ normal human keratinocytes. *J Clin Invest,* 93**,** 2275-9.

BEERMANN, F., ORLOW, S. J., BOISSY, R. E., SCHMIDT, A., BOISSY, Y. L. & LAMOREUX, M. L. 1995. Misrouting of tyrosinase with a truncated cytoplasmic tail as a result of the murine platinum (cp) mutation. *Exp Eye Res,* 61**,** 599-607.

BEERMANN, F., ORLOW, S. J. & LAMOREUX, M. L. 2004. The Tyr (albino) locus of the laboratory mouse. *Mamm Genome,* 15**,** 749-58.

BEERMANN, F., RUPPERT, S., HUMMLER, E., BOSCH, F. X., MULLER, G., RUTHER, U. & SCHUTZ, G. 1990. Rescue of the albino phenotype by introduction of a functional tyrosinase gene into mice. *EMBO J,* 9**,** 2819-26.

BENNETT, D. C. & LAMOREUX, M. L. 2003. The color loci of mice--a genetic century. *Pigment Cell Res,* 16**,** 333-44.

BENTLEY, N. J., EISEN, T. & GODING, C. R. 1994. Melanocyte-specific expression of the human tyrosinase promoter: activation by the microphthalmia gene product and role of the initiator. *Mol Cell Biol,* 14**,** 7996-8006.

BERSON, J. F., HARPER, D. C., TENZA, D., RAPOSO, G. & MARKS, M. S. 2001. Pmel17 initiates premelanosome morphogenesis within multivesicular bodies. *Mol Biol Cell,* 12**,** 3451-64.

BERTOLOTTO, C., ABBE, P., HEMESATH, T. J., BILLE, K., FISHER, D. E., ORTONNE, J. P. & BALLOTTI, R. 1998. Microphthalmia gene product as a signal transducer in cAMP-induced differentiation of melanocytes. *J Cell Biol,* 142**,** 827-35.

BHARTI, K., LIU, W., CSERMELY, T., BERTUZZI, S. & ARNHEITER, H. 2008. Alternative promoter use in eye development: the complex role and regulation of the transcription factor MITF. *Development,* 135**,** 1169-78.

BHARTI, K., NGUYEN, M. T., SKUNTZ, S., BERTUZZI, S. & ARNHEITER, H. 2006. The other pigment cell: specification and development of the pigmented epithelium of the vertebrate eye. *Pigment Cell Res,* 19**,** 380-94.

BLACK, W. & VASILIOU, V. 2005. **Ocular Metabolism and Disposition of 4-Hydroxy-2-nonenal**. *Cutaneous and Ocular Toxicology,* 24**,** 165-176.

BLACK, W. J., STAGOS, D., MARCHITTI, S. A., NEBERT, D. W., TIPTON, K. F., BAIROCH, A. & VASILIOU, V. 2009. Human aldehyde dehydrogenase genes: alternatively spliced transcriptional variants and their suggested nomenclature. *Pharmacogenet Genomics,* 19**,** 893-902.

BLAGOVESHCHENSKAYA, A. D., HEWITT, E. W. & CUTLER, D. F. 1999. Di-leucine signals mediate targeting of tyrosinase and synaptotagmin to synaptic-like microvesicles within PC12 cells. *Mol Biol Cell,* 10**,** 3979-90.

BLOMHOFF, R. 1994. Transport and metabolism of vitamin A. *Nutr Rev,* 52**,** S13-23.

BOISSY, R. E. & NORDLUND, J. J. 2011. Vitiligo: current medical and scientific understanding. *G Ital Dermatol Venereol,* 146**,** 69-75.

BOISSY, R. E., SAKAI, C., ZHAO, H., KOBAYASHI, T. & HEARING, V. J. 1998. Human tyrosinase related protein-1 (TRP-1) does not function as a DHICA oxidase activity in contrast to murine TRP-1. *Exp Dermatol,* 7**,** 198-204.

BOISSY, R. E. & SPRITZ, R. A. 2009. Frontiers and controversies in the pathobiology of vitiligo: separating the wheat from the chaff. *Exp Dermatol,* 18**,** 583-5.

BONIFACINO, J. S. & TRAUB, L. M. 2003. Signals for sorting of transmembrane proteins to endosomes and lysosomes. *Annu Rev Biochem,* 72**,** 395-447.

BONILLA, C., BOXILL, L. A., DONALD, S. A., WILLIAMS, T., SYLVESTER, N., PARRA, E. J., DIOS, S., NORTON, H. L., SHRIVER, M. D. & KITTLES, R. A. 2005. The 8818G allele of the agouti signaling protein (ASIP) gene is ancestral and is associated with darker skin color in African Americans. *Hum Genet,* 116**,** 402-6.

BOTCHKAREVA, N. V., BOTCHKAREV, V. A. & GILCHREST, B. A. 2003. Fate of melanocytes during development of the hair follicle pigmentary unit. *J Investig Dermatol Symp Proc,* 8**,** 76-9.

BOUCHARD, B., FULLER, B. B., VIJAYASARADHI, S. & HOUGHTON, A. N. 1989. Induction of pigmentation in mouse fibroblasts by expression of human tyrosinase cDNA. *J Exp Med,* 169**,** 2029-42.

BRANDA, R. F. & EATON, J. W. 1978. Skin color and nutrient photolysis: an evolutionary hypothesis. *Science,* 201**,** 625-6.

BRENNER, M. & HEARING, V. J. 2008. Modifying skin pigmentation - approaches through intrinsic biochemistry and exogenous agents. *Drug Discov Today Dis Mech,* 5**,** e189-e199.

BUCHHOLZ, F., ANGRAND, P. O. & STEWART, A. F. 1998. Improved properties of FLP recombinase evolved by cycling mutagenesis. *Nat Biotechnol,* 16**,** 657-62.

BURCHILL, S. A., THODY, A. J. & ITO, S. 1986. Melanocyte-stimulating hormone, tyrosinase activity and the regulation of eumelanogenesis and phaeomelanogenesis in the hair follicular melanocytes of the mouse. *J Endocrinol,* 109**,** 15-21.

BUSCA, R. & BALLOTTI, R. 2000. Cyclic AMP a key messenger in the regulation of skin pigmentation. *Pigment Cell Res,* 13**,** 60-9.

BYERS, H. R., YAAR, M., ELLER, M. S., JALBERT, N. L. & GILCHREST, B. A. 2000. Role of cytoplasmic dynein in melanosome transport in human melanocytes. *J Invest Dermatol,* 114**,** 990-7.

CALLÉJA, C., MESSADDEQ, N., CHAPELLIER, B., YANG, H., KREZEL, W., LI, M., METZGER, D., MASCREZ, B., OHTA, K., KAGECHIKA, H., ENDO, Y., MARK, M., GHYSELINCK, N. B. & CHAMBON, P. 2006. Genetic and pharmacological evidence that a retinoic acid cannot be the RXR-activating ligand in mouse epidermis keratinocytes. *Genes Dev,* 20**,** 1525-38.

CALVO, P. A., FRANK, D. W., BIELER, B. M., BERSON, J. F. & MARKS, M. S. 1999. A cytoplasmic sequence in human tyrosinase defines a second class of di-leucine-based sorting signals for late endosomal and lysosomal delivery. *J Biol Chem,* 274**,** 12780-9.

CASTANET, J. & ORTONNE, J. P. 1997. Pathophysiology of vitiligo. *Clin Dermatol,* 15**,** 845-51.

CAVALLI, G. & MISTELI, T. 2013. Functional implications of genome topology. *Nat Struct Mol Biol,* 20**,** 290-9.

CHAMBON, P. 1996. A decade of molecular biology of retinoic acid receptors. *FASEB J,* 10**,** 940-54.

CHANG, T. S. 2009. An updated review of tyrosinase inhibitors. *Int J Mol Sci,* 10**,** 2440-75.

CHEN, J. Y., CLIFFORD, J., ZUSI, C., STARRETT, J., TORTOLANI, D., OSTROWSKI, J., RECZEK, P. R., CHAMBON, P. & GRONEMEYER, H. 1996. Two distinct actions of retinoid-receptor ligands. *Nature,* 382**,** 819-22.

CHEN, Y., KOPPAKA, V., THOMPSON, D. C. & VASILIOU, V. 2012. Focus on molecules: ALDH1A1: from lens and corneal crystallin to stem cell marker. *Exp Eye Res,* 102**,** 105-6.

CHEN, Y., MEHTA, G. & VASILIOU, V. 2009. Antioxidant defenses in the ocular surface. *Ocul Surf,* 7**,** 176-85.

CHIAVERINI, C., BEURET, L., FLORI, E., BUSCA, R., ABBE, P., BILLE, K., BAHADORAN, P., ORTONNE, J. P., BERTOLOTTO, C. & BALLOTTI, R. 2008. Microphthalmia-associated transcription factor regulates RAB27A gene expression and controls melanosome transport. *J Biol Chem,* 283**,** 12635-42.

COSTIN, G. E. & HEARING, V. J. 2007. Human skin pigmentation: melanocytes modulate skin color in response to stress. *FASEB J,* 21**,** 976-94.

CUI, R., WIDLUND, H. R., FEIGE, E., LIN, J. Y., WILENSKY, D. L., IGRAS, V. E., D'ORAZIO, J., FUNG, C. Y., SCHANBACHER, C. F., GRANTER, S. R. & FISHER, D. E. 2007. Central role of p53 in the suntan response and pathologic hyperpigmentation. *Cell,* 128**,** 853-64.

DAILY, K., PATEL, V. R., RIGOR, P., XIE, X. & BALDI, P. 2011. MotifMap: integrative genome-wide maps of regulatory motif sites for model species. *BMC Bioinformatics,* 12**,** 495.

DANESHPAZHOOH, M., MOSTOFIZADEH, G. M., BEHJATI, J., AKHYANI, M. & ROBATI, R. M. 2006. Anti-thyroid peroxidase antibody and vitiligo: a controlled study. *BMC Dermatol,* 6**,** 3.

DEL MARMOL, V., ITO, S., JACKSON, I., VACHTENHEIM, J., BERR, P., GHANEM, G., MORANDINI, R., WAKAMATSU, K. & HUEZ, G. 1993. TRP-1 expression correlates with eumelanogenesis in human pigment cells in culture. *FEBS Lett,* 327**,** 307-10.

DI PIETRO, S. M. & DELL'ANGELICA, E. C. 2005. The cell biology of Hermansky-Pudlak syndrome: recent advances. *Traffic,* 6**,** 525-33.

DILWORTH, F. J., FROMENTAL-RAMAIN, C., REMBOUTSIKA, E., BENECKE, A. & CHAMBON, P. 1999. Ligand-dependent activation of transcription in vitro by retinoic acid receptor alpha/retinoid X receptor alpha heterodimers that mimics transactivation by retinoids in vivo. *Proc Natl Acad Sci U S A,* 96**,** 1995-2000.

DILWORTH, F. J., FROMENTAL-RAMAIN, C., YAMAMOTO, K. & CHAMBON, P. 2000. ATP-driven chromatin remodeling activity and histone acetyltransferases act sequentially during transactivation by RAR/RXR In vitro. *Mol Cell,* 6**,** 1049-58.

DONG, D. & NOY, N. 1998. Heterodimer formation by retinoid X receptor: regulation by ligands and by the receptor's self-association properties. *Biochemistry,* 37**,** 10691-700.

DOW, L. E., PREMSRIRUT, P. K., ZUBER, J., FELLMANN, C., MCJUNKIN, K., MIETHING, C., PARK, Y., DICKINS, R. A., HANNON, G. J. & LOWE, S. W. 2012. A pipeline for the generation of shRNA transgenic mice. *Nat Protoc,* 7**,** 374-93.

DOWNES, J. & HOLMES, R. 1992. Development of aldehyde dehydrogenase and alcohol dehydrogenase in mouse eye: evidence for light-induced changes. *Biol Neonate,* 61**,** 118-23.

DU, J., MILLER, A. J., WIDLUND, H. R., HORSTMANN, M. A., RAMASWAMY, S. & FISHER, D. E. 2003. MLANA/MART1 and SILV/PMEL17/GP100 are transcriptionally regulated by MITF in melanocytes and melanoma. *Am J Pathol,* 163**,** 333-43.

DU, X., TABETA, K., MANN, N., CROZAT, K., MUDD, S. & BEUTLER, B. 2005. An essential role for Rxr alpha in the development of Th2 responses. *Eur J Immunol,* 35**,** 3414-23.

DUESTER, G. 2000. Families of retinoid dehydrogenases regulating vitamin A function: production of visual pigment and retinoic acid. *Eur J Biochem,* 267**,** 4315-24.

DUFFY, D. L., BOX, N. F., CHEN, W., PALMER, J. S., MONTGOMERY, G. W., JAMES, M. R., HAYWARD, N. K., MARTIN, N. G. & STURM, R. A. 2004. Interactive effects of MC1R and OCA2 on melanoma risk phenotypes. *Hum Mol Genet,* 13**,** 447-61.

DUPIN, E. & LE DOUARIN, N. M. 1995. Retinoic acid promotes the differentiation of adrenergic cells and melanocytes in quail neural crest cultures. *Dev Biol,* 168**,** 529-48.

EGEA, P. F., KLAHOLZ, B. P. & MORAS, D. 2000. Ligand-protein interactions in nuclear receptors of hormones. *FEBS Lett,* 476**,** 62-7.

EGEA, P. F., ROCHEL, N., BIRCK, C., VACHETTE, P., TIMMINS, P. A. & MORAS, D. 2001. Effects of ligand binding on the association properties and conformation in solution of retinoic acid receptors RXR and RAR. *J Mol Biol,* 307**,** 557-76.

ELDER, J. T., ASTROM, A., PETTERSSON, U., TAVAKKOL, A., GRIFFITHS, C. E., KRUST, A., KASTNER, P., CHAMBON, P. & VOORHEES, J. J. 1992a. Differential regulation of retinoic acid receptors and binding proteins in human skin. *J Invest Dermatol,* 98**,** 673-9.

ELDER, J. T., ASTRÖM, A., PETTERSSON, U., TAVAKKOL, A., GRIFFITHS, C. E., KRUST, A., KASTNER, P., CHAMBON, P. & VOORHEES, J. J. 1992b. Differential regulation of retinoic acid receptors and binding proteins in human skin. *J Invest Dermatol,* 98**,** 673-9.

ELIAS, P. M. 2005. Stratum corneum defensive functions: an integrated view. *J Invest Dermatol,* 125**,** 183-200.

ELIAS, P. M. & CHOI, E. H. 2005. Interactions among stratum corneum defensive functions. *Exp Dermatol,* 14**,** 719-26.

ELIASON, C. M., BITTON, P.-P. & SHAWKEY, M. D. 2013. How hollow melanosomes affect iridescent colour production in birds. *Proceedings of the Royal Society B: Biological Sciences,* 280**,** 20131505.

ELLER, M. S. & GILCHREST, B. A. 2000. Tanning as part of the eukaryotic SOS response. *Pigment Cell Res,* 13 Suppl 8**,** 94-7.

ELLER, M. S., OSTROM, K. & GILCHREST, B. A. 1996. DNA damage enhances melanogenesis. *Proc Natl Acad Sci U S A,* 93**,** 1087-92.

ERICKSON, C. A., DUONG, T. D. & TOSNEY, K. W. 1992. Descriptive and experimental analysis of the dispersion of neural crest cells along the dorsolateral path and their entry into ectoderm in the chick embryo. *Dev Biol,* 151**,** 251-72.

ESTEY, T., CANTORE, M., WESTON, P. A., CARPENTER, J. F., PETRASH, J. M. & VASILIOU, V. 2007. Mechanisms involved in the protection of UV-induced protein inactivation by the corneal crystallin ALDH3A1. *J Biol Chem,* 282**,** 4382-92.

ESTEY, T., CHEN, Y., CARPENTER, J. F. & VASILIOU, V. 2010. Structural and functional modifications of corneal crystallin ALDH3A1 by UVB light. *PLoS One,* 5**,** e15218.

FAN, X., MOLOTKOV, A., MANABE, S., DONMOYER, C. M., DELTOUR, L., FOGLIO, M. H., CUENCA, A. E., BLANER, W. S., LIPTON, S. A. & DUESTER, G. 2003. Targeted disruption of Aldh1a1 (Raldh1) provides evidence for a complex mechanism of retinoic acid synthesis in the developing retina. *Mol Cell Biol,* 23**,** 4637-48.

FARAGE, M. A., MILLER, K. W., ELSNER, P. & MAIBACH, H. I. 2007. Structural characteristics of the aging skin: a review. *Cutan Ocul Toxicol,* 26**,** 343-57.

FECKER, L. F., EBERLE, J., ORFANOS, C. E. & GEILEN, C. C. 2002. Inducible nitric oxide synthase is expressed in normal human melanocytes but not in melanoma cells in response to tumor necrosis factor-alpha, interferon-gamma, and lipopolysaccharide. *J Invest Dermatol,* 118**,** 1019-25.

FELLMANN, C., ZUBER, J., MCJUNKIN, K., CHANG, K., MALONE, C. D., DICKINS, R. A., XU, Q., HENGARTNER, M. O., ELLEDGE, S. J., HANNON, G. J. & LOWE, S. W. 2011. Functional identification of optimized RNAi triggers using a massively parallel sensor assay. *Mol Cell,* 41**,** 733-46.

FERNANDES, S. S., ARCURI, R., MORGADO-DIAZ, J. A. & BENCHIMOL, M. 2004a. Increase of melanogenesis by retinoic acid: an ultrastructural and morphometric study. *Tissue Cell,* 36**,** 95-105.

FERNANDES, S. S., ARCURI, R., MORGADO-DÍAZ, J. A. & BENCHIMOL, M. 2004b. Increase of melanogenesis by retinoic acid: an ultrastructural and morphometric study. *Tissue Cell,* 36**,** 95-105.

FISHER, G. J., TALWAR, H. S., XIAO, J. H., DATTA, S. C., REDDY, A. P., GAUB, M. P., ROCHETTE-EGLY, C., CHAMBON, P. & VOORHEES, J. J. 1994. Immunological identification and functional quantitation of retinoic acid and retinoid X receptor proteins in human skin. *J Biol Chem,* 269**,** 20629-35.

FISHER, G. J. & VOORHEES, J. J. 1996. Molecular mechanisms of retinoid actions in skin. *FASEB J,* 10**,** 1002-13.

FITZPATRICK, T. B. & BREATHNACH, A. S. 1963. [the Epidermal Melanin Unit System]. *Dermatol Wochenschr,* 147**,** 481-9.

FOWLER, D. M., KOULOV, A. V., ALORY-JOST, C., MARKS, M. S., BALCH, W. E. & KELLY, J. W. 2006. Functional amyloid formation within mammalian tissue. *PLoS Biol,* 4**,** e6.

FRANDBERG, P. A., DOUFEXIS, M., KAPAS, S. & CHHAJLANI, V. 1998. Human pigmentation phenotype: a point mutation generates nonfunctional MSH receptor. *Biochem Biophys Res Commun,* 245**,** 490-2.

FREEDBERG, I. M. & FITZPATRICK, T. B. 1999. *Fitzpatrick's dermatology in general medicine,* New York, McGraw-Hill, Health Professions Division.

FREEMAN, S. E., HACHAM, H., GANGE, R. W., MAYTUM, D. J., SUTHERLAND, J. C. & SUTHERLAND, B. M. 1989. Wavelength dependence of pyrimidine dimer formation in DNA of human skin irradiated in situ with ultraviolet light. *Proc Natl Acad Sci U S A,* 86**,** 5605-9.

FRIEDMANN, P. S. & GILCHREST, B. A. 1987. Ultraviolet radiation directly induces pigment production by cultured human melanocytes. *J Cell Physiol,* 133**,** 88-94.

FUJIMURA, N., TAKETO, M. M., MORI, M., KORINEK, V. & KOZMIK, Z. 2009. Spatial and temporal regulation of Wnt/beta-catenin signaling is essential for development of the retinal pigment epithelium. *Dev Biol,* 334**,** 31-45.

FUNASAKA, Y., CHAKRABORTY, A. K., HAYASHI, Y., KOMOTO, M., OHASHI, A., NAGAHAMA, M., INOUE, Y., PAWELEK, J. & ICHIHASHI, M. 1998. Modulation of melanocyte-stimulating hormone receptor expression on normal human melanocytes: evidence for a regulatory role of ultraviolet B, interleukin-1alpha, interleukin-1beta, endothelin-1 and tumour necrosis factor-alpha. *Br J Dermatol,* 139**,** 216-24.

FUSE, N., YASUMOTO, K., SUZUKI, H., TAKAHASHI, K. & SHIBAHARA, S. 1996. Identification of a melanocyte-type promoter of the microphthalmia-associated transcription factor gene. *Biochem Biophys Res Commun,* 219**,** 702-7.

FUTTERMAN, S. & ROLLINS, M. H. 1973. The catalytic isomerization of all-trans-retinal to 9-cis-retinal and 13-cis-retinal. *J Biol Chem,* 248**,** 7773-9.

GANESAN, A. K., HO, H., BODEMANN, B., PETERSEN, S., ARURI, J., KOSHY, S., RICHARDSON, Z., LE, L. Q., KRASIEVA, T., ROTH, M. G., FARMER, P. & WHITE, M. A. 2008. Genome-wide siRNA-based functional genomics of pigmentation identifies novel genes and pathways that impact melanogenesis in human cells. *PLoS Genet,* 4**,** e1000298.

GILCHREST, B. A., PARK, H. Y., ELLER, M. S. & YAAR, M. 1996. Mechanisms of ultraviolet light-induced pigmentation. *Photochem Photobiol,* 63**,** 1-10.

GILLBRO, J. M., MARLES, L. K., HIBBERTS, N. A. & SCHALLREUTER, K. U. 2004. Autocrine catecholamine biosynthesis and the beta-adrenoceptor signal promote pigmentation in human epidermal melanocytes. *J Invest Dermatol,* 123**,** 346-53.

GLASS, C. K. 1996. Some new twists in the regulation of gene expression by thyroid hormone and retinoic acid receptors. *J Endocrinol,* 150**,** 349-57.

GLOSTER, H. M., JR. & BRODLAND, D. G. 1996. The epidemiology of skin cancer. *Dermatol Surg,* 22**,** 217-26.

GODING, C. R. 2000. Mitf from neural crest to melanoma: signal transduction and transcription in the melanocyte lineage. *Genes Dev,* 14**,** 1712-28.

GOH, M. J., PARK, J. S., BAE, J. H., KIM, D. H., KIM, H. K. & NA, Y. J. 2012. Effects of ortho-dihydroxyisoflavone derivatives from Korean fermented soybean paste on melanogenesis in B16 melanoma cells and human skin equivalents. *Phytother Res,* 26**,** 1107-12.

GOLDSMITH, L. A. & FITZPATRICK, T. B. 2012. *Fitzpatrick's dermatology in general medicine,* New York, McGraw-Hill Professional.

GRANDO, S. A., PITTELKOW, M. R. & SCHALLREUTER, K. U. 2006. Adrenergic and cholinergic control in the biology of epidermis: physiological and clinical significance. *J Invest Dermatol,* 126**,** 1948-65.

GREEN, M. C. 1961. Himalayan, a new allele of albino in the mouse. *Journal of Heredity,* 52**,** 73-75.

GRIMES, P., NORDLUND, J. J., PANDYA, A. G., TAYLOR, S., RENDON, M. & ORTONNE, J. P. 2006. Increasing our understanding of pigmentary disorders. *J Am Acad Dermatol,* 54**,** S255-61.

GRIMES, P. E. 1995. Melasma. Etiologic and therapeutic considerations. *Arch Dermatol,* 131**,** 1453-7.

GRIMES, P. E., YAMADA, N. & BHAWAN, J. 2005. Light microscopic, immunohistochemical, and ultrastructural alterations in patients with melasma. *Am J Dermatopathol,* 27**,** 96-101.

GRUN, F., HIROSE, Y., KAWAUCHI, S., OGURA, T. & UMESONO, K. 2000. Aldehyde dehydrogenase 6, a cytosolic retinaldehyde dehydrogenase prominently expressed in sensory neuroepithelia during development. *J Biol Chem,* 275**,** 41210-8.

GUPTA, A. K., GOVER, M. D., NOURI, K. & TAYLOR, S. 2006. The treatment of melasma: a review of clinical trials. *J Am Acad Dermatol,* 55**,** 1048-65.

HACHIYA, A., KOBAYASHI, A., OHUCHI, A., TAKEMA, Y. & IMOKAWA, G. 2001. The paracrine role of stem cell factor/c-kit signaling in the activation of human melanocytes in ultraviolet-B-induced pigmentation. *J Invest Dermatol,* 116**,** 578-86.

HALABAN, R., MOELLMANN, G., TAMURA, A., KWON, B. S., KUKLINSKA, E., POMERANTZ, S. H. & LERNER, A. B. 1988. Tyrosinases of murine melanocytes with mutations at the albino locus. *Proceedings of the National Academy of Sciences,* 85**,** 7241-7245.

HALABAN, R., POMERANTZ, S. H., MARSHALL, S., LAMBERT, D. T. & LERNER, A. B. 1983. Regulation of tyrosinase in human melanocytes grown in culture. *J Cell Biol,* 97**,** 480-8.

HALABAN, R., SVEDINE, S., CHENG, E., SMICUN, Y., ARON, R. & HEBERT, D. N. 2000. Endoplasmic reticulum retention is a common defect associated with tyrosinase-negative albinism. *Proc Natl Acad Sci U S A,* 97**,** 5889-94.

HARA, M., YAAR, M., BYERS, H. R., GOUKASSIAN, D., FINE, R. E., GONSALVES, J. & GILCHREST, B. A. 2000. Kinesin participates in melanosomal movement along melanocyte dendrites. *J Invest Dermatol,* 114**,** 438-43.

HARA, M., YAAR, M. & GILCHREST, B. A. 1995. Endothelin-1 of keratinocyte origin is a mediator of melanocyte dendricity. *J Invest Dermatol,* 105**,** 744-8.

HARDING, R. M., HEALY, E., RAY, A. J., ELLIS, N. S., FLANAGAN, N., TODD, C., DIXON, C., SAJANTILA, A., JACKSON, I. J., BIRCH-MACHIN, M. A. & REES, J. L. 2000. Evidence for variable selective pressures at MC1R. *Am J Hum Genet,* 66**,** 1351-61.

HARRIS, M. L., BAXTER, L. L., LOFTUS, S. K. & PAVAN, W. J. 2010. Sox proteins in melanocyte development and melanoma. *Pigment Cell Melanoma Res,* 23**,** 496-513.

HEARING, V. J. 2000. The melanosome: the perfect model for cellular responses to the environment. *Pigment Cell Res,* 13 Suppl 8**,** 23-34.

HEARING, V. J. & JIMENEZ, M. 1987. Mammalian tyrosinase--the critical regulatory control point in melanocyte pigmentation. *Int J Biochem,* 19**,** 1141-7.

HEARING, V. J. & JIMENEZ, M. 1989. Analysis of mammalian pigmentation at the molecular level. *Pigment Cell Res,* 2**,** 75-85.

HEARING, V. J. & TSUKAMOTO, K. 1991. Enzymatic control of pigmentation in mammals. *FASEB J,* 5**,** 2902-9.

HECK, D. E., LASKIN, D. L., GARDNER, C. R. & LASKIN, J. D. 1992. Epidermal growth factor suppresses nitric oxide and hydrogen peroxide production by keratinocytes. Potential role for nitric oxide in the regulation of wound healing. *J Biol Chem,* 267**,** 21277-80.

HEMESATH, T. J., STEINGRIMSSON, E., MCGILL, G., HANSEN, M. J., VAUGHT, J., HODGKINSON, C. A., ARNHEITER, H., COPELAND, N. G., JENKINS, N. A. & FISHER, D. E. 1994. microphthalmia, a critical factor in melanocyte development, defines a discrete transcription factor family. *Genes Dev,* 8**,** 2770-80.

HERSHEY, C. L. & FISHER, D. E. 2005. Genomic analysis of the Microphthalmia locus and identification of the MITF-J/Mitf-J isoform. *Gene,* 347**,** 73-82.

HEYMAN, R. A., MANGELSDORF, D. J., DYCK, J. A., STEIN, R. B., EICHELE, G., EVANS, R. M. & THALLER, C. 1992. 9-cis retinoic acid is a high affinity ligand for the retinoid X receptor. *Cell,* 68**,** 397-406.

HIROBE, T. 1984. Histochemical survey of the distribution of the epidermal melanoblasts and melanocytes in the mouse during fetal and postnatal periods. *Anat Rec,* 208**,** 589-94.

HO, H. & GANESAN, A. K. 2011. The pleiotropic roles of autophagy regulators in melanogenesis. *Pigment Cell Melanoma Res,* 24**,** 595-604.

HO, H., KAPADIA, R., AL-TAHAN, S., AHMAD, S. & GANESAN, A. K. 2011. WIPI1 coordinates melanogenic gene transcription and melanosome formation via TORC1 inhibition. *J Biol Chem,* 286**,** 12509-23.

HO, K. K., HALLIDAY, G. M. & BARNETSON, R. S. 1992. Topical retinoic acid augments ultraviolet light-induced melanogenesis. *Melanoma Res,* 2**,** 41-5.

HOEK, K., RIMM, D. L., WILLIAMS, K. R., ZHAO, H., ARIYAN, S., LIN, A., KLUGER, H. M., BERGER, A. J., CHENG, E., TROMBETTA, E. S., WU, T., NIINOBE, M., YOSHIKAWA, K., HANNIGAN, G. E. & HALABAN, R. 2004. Expression profiling reveals novel pathways in the transformation of melanocytes to melanomas. *Cancer Res,* 64**,** 5270-82.

HOLBROOK, K. A., UNDERWOOD, R. A., VOGEL, A. M., GOWN, A. M. & KIMBALL, H. 1989. The appearance, density and distribution of melanocytes in human embryonic and fetal skin revealed by the anti-melanoma monoclonal antibody, HMB-45. *Anat Embryol (Berl),* 180**,** 443-55.

HOLICK, M. F. 1995. Noncalcemic actions of 1,25-dihydroxyvitamin D3 and clinical applications. *Bone,* 17**,** 107S-111S.

HOLICK, M. F. 2003a. Evolution and function of vitamin D. *Recent Results Cancer Res,* 164**,** 3-28.

HOLICK, M. F. 2003b. Vitamin D: A millenium perspective. *J Cell Biochem,* 88**,** 296-307.

HOLICK, M. F. 2005. The vitamin D epidemic and its health consequences. *J Nutr,* 135**,** 2739S-48S.

HOLICK, M. F. 2007. Vitamin D deficiency. *N Engl J Med,* 357**,** 266-81.

HONING, S., SANDOVAL, I. V. & VON FIGURA, K. 1998. A di-leucine-based motif in the cytoplasmic tail of LIMP-II and tyrosinase mediates selective binding of AP-3. *EMBO J,* 17**,** 1304-14.

HOSOI, J., ABE, E., SUDA, T. & KUROKI, T. 1985. Regulation of melanin synthesis of B16 mouse melanoma cells by 1 alpha, 25-dihydroxyvitamin D3 and retinoic acid. *Cancer Res,* 45**,** 1474-8.

HUAN, B., KOSOVSKY, M. J. & SIDDIQUI, A. 1995. Retinoid X receptor alpha transactivates the hepatitis B virus enhancer 1 element by forming a heterodimeric complex with the peroxisome proliferator-activated receptor. *J Virol,* 69**,** 547-51.

HUBER, W. E., PRICE, E. R., WIDLUND, H. R., DU, J., DAVIS, I. J., WEGNER, M. & FISHER, D. E. 2003. A tissue-restricted cAMP transcriptional response: SOX10 modulates alpha-melanocyte-stimulating hormone-triggered expression of microphthalmia-associated transcription factor in melanocytes. *J Biol Chem,* 278**,** 45224-30.

HUGGINS, R. H., SCHWARTZ, R. A. & JANNIGER, C. 2005. Vitiligo. *Acta Dermatovenerol Alp Pannonica Adriat,* 14**,** 137-42, 144-5.

HUIZING, M., SARANGARAJAN, R., STROVEL, E., ZHAO, Y., GAHL, W. A. & BOISSY, R. E. 2001. AP-3 mediates tyrosinase but not TRP-1 trafficking in human melanocytes. *Mol Biol Cell,* 12**,** 2075-85.

HURBAIN, I., GEERTS, W. J., BOUDIER, T., MARCO, S., VERKLEIJ, A. J., MARKS, M. S. & RAPOSO, G. 2008. Electron tomography of early melanosomes: implications for melanogenesis and the generation of fibrillar amyloid sheets. *Proc Natl Acad Sci U S A,* 105**,** 19726-31.

IHAKA, R., GENTLEMAN, R 1995. R: A Language for Data Analysis and Graphics. *Journal of Computational and Graphical Statistics,* 5**,** 299-314.

IJPENBERG, A., TAN, N. S., GELMAN, L., KERSTEN, S., SEYDOUX, J., XU, J., METZGER, D., CANAPLE, L., CHAMBON, P., WAHLI, W. & DESVERGNE, B. 2004. In vivo activation of PPAR target genes by RXR homodimers. *EMBO J,* 23**,** 2083-91.

IMOKAWA, G., KOBAYASI, T. & MIYAGISHI, M. 2000. Intracellular signaling mechanisms leading to synergistic effects of endothelin-1 and stem cell factor on proliferation of cultured human melanocytes. Cross-talk via trans-activation of the tyrosine kinase c-kit receptor. *J Biol Chem,* 275**,** 33321-8.

IMOKAWA, G., YADA, Y. & HORI, Y. 1988. Induction of melanization within hair bulb melanocytes in chinchilla mutant by melanogenic stimulants. *Journal of investigative dermatology,* 91**,** 106-113.

IMOKAWA, G., YADA, Y. & MIYAGISHI, M. 1992. Endothelins secreted from human keratinocytes are intrinsic mitogens for human melanocytes. *J Biol Chem,* 267**,** 24675-80.

ITO, S., NAKANISHI, Y., VALENZUELA, R. K., BRILLIANT, M. H., KOLBE, L. & WAKAMATSU, K. 2011. Usefulness of alkaline hydrogen peroxide oxidation to analyze eumelanin and pheomelanin in various tissue samples: application to chemical analysis of human hair melanins. *Pigment cell & melanoma research,* 24**,** 605-613.

ITO, S., WAKAMATSU, K. & OZEKI, H. 2000. Chemical analysis of melanins and its application to the study of the regulation of melanogenesis. *Pigment Cell Res,* 13 Suppl 8**,** 103-9.

JABLONSKI, N. G. 2004. The evolution of human skin and skin color. *Annual Review of Anthropology***,** 585-623.

JABLONSKI, N. G. & CHAPLIN, G. 2000. The evolution of human skin coloration. *Journal of human evolution,* 39**,** 57-106.

JABLONSKI, N. G. & CHAPLIN, G. 2010. Colloquium paper: human skin pigmentation as an adaptation to UV radiation. *Proc Natl Acad Sci U S A,* 107 Suppl 2**,** 8962-8.

JACKSON, I. J. 1994. Molecular and developmental genetics of mouse coat color. *Annu Rev Genet,* 28**,** 189-217.

JACKSON, I. J., CHAMBERS, D., RINCHIK, E. M. & BENNETT, D. C. 1990. Characterization of TRP-1 mRNA levels in dominant and recessive mutations at the mouse brown (b) locus. *Genetics,* 126**,** 451-9.

JACKSON, I. J., CHAMBERS, D. M., BUDD, P. S. & JOHNSON, R. 1991. The tyrosinase-related protein-1 gene has a structure and promoter sequence very different from tyrosinase. *Nucleic Acids Res,* 19**,** 3799-804.

JACKSON, I. J., CHAMBERS, D. M., TSUKAMOTO, K., COPELAND, N. G., GILBERT, D. J., JENKINS, N. A. & HEARING, V. 1992. A second tyrosinase-related protein, TRP-2, maps to and is mutated at the mouse slaty locus. *EMBO J,* 11**,** 527-35.

JACQUEMIN, P., LANNOY, V. J., O'SULLIVAN, J., READ, A., LEMAIGRE, F. P. & ROUSSEAU, G. G. 2001. The transcription factor onecut-2 controls the microphthalmia-associated transcription factor gene. *Biochem Biophys Res Commun,* 285**,** 1200-5.

JAIN, P., SONTI, S., GARRUTO, J., MEHTA, R. & BANGA, A. K. 2012. Formulation optimization, skin irritation, and efficacy characterization of a novel skin-lightening agent. *J Cosmet Dermatol,* 11**,** 101-10.

JIMBOW, K., OIKAWA, O., SUGIYAMA, S. & TAKEUCHI, T. 1979. Comparison of eumelanogenesis and pheomelanogenesis in retinal and follicular melanocytes; role of vesiculo-globular bodies in melanosome differentiation. *J Invest Dermatol,* 73**,** 278-84.

JIMENEZ, M., KAMEYAMA, K., MALOY, W. L., TOMITA, Y. & HEARING, V. J. 1988. Mammalian tyrosinase: biosynthesis, processing, and modulation by melanocyte-stimulating hormone. *Proc Natl Acad Sci U S A,* 85**,** 3830-4.

JOSHI, M., STRANDHOY, J. & WHITE, W. L. 1996. Nitric oxide synthase activity is up-regulated in melanoma cell lines: a potential mechanism for metastases formation. *Melanoma Res,* 6**,** 121-6.

KADAUKE, S. & BLOBEL, G. A. 2009. Chromatin loops in gene regulation. *Biochim Biophys Acta,* 1789**,** 17-25.

KANETSKY, P. A., SWOYER, J., PANOSSIAN, S., HOLMES, R., GUERRY, D. & REBBECK, T. R. 2002. A polymorphism in the agouti signaling protein gene is associated with human pigmentation. *Am J Hum Genet,* 70**,** 770-5.

KANG, W. H., YOON, K. H., LEE, E. S., KIM, J., LEE, K. B., YIM, H., SOHN, S. & IM, S. 2002. Melasma: histopathological characteristics in 56 Korean patients. *Br J Dermatol,* 146**,** 228-37.

KASTNER, P., MARK, M. & CHAMBON, P. 1995. Nonsteroid nuclear receptors: what are genetic studies telling us about their role in real life? *Cell,* 83**,** 859-69.

KAUSER, S., SCHALLREUTER, K. U., THODY, A. J., GUMMER, C. & TOBIN, D. J. 2003. Regulation of human epidermal melanocyte biology by beta-endorphin. *J Invest Dermatol,* 120**,** 1073-80.

KERSTEN, S., GRONEMEYER, H. & NOY, N. 1997. The DNA binding pattern of the retinoid X receptor is regulated by ligand-dependent modulation of its oligomeric state. *J Biol Chem,* 272**,** 12771-7.

KHLGATIAN, M. K., HADSHIEW, I. M., ASAWANONDA, P., YAAR, M., ELLER, M. S., FUJITA, M., NORRIS, D. A. & GILCHREST, B. A. 2002. Tyrosinase gene expression is regulated by p53. *J Invest Dermatol,* 118**,** 126-32.

KIM, K. J., PEARL, P. L., JENSEN, K., SNEAD, O. C., MALASPINA, P., JAKOBS, C. & GIBSON, K. M. 2011. Succinic semialdehyde dehydrogenase: biochemical-molecular-clinical disease mechanisms, redox regulation, and functional significance. *Antioxid Redox Signal,* 15**,** 691-718.

KIPPENBERGER, S., LOITSCH, S., SOLANO, F., BERND, A. & KAUFMANN, R. 1998. Quantification of tyrosinase, TRP-1, and Trp-2 transcripts in human melanocytes by reverse transcriptase-competitive multiplex PCR--regulation by steroid hormones. *J Invest Dermatol,* 110**,** 364-7.

KLIEWER, S. A., UMESONO, K., NOONAN, D. J., HEYMAN, R. A. & EVANS, R. M. 1992. Convergence of 9-cis retinoic acid and peroxisome proliferator signalling pathways through heterodimer formation of their receptors. *Nature,* 358**,** 771-4.

KOBAYASHI, N., NAKAGAWA, A., MURAMATSU, T., YAMASHINA, Y., SHIRAI, T., HASHIMOTO, M. W., ISHIGAKI, Y., OHNISHI, T. & MORI, T. 1998a. Supranuclear melanin caps reduce ultraviolet induced DNA photoproducts in human epidermis. *J Invest Dermatol,* 110**,** 806-10.

KOBAYASHI, T., IMOKAWA, G., BENNETT, D. C. & HEARING, V. J. 1998b. Tyrosinase stabilization by Tyrp1 (the brown locus protein). *J Biol Chem,* 273**,** 31801-5.

KOBAYASHI, T., URABE, K., WINDER, A., JIMENEZ-CERVANTES, C., IMOKAWA, G., BREWINGTON, T., SOLANO, F., GARCIA-BORRON, J. C. & HEARING, V. J. 1994.

Tyrosinase related protein 1 (TRP1) functions as a DHICA oxidase in melanin biosynthesis. *EMBO J,* 13**,** 5818-25.

KONDO, S., TAKAHASHI, T., YOSHIDA, K. & MIZOGUCHI, H. 2012. Inhibitory effects of autolysate of Leuconostoc mesenteroides isolated from kimoto on melanogenesis. *J Biosci Bioeng,* 114**,** 424-8.

KOPPAKA, V., THOMPSON, D. C., CHEN, Y., ELLERMANN, M., NICOLAOU, K. C., JUVONEN, R. O., PETERSEN, D., DEITRICH, R. A., HURLEY, T. D. & VASILIOU, V. 2012. Aldehyde dehydrogenase inhibitors: a comprehensive review of the pharmacology, mechanism of action, substrate specificity, and clinical application. *Pharmacol Rev,* 64**,** 520-39.

KORESSAAR, T. & REMM, M. 2007. Enhancements and modifications of primer design program Primer3. *Bioinformatics,* 23**,** 1289-91.

KORIA, P. & ANDREADIS, S. T. 2006. Epidermal morphogenesis: the transcriptional program of human keratinocytes during stratification. *J Invest Dermatol,* 126**,** 1834-41.

KOSTNER, K., DENZER, N., MULLER, C. S., KLEIN, R., TILGEN, W. & REICHRATH, J. 2009. The relevance of vitamin D receptor (VDR) gene polymorphisms for cancer: a review of the literature. *Anticancer Res,* 29**,** 3511-36.

KUROKAWA, R., SODERSTROM, M., HORLEIN, A., HALACHMI, S., BROWN, M., ROSENFELD, M. G. & GLASS, C. K. 1995. Polarity-specific activities of retinoic acid receptors determined by a co-repressor. *Nature,* 377**,** 451-4.

KUSHIMOTO, T., BASRUR, V., VALENCIA, J., MATSUNAGA, J., VIEIRA, W. D., FERRANS, V. J., MULLER, J., APPELLA, E. & HEARING, V. J. 2001. A model for melanosome biogenesis based on the purification and analysis of early melanosomes. *Proc Natl Acad Sci U S A,* 98**,** 10698-703.

KWON, B. S., HAQ, A. K., POMERANTZ, S. H. & HALABAN, R. 1987. Isolation and sequence of a cDNA clone for human tyrosinase that maps at the mouse c-albino locus. *Proc Natl Acad Sci U S A,* 84**,** 7473-7.

KWON, B. S., HAQ, A. K., WAKULCHIK, M., KESTLER, D., BARTON, D. E., FRANCKE, U., LAMOREUX, M. L., WHITNEY, J. B., 3RD & HALABAN, R. 1989. Isolation, chromosomal mapping, and expression of the mouse tyrosinase gene. *J Invest Dermatol,* 93**,** 589-94.

LABRECQUE, J., DUMAS, F., LACROIX, A. & BHAT, P. V. 1995. A novel isoenzyme of aldehyde dehydrogenase specifically involved in the biosynthesis of 9-cis and all-trans retinoic acid. *Biochem J,* 305 (Pt 2)**,** 681-4.

LAMASON, R. L., MOHIDEEN, M. A., MEST, J. R., WONG, A. C., NORTON, H. L., AROS, M. C., JURYNEC, M. J., MAO, X., HUMPHREVILLE, V. R., HUMBERT, J. E., SINHA, S., MOORE, J. L., JAGADEESWARAN, P., ZHAO, W., NING, G.,

MAKALOWSKA, I., MCKEIGUE, P. M., O'DONNELL, D., KITTLES, R., PARRA, E. J., MANGINI, N. J., GRUNWALD, D. J., SHRIVER, M. D., CANFIELD, V. A. & CHENG, K. C. 2005. SLC24A5, a putative cation exchanger, affects pigmentation in zebrafish and humans. *Science,* 310**,** 1782-6.

LAMOREUX, M., WAKAMATSU, K. & ITO, S. 2001. Interaction of major coat color gene functions in mice as studied by chemical analysis of eumelanin and pheomelanin. *Pigment Cell Research,* 14**,** 23-31.

LASSEN, N., BATEMAN, J. B., ESTEY, T., KUSZAK, J. R., NEES, D. W., PIATIGORSKY, J., DUESTER, G., DAY, B. J., HUANG, J., HINES, L. M. & VASILIOU, V. 2007. Multiple and additive functions of ALDH3A1 and ALDH1A1: cataract phenotype and ocular oxidative damage in Aldh3a1(-/-)/Aldh1a1(-/-) knock-out mice. *J Biol Chem,* 282**,** 25668-76.

LASSEN, N., BLACK, W. J., ESTEY, T. & VASILIOU, V. 2008. The role of corneal crystallins in the cellular defense mechanisms against oxidative stress. *Semin Cell Dev Biol,* 19**,** 100-12.

LE POOLE, I. C., BOISSY, R. E., SARANGARAJAN, R., CHEN, J., FORRISTAL, J. J., SHETH, P., WESTERHOF, W., BABCOCK, G., DAS, P. K. & SAELINGER, C. B. 2000. PIG3V, an immortalized human vitiligo melanocyte cell line, expresses dilated endoplasmic reticulum. *In Vitro Cell Dev Biol Anim,* 36**,** 309-19.

LE POOLE, I. C., DAS, P. K., VAN DEN WIJNGAARD, R. M., BOS, J. D. & WESTERHOF, W. 1993. Review of the etiopathomechanism of vitiligo: a convergence theory. *Exp Dermatol,* 2**,** 145-53.

LE POOLE, I. C. & LUITEN, R. M. 2008. Autoimmune etiology of generalized vitiligo. *Curr Dir Autoimmun,* 10**,** 227-43.

LEE, M. S., YOON, H. D., KIM, J. I., CHOI, J. S., BYUN, D. S. & KIM, H. R. 2012. Dioxinodehydroeckol inhibits melanin synthesis through PI3K/Akt signalling pathway in α-melanocyte-stimulating hormone-treated B16F10 cells. *Exp Dermatol,* 21**,** 471-3.

LEID, M., KASTNER, P. & CHAMBON, P. 1992a. Multiplicity generates diversity in the retinoic acid signalling pathways. *Trends Biochem Sci,* 17**,** 427-33.

LEID, M., KASTNER, P., LYONS, R., NAKSHATRI, H., SAUNDERS, M., ZACHAREWSKI, T., CHEN, J. Y., STAUB, A., GARNIER, J. M., MADER, S. & ET AL. 1992b. Purification, cloning, and RXR identity of the HeLa cell factor with which RAR or TR heterodimerizes to bind target sequences efficiently. *Cell,* 68**,** 377-95.

LERNER, A. B. & MCGUIRE, J. S. 1961. Effect of alpha- and betamelanocyte stimulating hormones on the skin colour of man. *Nature,* 189**,** 176-9.

LEVIN, A. A., STURZENBECKER, L. J., KAZMER, S., BOSAKOWSKI, T., HUSELTON, C., ALLENBY, G., SPECK, J., KRATZEISEN, C., ROSENBERGER, M., LOVEY, A. &

ET AL. 1992. 9-cis retinoic acid stereoisomer binds and activates the nuclear receptor RXR alpha. *Nature,* 355**,** 359-61.

LEVINE, N., SHEFTEL, S. N., EYTAN, T., DORR, R. T., HADLEY, M. E., WEINRACH, J. C., ERTL, G. A., TOTH, K., MCGEE, D. L. & HRUBY, V. J. 1991. Induction of skin tanning by subcutaneous administration of a potent synthetic melanotropin. *JAMA,* 266**,** 2730-6.

LEVITT, J. 2007. The safety of hydroquinone: a dermatologist's response to the 2006 Federal Register. *J Am Acad Dermatol,* 57**,** 854-72.

LEVY, C., KHALED, M. & FISHER, D. E. 2006. MITF: master regulator of melanocyte development and melanoma oncogene. *Trends Mol Med,* 12**,** 406-14.

LI, M., CHIBA, H., WAROT, X., MESSADDEQ, N., GERARD, C., CHAMBON, P. & METZGER, D. 2001a. RXR-alpha ablation in skin keratinocytes results in alopecia and epidermal alterations. *Development,* 128**,** 675-88.

LI, M., CHIBA, H., WAROT, X., MESSADDEQ, N., GÉRARD, C., CHAMBON, P. & METZGER, D. 2001b. RXR-alpha ablation in skin keratinocytes results in alopecia and epidermal alterations. *Development,* 128**,** 675-88.

LI, M., INDRA, A. K., WAROT, X., BROCARD, J., MESSADDEQ, N., KATO, S., METZGER, D. & CHAMBON, P. 2000. Skin abnormalities generated by temporally controlled RXRalpha mutations in mouse epidermis. *Nature,* 407**,** 633-6.

LIANG, C. H. 2011. Ov-16 [4-(3,4-dihydroxybenzoyloxymethyl)phenyl-O-β-D-glucopyranoside] inhibits melanin synthesis by regulating expressions of melanogenesis-regulated gene and protein. *Exp Dermatol,* 20**,** 743-8.

LIN, B. C., WONG, C. W., CHEN, H. W. & PRIVALSKY, M. L. 1997. Plasticity of tetramer formation by retinoid X receptors. An alternative paradigm for DNA recognition. *J Biol Chem,* 272**,** 9860-7.

LIN, J. Y. & FISHER, D. E. 2007. Melanocyte biology and skin pigmentation. *Nature,* 445**,** 843-50.

LISTER, J. A., ROBERTSON, C. P., LEPAGE, T., JOHNSON, S. L. & RAIBLE, D. W. 1999. nacre encodes a zebrafish microphthalmia-related protein that regulates neural-crest-derived pigment cell fate. *Development,* 126**,** 3757-67.

LIU, Y., KEMPF, V. R., NOFSINGER, J. B., WEINERT, E. E., RUDNICKI, M., WAKAMATSU, K., ITO, S. & SIMON, J. D. 2003. Comparison of the structural and physical properties of human hair eumelanin following enzymatic or acid/base extraction. *Pigment Cell Res,* 16**,** 355-65.

LOOMIS, W. F. 1967. Skin-pigment regulation of vitamin-D biosynthesis in man. *Science,* 157**,** 501-6.

LOTAN, R. & LOTAN, D. 1980. Stimulation of melanogenesis in a human melanoma cell line by retinoids. *Cancer Res,* 40**,** 3345-50.

LOTTI, T., GORI, A., ZANIERI, F., COLUCCI, R. & MORETTI, S. 2008. Vitiligo: new and emerging treatments. *Dermatol Ther,* 21**,** 110-7.

LU, D., WILLARD, D., PATEL, I. R., KADWELL, S., OVERTON, L., KOST, T., LUTHER, M., CHEN, W., WOYCHIK, R. P., WILKISON, W. O. & ET AL. 1994. Agouti protein is an antagonist of the melanocyte-stimulating-hormone receptor. *Nature,* 371**,** 799-802.

LUCOCK, M. 2000. Folic acid: nutritional biochemistry, molecular biology, and role in disease processes. *Mol Genet Metab,* 71**,** 121-38.

LUGER, T. A., SCHOLZEN, T. & GRABBE, S. 1997. The role of alpha-melanocyte-stimulating hormone in cutaneous biology. *J Investig Dermatol Symp Proc,* 2**,** 87-93.

MA, I. & ALLAN, A. L. 2011. The role of human aldehyde dehydrogenase in normal and cancer stem cells. *Stem Cell Rev,* 7**,** 292-306.

MAKOVA, K. & NORTON, H. 2005. Worldwide polymorphism at the MC1R locus and normal pigmentation variation in humans. *Peptides,* 26**,** 1901-8.

MANDELCORN-MONSON, R. L., SHEAR, N. H., YAU, E., SAMBHARA, S., BARBER, B. H., SPANER, D. & DEBENEDETTE, M. A. 2003. Cytotoxic T lymphocyte reactivity to gp100, MelanA/MART-1, and tyrosinase, in HLA-A2-positive vitiligo patients. *J Invest Dermatol,* 121**,** 550-6.

MANGA, P., KROMBERG, J. G., BOX, N. F., STURM, R. A., JENKINS, T. & RAMSAY, M. 1997. Rufous oculocutaneous albinism in southern African Blacks is caused by mutations in the TYRP1 gene. *Am J Hum Genet,* 61**,** 1095-101.

MANGELSDORF, D. J., BORGMEYER, U., HEYMAN, R. A., ZHOU, J. Y., ONG, E. S., ORO, A. E., KAKIZUKA, A. & EVANS, R. M. 1992. Characterization of three RXR genes that mediate the action of 9-cis retinoic acid. *Genes Dev,* 6**,** 329-44.

MANGELSDORF, D. J., KLIEWER, S. A., KAKIZUKA, A., UMESONO, K. & EVANS, R. M. 1993. Retinoid receptors. *Recent Prog Horm Res,* 48**,** 99-121.

MANGELSDORF, D. J., THUMMEL, C., BEATO, M., HERRLICH, P., SCHUTZ, G., UMESONO, K., BLUMBERG, B., KASTNER, P., MARK, M., CHAMBON, P. & EVANS, R. M. 1995. The nuclear receptor superfamily: the second decade. *Cell,* 83**,** 835-9.

MANOLACHE, L. & BENEA, V. 2007. Stress in patients with alopecia areata and vitiligo. *J Eur Acad Dermatol Venereol,* 21**,** 921-8.

MANSKY, K. C., SANKAR, U., HAN, J. & OSTROWSKI, M. C. 2002. Microphthalmia transcription factor is a target of the p38 MAPK pathway in response to receptor activator of NF-kappa B ligand signaling. *J Biol Chem,* 277**,** 11077-83.

MARCHITTI, S. A., BROCKER, C., STAGOS, D. & VASILIOU, V. 2008. Non-P450 aldehyde oxidizing enzymes: the aldehyde dehydrogenase superfamily. *Expert Opin Drug Metab Toxicol,* 4**,** 697-720.

MARK, M., GHYSELINCK, N. B. & CHAMBON, P. 2006. Function of retinoid nuclear receptors: lessons from genetic and pharmacological dissections of the retinoic acid signaling pathway during mouse embryogenesis. *Annu Rev Pharmacol Toxicol,* 46**,** 451-80.

MARK, M., GHYSELINCK, N. B., WENDLING, O., DUPE, V., MASCREZ, B., KASTNER, P. & CHAMBON, P. 1999. A genetic dissection of the retinoid signalling pathway in the mouse. *Proc Nutr Soc,* 58**,** 609-13.

MARKS, M. S. & SEABRA, M. C. 2001. The melanosome: membrane dynamics in black and white. *Nat Rev Mol Cell Biol,* 2**,** 738-48.

MATHUR, U., DATTA, S. L. & MATHUR, B. B. 1977. The effect of aminopterin-induced folic acid deficiency on spermatogenesis. *Fertil Steril,* 28**,** 1356-60.

MATTS, P. J., DYKES, P. J. & MARKS, R. 2007. The distribution of melanin in skin determined in vivo. *Br J Dermatol,* 156**,** 620-8.

MCKENNA, N. J. & O'MALLEY, B. W. 2002. Combinatorial control of gene expression by nuclear receptors and coregulators. *Cell,* 108**,** 465-74.

MINUCCI, S., LEID, M., TOYAMA, R., SAINT-JEANNET, J. P., PETERSON, V. J., HORN, V., ISHMAEL, J. E., BHATTACHARYYA, N., DEY, A., DAWID, I. B. & OZATO, K. 1997. Retinoid X receptor (RXR) within the RXR-retinoic acid receptor heterodimer binds its ligand and enhances retinoid-dependent gene expression. *Mol Cell Biol,* 17**,** 644-55.

MOCHLY-ROSEN, D. 1995. Localization of protein kinases by anchoring proteins: a theme in signal transduction. *Science,* 268**,** 247-51.

MOLOTKOV, A. & DUESTER, G. 2003. Genetic evidence that retinaldehyde dehydrogenase Raldh1 (Aldh1a1) functions downstream of alcohol dehydrogenase Adh1 in metabolism of retinol to retinoic acid. *J Biol Chem,* 278**,** 36085-90.

MONCADA, S., PALMER, R. M. & HIGGS, E. A. 1991. Nitric oxide: physiology, pathophysiology, and pharmacology. *Pharmacol Rev,* 43**,** 109-42.

MORRIS, J. K. 1965. A formaldehyde glutaraldehyde fixative of high osmolality for use in electron microscopy. *J. cell. Biol,* 27**,** 137-139.

MORRISS-KAY, G. M. & WARD, S. J. 1999. Retinoids and mammalian development. *Int Rev Cytol,* 188**,** 73-131.

MOUNTJOY, K. G., ROBBINS, L. S., MORTRUD, M. T. & CONE, R. D. 1992. The cloning of a family of genes that encode the melanocortin receptors. *Science,* 257**,** 1248-51.

NAGY, L., KAO, H. Y., CHAKRAVARTI, D., LIN, R. J., HASSIG, C. A., AYER, D. E., SCHREIBER, S. L. & EVANS, R. M. 1997. Nuclear receptor repression mediated by a complex containing SMRT, mSin3A, and histone deacetylase. *Cell,* 89**,** 373-80.

NAGY, L., KAO, H. Y., LOVE, J. D., LI, C., BANAYO, E., GOOCH, J. T., KRISHNA, V., CHATTERJEE, K., EVANS, R. M. & SCHWABE, J. W. 1999. Mechanism of corepressor binding and release from nuclear hormone receptors. *Genes Dev,* 13**,** 3209-16.

NAKAYAMA, A., NGUYEN, M. T., CHEN, C. C., OPDECAMP, K., HODGKINSON, C. A. & ARNHEITER, H. 1998. Mutations in microphthalmia, the mouse homolog of the human deafness gene MITF, affect neuroepithelial and neural crest-derived melanocytes differently. *Mech Dev,* 70**,** 155-66.

NAMAZI, M. R. 2005. Phenytoin as a novel anti-vitiligo weapon. *J Autoimmune Dis,* 2**,** 11.

NGUYEN, T., NOVAK, E. K., KERMANI, M., FLUHR, J., PETERS, L. L., SWANK, R. T. & WEI, M. L. 2002. Melanosome morphologies in murine models of hermansky-pudlak syndrome reflect blocks in organelle development. *J Invest Dermatol,* 119**,** 1156-64.

NI-KOMATSU, L., TONG, C., CHEN, G., BRINDZEI, N. & ORLOW, S. J. 2008. Identification of quinolines that inhibit melanogenesis by altering tyrosinase family trafficking. *Mol Pharmacol,* 74**,** 1576-86.

NICOLAIDOU, E., ANTONIOU, C., STRATIGOS, A. & KATSAMBAS, A. D. 2009. Narrowband ultraviolet B phototherapy and 308-nm excimer laser in the treatment of vitiligo: a review. *J Am Acad Dermatol,* 60**,** 470-7.

NIEDERREITHER, K. & DOLLE, P. 2008. Retinoic acid in development: towards an integrated view. *Nat Rev Genet,* 9**,** 541-53.

NORDLUND, J. J., BOISSY, R. E., HEARING, V. J., KING, R. A., OETTING, W. S. & ORTONNE, J.-P. 2006. *The pigmentary system: physiology and pathophysiology*, Wiley-Blackwell.

NORMAN, A. W. 2008. From vitamin D to hormone D: fundamentals of the vitamin D endocrine system essential for good health. *Am J Clin Nutr,* 88**,** 491S-499S.

NYLANDER, K., BOURDON, J. C., BRAY, S. E., GIBBS, N. K., KAY, R., HART, I. & HALL, P. A. 2000. Transcriptional activation of tyrosinase and TRP-1 by p53 links UV irradiation to the protective tanning response. *J Pathol,* 190**,** 39-46.

OETTING, W. S. 2000. The tyrosinase gene and oculocutaneous albinism type 1 (OCA1): A model for understanding the molecular biology of melanin formation. *Pigment Cell Res,* 13**,** 320-5.

OETTING, W. S. & KING, R. A. 1999. Molecular basis of albinism: mutations and polymorphisms of pigmentation genes associated with albinism. *Hum Mutat,* 13**,** 99-115.

OETTING, W. S., SUMMERS, C. G. & KING, R. A. 1994. Albinism and the associated ocular defects. *Metab Pediatr Syst Ophthalmol,* 17**,** 5-9.

OFF, M. K., STEINDAL, A. E., POROJNICU, A. C., JUZENIENE, A., VOROBEY, A., JOHNSSON, A. & MOAN, J. 2005. Ultraviolet photodegradation of folic acid. *J Photochem Photobiol B,* 80**,** 47-55.

OLLMANN, M. M., WILSON, B. D., YANG, Y. K., KERNS, J. A., CHEN, Y., GANTZ, I. & BARSH, G. S. 1997. Antagonism of central melanocortin receptors in vitro and in vivo by agouti-related protein. *Science,* 278**,** 135-8.

ONGENAE, K., VAN GEEL, N. & NAEYAERT, J. M. 2003. Evidence for an autoimmune pathogenesis of vitiligo. *Pigment Cell Res,* 16**,** 90-100.

OPDECAMP, K., NAKAYAMA, A., NGUYEN, M. T., HODGKINSON, C. A., PAVAN, W. J. & ARNHEITER, H. 1997. Melanocyte development in vivo and in neural crest cell cultures: crucial dependence on the Mitf basic-helix-loop-helix-zipper transcription factor. *Development,* 124**,** 2377-86.

ORLOW, S. J. 1995. Melanosomes are specialized members of the lysosomal lineage of organelles. *J Invest Dermatol,* 105**,** 3-7.

ORLOW, S. J., BOISSY, R. E., MORAN, D. J. & PIFKO-HIRST, S. 1993. Subcellular distribution of tyrosinase and tyrosinase-related protein-1: implications for melanosomal biogenesis. *J Invest Dermatol,* 100**,** 55-64.

ORLOW, S. J., CHAKRABORTY, A. K. & PAWELEK, J. M. 1990. Retinoic acid is a potent inhibitor of inducible pigmentation in murine and hamster melanoma cell lines. *J Invest Dermatol,* 94**,** 461-4.

OZEKI, H., ITO, S. & WAKAMATSU, K. 1996a. Chemical characterization of melanins in sheep wool and human hair. *Pigment Cell Res,* 9**,** 51-7.

OZEKI, H., ITO, S., WAKAMATSU, K. & HIROBE, T. 1995. Chemical Characterization of Hair Melanins in Various Coat—Color Mutants of Nlice.

OZEKI, H., ITO, S., WAKAMATSU, K. & ISHIGURO, I. 1997. Chemical characterization of pheomelanogenesis starting from dihydroxyphenylalanine or tyrosine and cysteine. Effects of tyrosinase and cysteine concentrations and reaction time. *Biochim Biophys Acta,* 1336**,** 539-48.

OZEKI, H., ITO, S., WAKAMATSU, K. & THODY, A. J. 1996b. Spectrophotometric characterization of eumelanin and pheomelanin in hair. *Pigment Cell Res,* 9**,** 265-70.

PALCZEWSKI, K. 2006. G protein-coupled receptor rhodopsin. *Annu Rev Biochem,* 75**,** 743-67.

PARK, H. Y. & GILCHREST, B. A. 1999. Signaling pathways mediating melanogenesis. *Cell Mol Biol (Noisy-le-grand),* 45**,** 919-30.

PARK, H. Y., KOSMADAKI, M., YAAR, M. & GILCHREST, B. A. 2009. Cellular mechanisms regulating human melanogenesis. *Cell Mol Life Sci,* 66**,** 1493-506.

PARK, H. Y., WU, H., KILLORAN, C. E. & GILCHREST, B. A. 2004. The receptor for activated C-kinase-I (RACK-I) anchors activated PKC-beta on melanosomes. *J Cell Sci,* 117**,** 3659-68.

PARRA, E. J. 2007. Human pigmentation variation: evolution, genetic basis, and implications for public health. *Am J Phys Anthropol,* Suppl 45**,** 85-105.

PARRISH, J. A., JAENICKE, K. F. & ANDERSON, R. R. 1982. Erythema and melanogenesis action spectra of normal human skin. *Photochem Photobiol,* 36**,** 187-91.

PATERSON, E. K., HO, H., KAPADIA, R. & GANESAN, A. K. 2013. 9‐cis retinoic acid is the ALDH1A1 product that stimulates melanogenesis. *Experimental dermatology,* 22**,** 202-209.

PATHAK, M. A., RILEY, F. C. & FITZPATRICK, T. B. 1962. Melanogenesis in human skin following exposure to long-wave ultraviolet and visible light. *J Invest Dermatol,* 39**,** 435-43.

PATHAK, M. A. & STRATTON, K. 1968. Free radicals in human skin before and after exposure to light. *Arch Biochem Biophys,* 123**,** 468-76.

PEDEN, A. A., OORSCHOT, V., HESSER, B. A., AUSTIN, C. D., SCHELLER, R. H. & KLUMPERMAN, J. 2004. Localization of the AP-3 adaptor complex defines a novel endosomal exit site for lysosomal membrane proteins. *J Cell Biol,* 164**,** 1065-76.

PEREZ, E., BOURGUET, W., GRONEMEYER, H. & DE LERA, A. R. 2012. Modulation of RXR function through ligand design. *Biochim Biophys Acta,* 1821**,** 57-69.

POGENBERG, V., GUICHOU, J. F., VIVAT-HANNAH, V., KAMMERER, S., PÉREZ, E., GERMAIN, P., DE LERA, A. R., GRONEMEYER, H., ROYER, C. A. & BOURGUET, W. 2005. Characterization of the interaction between retinoic acid receptor/retinoid X receptor (RAR/RXR) heterodimers and transcriptional coactivators through structural and fluorescence anisotropy studies. *J Biol Chem,* 280**,** 1625-33.

PREMSRIRUT, P. K., DOW, L. E., KIM, S. Y., CAMIOLO, M., MALONE, C. D., MIETHING, C., SCUOPPO, C., ZUBER, J., DICKINS, R. A. & KOGAN, S. C. 2011. A

rapid and scalable system for studying gene function in mice using conditional RNA interference. *Cell,* 145**,** 145-158.

PRICE, E. R., HORSTMANN, M. A., WELLS, A. G., WEILBAECHER, K. N., TAKEMOTO, C. M., LANDIS, M. W. & FISHER, D. E. 1998. alpha-Melanocyte-stimulating hormone signaling regulates expression of microphthalmia, a gene deficient in Waardenburg syndrome. *J Biol Chem,* 273**,** 33042-7.

PROTA, G. 2000. Melanins, melanogenesis and melanocytes: looking at their functional significance from the chemist's viewpoint. *Pigment Cell Research,* 13**,** 283-293.

RANA, B. K., HEWETT-EMMETT, D., JIN, L., CHANG, B. H., SAMBUUGHIN, N., LIN, M., WATKINS, S., BAMSHAD, M., JORDE, L. B., RAMSAY, M., JENKINS, T. & LI, W. H. 1999. High polymorphism at the human melanocortin 1 receptor locus. *Genetics,* 151**,** 1547-57.

RANSON, M., POSEN, S. & MASON, R. S. 1988. Human melanocytes as a target tissue for hormones: in vitro studies with 1 alpha-25, dihydroxyvitamin D3, alpha-melanocyte stimulating hormone, and beta-estradiol. *J Invest Dermatol,* 91**,** 593-8.

RAPOSO, G. & MARKS, M. S. 2007. Melanosomes--dark organelles enlighten endosomal membrane transport. *Nat Rev Mol Cell Biol,* 8**,** 786-97.

RAPOSO, G., TENZA, D., MURPHY, D. M., BERSON, J. F. & MARKS, M. S. 2001. Distinct protein sorting and localization to premelanosomes, melanosomes, and lysosomes in pigmented melanocytic cells. *J Cell Biol,* 152**,** 809-24.

REES, J. L. 2003. Genetics of hair and skin color. *Annu Rev Genet,* 37**,** 67-90.

REES, J. L. 2004. The genetics of sun sensitivity in humans. *Am J Hum Genet,* 75**,** 739-51.

REICHRATH, J., MUNSSINGER, T., KERBER, A., ROCHETTE-EGLY, C., CHAMBON, P., BAHMER, F. A. & BAUM, H. P. 1995. In situ detection of retinoid-X receptor expression in normal and psoriatic human skin. *Br J Dermatol,* 133**,** 168-75.

RESNIK, S. 1967a. Melasma induced by oral contraceptive drugs. *JAMA,* 199**,** 601-5.

RESNIK, S. S. 1967b. Melasma and other skin manifestations or oral contraceptives. *Trans N Engl Obstet Gynecol Soc,* 21**,** 101-7.

RIVAS, S. & PANDYA, A. G. 2013. Treatment of melasma with topical agents, peels and lasers: an evidence-based review. *Am J Clin Dermatol,* 14**,** 359-76.

ROBINSON, M. S. & BONIFACINO, J. S. 2001. Adaptor-related proteins. *Curr Opin Cell Biol,* 13**,** 444-53.

ROMÉRO, C., ABERDAM, E., LARNIER, C. & ORTONNE, J. P. 1994. Retinoic acid as modulator of UVB-induced melanocyte differentiation. Involvement of the melanogenic enzymes expression. *J Cell Sci,* 107 (Pt 4)**,** 1095-103.

ROMERO-GRAILLET, C., ABERDAM, E., CLEMENT, M., ORTONNE, J. P. & BALLOTTI, R. 1997. Nitric oxide produced by ultraviolet-irradiated keratinocytes stimulates melanogenesis. *J Clin Invest,* 99**,** 635-42.

ROUZAUD, F., KADEKARO, A. L., ABDEL-MALEK, Z. A. & HEARING, V. J. 2005. MC1R and the response of melanocytes to ultraviolet radiation. *Mutat Res,* 571**,** 133-52.

SAITO, H., YASUMOTO, K., TAKEDA, K., TAKAHASHI, K., FUKUZAKI, A., ORIKASA, S. & SHIBAHARA, S. 2002. Melanocyte-specific microphthalmia-associated transcription factor isoform activates its own gene promoter through physical interaction with lymphoid-enhancing factor 1. *J Biol Chem,* 277**,** 28787-94.

SATO, K., MORITA, M., ICHIKAWA, C., TAKAHASHI, H. & TORIYAMA, M. 2008. Depigmenting mechanisms of all-trans retinoic acid and retinol on B16 melanoma cells. *Biosci Biotechnol Biochem,* 72**,** 2589-97.

SCHALLREUTER, K. U. 1999. A review of recent advances on the regulation of pigmentation in the human epidermis. *Cell Mol Biol (Noisy-le-grand),* 45**,** 943-9.

SCHALLREUTER, K. U., KOTHARI, S., CHAVAN, B. & SPENCER, J. D. 2008. Regulation of melanogenesis--controversies and new concepts. *Exp Dermatol,* 17**,** 395-404.

SCHALLREUTER, K. U., WOOD, J. M., PITTELKOW, M. R., GUTLICH, M., LEMKE, K. R., RODL, W., SWANSON, N. N., HITZEMANN, K. & ZIEGLER, I. 1994. Regulation of melanin biosynthesis in the human epidermis by tetrahydrobiopterin. *Science,* 263**,** 1444-6.

SCHIOTH, H. B., PHILLIPS, S. R., RUDZISH, R., BIRCH-MACHIN, M. A., WIKBERG, J. E. & REES, J. L. 1999. Loss of function mutations of the human melanocortin 1 receptor are common and are associated with red hair. *Biochem Biophys Res Commun,* 260**,** 488-91.

SCHNEIDER, C. A., RASBAND, W. S. & ELICEIRI, K. W. 2012. NIH Image to ImageJ: 25 years of image analysis. *Nat Methods,* 9**,** 671-5.

SCHNUR, R. E., SELLINGER, B. T., HOLMES, S. A., WICK, P. A., TATSUMURA, Y. O. & SPRITZ, R. A. 1996. Type I oculocutaneous albinism associated with a full-length deletion of the tyrosinase gene. *J Invest Dermatol,* 106**,** 1137-40.

SCOTT, G., LEOPARDI, S., PRINTUP, S. & MADDEN, B. C. 2002a. Filopodia are conduits for melanosome transfer to keratinocytes. *J Cell Sci,* 115**,** 1441-51.

SCOTT, M. C., WAKAMATSU, K., ITO, S., KADEKARO, A. L., KOBAYASHI, N., GRODEN, J., KAVANAGH, R., TAKAKUWA, T., VIRADOR, V., HEARING, V. J. &

ABDEL-MALEK, Z. A. 2002b. Human melanocortin 1 receptor variants, receptor function and melanocyte response to UV radiation. *J Cell Sci,* 115**,** 2349-55.

SEIBERG, M., PAINE, C., SHARLOW, E., ANDRADE-GORDON, P., COSTANZO, M., EISINGER, M. & SHAPIRO, S. S. 2000. Inhibition of melanosome transfer results in skin lightening. *J Invest Dermatol,* 115**,** 162-7.

SEIJI, M., FITZPATRICK, T. B., SIMPSON, R. T. & BIRBECK, M. S. 1963a. Chemical composition and terminology of specialized organelles (melanosomes and melanin granules) in mammalian melanocytes. *Nature,* 197**,** 1082-4.

SEIJI, M., SHIMAO, K., BIRBECK, M. & FITZPATRICK, T. B. 1963b. Subcellular localization of melanin biosynthesis. *Annals of the New York Academy of Sciences,* 100**,** 497-533.

SERBEDZIJA, G. N., BRONNER-FRASER, M. & FRASER, S. E. 1989. A vital dye analysis of the timing and pathways of avian trunk neural crest cell migration. *Development,* 106**,** 809-16.

SETTY, S. R., TENZA, D., TRUSCHEL, S. T., CHOU, E., SVIDERSKAYA, E. V., THEOS, A. C., LAMOREUX, M. L., DI PIETRO, S. M., STARCEVIC, M., BENNETT, D. C., DELL'ANGELICA, E. C., RAPOSO, G. & MARKS, M. S. 2007. BLOC-1 is required for cargo-specific sorting from vacuolar early endosomes toward lysosome-related organelles. *Mol Biol Cell,* 18**,** 768-80.

SHAMEER, P., PRASAD, P. V. & KAVIARASAN, P. K. 2005. Serum zinc level in vitiligo: a case control study. *Indian J Dermatol Venereol Leprol,* 71**,** 206-7.

SHIBAHARA, S., TAKEDA, K., YASUMOTO, K., UDONO, T., WATANABE, K., SAITO, H. & TAKAHASHI, K. 2001. Microphthalmia-associated transcription factor (MITF): multiplicity in structure, function, and regulation. *J Investig Dermatol Symp Proc,* 6**,** 99-104.

SHIBAHARA, S., YASUMOTO, K., AMAE, S., UDONO, T., WATANABE, K., SAITO, H. & TAKEDA, K. 2000. Regulation of pigment cell-specific gene expression by MITF. *Pigment Cell Res,* 13 Suppl 8**,** 98-102.

SHIH, T. W., LIN, T. H., SHEALY, Y. F. & HILL, D. L. 1997. Nonenzymatic isomerization of 9-cis-retinoic acid catalyzed by sulfhydryl compounds. *Drug Metab Dispos,* 25**,** 27-32.

SIEGRIST, W., DROZDZ, R., COTTI, R., WILLARD, D. H., WILKISON, W. O. & EBERLE, A. N. 1997. Interactions of alpha-melanotropin and agouti on B16 melanoma cells: evidence for inverse agonism of agouti. *J Recept Signal Transduct Res,* 17**,** 75-98.

SILVERS, W. K. 1979. *The Coat Colors of Mice: A Model for Mammalian Gene Action and Interaction,* New York, Springer-Verlag.

SIMMEN, T., SCHMIDT, A., HUNZIKER, W. & BEERMANN, F. 1999. The tyrosinase tail mediates sorting to the lysosomal compartment in MDCK cells via a di-leucine and a tyrosine-based signal. *J Cell Sci,* 112 (Pt 1)**,** 45-53.

SLOMINSKI, A. & PAUS, R. 1993. Melanogenesis is coupled to murine anagen: toward new concepts for the role of melanocytes and the regulation of melanogenesis in hair growth. *J Invest Dermatol,* 101**,** 90S-97S.

SLOMINSKI, A., PAUS, R. & COSTANTINO, R. 1991. Differential expression and activity of melanogenesis-related proteins during induced hair growth in mice. *J Invest Dermatol,* 96**,** 172-9.

SLOMINSKI, A., PLONKA, P. M., PISARCHIK, A., SMART, J. L., TOLLE, V., WORTSMAN, J. & LOW, M. J. 2005. Preservation of eumelanin hair pigmentation in proopiomelanocortin-deficient mice on a nonagouti (a/a) genetic background. *Endocrinology,* 146**,** 1245-53.

SLOMINSKI, A., TOBIN, D. J., SHIBAHARA, S. & WORTSMAN, J. 2004. Melanin pigmentation in mammalian skin and its hormonal regulation. *Physiol Rev,* 84**,** 1155-228.

SLOMINSKI, A. & WORTSMAN, J. 2000. Neuroendocrinology of the skin. *Endocr Rev,* 21**,** 457-87.

SLOMINSKI, A., ZMIJEWSKI, M. A. & PAWELEK, J. 2012. L-tyrosine and L-dihydroxyphenylalanine as hormone-like regulators of melanocyte functions. *Pigment Cell Melanoma Res,* 25**,** 14-27.

SMILES, K. A., DONG, K. K., CANNING, M. T., GRIMSON, R., WALFIELD, A. M. & YAROSH, D. B. 2007. A hydroquinone formulation with increased stability and decreased potential for irritation. *J Cosmet Dermatol,* 6**,** 83-8.

SMITH, A. G., SHUSTER, S., THODY, A. J. & PEBERDY, M. 1977. Chloasma, oral contraceptives, and plasma immunoreactive beta-melanocyte-stimulating hormone. *J Invest Dermatol,* 68**,** 169-70.

SOPHOS, N. A. & VASILIOU, V. 2003. Aldehyde dehydrogenase gene superfamily: the 2002 update. *Chem Biol Interact,* 143-144**,** 5-22.

STEINMETZ, A. C., RENAUD, J. P. & MORAS, D. 2001. Binding of ligands and activation of transcription by nuclear receptors. *Annu Rev Biophys Biomol Struct,* 30**,** 329-59.

STORMS, R. W., GREEN, P. D., SAFFORD, K. M., NIEDZWIECKI, D., COGLE, C. R., COLVIN, O. M., CHAO, N. J., RICE, H. E. & SMITH, C. A. 2005. Distinct hematopoietic progenitor compartments are delineated by the expression of aldehyde dehydrogenase and CD34. *Blood,* 106**,** 95-102.

STORMS, R. W., TRUJILLO, A. P., SPRINGER, J. B., SHAH, L., COLVIN, O. M., LUDEMAN, S. M. & SMITH, C. 1999. Isolation of primitive human hematopoietic

progenitors on the basis of aldehyde dehydrogenase activity. *Proc Natl Acad Sci U S A,* 96**,** 9118-23.

STURM, R. A., O'SULLIVAN, B. J., BOX, N. F., SMITH, A. G., SMIT, S. E., PUTTICK, E. R., PARSONS, P. G. & DUNN, I. S. 1995. Chromosomal structure of the human TYRP1 and TYRP2 loci and comparison of the tyrosinase-related protein gene family. *Genomics,* 29**,** 24-34.

STURM, R. A., TEASDALE, R. D. & BOX, N. F. 2001. Human pigmentation genes: identification, structure and consequences of polymorphic variation. *Gene,* 277**,** 49-62.

SVIDERSKAYA, E. V., WAKELING, W. F. & BENNETT, D. C. 1995. A cloned, immortal line of murine melanoblasts inducible to differentiate to melanocytes. *Development,* 121**,** 1547-57.

SZABÓ, G., GERALD, A. B., PATHAK, M. A. & FITZPATRICK, T. B. 1969. Racial differences in the fate of melanosomes in human epidermis. *Nature,* 222**,** 1081-1082.

SZCZURKO, O. & BOON, H. S. 2008. A systematic review of natural health product treatment for vitiligo. *BMC Dermatol,* 8**,** 2.

TAKEDA, K., TAKEMOTO, C., KOBAYASHI, I., WATANABE, A., NOBUKUNI, Y., FISHER, D. E. & TACHIBANA, M. 2000. Ser298 of MITF, a mutation site in Waardenburg syndrome type 2, is a phosphorylation site with functional significance. *Hum Mol Genet,* 9**,** 125-32.

TAKIGUCHI, M., DOW, L. E., PRIER, J. E., CARMICHAEL, C. L., KILE, B. T., TURNER, S. J., LOWE, S. W., HUANG, D. C. & DICKINS, R. A. 2013. Variability of inducible expression across the hematopoietic system of tetracycline transactivator transgenic mice. *PLoS One,* 8**,** e54009.

THEOS, A. C., BERSON, J. F., THEOS, S. C., HERMAN, K. E., HARPER, D. C., TENZA, D., SVIDERSKAYA, E. V., LAMOREUX, M. L., BENNETT, D. C., RAPOSO, G. & MARKS, M. S. 2006a. Dual loss of ER export and endocytic signals with altered melanosome morphology in the silver mutation of Pmel17. *Mol Biol Cell,* 17**,** 3598-612.

THEOS, A. C., TENZA, D., MARTINA, J. A., HURBAIN, I., PEDEN, A. A., SVIDERSKAYA, E. V., STEWART, A., ROBINSON, M. S., BENNETT, D. C., CUTLER, D. F., BONIFACINO, J. S., MARKS, M. S. & RAPOSO, G. 2005. Functions of adaptor protein (AP)-3 and AP-1 in tyrosinase sorting from endosomes to melanosomes. *Mol Biol Cell,* 16**,** 5356-72.

THEOS, A. C., TRUSCHEL, S. T., TENZA, D., HURBAIN, I., HARPER, D. C., BERSON, J. F., THOMAS, P. C., RAPOSO, G. & MARKS, M. S. 2006b. A lumenal domain-dependent pathway for sorting to intralumenal vesicles of multivesicular endosomes involved in organelle morphogenesis. *Dev Cell,* 10**,** 343-54.

THOMAS, A. J. & ERICKSON, C. A. 2009. FOXD3 regulates the lineage switch between neural crest-derived glial cells and pigment cells by repressing MITF through a non-canonical mechanism. *Development,* 136**,** 1849-58.

THONG, H. Y., JEE, S. H., SUN, C. C. & BOISSY, R. 2003. The patterns of melanosome distribution in keratinocytes of human skin as one determining factor of skin colour. *British Journal of Dermatology,* 149**,** 498-505.

TOBIN, D. J. 2006. Biochemistry of human skin--our brain on the outside. *Chem Soc Rev,* 35**,** 52-67.

TODA, K., PATHAK, M. A., PARRISH, J. A., FITZPATRICK, T. B. & QUEVEDO, W. C., JR. 1972. Alteration of racial differences in melanosome distribution in human epidermis after exposure to ultraviolet light. *Nat New Biol,* 236**,** 143-5.

TOROK, H. M. 2006. A comprehensive review of the long-term and short-term treatment of melasma with a triple combination cream. *Am J Clin Dermatol,* 7**,** 223-30.

TOYOFUKU, K., WADA, I., SPRITZ, R. A. & HEARING, V. J. 2001a. The molecular basis of oculocutaneous albinism type 1 (OCA1): sorting failure and degradation of mutant tyrosinases results in a lack of pigmentation. *Biochem J,* 355**,** 259-69.

TOYOFUKU, K., WADA, I., VALENCIA, J. C., KUSHIMOTO, T., FERRANS, V. J. & HEARING, V. J. 2001b. Oculocutaneous albinism types 1 and 3 are ER retention diseases: mutation of tyrosinase or Tyrp1 can affect the processing of both mutant and wild-type proteins. *The FASEB Journal,* 15**,** 2149-2161.

TRUAX, A. D. & GREER, S. F. 2012. ChIP and Re-ChIP assays: investigating interactions between regulatory proteins, histone modifications, and the DNA sequences to which they bind. *Methods Mol Biol,* 809**,** 175-88.

TSAI, M. J. & O'MALLEY, B. W. 1994. Molecular mechanisms of action of steroid/thyroid receptor superfamily members. *Annu Rev Biochem,* 63**,** 451-86.

TSUKAMOTO, K., JACKSON, I. J., URABE, K., MONTAGUE, P. M. & HEARING, V. J. 1992. A second tyrosinase-related protein, TRP-2, is a melanogenic enzyme termed DOPAchrome tautomerase. *EMBO J,* 11**,** 519-26.

TURNER, W. A., TAYLOR, J. D. & TCHEN, T. T. 1975. Melanosome formation in the goldfish: the role of multivesicular bodies. *J Ultrastruct Res,* 51**,** 16-31.

UDONO, T., YASUMOTO, K., TAKEDA, K., AMAE, S., WATANABE, K., SAITO, H., FUSE, N., TACHIBANA, M., TAKAHASHI, K., TAMAI, M. & SHIBAHARA, S. 2000. Structural organization of the human microphthalmia-associated transcription factor gene containing four alternative promoters. *Biochim Biophys Acta,* 1491**,** 205-19.

UNTERGASSER, A., CUTCUTACHE, I., KORESSAAR, T., YE, J., FAIRCLOTH, B. C., REMM, M. & ROZEN, S. G. 2012. Primer3--new capabilities and interfaces. *Nucleic Acids Res,* 40**,** e115.

URABE, K., AROCA, P., TSUKAMOTO, K., MASCAGNA, D., PALUMBO, A., PROTA, G. & HEARING, V. J. 1994. The inherent cytotoxicity of melanin precursors: a revision. *Biochim Biophys Acta,* 1221**,** 272-8.

VACHTENHEIM, J. & BOROVANSKÝ, J. 2010. "Transcription physiology" of pigment formation in melanocytes: central role of MITF. *Experimental dermatology,* 19**,** 617-627.

VASILIOU, V. & NEBERT, D. W. 2005. Analysis and update of the human aldehyde dehydrogenase (ALDH) gene family. *Hum Genomics,* 2**,** 138-43.

VASILIOU, V. & PAPPA, A. 2000. Polymorphisms of human aldehyde dehydrogenases. Consequences for drug metabolism and disease. *Pharmacology,* 61**,** 192-8.

VASILIOU, V., PAPPA, A. & PETERSEN, D. R. 2000. Role of aldehyde dehydrogenases in endogenous and xenobiotic metabolism. *Chem Biol Interact,* 129**,** 1-19.

VICTOR, F. C., GELBER, J. & RAO, B. 2004. Melasma: a review. *J Cutan Med Surg,* 8**,** 97-102.

VIJAYASARADHI, S., XU, Y., BOUCHARD, B. & HOUGHTON, A. N. 1995. Intracellular sorting and targeting of melanosomal membrane proteins: identification of signals for sorting of the human brown locus protein, gp75. *J Cell Biol,* 130**,** 807-20.

VO, N. & GOODMAN, R. H. 2001. CREB-binding protein and p300 in transcriptional regulation. *J Biol Chem,* 276**,** 13505-8.

VOISEY, J., GOMEZ-CABRERA MDEL, C., SMIT, D. J., LEONARD, J. H., STURM, R. A. & VAN DAAL, A. 2006. A polymorphism in the agouti signalling protein (ASIP) is associated with decreased levels of mRNA. *Pigment Cell Res,* 19**,** 226-31.

WAKAMATSU, K. & ITO, S. 2002. Advanced chemical methods in melanin determination. *Pigment Cell Res,* 15**,** 174-83.

WAKAMATSU, K., ITO, S. & REES, J. L. 2002. The Usefulness of 4‐Amino‐3‐hydroxyphenylalanine as a Specific Marker of Pheomelanin. *Pigment Cell Research,* 15**,** 225-232.

WANG, S. Q., SETLOW, R., BERWICK, M., POLSKY, D., MARGHOOB, A. A., KOPF, A. W. & BART, R. S. 2001. Ultraviolet A and melanoma: a review. *J Am Acad Dermatol,* 44**,** 837-46.

WANG, Z., ZANG, C., ROSENFELD, J. A., SCHONES, D. E., BARSKI, A., CUDDAPAH, S., CUI, K., ROH, T. Y., PENG, W., ZHANG, M. Q. & ZHAO, K. 2008. Combinatorial

patterns of histone acetylations and methylations in the human genome. *Nat Genet,* 40**,** 897-903.

WEI, L. N. 2003. Retinoid receptors and their coregulators. *Annu Rev Pharmacol Toxicol,* 43**,** 47-72.

WEI, M. L. 2006. Hermansky-Pudlak syndrome: a disease of protein trafficking and organelle function. *Pigment Cell Res,* 19**,** 19-42.

WEILBAECHER, K. N., MOTYCKOVA, G., HUBER, W. E., TAKEMOTO, C. M., HEMESATH, T. J., XU, Y., HERSHEY, C. L., DOWLAND, N. R., WELLS, A. G. & FISHER, D. E. 2001. Linkage of M-CSF signaling to Mitf, TFE3, and the osteoclast defect in Mitf(mi/mi) mice. *Mol Cell,* 8**,** 749-58.

WELSH, B. M., MASON, R. S. & HALLIDAY, G. M. 1999. Topical all-trans retinoic acid augments ultraviolet radiation-induced increases in activated melanocyte numbers in mice. *J Invest Dermatol,* 112**,** 271-8.

WHITTON, M. E., ASHCROFT, D. M. & GONZALEZ, U. 2008. Therapeutic interventions for vitiligo. *J Am Acad Dermatol,* 59**,** 713-7.

WICKS, N. L., CHAN, J. W., NAJERA, J. A., CIRIELLO, J. M. & OANCEA, E. 2011. UVA phototransduction drives early melanin synthesis in human melanocytes. *Curr Biol,* 21**,** 1906-11.

WU, H. & PARK, H. Y. 2003. Protein kinase C-beta-mediated complex formation between tyrosinase and TRP-1. *Biochem Biophys Res Commun,* 311**,** 948-53.

WU, M., HEMESATH, T. J., TAKEMOTO, C. M., HORSTMANN, M. A., WELLS, A. G., PRICE, E. R., FISHER, D. Z. & FISHER, D. E. 2000. c-Kit triggers dual phosphorylations, which couple activation and degradation of the essential melanocyte factor Mi. *Genes Dev,* 14**,** 301-12.

XIE, X., RIGOR, P. & BALDI, P. 2009. MotifMap: a human genome-wide map of candidate regulatory motif sites. *Bioinformatics,* 25**,** 167-74.

XU, X., THORNWALL, M., LUNDIN, L. G. & CHHAJLANI, V. 1996. Val92Met variant of the melanocyte stimulating hormone receptor gene. *Nat Genet,* 14**,** 384.

YADA, Y., HIGUCHI, K. & IMOKAWA, G. 1991. Effects of endothelins on signal transduction and proliferation in human melanocytes. *J Biol Chem,* 266**,** 18352-7.

YAGHOOBI, R., OMIDIAN, M. & BAGHERANI, N. 2011. Vitiligo: a review of the published work. *J Dermatol,* 38**,** 419-31.

YAKUBU, A. & MABOGUNJE, O. A. 1993. Skin cancer in African albinos. *Acta Oncol,* 32**,** 621-2.

YASUMOTO, K., TAKEDA, K., SAITO, H., WATANABE, K., TAKAHASHI, K. & SHIBAHARA, S. 2002. Microphthalmia-associated transcription factor interacts with LEF-1, a mediator of Wnt signaling. *EMBO J,* 21**,** 2703-14.

YASUMOTO, K., YOKOYAMA, K., SHIBATA, K., TOMITA, Y. & SHIBAHARA, S. 1994. Microphthalmia-associated transcription factor as a regulator for melanocyte-specific transcription of the human tyrosinase gene. *Mol Cell Biol,* 14**,** 8058-70.

YOHN, J. J., MORELLI, J. G., WALCHAK, S. J., RUNDELL, K. B., NORRIS, D. A. & ZAMORA, M. R. 1993. Cultured human keratinocytes synthesize and secrete endothelin-1. *J Invest Dermatol,* 100**,** 23-6.

YOKOYAMA, K., SUZUKI, H., YASUMOTO, K., TOMITA, Y. & SHIBAHARA, S. 1994. Molecular cloning and functional analysis of a cDNA coding for human DOPAchrome tautomerase/tyrosinase-related protein-2. *Biochim Biophys Acta,* 1217**,** 317-21.

YOSHIDA, A., HSU, L. C. & DAVE, V. 1992. Retinal oxidation activity and biological role of human cytosolic aldehyde dehydrogenase. *Enzyme,* 46**,** 239-44.

YU, V. C., DELSERT, C., ANDERSEN, B., HOLLOWAY, J. M., DEVARY, O. V., NAAR, A. M., KIM, S. Y., BOUTIN, J. M., GLASS, C. K. & ROSENFELD, M. G. 1991. RXR beta: a coregulator that enhances binding of retinoic acid, thyroid hormone, and vitamin D receptors to their cognate response elements. *Cell,* 67**,** 1251-66.